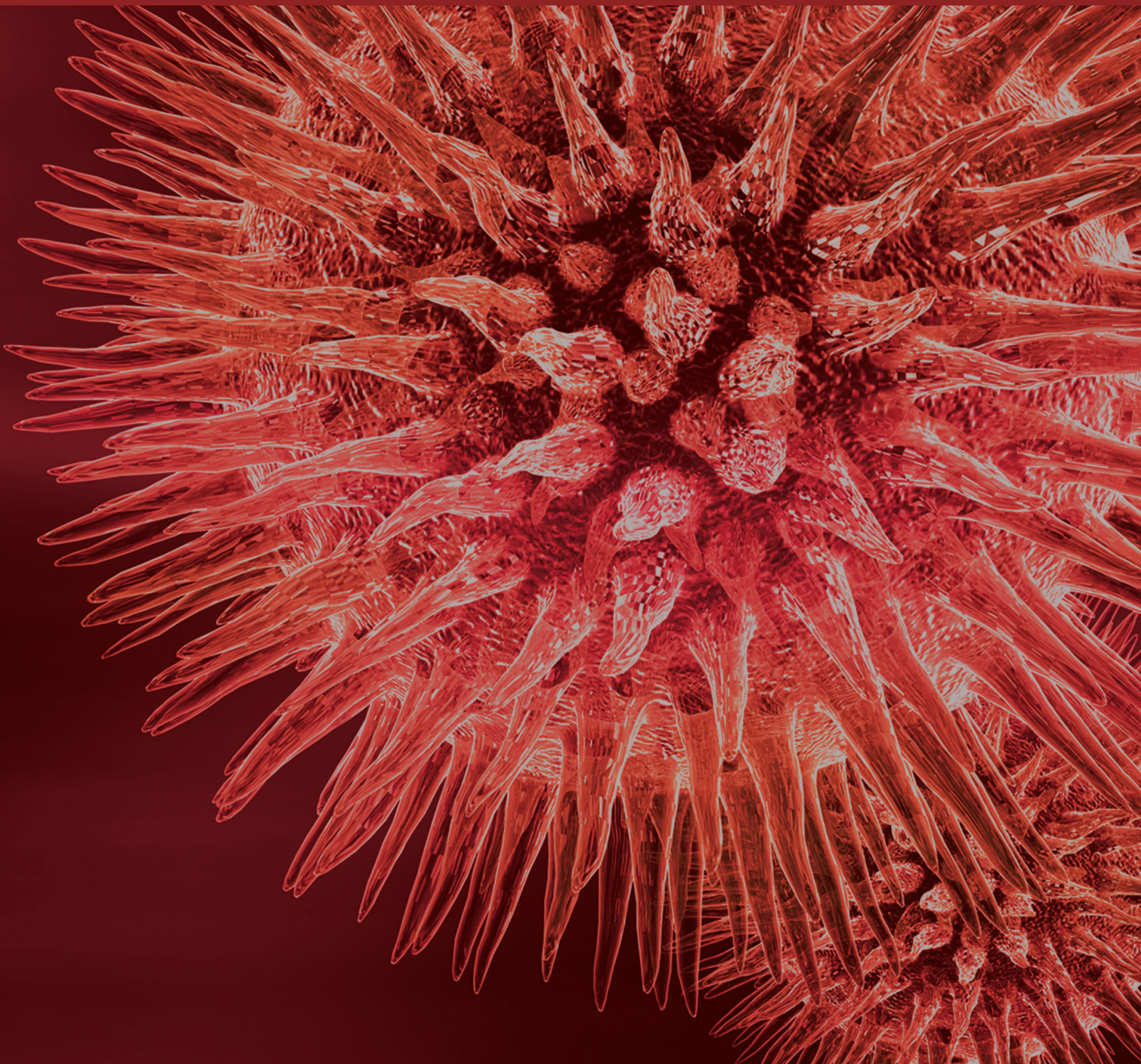


Bioarcheology: Medicine, Biology, and Forensic Sciences

Guest Editors: Otto Appenzeller, Timothy G. Bromage, Rabab Khairat,
Andreas G. Nerlich, and Frank Jakobus Rühli





**Bioarcheology: Medicine, Biology,
and Forensic Sciences**

BioMed Research International

**Bioarcheology: Medicine, Biology,
and Forensic Sciences**

Guest Editors: Otto Appenzeller, Timothy G. Bromage,
Rabab Khairat, Andreas G. Nerlich, and Frank Jakobus Rühli



Copyright © 2015 Hindawi Publishing Corporation. All rights reserved.

This is a special issue published in “BioMed Research International.” All articles are open access articles distributed under the Creative Commons Attribution License, which permits unrestricted use, distribution, and reproduction in any medium, provided the original work is properly cited.

Contents

Bioarcheology: Medicine, Biology, and Forensic Sciences, Otto Appenzeller, Timothy G. Bromage, Rabab Khairat, Andreas G. Nerlich, and Frank Jakobus Rühli
Volume 2015, Article ID 671206, 2 pages

Paleopathology and Nutritional Analysis of a South German Monastery Population, Andreas G. Nerlich, Alfred Riepertinger, Ralph Gillich, and Stephanie Panzer
Volume 2015, Article ID 486467, 8 pages

A Systematic Approach to the Application of Soft Tissue Histopathology in Paleopathology, Christina Grove, Oliver Peschel, and Andreas G. Nerlich
Volume 2015, Article ID 631465, 9 pages

New Ancient Egyptian Human Mummies from the Valley of the Kings, Luxor: Anthropological, Radiological, and Egyptological Investigations, Frank Rühli, Salima Ikram, and Susanne Bickel
Volume 2015, Article ID 530362, 8 pages

Modeling Clinical States and Metabolic Rhythms in Bioarcheology, Clifford Qualls, Raffaella Bianucci, Michael N. Spilde, Genevieve Phillips, Cecilia Wu, and Otto Appenzeller
Volume 2015, Article ID 818724, 7 pages

Frozen Mummies from Andean Mountaintop Shrines: Bioarchaeology and Ethnohistory of Inca Human Sacrifice, Maria Constanza Ceruti
Volume 2015, Article ID 439428, 12 pages

Resilience at the Transition to Agriculture: The Long-Term Landscape and Resource Development at the Aceramic Neolithic Tell Site of Chogha Golan (Iran), S. Riehl, E. Asouti, D. Karakaya, B. M. Starkovich, M. Zeidi, and N. J. Conard
Volume 2015, Article ID 532481, 22 pages

The Use and Effectiveness of Triple Multiplex System for Coding Region Single Nucleotide Polymorphism in Mitochondrial DNA Typing of Archaeologically Obtained Human Skeletons from Premodern Joseon Tombs of Korea, Chang Seok Oh, Soong Deok Lee, Yi-Suk Kim, and Dong Hoon Shin
Volume 2015, Article ID 850648, 7 pages

Reconstructing Ancient Egyptian Diet through Bone Elemental Analysis Using LIBS (Qubbet el Hawa Cemetery), Ghada Darwish Al-Khafif and Rokia El-Banna
Volume 2015, Article ID 281056, 7 pages

Invasive versus Non Invasive Methods Applied to Mummy Research: Will This Controversy Ever Be Solved?, Despina Moissidou, Jasmine Day, Dong Hoon Shin, and Raffaella Bianucci
Volume 2015, Article ID 192829, 7 pages

Modeling Metabolism and Disease in Bioarcheology, Clifford Qualls and Otto Appenzeller
Volume 2015, Article ID 548704, 8 pages

Editorial

Bioarcheology: Medicine, Biology, and Forensic Sciences

**Otto Appenzeller,¹ Timothy G. Bromage,² Rabab Khairat,³
Andreas G. Nerlich,⁴ and Frank Jakobus Rühli⁵**

¹New Mexico Health Enhancement and Marathon Clinics Research Foundation, Albuquerque, NM 87122-1424, USA

²Hard Tissue Research Unit, Department of Biomaterials & Biomimetics, New York University College of Dentistry, New York, NY 10010-4086, USA

³Department of Medical Molecular Genetics, Division of Human Genome and Genome Research, National Research Center, Cairo, Egypt

⁴Section of Paleopathology, Pathology Institute, Klinikum München-Bogenhausen, Munich, Germany

⁵Institute of Evolutionary Medicine, University of Zurich, 8057 Zürich, Switzerland

Correspondence should be addressed to Otto Appenzeller; ottoarun12@aol.com

Received 2 July 2015; Accepted 2 July 2015

Copyright © 2015 Otto Appenzeller et al. This is an open access article distributed under the Creative Commons Attribution License, which permits unrestricted use, distribution, and reproduction in any medium, provided the original work is properly cited.

Bioarcheology is the study of archived human and animal remains. The term was first proposed by the British archaeologist Grahame Clark to denote the investigations of animal bones from archeological sites. Since its introduction in 1972, this term has been applied to encompass additional scientific domains and has also been used for the multidisciplinary papers collected in this special issue.

Agriculture's first appearance on the archeological horizon is a matter of debate. Evidence provided by multidisciplinary studies encompassing archaeobotany and zooarchaeology and the emergence of agricultural practices in the "fertile crescent" (a crescent shaped area containing fertile lands amidst semiarid regions of Western Asia, the Nile valley, and northeast Africa) in Iran add to the science of ancient agriculture (S. Riehl et al.).

Egyptian archeology has been a widely accepted aspect of bioarcheology. Here a wealth of information has been collected with the applications of new techniques to ancient tissues such as X-ray analyses applied in the field to archived human bones (F. Rühli et al.).

Mandibles excavated from Qubbet el-Hawa cemetery in Aswan, Egypt, have yielded information on the food consumed by middle class people during several periods of ancient Egyptian history. The elemental analysis of the bones hinted at social and climatic changes affecting ancient

populations and shows the effects of state socialism (a variant socialism in which the power of the state is employed to creating an egalitarian society through the control of production of all goods) and agricultural conditions during the 17th Dynasty in Upper Egypt (G. D. AL-Khafif and R. El-Banna).

South American frozen mummies from mountain tops of the high Andes have only recently become available for bioarcheological studies. Such studies have revealed important aspects of human sacrificial practices in pre-Hispanic times. Because of the exceptional preservation of the soft tissues of these mummies due to the intense cold and ambient dryness at altitudes at which they were found, important human pathologies accompanying life under Inca rule have become accessible to modern techniques (M. C. Ceruti).

The histology of soft tissues is a well-accepted diagnostic method in modern human pathology. However, its application to ancient tissues brings challenges to the standard interpretation of histological stains because of the variable preservation of specimens depending on numerous unforeseeable factors. The postmortem interval before histological study is one crucial obstacle. The longer this time the less dependable the results. Paleopathological examinations provided guidelines to the tissues likely to be best preserved and allowed the most reliable diagnoses (C. Grove et al.).

Successful and cheap methods recently developed for the extraction of ancient DNA (aDNA) have led to important studies in evolution and worldwide human migrations. East Asian mitochondrial DNA (mtDNA) especially of Koreans has been used to determine single nucleotide polymorphisms in mtDNA in human bone samples from premodern Joseon tombs in Republic of Korea (C. S. Oh et al.).

Archeological materials useful for the study of bioarcheology are conserved in museums throughout the world. Curators prefer the study of their collections by noninvasive methods. The desire to maintain specimens intact is shared by bioarcheologists too. Nevertheless, invasive methods such as autopsies, endoscopies, and biopsies are sometimes unavoidable for accurate diagnosis. In this setting controversies are unavoidable but scientific criteria coupled with ethical considerations are proposed which may resolve disputes (D. Moissidou et al.).

Monastic inhabitants of ancient institutions provide fertile grounds for the investigations of diseases and social aspects of a particularly privileged population. Regional differences are not often revealed but when such studies are restricted to defined populations such as those in Bavaria, Germany, insights into paleopathology, nutrition, and lifestyles of a well-defined human group become apparent (A. G. Nerlich et al.).

Statistical modeling has advanced science in general and bioarcheology in particular. Growth lines in archived biological materials such as teeth and hair proved valuable in providing evidence of metabolic health, physiology, and lifestyles of long dead individuals. Thus new noninvasive methods for the analyses of curated archeological specimens could avoid ethical consideration in bioarcheological investigations (C. Qualls and O. Appenzeller).

Computational methods could also predict the physical appearance, mood, and clinical diagnosis such as hirsutism (excessive hair growth) also known in some individuals as Cantú syndrome (C. Qualls et al.).

Recent massive sequencing of ancient DNA has transformed the study of human evolution and human history. Such studies are only now beginning in bioarcheology but important insights into modern diseases are likely to be gleaned from analyses of bioarcheological specimens.

Acknowledgment

We are grateful to the New Mexico Health Enhancement and Marathon Clinics Research Foundation for financial support.

*Otto Appenzeller
Timothy G. Bromage
Rabab Khairat
Andreas G. Nerlich
Frank Jakobus Rühli*

Research Article

Paleopathology and Nutritional Analysis of a South German Monastery Population

Andreas G. Nerlich,¹ Alfred Riepertinger,¹ Ralph Gillich,¹ and Stephanie Panzer^{2,3}

¹*Division of Paleopathology, Institute of Pathology, Academic Clinics München-Bogenhausen and München-Schwabing, 81925 Munich, Germany*

²*Department of Radiology, Murnau Trauma Center, 82418 Murnau am Staffelsee, Germany*

³*Biomechanics Laboratory, Paracelsus Medical University Salzburg at the Murnau Trauma Center, 82418 Murnau am Staffelsee, Germany*

Correspondence should be addressed to Andreas G. Nerlich; andreas.nerlich@extern.lrz-muenchen.de

Received 16 December 2014; Accepted 27 April 2015

Academic Editor: Ronald L. Klein

Copyright © 2015 Andreas G. Nerlich et al. This is an open access article distributed under the Creative Commons Attribution License, which permits unrestricted use, distribution, and reproduction in any medium, provided the original work is properly cited.

The monastery of Attel, Upper Bavaria, which was founded in AD 1030, harbours a series of crypt burials from the time period between AD 1700 and 1750. Due to a restoration of the church, 16 crypts had to be removed and were subjected to an extensive anthropological-paleopathological and isotope analysis. The 16 crypts contained 19 burials in open wooden coffins. All bodies were covered by an extensive layer of calcium carbonate. Despite this “treatment,” bone and teeth were excellently preserved (mean degree of conservation > 75%, completeness > 85%). The anthropological investigation revealed a mean age of 38.5 years and a body height of 1.71 m. Paleopathologically, a surprisingly high rate of trauma was seen (13 injuries in 7 different individuals, i.e., 36.8% of individuals affected), 2 cases presented signs of extensive arthritis urica (gout), and several monks were affected by arthrosis of shoulder and knee joints. Extensive dental attrition, numerous foci of dental caries, and dentogenic abscesses coincided with considerable dental calculus indicating poor oral hygienic conditions. Stable isotope analysis showed adequate mixed carnivore-herbivore nutrition, comparable to that of contemporaneous upper class individuals. This extensive combined analysis provides considerable insight into the nutrition and disease pattern of a middle-class monastery of early 18th century South Germany.

1. Introduction

Most paleopathologic studies analyze human remains from defined spatial and temporal settings and try to deduce certain aspects of living conditions and diseases within this population. Surprisingly little attention is paid to selected populations, such as monasteries [1].

Monks represent a particular part of any past or present population. This holds true for various time periods and regions, although historic (mainly literary) evidence suggests differences in tasks, structure, and living conditions between various monasteries. Therefore, the multidisciplinary analysis of the human remains of monastery populations is of major interest.

Recent advances have clearly shown that the successful investigation of ancient human remains requires the application of a multitude of analytical techniques, depending on the

available tissue and its degree of conservation, but also on the applicable techniques [2].

The present study was therefore designed to fill part of this gap by an interdisciplinary analysis of a population of very well-preserved skeletons from a South German “middle-class” monastery of a distinct time period between 1700 and 1750 AD. Since some of the individuals could be identified, the available monastery archive [3] helped us to reconstruct even individual disease histories.

2. Material and Methods

In this study, we investigated the human remains from 19 individuals that have been recovered during a renovation project of the crypt of the monastery church of Attel. This small monastery which was founded in the year 1037



FIGURE 1: The monastery of Attel, Upper Bavaria, in 1700 (image: collection A. Nerlich).

AD, destroyed in 1070 AD, and reopened in 1110 AD was continuously inhabited until the year 1803 AD (when all monasteries in Bavaria were closed due to secularization). It is located on the banks of the river Inn (Figure 1). Although the monastery was repeatedly damaged by flooding of the river Inn, this site was also advantageous for economic reasons, since the river provided a good opportunity as an efficient transport route for various goods. Accordingly, the written records document a moderate wealth of the monastery for several centuries. Besides the danger of flooding by the river Inn, recurrent warfare endangered the monastery for several times, such as what happened during the Thirty Years' War. However, in the period of "our" monastic population (i.e., between AD 1700 and 1750), there is no record of such an event. Accordingly, at this period, economy seems to have been stable and the support of monks and both employed and dependent people of the monastery should have been sufficiently good [3].

The records of the monastery, recently worked up into a large monograph [3], not only provide insight into the organization of daily life and the economic development but also give some detailed data on individual persons within the monastic community, including names, age at death, and function within the community, and also some hint on distinct diseases in certain individuals and eventually their cause of death. The burial place in the monastery church is below the church's altar and was reserved for monks. The crypt consists of 40 burial chambers that had been closed by brick walls. Although we assume that all chambers initially carried the names of the buried person, only a few of these inscriptions have been retained until today.

Since that church was completely renovated at the end of the 17th century, the burials cover a time period between approximately 1700 and 1750 AD, with later burial (i.e., after 1750 AD) having been performed on the newly formed cemetery close to the church. In this study, we only had access to 16 chambers which had to be removed for structural problems of the church, while the other 24 chambers remained unopened. On the wall of 4 of the chambers under investigation, an identification tag was present; 2 further individuals could be identified according to their precise location in one of the untagged chambers. All residual individuals remained unidentified.

After opening of the 16 burial chambers, all material was removed, prescreened into those residues of the (exclusively wooden) coffins, remains of clothes and grave goods, such as rosaries and crucifixes, cloths, and leather shoes, and the human remains. The open wooden coffins were mostly covered by large amounts of a whitish crumbly material that proved to be calcium carbonate and had obviously been used to "preserve" the cadavers and to avoid the undesired bad smell of the decomposing corpses following the burial. Despite this "treatment," the skeletal elements (and teeth) proved to be well preserved. Soft tissue and hair, however, were present only very occasionally.

2.1. Evaluation of the Tissue Material. In the first step, all human biomaterial was cleaned, registered, and evaluated according to the presence of the skeletal elements (termed "representativity") and the conditions of the bone substance ("preservation"). In order to standardize, we used the previously developed and applied scheme that covers 40 regions of the human skeleton and evaluates the presence of the respective skeletal material (0–40 points) and the condition of the bone (0–126 points) with low figures indicating an absent or very fragmented skeleton and an extremely poorly conserved bone substance, respectively [4]. In contrast, high figures indicate the presence of all/most skeletal elements and good/excellent preservation of the bone substance, respectively. This system has previously been successfully applied to other small skeletal series [5].

2.2. Anthropological Investigation. Following the above indicated evaluation, an anthropological survey of the bones provided data on sex, age at death, body height, and physiological characteristics of the individuals. Likewise, individual gender was determined on the pelvic suture and skull bone characteristics; age at death was calculated from skull bone sutures, symphyseal surface, and the ossification pattern of the first costosternal joints. Body height was estimated from the length of long bones according to established protocols. Physical properties, such as handedness, mobility pattern, and development of skeletal musculature, were determined from bone measurement ratios and extent of muscular insertion zones on long bones [6, 7].

2.3. Paleopathological Analysis. Features of pathological conditions were also determined as shown in previous studies, including sequels of trauma, chronic metabolic deficiencies, and dental pathology. Degenerative diseases of large joints and the vertebral column were evaluated using established criteria and standardized protocols [8].

2.4. Radiological Investigations. In order to enhance the paleopathological diagnostics, we performed X-rays and/or CT scans on isolated skeletal elements. Here, again, previous protocols were followed and the technical details of the analysis are given in [2].

2.5. Stable Isotope Analyses. For the investigation of the nutritional composition of the investigated individuals, we used standard bone samples from vertebral bodies of all



FIGURE 2: The skeleton of Gregorius Lechner (number 6) following removal from the burial chamber and cleaning. The skeleton is almost complete; the bone substance is excellently preserved.

identified persons. The analysis of nitrogen and carbon isotopes was performed according to established protocols [9]. Stable isotope analysis and concentration measurements of nitrogen and carbon were performed using ratio mass spectrometry (IsoAnalytical, Crewe, UK) as previously described in detail [2].

3. Results

3.1. Macroscopic and Anthropological Findings. In the 16 burial chambers, we were able to identify 19 individuals with double burials in 3 of the chambers. Generally, all bones were good to excellently preserved (Figure 2). The scoring of bone tissue preservation revealed values between 75 and 100% of maximum values (between 32 and 40 maximal points, average 81.9%). In parallel, the extent of skeletal representativity was also in most cases considerably high again reaching between c. 80 and 100% of maximum values (between 95 and 126 points of maximum 126 points, average 89.2%).

All individuals showed skeletal features of male persons. Most of them died in the 4th to 6th decade of age with

2 monks dying between 20 and 30 years, 7 individuals between 30 and 40 years, 6 persons between 40 and 50 years, and two cases reaching 50 to 60 and further two cases showing more than 60 years of age (on the average of 38.5 years). This age distribution correlates very well with the values that can be retrieved from written sources [3]. In a detailed evaluation, most monks died in the period between 1700 AD and 1750 AD at the age between 40 and 60 years and the resulting distribution curves are quite similar between the overall population of 37 Attel monks and the 19 individuals that we investigated. Furthermore, 6 persons were identified by either the inscriptions on the burial chamber walls and/or the written records. The anthropological age estimation correlates very well with the written data ($r = 0.88$).

Finally, certain physical properties could be identified. The body height ranged between 1.67 m and 1.78 m (on the average of 1.71 m) which is well above the values in various 18th to early 19th century populations in Southern Bavaria and neighbouring Austria where the average body height in males ranges at 1.62–1.64 m [10–12].

The determination of osteometric indices provides evidence for right handedness in 11 monks and left handedness in 7 persons. The mobility index (index platycnemius) reveals low mobility ratios (stenomeric). The muscular insertion zones were in all 19 individuals not significantly prominent and confirmed low physical activity profiles.

3.2. Paleopathologic Investigation. In 7 of the 19 individuals, the sequelae of trauma could be identified (36,8%). Some cases presented with multiple lesions which thereby summed up to 13 trauma lesions in those 7 affected individuals.

These comprised one case with a large skull defect. This unique finding strongly suggests an attack with a sharp weapon such as a sword blow that had removed an almost 15×6 cm large piece of bone out of the temporoparietal region. This diagnosis is based on the lack of any adequate piece of bone in the skull region of the individual. In consequence, the piece of bone must have been removed from the skull before burial; that is, we see a premortem removal of that piece of bone. Furthermore, the dark brown colouring of the cutting margin indicates an “old” lesion, obviously occurring in previous time. Finally, the cut surface at the high parietal margin runs from the external bone table (tabula externa) to the internal layer of bone, while the margin at the lower temporal margins runs in the opposite way (Figure 3(c)), fitting best with a sharp weapon blow downwards. In summary, these findings strongly argue for an “old,” presumably perimortem, defect with typical cutting margins of a violent attack. This is also consistent with a perimortem time course, since the defect margins did not show active bone remodelling reaction (resorption and/or new bone formation) on X-rays and CT scans. This suggests a terminal and potentially lethal trauma (Figures 3(a) and 3(b)).

In 3 cases, multiple old-healed fractures of several ribs were seen, in one case together with an also healed clavicle fracture suggesting massive trauma, for example, from falling from considerable height onto the thorax. In all cases,

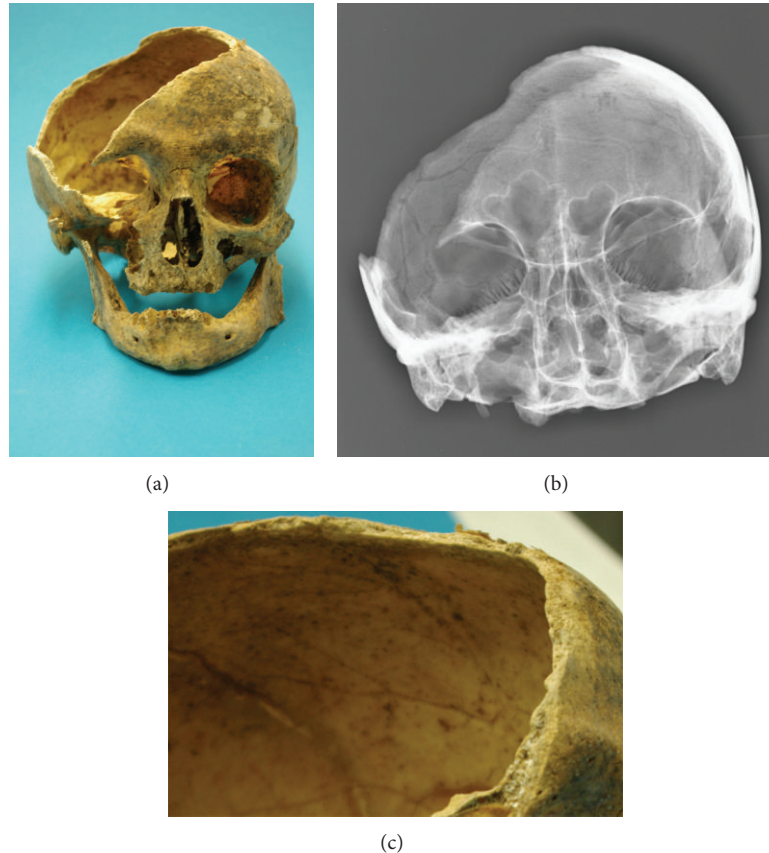


FIGURE 3: Massive defect of the skull bone suggesting severe trauma. The morphology indicates a massive attack by a sharp weapon, for example, a sword blow, without any bone reaction (a: macroscopy; b: radiology). A detailed aspect of the cut margin at the upper (temporal) skull bone (c) showing the brown colouring of the cut surface which runs from the outer table tangentially to the inner table such as in a sharp weapon blow.



FIGURE 4: Old-healed fracture of the clavicle with fusion of the dislocated fracture ends.

there were clear signs of new bone formation and callus-like bridging reaction of the defect zone. Further two cases revealed isolated healed clavicle fractures (Figure 4), one further case had an old-healed distal fracture of the radius, one case had a healed compression fracture of the right femoral condyle, and another case showed a torsion fracture of the ventral rim of the cervical vertebral body C7 without healing signs. Finally, 2 metacarpal bones had been fractured with extensive pseudoarthrosis and bone reaction and in two cases a complete unilateral fusion of the ileosacral joint suggests potential old-healed pelvic trauma.

In contrast to this high number of trauma residues, we had no case with cribra orbitalia (as a sign for chronic iron-deficiency and anemia) nor for chronic vitamin C-deficiency

(scurbut). One individual presented with slight to moderate bowing of several long bones such as in mild infantile/juvenile rickets and one monk (of c. 30–40 years of age) showed a moderate loss of bone substance indicating osteopenia which is most presumably the result of prolonged vitamin D deficiency (osteomalacia) at that age.

Despite this very low number of metabolic osteopathies, 2 monks revealed the very typical signs of chronic hyperuricemia (gout) as evidenced from massive bilateral osteolytic destruction of the first metatarsophalangeal joint which was confirmed by typical intraosseous lytic lesions on X-rays and CT scans of the affected bones (Figure 5). In both cases, we were able to identify the respective historic person and were able to correlate the paleopathological findings with corresponding evidence from the written sources that had indicated chronic gout in both persons.

These two persons are here briefly described in more detail.

Gregorius Lechner (cf. Figures 2 and 5) was born on 25/02/1672 in a small Upper Bavarian village. He took his vows at the age of 23 and the ordination of priesthood at the age of 26 years. At the age of 41, he was designated the “Oeconomus major”; that is, he was responsible for all external economic transactions of the monastery. He was said to be of “weak healthiness” suffering from chronic gout and dropsy.

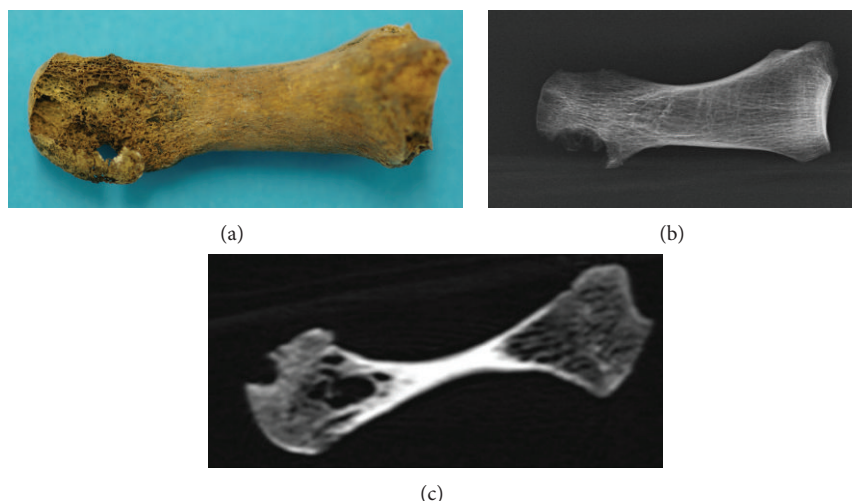


FIGURE 5: Severe osteolysis of the metatarsophalangeal joint in Gregorius Lechner indicating severe chronic gout (a: macroscopy; b: X-ray; c: CAT-scan).

At the age of 60, he died of both conditions. On paleopathological investigation, the most impressive finding was a severe bilateral arthritis urica of both first metatarsophalangeal joints, which was supplemented by a slight spondylosis of the lumbar spine, moderate osteoarthritis of both shoulder joints, and severe arthrosis of both femoropatellar joints suggesting frequent and extensive kneeling position such as in frequent praying. Finally, significant oral pathology presented with extensive dental calculus formation and severe parodontosis, one apical dental abscess, and moderate dental abrasion.

The second affected individual, Bernhardus Veldhofer, was born on 17/11/1683 in the small town of Erding which is approximately 30 km from Attel monastery. He entered the monastic society at the age of 14 years and took his vows on 11/11/1706. Four years later he received the ordination as a priest. Having served first as a keeper of the monasteries gate, he rapidly proceeded to become the organizer of pilgrimages and was involved in the daily religious services for the surrounding rural population. The records describe him to be of weak health finally developing gout and dropsy which also were regarded as cause of death. He died on 24/5/1731 at the age of 48 years. The paleopathologic examination again revealed the very typical signs of gout with massive destruction of the first metatarsophalangeal joints such as seen in the skeleton of Gregorius Lechner. As the second most extensive pathology, the dental apparatus was affected with multiple teeth having been lost intravitaly, two teeth with significant dental caries, and a large dentogenic abscess at the 26/27 region (upper left maxilla/teeth number 6 and 7) extending into the adjacent maxillary sinus and causing major remodelling of the osseous floor of this paranasal sinus. There was no evidence for major degenerative lesions of major joints or the vertebral column and also no signs of any other chronic disease affecting the skeleton nor any trauma sequelae.

The analysis of degeneration of large and small joints and that of the vertebral column revealed in several cases mild to moderate osteoarthritis in the right shoulder joint and

in both knee joints (according to the evaluation scheme by Schultz [8] average shoulder joint right 1.42 points versus left 0.89 points and right knee joint 1.24 points and left knee joint 1.38 points; all other values below 1). In parallel, the vertebral bodies (including the small facette joints) showed degeneration values ranging from 1.08 to 1.29 in the lumbar spine and from 0.43 to 0.92 points in the cervical and thoracal spine. Additionally, two cases presented with osteochondrosis dissecans of the knee joint.

As already indicated before, dental pathology was extensively present with moderate to severe dental abrasion, multiple cases with dental caries, and apical dental abscesses and also numerous cases with extensive dental calculus formation. As expected, those cases with dental calculus had lower frequencies of dental caries/dental abscesses and vice versa. The loss of teeth during lifetime was also a frequent event with only 4/19 cases without intravital dental loss and 5/19 cases with loss between 1 and 4 teeth, 3 cases between 5 and 9 teeth, 4 cases between 10 and 15 teeth, and 2 cases with a loss of more than 15 teeth (one with complete loss of dentition intravitaly).

3.3. Stable Isotope Analyses. In order to further evaluate the nutritional status of this monastery population, we determined the ratios of stable nitrogen and carbon isotopes. As a result, there was a very similar nutritional pattern with nitrogen $\delta^{15}\text{N}$ values ranging between 10.6 and 13.6 and carbon $\delta^{13}\text{C}$ lying between -19.5 and -18.8 . Most cases clustered closely together. Accordingly, the nutritional pattern is that of mixed carnivore-herbivore nutrition with considerable amounts of terrestrial protein and an adequate carbohydrate diet. There was no evidence for any dominant fish consumption. The two individuals with the massive gout were not different from their comonks (Figure 6).

4. Discussion

The circumstantial analysis of distinct past populations offers an excellent insight into ancient living conditions and

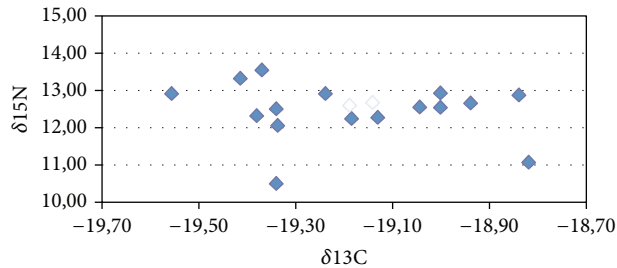


FIGURE 6: Isotopic results of the Attel monastery population. The two cases with paleopathological evidence for gout are indicated in open diamonds.

diseases. To this regard, monastery populations represent a particular setting, as these reveal a selected group of individuals within historic populations.

In our present study, we investigated a series of 19 monks that had lived between AD 1700 and 1750. The anthropological estimation of the age at death very well correlates with the data from written sources providing evidence that our subpopulation may be quite representative for the complete monastic population that lived in the Attel monastery at that time. Furthermore, all individuals investigated proved to be males. These observations strongly support the notion that we investigated the genuine monastic population that has been well documented in written sources [3].

Most interestingly, the physical properties of the individuals showed a tall stature, particularly when compared to 18th-19th century reference populations of Southern Bavaria where the mean body size of males ranged at 1.62–1.65 m [10–12]. Accordingly, a detailed analysis of nonmonastic rural populations in Bavaria/Austria of the 18th/19th century shows lower values than in the Attel population [11, 12]. Even a contemporary Swedish population provides lower mean values (mean 1.67 m [13]) than the Attel monks, although it is well known that the body height in Northern (Scandinavian) individuals was larger than in Southern (Mediterranean) populations with Middle European populations ranging in between [14]. Since the written records indicate that most monks had entered the monastery society at juvenile age, this suggests a good nourishment and avoidance of major consumptive, for example, infectious, diseases during their monasticism. Accordingly, the mean body height in our population can be interpreted to reflect “better” living conditions [14]. However, life expectancy did not differ significantly from other rural populations in Bavaria, Northern Germany, and rural Poland [15–17] possibly due to the enhanced rate of metabolic diseases in the monastic population, for example, by the severe gout. Finally, our observation also very well correlates with the stable isotope values that indicate a balanced diet with sufficient protein supply mainly from animal source and good carbohydrate diet. Despite its close location to the river Inn, the fish consumption may not have dominated their daily food. Well in line with the sufficient food supply is the almost complete lack of metabolic malnourishment diseases, such as *cribra orbitalia* or lack of essential vitamins (see above).

The most interesting, but not surprising, finding is the unambiguous presence of 2 cases with severe chronic hyperuricemia (gout). Both had at least somewhat higher positions within the monastery society (Gregorius Lechner was even “*oconomus major*” which means that he was the “chief” of all economic affairs of the monastery, Bernhardus Veldhofer obtained a less exposed position, but at least he was organizer of the pilgrimages and thereby he also must have had some influence on particular economic business). This suggests that they not only were well-maintained but also may have been subjected to excessive supply of alcohol, meat, and/or the consumption of protein from cell-rich internal organs, for example, liver.

Hyperuricemia is a chronic metabolic disease originating from a disturbance of the metabolism of purines characterized by the accumulation of its end product sodium urate within the body [1]. While a minor proportion of affected patients suffer from an inborn error of metabolism, in most instances hyperuricemia results from an excessive uptake of purines from the nourishment together with an enzymatic blockage of its degradation in the liver by toxic substances, such as alcohol and/or reduced excretion through the urinary system. The enhanced level of urate in the blood stream leads to its deposition in bradytrophic tissue, such as the capsule of peripheral small joints. This deposition occurs in crystal form thereby causing massive resorptive inflammation, with consequently swelling and redness of small joints, such as most preferentially the metatarsophalangeal and interphalangeal joints of the big toes. The chronic form of this condition leads to typical osseous resorption and joint destruction such as seen in our two present cases. The significant destruction of the first metatarsals further indicates that the metabolic condition in both affected individuals had persisted for considerable periods of time [1].

In paleopathology, chronic gout has repeatedly been identified dating back to ancient Egyptian mummies [18] where these findings could even be confirmed by laboratory investigations [19]. Furthermore, isolated cases have been seen in Roman cemetery findings [20] and mediaeval period skeletons [21], in several cases of the famous Medici family [22], but also as isolated findings or very small series in modern Pacific islanders [23]. Blondiaux et al. [24] described a familial accumulation of cases with arthritis urica in several skeletons of a French cemetery between the 7th century and the 18th century suggesting possible genetic links with living conditions in a historical privileged population. The most renowned case of as yet paleopathologically verified gout is Emperor Charles V [25]. The investigation of one of his fingers provided circumstantial evidence for gout.

In general, however, there exist neither data on the prevalence of this disorder in antiquity, nor on its occurrence in specific populations such as monastic inhabitants although written sources suggest that gout was very frequent in history [26]. To this regard, our present analysis adds to the previous knowledge, since the observed severe gout in two persons with documented gout.

Besides these two cases with gout, we surprisingly found a high number of individuals with trauma sequelae with at least several cases typical for more or less massive trauma,

such as falling from considerable height, but also minor trauma leading to broken metatarsals, and/or trauma from significant interpersonal conflict, such as a sharp weapon attack to the skull in one monk. These high figures highlight the dangerous daily life even within the monastic society, be it by accidental trauma or conflict situations. Unfortunately, no comparable data are available for any rural population in the region of that time period. However, in other 18th/19th century populations, trauma rates of rural population range up to 50% of individuals [26, 27].

Finally, massive pathology was seen in the dental apparatus with lack of oral hygiene and significant dental abrasion, most presumably by the consumption of food, for example, bread that had been prepared from cereals processed by stone mills. As a consequence, many monks suffered from caries, dental apical abscesses, and/or early intravital loss of teeth. In general, however, the high figures of dental pathology are not surprising in historic populations such as investigated here.

A comparison of the stable isotopic values with those of other historic populations from various regions and time periods indicates a similar level of nourishment between the Attel monks and Bavarian noblemen in terms of composition with adequate supply in terrestrial protein and carbohydrates. This is well in line with the written records that inform us that the Attel monastery of the early 18th century had a good economic basis. Furthermore, during this time we have indication that this economic stability must have not been endangered by warfare; the only major war at that time period was the “War of Spanish Succession” 1701–1714 which, however, did not affect the Attel region, nor by major environmental catastrophes, such as severe flooding by the river Inn.

In summary, our interdisciplinary study provides a further and extended insight into the living conditions of a very specific early 18th century monastic population, a new and profound example for the power of combined multidisciplinary historic studies that bring historic sciences together with natural historic ones.

Conflict of Interests

The authors declare that there is no conflict of interests regarding the publication of this paper.

Acknowledgments

The authors are very indebted to Pater K. Wagner, Katholisches Pfarramt St. Michael Attel, Staatliches Bauamt Rosenheim, Herrn B. Windhör, Bayerisches Landesamt für Denkmalpflege, for the permission to study the material. The initial very valuable help by Martin Bunzel in the preparation of samples for the isotope analyses is acknowledged. Finally, the authors are most thankful for the very helpful suggestions by the two anonymous reviewers.

References

- [1] A. C. Aufderheide and C. Rodriguez-Martin, *Human Paleopathology*, The Cambridge Encyclopedia, Cambridge University Press, Cambridge, UK, 1998.
- [2] S. Panzer, O. Peschel, B. Haas-Gebhard, B. E. Bachmeier, C. M. Pusch, and A. G. Nerlich, “Reconstructing the life of an unknown (ca. 500 years-old South American Inca) mummy—multidisciplinary study of a Peruvian Inca mummy suggests severe Chagas disease and ritual homicide,” *PLoS ONE*, vol. 9, no. 2, Article ID e89528, 2014.
- [3] P. Schinagl, *Die Abtei Attel in der Neuzeit*, vol. 31 of *Münchener Theologische Studien*, EOS, St. Ottilien, Erzabtei, Germany, 1990.
- [4] A. G. Nerlich, A. Riepertinger, R. Gillich, M. Bunzel, and S. Panzer, “Anthropological, paleopathological and istotope analysis of crypt burials,” in *Proceedings of the 10th International Meeting aDNA Research*, Munich, Germany, 2010.
- [5] A. G. Nerlich, “Anthropologisch-paläopathologische Untersuchung der Mumie aus dem Grab 5P12-1,” in *Ein neuartiger Denkmälerkomplex des Mittleren Reiches in Dahschur—Erste Einblicke und Perspektiven der Interpretation*, N. Alexanian, D. Blaschta, and S. Seidlmayer, Eds., SDAIK, 2015.
- [6] A. Nerlich, H. Rohrbach, and A. Zink, “Paläopathologie altägyptischer Mumien und Skelette,” *Der Pathologe*, vol. 23, no. 5, pp. 379–385, 2002.
- [7] A. Nerlich, A. Zink, H. G. Hagedorn, U. Szeimies, and C. Weyss, “Anthropological and palaeopathological analysis of the human remains from three ‘Tombs of the Nobles’ of the necropolis of Thebes-west, upper Egypt,” *Anthropologischer Anzeiger*, vol. 58, no. 4, pp. 321–343, 2000.
- [8] M. Schultz, “Paläopathologische diagnostik,” in *Handbuch der Vergleichenden Biologie des Menschen*, R. Knussmann, Ed., vol. 1, pp. 480–496, Schattauer, Stuttgart, Germany, 1988.
- [9] T. C. O’Connell and R. E. M. Hedges, “Isotopic comparison of hair and bone. Archaeological analyses,” *Journal of Archaeological Science*, vol. 26, no. 6, pp. 661–665, 1999.
- [10] J. Ranke, “Zur statistik und physiologie der körpergrösse der bayerischen militärpflichtigen,” in *Beiträge Zur Anthropologie Und Urgeschichte Bayerns*, vol. 4, Ulan Press, 1880.
- [11] J. Komlos, *Nutrition and Economic Development in the Eighteenth Century Habsburg Monarchy. An Anthropometric History*, Princeton University Press, Princeton, NJ, USA, 1989.
- [12] J. Komlos, “Modernes ökonomisches Wachstum und der biologische Lebensstandard,” in *Wirtschafts- und Sozialgeschichte—Gegenstand und Methode*, E. Schremmer, Ed., pp. 165–198, Steiner, Stuttgart, Germany, 1997.
- [13] L. G. Sandberg and R. H. Steckel, “Heights and economic history: the Swedish case,” *Annals of Human Biology*, vol. 14, no. 2, pp. 101–110, 1987.
- [14] R. Steckel, “Stature and the standard of living,” *Journal of Economic Literature*, vol. 33, pp. 1903–1940, 1995.
- [15] U. Pfister and G. Fertig, “The population history in Germany: research strategy and preliminary results,” MPIDR Working Paper 2010-035, Max-Planck Institute for Demographic Research, Rostock, Germany, 2010.
- [16] M. Luy, *Mortalitätsanalyse in der historischen Demographie*, Verlag Sozialwissenschaften, Wiesbaden, Germany, 2004.
- [17] A. Budnik, G. Liczbińska, and I. Gumna, “Demographic trends and biological status of historic populations from central Poland: the Ostrów Lednicki microregion,” *American Journal of Physical Anthropology*, vol. 125, no. 4, pp. 369–381, 2004.
- [18] G. E. Smith and W. R. Dawson, *Egyptian Mummies*, G. Allen Unwin, London, UK, 1924.
- [19] J. T. Rowling, “Pathological changes in mummies,” *Proceedings of the Royal Society of Medicine*, vol. 54, pp. 409–415, 1961.

- [20] C. Wells, "A palaeopathological rarity in a skeleton of Roman date," *Medical History*, vol. 17, no. 4, pp. 399–400, 1973.
- [21] J. Rogers, I. Watt, and P. Dieppe, "Arthritis in Saxon and mediaeval skeletons," *British Medical Journal*, vol. 283, no. 6307, pp. 1668–1670, 1981.
- [22] G. Fornaciari, V. Giuffra, S. Giusiani, A. Fornaciari, N. Villari, and A. Vitiello, "The 'gout' of the Medici, Grand Dukes of Florence: a palaeopathological study," *Rheumatology*, vol. 48, no. 4, pp. 375–377, 2009.
- [23] B. M. Rothschild and G. M. Heathcote, "Characterization of gout in a skeletal population sample: presumptive diagnosis in a micronesian population," *American Journal of Physical Anthropology*, vol. 98, no. 4, pp. 519–525, 1995.
- [24] J. Blondiaux, A. A.-L. Bagousse, X. Demondion, F. Delahaye, and C. Niel, "Maladie hyperostotique et maladie goutteuse, une diathèse familiale en normandie: thaon, calvados," *Bulletins et Mémoires de la Société d'Anthropologie de Paris*, vol. 19, pp. 7–20, 2007.
- [25] J. Ordi, P. L. Alonso, J. de Zulueta et al., "The severe gout of Holy Roman Emperor Charles V," *The New England Journal of Medicine*, vol. 355, no. 5, pp. 516–520, 2006.
- [26] G. Nuki and P. A. Simkin, "A concise history of gout and hyperuricemia and their treatment," *Arthritis Research and Therapy*, vol. 8, supplement 1, article S1, 2006.
- [27] C. M. Court-Brown and B. Caesar, "Epidemiology of adult fractures: a review," *Injury*, vol. 37, no. 8, pp. 691–697, 2006.

Research Article

A Systematic Approach to the Application of Soft Tissue Histopathology in Paleopathology

Christina Grove,¹ Oliver Peschel,¹ and Andreas G. Nerlich²

¹*Institute of Legal Medicine, Ludwig-Maximilians University of Munich, 80336 Munich, Germany*

²*Division of Paleopathology, Institute of Pathology, Academic Clinic Munich-Bogenhausen and Munich-Schwabing, 81925 Munich, Germany*

Correspondence should be addressed to Andreas G. Nerlich; andreas.nerlich@extern.lrz-muenchen.de

Received 19 December 2014; Revised 12 April 2015; Accepted 17 April 2015

Academic Editor: Paolo Fogagnolo

Copyright © 2015 Christina Grove et al. This is an open access article distributed under the Creative Commons Attribution License, which permits unrestricted use, distribution, and reproduction in any medium, provided the original work is properly cited.

The application of histology to soft tissue remains offers an important technique to obtain diagnostically important information on various physiological and pathological conditions in paleopathology. In a series of 29 cases with mummified tissue ranging between 16 months and c. 5.200 years of postmortem time interval, we systematically investigated paleohistology and the preservation of various tissues. We established a reproducible histological ranking system for the evaluation of mummified tissue preservation. The application of this scheme to the series showed good tissue preservation of tissues with high connective tissue content but also fat tissue and connective tissue rich organs, such as lung tissue, while most other internal organs were less well preserved despite highly different postmortem time intervals. There are some organs with only poor conservation even in short term periods such as the kidneys and CNS. Artificial mummification does not provide better conservation than naturally mummified tissues; “cold” mummies may be much better conserved than those from desert areas. The identification of specific pathologies underlines the potential power of paleohistology.

1. Introduction

“Some human diseases can be diagnosed from ancient skeletal tissue, but a much greater number can be discovered by examination of preserved soft tissues.” This statement by Aufderheide [1] from 2000 still holds very true and reflects a paradigm of modern paleopathology. Although used since very long times in paleopathology, soft tissue histopathology has only been applied in few instances. Nevertheless, some of the very first paleopathologic mummy studies provided conclusive results due to histopathology, for example, in the diagnosis of schistosomiasis [2]. The subsequent extensive “mummy projects,” for example, the Manchester mummy project [3] or the Philadelphia University mummy project [4], also included histology of soft tissue. Thereby, important data could be retrieved.

Besides the limited source of soft tissue remnants, the lack of a systematic investigation of the application of histology seems to be a limiting factor for the use of soft tissue histology. In the available literature as yet no such study

can be found. In the present study, we therefore performed a dual investigation, with one part covering a systematic investigation on human tissue samples from exhumations of more recent origin and a second part on human mummified tissue of various historic sources covering a wide range of time periods. Although especially the second part is strongly limited by the available tissue (which in turn depends on the accessibility of the tissue of a mummy), this study offers insight into the conservation of tissues under certain “storage” conditions. In summary, our study provides evidence that soft tissue histopathology is applicable to various organ pathologies and that the tissue conservation generally differs between certain organs.

2. Material and Methods

2.1. Material and Samples. The study was conducted on a total of 29 mummies covering a range of time between death and investigation between 1.25 years (yrs.) and c. 5.200 yrs. All

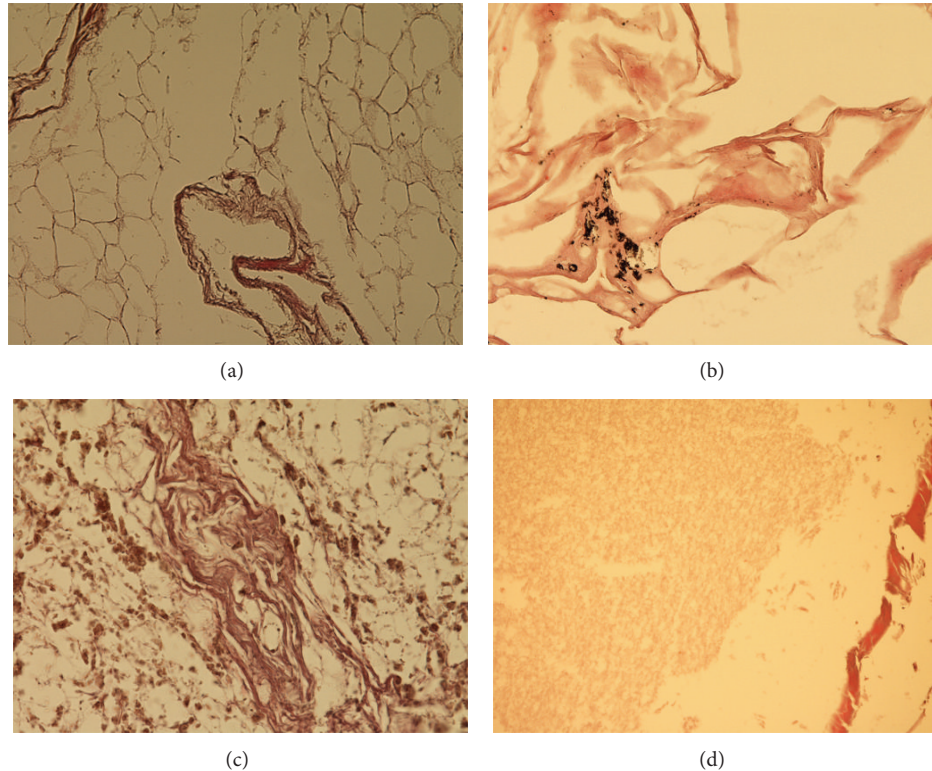


FIGURE 1: Histological features of mummified tissue from individuals with a postmortem time interval between 16 months and c. 5 yrs. (a) Fat and connective tissue (subcutis) from mummy 3 (17 months) showing good conservation of tissue structures despite the loss of cell nuclei. Note the similarly well-preserved small blood vessel. (b) Lung tissue from mummy 7 (18 months). The alveoli are distended, and in the interstitium small deposits of anthracosis pigment prove the pulmonary origin. (c) Liver tissue from mummy 12 (5 yrs.) showing severe postmortem diagenesis of the hepatocytes but retained tissue structure with small portal fields. Note the pigment that proved to be the results of postmortem oxidation products. (d) CNS tissue from mummy 12 (5 yrs.). The structure of the parenchyma has gone lost; on the right side a small sheath of connective tissue indicates the meninges (all examples: original magnification $\times 200$, staining: H&E).

cases were selected due to their good to excellent macroscopic state of conservation.

The study was initially divided into two groups: (i) the first group consisted of 17 complete/near complete mummies of the 19th till the 21st century where we had access to the whole body and were able to perform typical autopsies. (ii) The remaining 12 “cases” were significantly “older” and came from historic individuals of various places and time periods where we had mostly access only to limited material, mostly due to restrictions in the accessibility and in order to remain as little destructive as possible. In 4 of group II specimens, however, several organs were available for investigation, close to the material of group I.

Group I. Twelve of the most recent cases came from the files of the Department of Legal Medicine of the Ludwig Maximilians University of Munich that had been obtained after exhumation for medicolegal reasons between 16 months and 5 years after death with more or less intense natural mummification. Ten cases (with a postmortem time interval between 16 and 19 months) had been autopsied from one cemetery site in Southern Bavaria (Sonthofen) as a result of a homicide series investigation (Figure 1). Unfortunately, in those cases no skin tissue was retained since this seemed to

be not necessary for the forensic examination. Surprisingly, all these cases still presented with extensively preserved soft tissues including internal organs. Two more cases had been autopsied also for medicolegal reasons. One had been found as a naturally mummified corpse 5 years after death in her living apartment; the second case was a crypt burial (Figure 2).

In addition, we were able to investigate a small series of historic mummies of mostly natural mummification processes (except for one child mummy, see below). In this series the mummies came from a South German crypt dating to the post-Napoleonic period (AD 1841–1859) (Figure 3); one artificially mummified infant of that crypt had died in 1816 AD and had been prepared as an artificial mummy. This is described more in detail below.

Group II. These “cases” were significantly older than that of group I; however, in most cases the available samples were much more restricted due to conservatory reasons of the objects. From one young female mummy from South America, dating into the Nazca period between 1451 and 1642 AD [5], soft tissue samples were obtained from skin and the rectal wall. Additionally, three naturally mummified skulls from South American individuals were included dating to

TABLE I: Cases studied and results.

No.	ID	Origin	Age	Sex	Time	Skin	Conn	bl v	Fat t	Lung	Heart	Liver	Kidney	CNS
1	RM-1691	Germany	95	m	16 months	nd	3	3	3	2	2	nd	1	1
2	RM-1479	Germany	93	f	16 months	nd	3	3	3	2	1	nd	nd	1
3	RM-1689	Germany	79	f	17 months	nd	3	3	3	2	2	2	1	0
4	RM-1815	Germany	92	m	17 months	3	3	3	3	2	1	2	nd	1
5	RM-1480	Germany	81	f	17.5 months	nd	3	3	3	2	2	2	2	1
6	RM-1687	Germany	80	f	17.5 months	nd	2	3	3	nd	nd	2	nd	1
7	RM-1485	Germany	92	m	18 months	nd	3	3	2	2	1	nd	nd	nd
8	RM-1813	Germany	88	f	18 months	nd	3	3	3	2	2	2	2	1
9	RM-1811	Germany	82	f	18.5 months	nd	3	3	3	2	1	2	1	1
10	RM-1484	Germany	82	m	19 months	nd	3	3	3	2	2	2	2	0
11	RM-2418	Germany	78	f	5 yrs.	3	3	3	3	2	1	1	0	0
12	Path-12036	Germany	68	m	36 yrs.	2	3	3	3	2	2	1	nd	1
13	Wack-5	Germany	76	f	155 yrs.	2	3	3	3	2	1	1	1	0
14	Wack-4	Germany	88	m	163 yrs.	2	3	3	3	2	1	1	0	0
15	Wack-3	Germany	32	m	164 yrs.	2	3	3	3	2	2	1	1	1
16	Wack-2	Germany	69	m	173 yrs.	2	3	3	3	2	2	2	1	0
Gr. I	Mean value					2,3	2,9	3	2,9	2	1,5	1,6	1,1	0,6
	2SD					0,1	0,1	0	0,1	0	0,4	0,3	0,4	0,2
17	Wack-1*	Germany	1	f	198 yrs.	4	4	4	4	4	4	4	4	3
18	BSAM	Peru?	20–25	f	370–560 yrs.	2	3	3	3	nd	nd	nd	nd	nd
19	LT-15-465	Peru	30–40	f	c. 1.650 yrs.	2	3	3	2	nd	nd	nd	nd	nd
20	CAH-331	Peru	60–70	m	c. 1.650 yrs.	3	3	2	2	nd	nd	nd	nd	1
21	CAH-427	Peru	20–30	f	c. 1.650 yrs.	2	2	2	3	nd	nd	nd	nd	1
22	TT-95-2	Egypt	50–60	f	c. 2.700 yrs.	2	3	3	2	nd	nd	nd	nd	nd
23	ÄS-12d	Egypt	20–40	m	c. 2.900 yrs.	2	2	2	2	2	1	2	nd	nd
24	DAN-95-21	Egypt	40–60	m	c. 2.900 yrs.	2	2	3	2	nd	2	nd	nd	nd
25	TT-95-22	Egypt	20–30	f	c. 3.000 yrs.	3	3	3	3	3	3	3	nd	nd
26	TT-183-4	Egypt	20–40	m	c. 3.200 yrs.	2	2	2	2	nd	nd	nd	nd	nd
27	TT-84-18	Egypt	20–30	m	c. 3.200 yrs.	2	3	2	2	2	nd	nd	1	nd
28	DAN-02-5	Egypt	20–30	f	c. 3.900 yrs.	nd	2	nd	nd	3	nd	nd	nd	nd
29	Ötzi	Alps	35–45	m	c. 5.200 yrs.	3	3	3	3	nd	nd	nd	nd	nd
Gr. II	Mean value					2,2	2,6	2,5	2,4	2,5	2	2,5	1	1
	2SD					0,1	0,3	0,2	0,2	0,4	0,5	0,5	0	0

nd: not determined.

* Artificially mummified mummy; this case was not included in the statistical calculations of groups I and II.

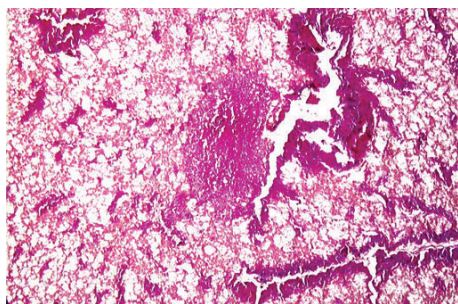


FIGURE 2: Liver tissue from the (natural) crypt mummy 12 (36 yrs.). Despite significant diagnosis here again the liver structure is retained by the presence of portal fields. In the center a nodular formation indicates the remnants of a tumor nodule (diagnosis: metastatic carcinoma) (original magnification $\times 100$, H&E).

c. 350–500 AD [6] (Figure 4). Furthermore 7 human mummies came from ancient Egypt (c. 1900–700 BC) [7, 8] (Figures 5 and 6) and several soft tissue samples were available for this study from the Neolithic glacier mummy “Ötzi” (c. 3.200 BC) [9, 10] (Figure 7). In four of the ancient Egyptian cases we had been able to perform more extensive analyses, since several internal organs had been preserved as organ packages within the body cavities or in adjacent Canopic jars providing access to comparable tissue types than in group I (Figures 5 and 6). Detailed information on the material and the underlying cases is summarized in Table 1.

The material had been obtained from autopsies or small local tissue excisions and covers in most cases (at least in group I) several organs from different regions of the body that had been identified by macroscopy. In some cases (group II),

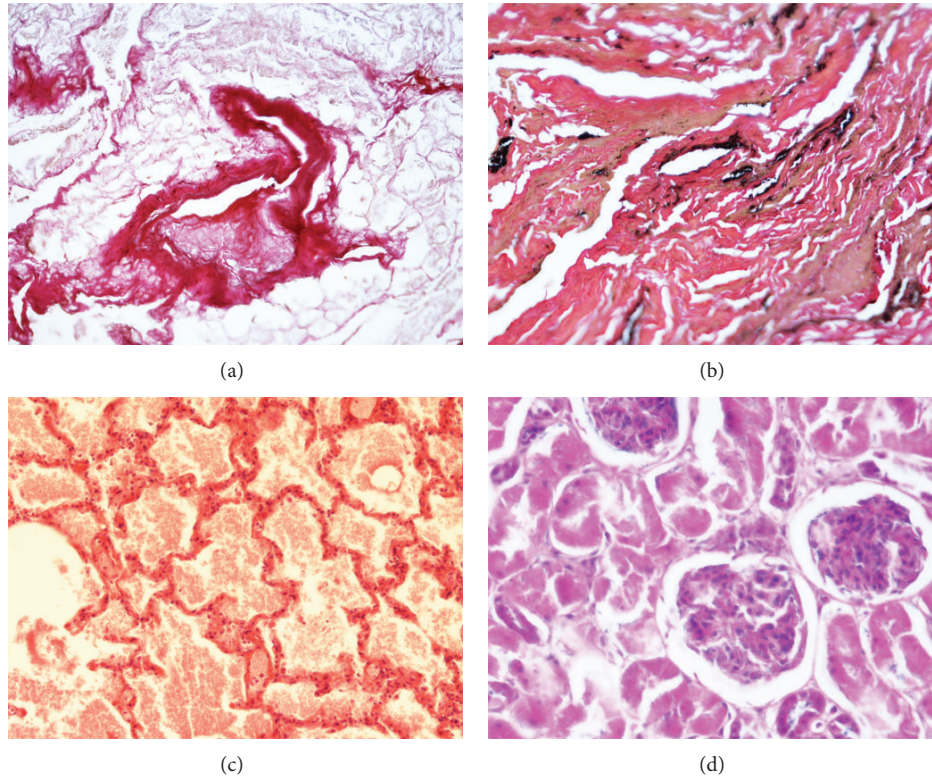


FIGURE 3: (a) A natural mummy from a German crypt of AD 1851 (14, 163 yrs.). The soft tissue is in a very well conservation status with fat cell residues and a small arteriolar blood vessel (center). (b) Lung tissue from mummy 14 with collapse of the air spaces, abundant anthracosis pigment, and small residues of a proteinaceous exudate (obviously remnants of a lung edema). (c) The artificially mummified infant 17 (198 yrs.) shows extremely well-preserved tissue structures of the lung, again with extensive residues of a (terminal) pulmonary edema. Here, the artificial conservation even has retained cell structures! (d) A section of kidney tissue from mummy 17 again with excellently preserved tissue structures as visible from glomeruli and residues of tubuli (original magnification $\times 200$; ((a)–(d)) H&E).

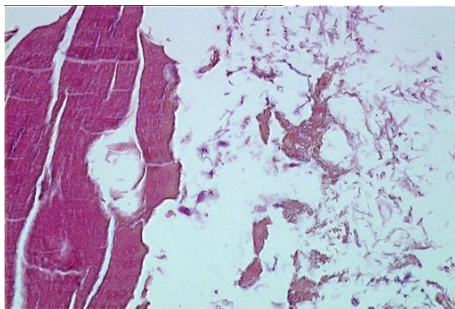


FIGURE 4: Soft tissue from the mummy skull 21 (c. 1.650 yrs.) showing a broad connective tissue plate (left) and fat tissue (right) with central extensions of a fresh perimortal bleeding (original magnification $\times 200$, H&E).

only isolated organs could be identified by macroscopy due to their position within the body and/or their morphology, while other internal organs obviously had disappeared or were not accessible without major destruction of the mummy. In the South American mummy skulls [6] and in the Neolithic Iceman [9, 10], only small samples from skin and subcutaneous soft tissues were available, but with no internal organs.

2.2. Tissue Processing. In order to be able to perform histology, the dry and brittle mummy tissue has to be rehydrated. This procedure is highly critical for the further processing of the material and seems to be crucial for the tissue preservation. The samples were generally prepared according to the technique described by Ruffer in 1909 [11] with slight modifications. Briefly, the samples were immersed into a solution composed of 2–4% formaldehyde solution, pH 7.4, supplemented with 5% sodium carbonate. The sample was gently shaken for 12–16 hours in order to ensure optimal penetration of the solution into the material. After this time period the solution was replaced by 4–6% formaldehyde, pH 7.4 without any further addition for another 12–16 hours (postfixation).

The rehydration procedure is very critical for the result. In general, only in a part of cases a successful rehydration is possible. As yet, there exists no indicator that may help to discriminate between both possibilities.

The organs of the artificial infant mummy (“Wack-1”) had not to be rehydrated, since those internal organs had been stored for 200 years in ethanol. In this case, however, skin and soft tissues had to be rehydrated and these were treated as in the other specimens. The samples of the Neolithic cold mummy Ötzi were treated as those of the other specimens.

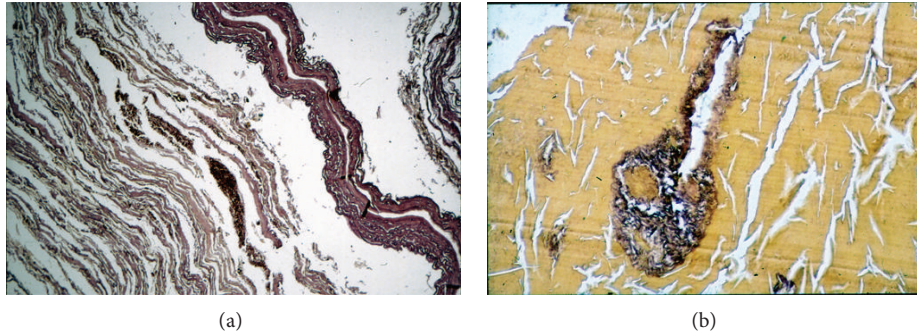


FIGURE 5: Ancient Egyptian mummy 23 (c. 2.900 yrs.) soft tissue histology. (a) Lung tissue sample showing a major blood vessel (upper part) and collapsed alveoli (lower part). Between the alveoli small deposits are seen that proved to be older bleeding residues due to a parasitic pulmonary infection. (b) Liver tissue from mummy 23 with excellently preserved portal fields (center) and the residues of the surrounding parenchyma (original magnification: (a) $\times 100$, (b) $\times 200$; (a) H&E; (b) van Gieson connective tissue stain).

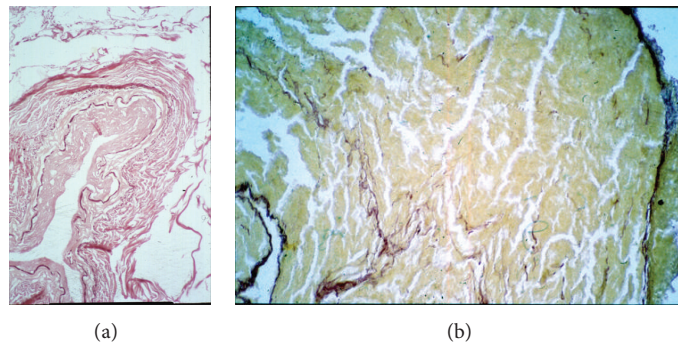


FIGURE 6: Ancient Egyptian mummy tissue from case 24 (c. 2.900 yrs.). (a) A small coronary artery shows significant intimal arteriosclerotic thickening. Note the excellently preserved internal elastic lamina. (b) Myocardial tissue with tiny connective tissue sheaths between the residues of the cardiomyocytes (original magnification: $\times 200$; Elastica-van Gieson stain).

Following rehydration and fixation, mostly the fixation fluid had turned (dark) brown indicating that the solution contained oxidation products that have been removed from the tissue. Poorly conserved tissue may completely be dissolved and “disappear.” Subsequently, the now rehydrated material is further processed as routinely done in a modern histopathology laboratory. It is finally embedded into paraffin wax.

From the paraffin blocks thin sections of 2-3 μm thickness are cut and stained with various routine stainings, including haematoxylin and eosin (HE), van Gieson’s connective tissue stain, PAS-stain, Prussian blue staining, and eventually other special stains if required. All detailed staining procedures have previously been described in detail [7, 8].

2.3. Tissue Evaluation. All sections were evaluated by light microscopy as routinely performed. In order to render the observations better comparable, we applied a semiquantitative scoring system with a series of criteria that may help to define the status of the embedded tissue.

These criteria are presented in detail in Table 2 and comprise identification of tissue integrity, presence of characteristic tissue structures or substructures (e.g., cartilage of the bronchial tree in lung samples; typical layering of elastic membranes in arterial/arteriolar blood vessels), presence and

extent of artefacts from preprocessing storage/decay, and staining properties in various routine stainings. In order to render this scoring system less subjective, we defined for each criterium distinct qualitative and whenever possible quantitative aspects that should enable a proper classification. The criteria are described in detail in Table 2. For further evaluation, these criteria were first tested in a subset of 10 tissue sections of the “modern” samples (group I); since this evaluation revealed good applicability, those were applied to all cases in a systematic manner. Finally, the resulting points were added to a specific summation score which was used to classify the conservation status of a sample/organ (Table 3). Generally, this indicates the histologic conservation status into 5 grades (grades 0 to 4, with 0 being the worst and 4 being the best status).

Besides this (semi)quantitative evaluation of the diagnostic features of all tissues/organs present, we recorded pathological findings in a qualitative way.

3. Results

3.1. Rate of Successful Analyses. All 29 cases included in this study provided tissue preservation sufficient for evaluation. We had no case with complete loss of tissue during the

TABLE 2: Evaluation criteria.

Points	Tissue overall structure (integrity)	Presence of specific (sub)structures	Presence of artefacts	Staining properties
0	Strong fragmentation, less than 25% of tissue intact	No substructures present/identifiable	Presence of numerous artefact foci (e.g., >10 crystal deposits >10 per HPF*)	No specific staining (only nonspecific staining)
1	26–50% of tissue intact	Few substructures present (in 1–3 HPF*)	Many artefact foci (5–10 artefacts per HPF*)	Weak staining of specific structures
2	51–75% of tissue intact	Occasional substructures present (in 4–10 HPF*)	Occasional artefact foci (1–4 artefact foci per HPF*)	Moderate staining of specific structures
3	76–90% of tissue intact	Many substructures present (in 10–20 HPF*)	No artefact foci	Good staining of specific structures
4	Tissue completely intact (91–100%)	Abundant substructures present (in >20 HPF*)	—	—

*HPF: high power field (visual field at magnification $\times 400$).

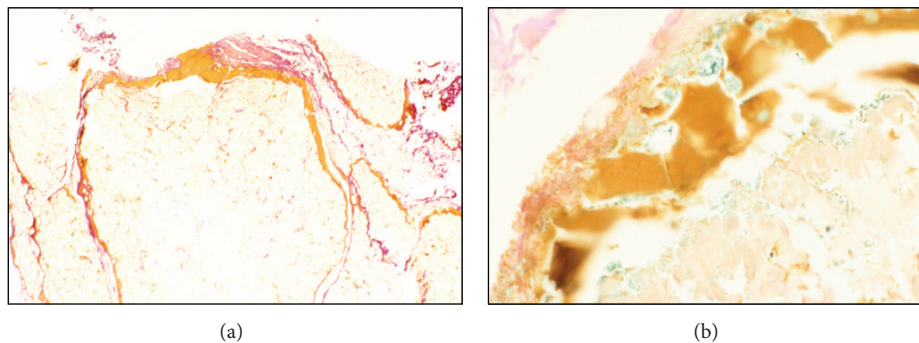


FIGURE 7: Subcutaneous tissue from the Iceman “Ötzi.” (a) The well-preserved fat tissue is separated by a fresh bleeding zone. (b) More on detail, the bleeding zone shows on special staining (Prussian blue) the remnants of haemosiderin-positive macrophages (blue) indicating a survival period of several days ante mortem (original magnification: (a) $\times 150$; (b) $\times 300$; (a): H&E; (b): Prussian blue stain).

TABLE 3: Scoring table.

Points	Score
0–3	0
4–6	1
7–9	2
10–12	3
13–14	4

rehydration procedure. This may clearly be due to a “preselection” of the cases, since we had selected only those cases with good to excellent macroscopic soft tissue conservation. Furthermore, we chose the most “ancient” technique of rehydration which proved, at least in our hands, to be the most successful when compared to other techniques [12–15].

3.2. Diagnostic Evaluation Scheme. The evaluation scheme applied in this study was tested first for its applicability for the evaluation of the material. The resulting points could be clearly transferred into the ranking system. Thereby, every tissue/organ under investigation could unambiguously be characterized and classified.

The application of the system was first tested by two independent researchers (Christina Grove and Andreas G. Nerlich) showing a high rate of concordance and low interobserver variability. This was evaluated using percent agreement and kappa statistics. According to Landis and Koch [16], the agreement was rated as follows: Kappa between 0 and 0.2 indicates slight agreement, between 0.21 and 0.4 fair agreement, between 0.41 and 0.60 moderate agreement, between 0.61 and 0.8 substantial agreement, and from 0.81 excellent agreement. Absolute agreement would be 1.0. Frequency of disagreement was calculated for each sample. In the present assessment the percent agreement ranged at 88,9% for all evaluated samples; the weighted kappa value was at 0.81 indicating good to excellent agreement.

Finally, the score values were statistically evaluated between the “cases” from groups I and II with a standard correlation test (with $p < 0.5$ being regarded as statistically significantly different).

3.3. Observations in Naturally Mummified versus Artificially Mummified Tissues as well as in “Cold Mummy” Tissues. Although the number of cases with artificial mummification is significantly lower than the naturally mummified ones in our series, the direct comparison shows no statistical difference in the values of tissue conservations between both ($p = 0.8$). The only exception is the young infant (“Wack.1”), dying at AD 1816 at the age of approximately 1 year, all internal organs had been kept in ethanol until present time, while the body obviously had been dried by external application (and internal treatment of the body cavities) by a mixture of sodium-/potassium- and magnesium-sulphate salts. Despite minor differences in conservation of internal organs and skin/soft tissues, all specimens in this case showed excellent conservation (Figures 3(c) and 3(d)). Only the extent of some artefacts was higher in the dried tissue than in the fixed material. Accordingly, skin and the subcutaneous fat and musculature were also excellently preserved.

The exceptionally old tissue samples from the Alpine iceman (Ötzi) were also very well preserved allowing the identification of various substructures of the tissue without difficulties. Here, unfortunately, we had no access to internal organ samples that were not available at the time when our study had been granted the authorities. A direct comparison between the conservation status of Ötzi’s skin and subcutaneous tissue structures with significantly “younger” ones revealed a significantly better preservation of the soft tissue in this “cold” mummy tissue.

3.4. Tissue Preservation with respect to the Postmortem Time Interval. In the next step we evaluated the tissue preservation with increasing postmortem time interval, especially with group I samples, and also in comparison to group II material. A (slightly) statistically better degree of preservation is seen for blood vessels ($p < 0.5$) and adipose tissue ($p < 0.5$), while the other tissues did not reveal a statistical degree of difference at all (skin and connective tissue) or obviously due to the few tissue samples available in group II (lung, heart, liver, kidney, and CNS). However, the values for

the kidneys and the CNS samples were very low in both groups. Thereby, we did not observe a general or even gradual loss of tissue structures with increasing postmortem time interval, at least in our series that covered the post-mortem time interval between several months and several centuries/millennia.

In addition, in our series we detected differences between some tissue types in terms of the identification of specific tissue structures. Thus, lungs are much more easily identified when bronchial cartilage and/or small deposits of anthracosis pigment are found, thereby also increasing the score rank of our evaluation scheme. Similarly, the identification of typical portal triads may facilitate the diagnosis “liver tissue.” Similarly, “key structures” are not present in other organs, such as kidney and the CNS. While the kidneys contain arteriolar blood vessels that might have even been identified even in less well-preserved status, the CNS proved to be the least well-preserved organ. Accordingly, in none of the cases we were able to identify CNS tissue in an adequately well-conservation status.

3.5. Identification of Pathologic Conditions. In our small series of cases some paleopathologic observations could be identified. This confirms the diagnostic power of paleohistology of soft tissues. Likewise, in one of the South American mummy skulls we detected an extensive bleeding within connective tissue structures obviously as a result of an acute rotational trauma [6]. One of the ancient Egyptian mummies revealed extensive intrapulmonary bleeding [7] most presumably due to an infection by a parasitosis. In another case, we were able to diagnose intramyocardial scarring of old-healed myocardial infarction [8]. The soft tissue sample from the rectal wall of a South American Inca mummy showed massive fibrosis of the submucosa, such as that seen in chronic inflammation due to Chagas-disease (*T. cruzi* infection) which was further confirmed in this particular case by molecular analysis [5]. Finally, the study of subcutaneous soft tissue samples from the Neolithic glacier mummy Ötzi allowed the diagnosis of an intravital laceration wound with bleeding residues with evidence for tissue reaction, such as that seen in shortly survived, but vital skin wounds [9]. Interestingly, even in relatively poorly conserved material some paleopathology was seen. In case 12, a crypt mummy with a postmortem time interval of 36 yrs. and the clinical diagnosis of metastatic tumor disease, an intrahepatic mass was seen highly suspicious for intrahepatic metastasis, despite the significant decomposition effects in the liver tissue.

4. Discussion

Despite its application even in early paleopathology at the beginning of the 20th century, soft tissue paleohistology has not been used widely. The reasons therefore may be multiple. First, paleohistology is a destructive technique and it is sometimes difficult (or even for ethical reasons impossible) to get access to the diagnostically relevant tissue/organ without major destruction of the mummy corpse; secondly, it requires rehydration, a “chemical” process that endangers the sample

to be destroyed during the rehydration period; this issue may be different between mummified tissues from “cold” mummies (i.e., mummies that had kept frozen for a long period of time, but that obviously had retained a better hydration status than both natural and artificial mummies from “hot” desert areas); thirdly, there exists up to now no systematic study that provides information on the potential success rate of paleohistology. In contrast, major scientific information has as yet been obtained by paleohistology (e.g., [1–4]) and the observations of the present study confirm the potential of this technique in paleopathology.

We are aware that our present study has several limitations: (i) the number of investigated cases is low, but this is the as yet most extensive study on a systematic approach to paleohistology in terms of case numbers and time range, (ii) a certain preselection of macroscopically well-preserved material might have influenced the outcome, (iii) especially in most of the “older” cases (group II) we had access only to very limited tissues/organs.

Despite these restrictions we provide here interesting information on the tissue preservation in mummified corpses: (i) macroscopically well-preserved material has a considerably high rate of successful rehydration; (ii) “cold” mummies may be investigated with even higher success rates (this statement has to be made with great care since we have seen only one case!); (iii) there is no major difference between artificially and naturally mummified specimens (except when the artificial preservation is done by a typical fixative, such as ethanol (case “Wack-1”) or, since the end of the 19th century, formaldehyde); (iv) selected tissues/organs are better preserved than others (subcutis, blood vessels, lung versus CNS, and heart/skeletal muscle); (v) we present here an evaluation scheme that may serve as a basis for future systematic research.

In general, the evaluation scheme for the preservation of mummy tissue proved to be easily applicable and it showed surprisingly high values of reproducibility. However, we clearly admit that the scheme may be refined in ongoing studies, particularly when no prescreened mummies with macroscopic evidence for adequate conservation are used. Nevertheless, this study provides clear evidence that a paleohistologic study may be important in those cases with adequate macroscopic conservation and that those cases offer a considerably high rate of successive analysis.

As a further important observation, we detected that tissue preservation is less dependent from the postmortem time interval than from

- (i) initial (i.e., within the first weeks/months) conservation of the mummy,
- (ii) type of tissue/organ under investigation (which in turn influences the diagnostic spectrum),
- (iii) experience in tissue preparation and histologic interpretation.

Accordingly, soft tissue pathology is more promising in those tissues with a high amount of connective tissue or “stable” tissue structures, such as fat tissue. These seem to undergo postmortem decomposition either very rapidly after death

or remaining “stable” for a long period of time (proper storage provided). As the least well-conserved organ we identified the CNS; it is evident that CNS does not contain much connective tissue; furthermore, brain tissue is not characterized by specific substructures (with the exception of pigmented cells in the pigmented nuclei that may indeed be seen even in less well-preserved brain tissue specimens). In several instances, even paleohistology may not be decisive in identifying the proper organ. However, the identification of particular tissue structures and their conservation even after long periods of postmortem time interval seems to be a promising perspective for paleohistology.

Finally, recent significant progress in imaging techniques, mainly by CT scans, has opened the question whether paleohistology (as a destructive technique) should be applied to mummies at all. Problems in the proper identification of specific lesions and the need to distinguish between pre- and postmortem alterations, however, have made clear that CT scanning alone cannot solve distinct questions [17]. Additionally, the application of modern molecular techniques, such as stable isotope analysis or ancient DNA investigations, requires tissue material and can often be interpreted successfully when combined with corresponding paleohistology. Therefore, the careful, precise, and knowledgeable application of this analytical technique will persist to be fundamentally important for multidisciplinary mummy research.

Conflict of Interests

The authors declare that there is no conflict of interests regarding the publication of this paper.

Acknowledgments

The authors are indebted to the various organizations that allowed them to use tissue samples for their studies. This holds particularly true for the Institute of Anthropology and Human Genetics, Ludwig Maximilians University of Munich, the Institute for Human Genetics and Anthropology, Karl-Eberhards-University Tübingen, and the Oberndorfer-Collection, Klinikum München-Schwabing for the Egyptian material; the South American material was kindly provided by the Bavarian State Collection of Archeology, Munich, and again the Oberndorfer-Collection, München; finally, the South Tyrolean Museum of Archaeology, in particular the conservator for the Iceman (Dr. E. Egarter-Vigl), had kindly supplied the authors with the tissue samples of the Iceman Ötzi. All mentioned institutions had granted the permission to perform paleohistology on selected tissue samples. For the technical performance of the paleohistological analysis, the authors are most thankful to Mrs. Ch. Reischl.

References

- [1] A. C. Aufderheide, “Progress in soft tissue paleopathology,” *The Journal of the American Medical Association*, vol. 284, no. 20, pp. 2571–2573, 2000.
- [2] M. A. Ruffer, “Note on the presence of ‘bilharzia haematobia’ in Egyptian mummies of the twentieth dynasty,” *The British Medical Journal*, vol. 1, no. 2557, p. 16, 1910.
- [3] A. R. David, *The Manchester Museum Mummy Project*, Manchester University Press, Manchester, UK, 1979.
- [4] A. Cockburn, R. A. Barraco, T. A. Reyman, and W. H. Peck, “Autopsy of an Egyptian mummy,” *Science*, vol. 187, no. 4182, pp. 1155–1160, 1975.
- [5] S. Panzer, O. Peschel, B. Haas-Gebhard, B. E. Bachmeier, C. M. Pusch, and A. G. Nerlich, “Reconstructing the life of an unknown (ca. 500 years-old South American Inca) mummy—multidisciplinary study of a Peruvian Inca mummy suggest severe Chagas disease and ritual homicide,” *PLoS ONE*, vol. 9, no. 2, Article ID e89528, 2014.
- [6] R. Sokiranski, W. Pirsig, H.-P. Richter, and A. G. Nerlich, “Unique paleopathology in a Pre-Columbian mummy remnant from Southern Peru—severe cervical rotation trauma with subluxation of the axis as cause of death,” *Acta Neurochirurgica*, vol. 153, no. 3, pp. 609–616, 2011.
- [7] A. G. Nerlich, F. Parsche, I. Wiest, P. Schramel, and U. Löhns, “Extensive pulmonary haemorrhage in an Egyptian mummy,” *Virchows Archiv*, vol. 427, no. 4, pp. 423–429, 1995.
- [8] A. G. Nerlich, I. Wiest, and J. Tübel, “Coronary arteriosclerosis in a male mummy from ancient Egypt,” *Journal of Paleopathology*, vol. 9, pp. 83–89, 1997.
- [9] A. G. Nerlich, B. Bachmeier, A. Zink, S. Thalhammer, and E. Egarter-Vigl, “Ötzi had a wound on his right hand,” *The Lancet*, vol. 362, no. 9380, p. 334, 2003.
- [10] A. G. Nerlich, O. Peschel, and E. Egarter-Vigl, “New evidence for Ötzi’s final trauma,” *Intensive Care Medicine*, vol. 35, no. 6, pp. 1138–1139, 2009.
- [11] M. A. Ruffer, “Preliminary note on the histology of Egyptian mummies,” *The British Medical Journal*, vol. 1, no. 2521, article 1005, 1909.
- [12] A. T. Sandison, “The histological examination of mummified material,” *Stain technology*, vol. 30, no. 6, pp. 277–283, 1955.
- [13] E. Fulcheri, E. Rabino Massa, and C. Fenoglio, “Improvement in the histological technique for mummified tissue,” *Verhandlungen der Deutschen Gesellschaft für Pathologie*, vol. 69, article 471, 1985.
- [14] E. Tapp, “Histology and histopathology of the Manchester mummies,” in *Science in Egyptology*, A. R. David, Ed., pp. 347–350, Manchester University Press, Manchester, UK, 1986.
- [15] A.-M. Mekota and M. Vermehren, “Determination of optimal rehydration, fixation and staining methods for histological and immunohistochemical analysis of mummified soft tissues,” *Biotechnic and Histochemistry*, vol. 80, no. 1, pp. 7–13, 2005.
- [16] J. R. Landis and G. G. Koch, “The measurement of observer agreement for categorical data,” *Biometrics*, vol. 33, no. 1, pp. 159–174, 1977.
- [17] N. Lynnerup, “Mummies,” *Yearbook of Physical Anthropology*, vol. 50, pp. 162–190, 2007.

Research Article

New Ancient Egyptian Human Mummies from the Valley of the Kings, Luxor: Anthropological, Radiological, and Egyptological Investigations

Frank Rühli,¹ Salima Ikram,² and Susanne Bickel³

¹Institute of Evolutionary Medicine, University of Zurich, 8057 Zurich, Switzerland

²Department of Egyptology, American University of Cairo, Cairo 11835, Egypt

³Egyptology, University of Basel, 4051 Basel, Switzerland

Correspondence should be addressed to Frank Rühli; frank.ruehli@iem.uzh.ch

Received 5 January 2015; Accepted 11 May 2015

Academic Editor: Laura Guidetti

Copyright © 2015 Frank Rühli et al. This is an open access article distributed under the Creative Commons Attribution License, which permits unrestricted use, distribution, and reproduction in any medium, provided the original work is properly cited.

The Valley of the Kings (arab. *Wadi al Muluk*; KV) situated on the West Bank near Luxor (Egypt) was the site for royal and elite burials during the New Kingdom (ca. 1500–1100 BC), with many tombs being reused in subsequent periods. In 2009, the scientific project “The University of Basel Kings’ Valley Project” was launched. The main purpose of this transdisciplinary project is the clearance and documentation of nonroyal tombs in the surrounding of the tomb of Pharaoh Thutmose III (ca. 1479–1424 BC; KV 34). This paper reports on newly discovered ancient Egyptian human mummified remains originating from the field seasons 2010–2012. Besides macroscopic assessments, the remains were conventionally X-rayed by a portable X-ray unit *in situ* inside KV 31. These image data serve as basis for individual sex and age determination and for the study of probable pathologies and embalming techniques. A total of five human individuals have been examined so far and set into an Egyptological context. This project highlights the importance of ongoing excavation and science efforts even in well-studied areas of Egypt such as the Kings’ Valley.

1. Introduction

The Valley of the Kings (arab. *Wadi al Muluk*; KV) situated on the West Bank near Luxor (Egypt) was the site for royal and elite burials during the New Kingdom (ca. 1500–1100 BC), with many tombs being subsequently reused by lesser elites (ca. 950–850 BC). Its remote and dry location helped for the preservation of the buried ancient human mummified remains [1–5]. The valley has been visited by robbers and tourists since antiquity; since the early 19th century AD, antiquarians and archaeologists have cleared and recorded tombs, with a total of 61 sepulchers being known by the start of the 20th century [6]. In 1912, The financier and excavator, Theodore Davis (1837–1915) famously declared the valley now “being exhausted” [7]. However, in late 1922, the archaeologist Howard Carter (1874–1939) and his colleagues discovered the now iconic tomb (KV 62) of Pharaoh Tutankhamun [8]. Since these days, almost one hundred years ago, discovering new tombs has become rare in the valley: in 2005, the Amenmesse

Project found KV 63, an embalming cache [9], and in 2012, the University of Basel Kings’ Valley Project found KV 64 [10–12]. Nowadays, most archeological research focuses on the documentation and precise recording of the hitherto known tombs and pits, reestablishing their precise location and analyzing their remaining contents.

Researchers of the University of Basel (Switzerland) have been involved in Egyptological projects in the Kings’ Valley since many years [13]. In 2009, the most recent scientific project “The University of Basel Kings Valley Project” (<http://www.ubkvp.ch/>; access date: 20 Dec. 2014) or (<http://aegyptologie.unibas.ch/forschung/projekte/university-of-basel-kings-valley-project/>; access date: 20 Dec. 2014) was started with Susanne Bickel as director and Elina Paulin-Grothe as field director. The main purpose of this transdisciplinary project is the investigation and documentation of nonroyal tombs in the surroundings of the tomb of Pharaoh Thutmose III (ca. 1450 BC; KV 34; Figure 1).

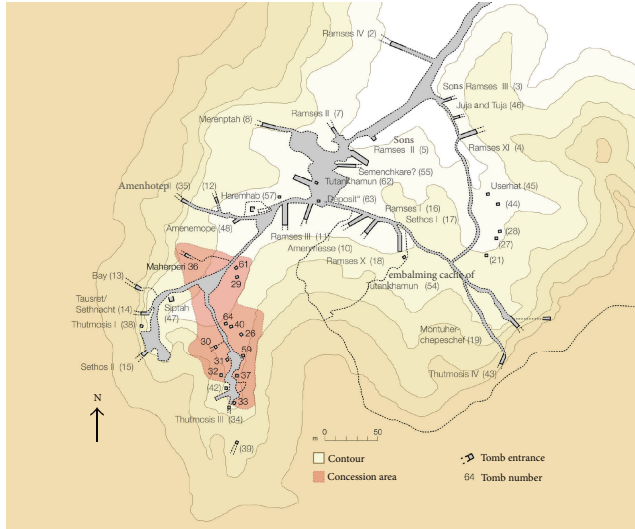


FIGURE 1: Map of the Kings' Valley with the concession area of the University of Basel Kings' Valley Project in red.

During the season of spring 2010, the project team started research on tomb KV 31, of which only the upper rim of the shaft was visible on the desert surface. No information about this tomb nor documentation of former archaeological explorations were known, although KV 31 has possibly been visited already by Giovanni Battista Belzoni (1778–1823) in 1817 and perhaps also by Victor Loret (1859–1946) or his team in 1898. As its shaft was entirely filled with sand and stones, it had not been surveyed by the Theban Mapping Project (<http://www.thebanmappingproject.com/>, for a first sketch of the tomb <http://aegyptologie.unibas.ch/?id=21700>, access date: Dec. 20, 2014).

Tomb KV 31 lies on a steep slope on the west flank of the lateral valley; it consists of a vertical shaft with a depth of about 5 m, which gives access to a central room B (ca. 470 cm × 370 cm). The main burial chamber (room C, ca. 530 cm × 320 cm, Figure 2) lies to the south of the central room, a less properly cut room D lies to the west. The central room was filled in with a thick layer of desert debris possibly indicating a later reuse of the tomb. Rooms C and D contained the very fragmented remains of several burials, probably five individuals, which can be assigned to the mid-18th dynasty (ca. 1450–1400 BC, from the reign of Thutmose III to that of Amenhotep II) on the basis of a large quantity of pottery and some fragments of canopic jars. The original burials were severely looted in antiquity (21st dynasty, 11th–10th c. BC), some decades before the probable reuse of the tomb, and further damage by modern robbers seems assured. Robbers of all periods sought for valuables, mainly jewellery; ancient looters moreover retrieved all wooden objects for reuse. No wooden coffins remained in KV 31. The mummies of the individuals were stripped of all their bandages and violently disarticulated. Most of the mummies' remains were found clustered in room C (thus labelled 31.C), with one mummy found in room D (31.D). The remaining objects do not reveal the identity of the individuals. However, the quality of

the fragmentary burial goods indicates their very high social status. During the mid-18th dynasty, the Kings' Valley was used as burial ground for members of the royal family and the kings' immediate entourage (queens, princesses, princes, wet-nurses, and royal companions, [14]). Future ancient DNA analyses might answer the question whether the individuals of KV 31 were related to each other and whether they belonged to the royal family or not.

The aim of this paper is to report on these ancient human mummified remains. The application of simple, on-site techniques (visual inspection, conventional X-rays) allows the investigators to reassemble the highly fragmented bodies as well as assess sex, individual age, and possible pre- and postmortem changes.

2. Material and Methods

All human remains found in KV 31 (chambers C and D), Valley of the Kings, Luxor, Egypt, were reassembled and analysed. The initial stage of analysis consisted of matching up body fragments to form complete individuals. The mummies and fragments thereof then were subjected to macroscopic examination by naked eye and magnifying glasses for mummification technology, taphonomic changes in the mummies, basic ageing and sexing, and identifying any particular lesions. This was finally followed by radiography. A total of 27 radiological images of all bodies were taken. Some of the images are of minor quality (field of view, exposure time); yet unfortunately no repetition of such lower quality images could be made due to local technical restrictions (traditional development over night only) and administrative restrictions prohibited the use of more modern and adequate radiographic equipment. The portable machine used was a Karmex Diagnostic X-ray Unit PX-20N (AC 115 V 50/60 HZ, 50–130 KVp 2–20 mA), together with Agfa industrial film. The kV was 60, 15 mAs, although there was some variation due to technical issues of electricity supply. The distance varied between 1.35 m and 1.45 m. The bodies were also photographed within the tomb. Ageing and sexing was based on standard anthropological criteria [15, 16] as far as possible based on the skeletonized, partially mummified, fully mummified, and in some cases even fully wrapped remains. After examination, the body parts were labelled and stored appropriately in individual modern coffins in KV 31.

3. Results

3.1. General Assessment and Macroscopic Appearance. First, an initial macroscopic assessment was undertaken. The various fragmented body parts, initially thought to be four mummies, were “matched.” Almost all of the bone and soft tissue fragments could be relocated correctly, leading to a much more complete appearance of the bodies. This “matching” led to a new total of five individuals. Body C1 consists of an isolated head as well as thorax and lower parts of the body. Body C2 is almost complete yet separated in four major parts (head, upper body, and two legs); its legs are still partially wrapped. Body C3 is headless but thorax, and

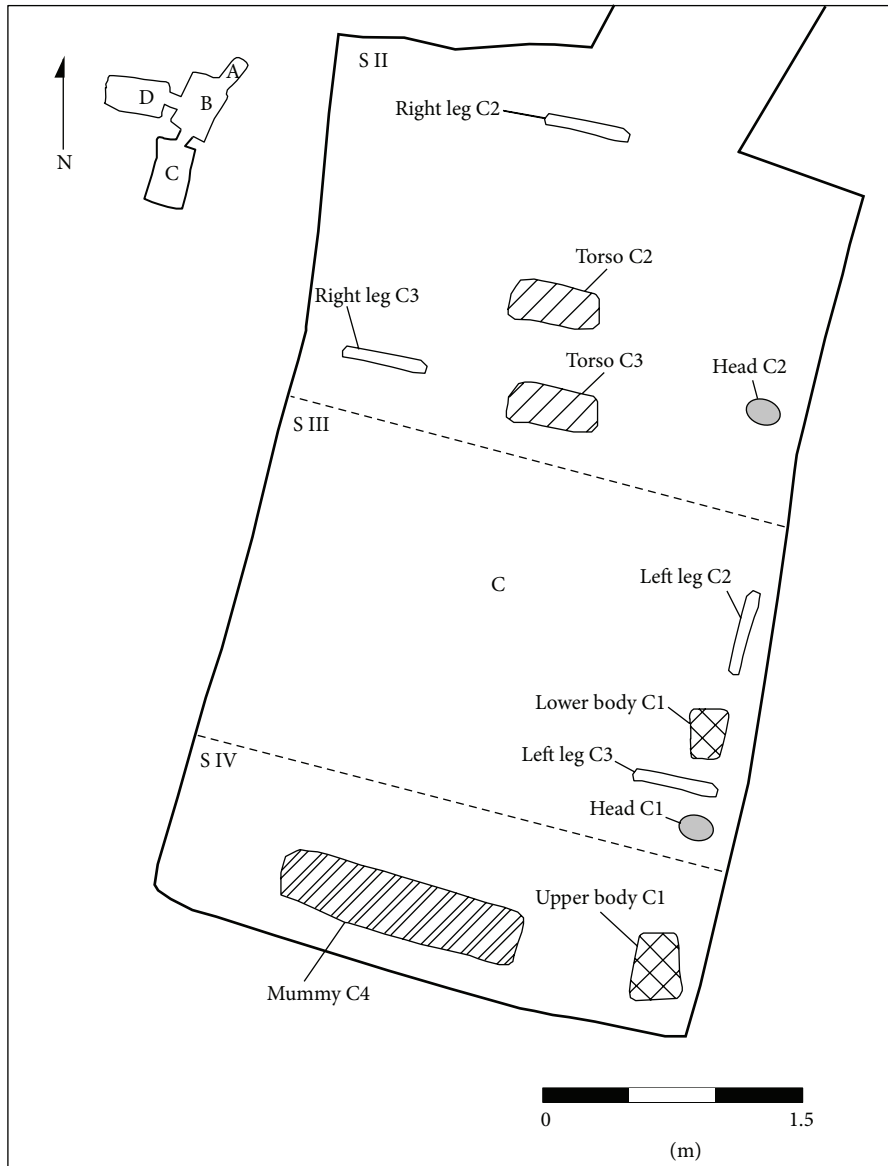


FIGURE 2: Room C of tomb KV 31 with the scattered fragments of mummy parts (survey: T. Alshaimer, University of Basel).

the majority of the left arm and both legs are in fragmented form preserved. Body C4 is almost complete, except for the feet and hands mostly fragmented. Body D consists of the pelvic girdle and most likely the head of the same individual. Thus, all bodies have suffered major postmortem damage and do not show by naked eye any inscriptions or amulets. The position of the arms of the mummies varies (Table 1).

3.2. *Mummy C1* (Figure 3). This fragmented mummy is fairly complete. It clearly shows a female with small, albeit deflated, breasts and a female pelvis (subpubic arcus). The individual age seems to be juvenile, maybe up to adult (ca. 18–25 yrs). Both arms lie straight along her torso; yet the hands have been broken off. The body is now in several components: head (separated from the torso between the seventh cervical and first thoracic vertebra), torso, and legs (the right foot

is missing the toes), all of which can be realigned, giving a length of ca. 160 cm (159 cm according to Bach [17], with the maximum length of humerus, as defined by Martin Mass Nr. 1 [18], to be bilaterally 290 mm). The head shows some frontal hacking marks most likely of postmortem nature. The head length is 170 mm and head width is 138 mm. The face is broken, but part of the maxilla and the entire mandible survives, complete with teeth, and the tongue is well preserved too. Twenty-eight teeth are erupted and do not show signs of excessive wear or any dental disease assumed. Some postmortem damage such as a lesion of the right lower first molar and in the frontal part of the left maxilla can be found. The right side of the chin is nicked by a blade. A few wrinkles are visible on the remaining left side of the face.

Unfortunately, the damage makes it impossible to determine if excerebration took place nasally, although from

TABLE 1: Basic description of mummies investigated (n.d.: not determinable).

Mummy	Sex	Age	Height (cm)	Eviscerated	Excerebrated	Position of arms	Disease (besides unhealed fractures)
31.C.1	F	Juvenile-young adult	155–165	Yes	Probably not	Side	None
31.C.2	M?	Young adult?	Ca. 165	Yes	Probably not	Pubes	None
31.C.3	M?	Juvenile-young adult	Ca. 175	Yes	No skull preserved	Crossed	None
31.C.4	M?	Adult	n.d.	Yes	n.d.	Pubes	None
31.D.1	F?	Adult	Ca. 155	n.d.	Certainly not	n.d.	Unclear finding in iliac fossa



FIGURE 3: (a), (b): overview of mummy C1 (a) and close-up view of postmortem exposed abdominal cavity showing packages of bandages (b).

the remaining anatomical elements excerebration looks rather unlikely. Rests of meninges are visible intracranially. The head is covered by short, fine, black, silky hair, with one lock of lighter coloured hair, possibly the result of an excess of natron. The ears are plugged with linen tamped in with resinous material. The body was eviscerated and the abdomen and the pelvic area are stuffed with dense embalming packing materials. The body was wrapped in several layers of linen; the legs and arms are packed separately; much of the bandaging has been removed later. The belly was hacked open and the interior packing was sliced by a sharp blade as is evidenced by cut-marks. The interior cavity is full with packages of bandages that are blackened, presumably by oils and resins. On the back, in the shoulder areas there are also signs of slashing. Based on the healthy teeth, an early adult age can be assumed.

The X-rays show that the head has been separated at the level of the seventh cervical and first thoracic vertebra. A big skull lesion with fragments in the posterior skull cavity can be seen; also parts of the maxilla are separated. Both epiphyses of the iliac bone crest are not fully closed.

The right hand is disarticulated, and of the left hand only three fingers are left; one of it with a fracture in the proximal phalangeal and metacarpal bone. The left ulna and radius are fractured. The left fibula head is most likely fractured too and the former proximal epiphyseal plate is still slightly visible. A fracture at the right lower limb is visible; also the left foot is disarticulated at the upper ankle joint; the distal phalanges of the first toe as well as the middle and distal phalanges of the fifth toe are missing. A subluxation can be found at the calcaneocuboid joint. All these traumata seem to be of postmortem nature. On the conventional X-ray, the thorax

shows dense packing in the right part, but no clear signs of remnants of a heart or other mediastinal or pulmonary tissues can be found. The symphysis pubis is hardly visible due to the superimposition of the stuffing material located in the small pelvis; yet specifically both medial menisci are clearly visible.

3.3. Mummy C2 (Figure 4). The head is separated from the torso. The legs, with feet attached, are also separated from the body, with the pelvis attached to the legs. The clavicles are pushed up and the humeri are squashed into the body. The upper arms lay along the body, and the lower arms are moved in so that the hands rested over the pubes. The belly area is broken postmortem, and the left hand is missing, as are portions of the left distal foot.

The remnants of the brain seem to be left in the cranium. Parts of the head, especially the face, are still well wrapped in linen bandages, with the back of the head and hair remaining exposed.

Postmortem cut-marks are visible in the facial bandages on the right side and these are at least four to five centimeters deep. The right eye is sunk in and the bandages are missing, whereas the left eye is fully covered by bandages. The back and top of the head are partially covered by hair that is braided and does not appear to be a wig but the deceased's own hair, although it is possible that some of the braids are woven into the natural hair. The crown of the head is solidly matted, as if oil had been placed there and dribbled into the hair. The ears, however, might have been plugged with linen as the ear openings are distended. The thoracic cavity is completely stuffed with a granular material. In the left thorax region, there is a small soft tissue defect visible. There is a complete



FIGURE 4: (a) overview of mummy C2, (b) Conventional x-ray (ap direction) of thorax showing among others in the right upper thoracic cavity two dense structures most likely to be organ or other packages.

separation of the body at the level of the fourth lumbar vertebra.

The robbers have also hacked the body in the belly area and removed the abdominal wall, rendering visible the fact that the body cavity is densely stuffed with rolls of linen impregnated with resinous material. Some sand and gravel are also visible in the body cavity.

The metacarpal bones are present on the right side, whereas for the rest of the left and right side the fingers and wrists are completely missing. Each arm is individually wrapped, spirally, as are the legs. One can count at least a dozen of layers of bandages on the right arm, although originally there were probably more. The legs were similarly wrapped, with the left thigh being wrapped in dozens of layers of linen. The right leg seems to be ca. 1-2 cm longer than the left one; however, this is most likely related to postmortem positioning. Blade marks made by a very sharp implement can be seen in the compacted wrappings of both thighs. The toes are wrapped individually although they are in fewer layers of bandages—two or three—and then wrapped together with the rest of the foot.

On the conventional X-rays, well pneumatized frontal sinuses, a soft tissue defect at the right neck area, and a radio-dense structure of unknown nature at the left ear can be seen. In the right upper thoracic aperture, a radio-dense structure consisting of two parts can be found. A fracture of the right first rib is also visible; also the left 11th rib is broken, most likely postmortem. The iliosacral joint is also most likely fractured postmortem and the left iliac crest is not yet fused. A radio-dense structure of unknown nature can be found between the trapezoid bone and the first metacarpal bone of the right hand.

The stature *in situ* measures ca. 156 cm. However, based on the measurement of humerus, radius, and tibia [19] an average of ca. 165 cm can be assumed—rather a dramatic difference. Based on the pelvis morphology, this is rather a female individual, whereas the skull shows a slight masculine tendency. Its age is most likely young adult, most long bone epiphyses seem fused, and the teeth show a rather low degree of abrasion; yet both iliac crest epiphyses are slightly visible (ca. 20–25 yrs). On the whole, it is more likely to be a male individual.

3.4. Mummy C3 (Figure 5). This mummy is a fairly complete body, although the head and right foot are missing and some

extremities damaged. Multiple, uncountable layers of linen, at least four centimeters deep/thick, cover the body. The arms were crossed over the chest, with the left fingers II–V being flexed, with a straight thumb as if it were holding an object. All extremities are multiply broken and the abdomen is exposed. Some soft tissue is missing in the left leg. It is most likely a juvenile to adult individual; most of the epiphyses seem to be closed (ca. 18–25 yrs). The sex is difficult to determine from the pelvis: while the arc composé is rather female, the incisura ischiadica major is indeterminate, and the pelvis in general seems to be rather male. Also, there are no breasts visible. The right humerus length is ca. 345 mm, the tibial length bilaterally each ca. 390 mm; thus, based on Breitingner [19], this would represent ca. 175 cm in total height, more in keeping for males.

The X-rays reveal a.o. a proximal left humerus fracture of most likely postmortem origin. The presence of mediastinal tissue, particularly the heart, cannot be determined due to the filling of the majority of the thorax and abdomen with rather dense stuffing material particularly in the lower abdomen and pelvis. Multiple fractures and anatomical dislocations can be seen: in the left distal lower arm and in the left subtrochanteric region as well as in the left tibia condyles. In the right axillar region, a discontinuity with a soft tissue defect in the humeral head region can be found; as differential diagnosis, a nondislocated humeral fracture of most likely postmortem origin as well as an artefact due to the superimposition of a soft tissue lesion is most likely. Also, the right first metatarsal shows a possible postmortem fracture. Finally, a mildly scoliotic upper thoracic spine toward the left side mostly due to positioning can be seen.

3.5. Mummy C4 (Figure 6). Fairly complete mummy, yet several fragments, parts of feet, and particularly the right arm are missing. It seems to be an adult individual of unknown sex, with a rather female pelvis shape; however, based on secondary sex characteristics (clear absence of female breasts), this is the broken up body of a man, although there is no male genital visible at all. The stature *in situ* is ca. 154 cm. Based on the long bone lengths (length of femur bilaterally ca. 380 mm, medial tibia length right ca. 345 mm, and left ca. 340 mm), the total stature according to Breitingner [19] for a male would be ca. 160 cm.

The partially fully exposed head has thin hanks of hair attached to it, some of which, on the right side, are fairly long.



FIGURE 5: (a), (b): overview of mummy C3 (a), close-up of left hand with flexed fingers II–V (b).



FIGURE 6: (a), (b): overview of mummy C4 (a) and conventional X-ray (ap direction) of midfemoral region (with parts of isolated lower limbs visible too) showing a.o. the massive soft tissue defects in the region of the adductor muscles.

The right ear is crinkled and does not look as if it was pierced. The nose is flattened and there is no indication that it was ever filled with linen plugs to keep its shape. The maxilla shows that all teeth but the third molars had erupted. The teeth show signs of wear and some, particularly the frontal ones, are altered postmortem but no obvious disease is apparent. The mandible is missing. The vast majority of the prevertebral throat area is completely missing.

Only the proximal half of the right humerus survives, and the right radius and ulna are missing. The left arm is broken but present. The upper arms lay along the side of the body; the hands seem to have been placed over the pubes but this is difficult to ascertain due to the mummy's broken state. Both shoulders are positioned cranially (shoulder elevation). The evisceration was in the left lumbar region (ca. 8 cm long), with the cut looking fairly vertical (ca. 15° proximally oriented towards lateral), which might indicate that this mummy was made prior to the end of the reign of Thutmose III (1479–1425) [20]. However, the cut is not clear enough to be completely confident of this dating. The body cavity was filled. The robbers who are responsible for the destruction of the body also cut out a piece of flesh just above the left buttock apparently with a sharp implement.

The X-rays show an unidentifiable small bone fragment at the left femur condyles and a fractured fibula collum as well as a soft tissue defect. The left clavicle is fractured. Also, a massive soft tissue defect right medial in the area of the adductor muscles as well as a unique contour of the femurs bilaterally up to the condyle region can be found. Also, left-sided defects of the pubic bone and symphysis can be seen.

All traumata are most likely of postmortem nature. Finally, the massive thoracic (with the exception of the left apex area) and abdominal stuffing can be seen bilaterally.

3.6. Mummy D1 (Figure 7). This body is highly fragmented consisting of a fractured head, the majority of the cervical and thoracic spine, parts of the shoulder blades, the sternum, the proximal part of the right humerus, the pelvis girdle, and major parts of the lower limbs only. This highly tentative grouping is also based on the fact that the legs and pelvic bones definitively match, and this is the only spare head left in the tomb (which from visual inspection may match too). The bandages are virtually all stripped off from the head and the legs.

The frontal part of the head is badly damaged, but there are no clear indications of excerebration via the ethmoid bone as it seems to be intact. The brain as well as the falx cerebri is visible intracranially; also most likely remnants of the brain have been identified in the conventional radiograph (see below). The hair is short and reddish; the color might be the result of ageing or bleaching due to embalming agents. The ears were plugged with linen soaked in resin. The eyes are closed and some of the eyelashes survive. Some natron, the substance which was identified by visual testing, is visible on the occipital area and on the left and right sides of the head and neck, below the jaw line. The following teeth are preserved (Fédération Dentaire Internationale (FDI)/World Dental Federation Notation, ISO-3950 Notation): 13 with postmortem damage, 14 ditto, 15, 16, 17, 22, 23, 24, 25, 26, 27; 35, 36, 37, 46, and 47. They show some degree of abrasion.

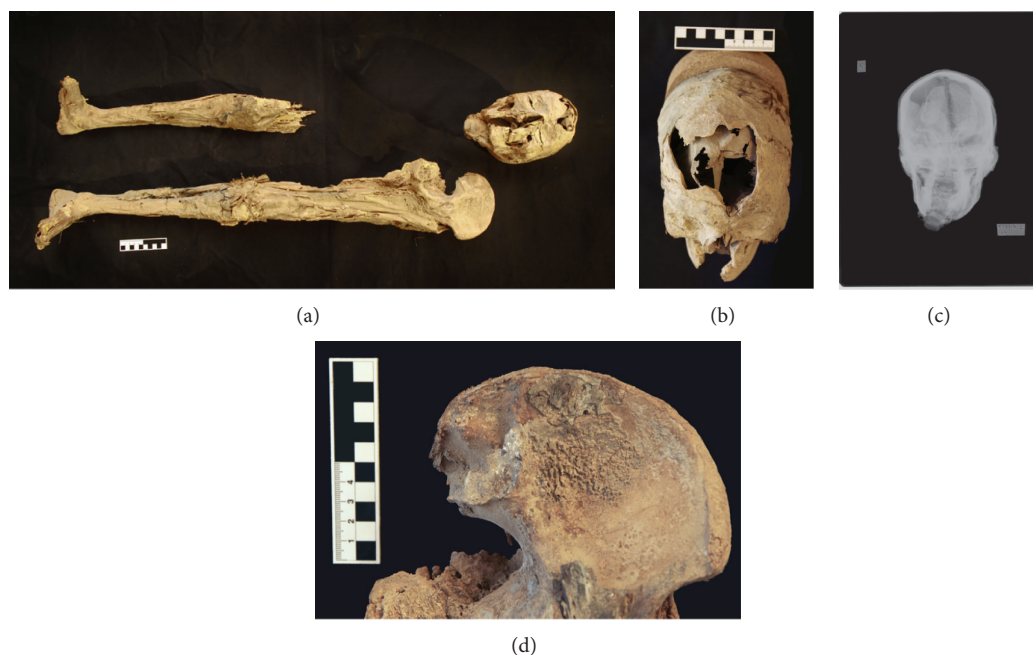


FIGURE 7: (a), (b), (c), and (d): overview of mummified remains D1 (a), frontal view of head D1 (b), conventional X-ray of head D1 showing among others most likely remnants of the shrunken brain (c), and close-up of alteration in left iliac fossa region of unclear etiology (d).

The right leg still has some flesh and skin covering the bone, with a few straggling bandages remaining. It is preserved with the exception of the middle part of the femur. The bandages closest to the skin on both legs are dark with oils and resins. The ones further from the skin are brown-beige. The left leg is better preserved. It is possible that part of the genitals (portion of the penis) is preserved, but the soft tissues are difficult to identify, partially due to postmortem damage. The legs show that the individual was probably rather plump during his lifetime as the flesh was folded over at various places.

An inconclusive alteration of the left iliac fossa (area of origin of iliac muscle) can be seen; possible differential diagnoses include those of taphonomic origin (crusts due to water/sand) or to be a periosteal reaction such as a calcified hematoma, though the latter is visually unlikely.

The remnants appear rather female, but it is quite uncertain. It is an adult individual of unknown age, based on the degree of dental alterations most likely within the adult age group (ca. 20–30 yrs). The left medial tibial length is ca. 340 mm; thus, an estimated stature of ca. 155 cm [17] can be assumed for a male individual.

The X-rays show a.o. the cervical spine to be preserved up to the 6th cervical vertebra. A massive soft tissue lesion can be found frontally, with particularly a fractured upper jaw. A fracture and impression of the frontoparietal bones with some bony parts within the skull can also be found. All traumata seem to be of postmortem nature. In the posterior part of the skull, one finds an inhomogeneous substance with no obvious fluid levels; these are most likely remnants of the brain.

4. Discussion

Despite being unnamed and only loosely dated, the human remains from KV 31 are useful and significant subjects of study as they provide insight into the mummification practices of mid-18th dynasty elite individuals and into the turbulent later history of the necropolis. The various intense looting phases hamper, however, the analysis of the mummies. The unwrapping of the bodies as well as much of the damage is most probably due to the activity of retrieving valuables and wood at the beginning of the Third Intermediate Period, whereas the scattering of the body parts and the theft of specific mummified body parts (head, hands) can presumably be attributed to robbers of the 19th century AD who sold these pieces to the early tourists. As stated above, these bodies must belong either to members of the royal family or to elite individuals who were in personal contact with the pharaoh. Based on the number of large storage jars found in the tomb, it can be assumed that all five individuals were originally buried here.

All the bodies were carefully mummified, being eviscerated, well desiccated, anointed with oils, and then wrapped with generous amounts of linen. Due to the destructive activities of robbers, one cannot determine the exact position of the evisceration incision on most of the mummies.

The arm positions for all those whose arms seem to follow the traditional division that was common throughout the New Kingdom and into the Third Intermediate Period, if not beyond: along the sides for women, and over the pubes for men. There is, however, one exception, mummy C3, whose arms are crossed over his chest, with the surviving hand posed as if it had been gripping something. This pose, from

the mid-Eighteenth dynasty to the end of the New Kingdom was regularly applied for kings; it became more frequent in later periods. It is, however, still difficult to relate arm positions of mummies to a specific social status or historical period with any degree of certainty. There is, for example, hardly any information available concerning the arm position of royal sons in the 18th dynasty. Also sexing and ageing is difficult to assess due to the partial destruction (and in some cases even crucial missing body parts) and the limited quality of conventional X-rays as well as the superimposition of embalming-related artifacts. Thus, the data need to be taken with enormous caution for these individual criteria. However, in general the bodies seem to be all of adult age. A higher-quality diagnostic imaging approach such as, for example, by CT scanning shall help to better determine individual sex and age and allow an improved evaluation of individual health and disease; the goal of the current excavation project is to get approval for such an advanced logistically more challenging imaging attempt in one of the future field seasons.

The lack of clear medical diagnosis is caused by various factors. Some of the human remains are still wrapped and thus any macroscopic investigation of tissues is impossible. Also, the enormous postmortem damage caused by tomb robbers and the numerous subsequent fractures make a clear distinction of pre- and postmortem origin of the numerous skeletal lesions de facto impossible. Finally, more sophisticated examinations methods were not available *in situ*.

Future studies shall hopefully include ancient DNA analyses as well as C^{14} dating of some of these mummies to possibly match them with existing New Kingdom royal mummy data (e.g., [21]). Especially, a more precise reconstruction of embalming techniques may help to set these individuals into a more exact historical context. Finally, the hereby-described unique human remains show again that the famous Valley of the Kings is still “not exhausted” and may also in the future reveal more insight into ancient life conditions and funerary customs.

Conflict of Interests

The authors declare that there is no conflict of interests regarding the publication of this paper.

Acknowledgments

The authors are grateful to Dr. W. R. Johnson, director of Chicago House, Luxor, for graciously permitting the use of Chicago House and its darkroom and are very especially thankful to Y. Kobylecky, photographer at Chicago House, for his expertise and generosity in the development of the radiographs and to the Institute of Bioarchaeology of the American University Cairo for the use of its radiographic equipment as well as KD Dr. T. Böni, Orthopaedic University Clinic Balgrist Zurich, for some helpful comments on interpretation of conventional X-rays. This research is funded by the Mäxi Foundation Zurich (Frank Rühli) and the Basel University and private sponsors (Susanne Bickel). Special thanks go to the Egyptian Supreme Council of Antiquities, the Egyptian

Ministry of State of Antiquities, and its numerous officers who supported and accompanied the authors' work.

References

- [1] G. E. Smith, *The Royal Mummies*, Imprimerie de l'Institut Français d'Archéologie Orientale, Cairo, Egypt; Duckworth, London, UK, 2000.
- [2] R. B. Partridge, *Faces of Pharaohs, Royal Mummies and Coffins from Ancient Thebes*, Rubicon Press, London, UK, 1994.
- [3] A. D. Bickerstaffe, *Refugees for Eternity: Identifying the Royal Mummies Pt. 4: The Royal Mummies of Thebes*, SOS Free Stock Canopus Press, London, UK, 2009.
- [4] J. Taylor, *Egyptian Mummies*, British Museum Press, London, UK, 2010.
- [5] J. Taylor, *Ancient Lives, New Discoveries: Eight Mummies, Eight Stories*, British Museum Press, London, UK, 2014.
- [6] N. Reeves and R. Wilkinson, *The Complete Valley of the Kings*, Thames and Hudson, London, UK, 1996.
- [7] T. Davis, *The Tombs of Harmhabi and Touatânkhamanou*, Duckworth Publishing, London, UK, 2001.
- [8] H. Carter and A. C. Mace, *The Tomb of Tutankhamen*, Cassell and Company, London, UK, 1923.
- [9] E. Ertman, R. Wilson, and O. Schaden, “Unraveling the mysteries of KV63,” *KMT: A Modern Journal of Ancient Egypt*, vol. 18, pp. 18–27, 2006.
- [10] S. Bickel and E. Paulin-Grothe, “KV 64: two burials in one tomb,” *Egyptian Archaeology*, vol. 41, pp. 36–40, 2012.
- [11] S. Bickel, “Nicht nur Pharaonen. Neue Untersuchungen zu nicht-königlichen Gräbern im Tal der Könige,” *Sokar*, vol. 26, pp. 60–71, 2013.
- [12] S. Bickel and E. Paulin-Grothe, “KV 40: a burial place for the royal entourage,” *Egyptian Archeology*, vol. 45, pp. 21–24, 2014.
- [13] E. Hornung, *The Valley of the Kings: Horizon of Eternity*, Timken, New York, NY, USA, 1990.
- [14] S. Bickel, “Other tombs: queens and commoners,” in *Oxford Handbook of the Valley of the Kings*, K. Weeks and R. Wilkinson, Eds., Oxford Press, Oxford, UK, 2015.
- [15] J. E. Buikstra and D. H. Ubelaker, “Standards for data collection from human skeletal remains,” *Arkansas Archeological Survey Report 44*, Arkansas Archeological Survey, Fayetteville, Ark, USA, 1994.
- [16] B. Herrmann, G. Grupe, S. Hummel, H. Piepenbrink, and H. Schutkowski, *Prähistorische Anthropologie, Leitfaden der Feld- und Labormethoden*, Springer, Berlin, Germany, 1990.
- [17] H. Bach, “Zur Berechnung der Körperhöhe aus den langen Gliedmassenknochen weiblicher Skelette,” *Anthropologischer Anzeiger*, vol. 29, pp. 12–21, 1965.
- [18] R. Martin, *Lehrbuch der Anthropologie*, vol. 2, Gustav Fischer, Jena, Germany, 1928.
- [19] E. Breitingner, “Zur Berechnung der Körperhöhe an den langen Gliedmassenknochen,” *Anthropologischer Anzeiger*, vol. 14, pp. 249–274, 1939.
- [20] S. Ikram and A. Dodson, *Mummy in Ancient Egypt: Equipping the Dead for Eternity*, Thames and Hudson, New York, NY, USA, 1998.
- [21] Z. Hawass, Y. Z. Gad, S. Ismail et al., “Ancestry and pathology in King Tutankhamun's family,” *The Journal of the American Medical Association*, vol. 303, no. 7, pp. 638–647, 2010.

Research Article

Modeling Clinical States and Metabolic Rhythms in Bioarcheology

Clifford Qualls,¹ Raffaella Bianucci,^{2,3} Michael N. Spilde,⁴
Genevieve Phillips,⁵ Cecilia Wu,⁶ and Otto Appenzeller⁷

¹Health Sciences Center, University of New Mexico, Albuquerque, NM, USA

²Department of Biosciences, Centre for Ecological and Evolutionary Synthesis (CEES), University of Oslo, Oslo, Norway

³Department of Public Health and Pediatric Sciences, University of Turin, Turin, Italy

⁴Department of Earth and Planetary Sciences, Institute of Meteoritics, University of New Mexico, Albuquerque, NM, USA

⁵Cancer Research and Treatment, Center Fluorescence Microscopy Facility, University of New Mexico, Albuquerque, NM, USA

⁶Department of Pathology, University of New Mexico, Albuquerque, NM, USA

⁷New Mexico Health Enhancement and Marathon Clinics Research Foundation, Albuquerque, NM, USA

Correspondence should be addressed to Otto Appenzeller; ottoarun12@aol.com

Received 22 October 2014; Revised 26 November 2014; Accepted 11 December 2014

Academic Editor: Giuseppe Piccione

Copyright © 2015 Clifford Qualls et al. This is an open access article distributed under the Creative Commons Attribution License, which permits unrestricted use, distribution, and reproduction in any medium, provided the original work is properly cited.

Bioarcheology is cross disciplinary research encompassing the study of human remains. However, life's activities have, up till now, eluded bioarcheological investigation. We hypothesized that growth lines in hair might archive the biologic rhythms, growth rate, and metabolism during life. Computational modeling predicted the physical appearance, derived from hair growth rate, biologic rhythms, and mental state for human remains from the Roman period. The width of repeat growth intervals (RI's) on the hair, shown by confocal microscopy, allowed computation of time series of periodicities of the RI's to model growth rates of the hairs. Our results are based on four hairs from controls yielding 212 data points and the RI's of six cropped hairs from Zweeloo woman's scalp yielding 504 data points. Hair growth was, ten times faster than normal consistent with hypertrichosis. Cantú syndrome consists of hypertrichosis, dyschondrosteosis, short stature, and cardiomegaly. Sympathetic activation and enhanced metabolic state suggesting arousal was also present. Two-photon microscopy visualized preserved portions of autonomic nerve fibers surrounding the hair bulb. Scanning electron microscopy found evidence that a knife was used to cut the hair three to five days before death. Thus computational modeling enabled the elucidation of life's activities 2000 years after death in this individual with Cantu syndrome. This may have implications for archeology and forensic sciences.

1. Introduction

"Zweeloo woman," now held in the Drents Museum in Assen, the Netherlands, was discovered in 1951 in a bog and exhumed in the presence of an archeologist and a paleobotanist. Subsequent studies of her remains showed that she was of short stature and affected by bony abnormalities consistent with Léri-Weill dyschondrosteosis [1]. Her scalp hair, when examined 2000 years after her death, was found to have been crudely cropped [1]. We found she also suffered from hypertrichosis, an excessive hair growth over her entire body including the face [2].

Dyschondrosteosis together with hypertrichosis and cardiomegaly, an enlarged heart, is characteristics of a recently described genetic disorder called Cantú syndrome (CS) [3].

Fifteen CS cases have been described, the majority of Mexican-Mestizo descent. The condition is suspected to be dominantly inherited [3].

Here we use modern histological methods and computational modeling, applied to scalp hair. The results give insights into her clinical and mental state for a few days before her death ~2000 year ago and may shed light on her burial in a bog instead of the customary cremation and interment in a cemetery.

We used modeling to show that the neuroautonomic control of biologic rhythms, metabolism, and behavior can be deduced from ancient material such as hair.

Thus our aim of determining life's activities from archived remains has been validated by widely applicable computational methods.

2. Materials and Methods

The Drents Museum in Assen, the Netherlands, donated the tissues obtained from specimen #1957/XII-13. Vincent van Vilsteren, curator of the Drents Museums of Assen, the Netherlands, gave permission to study the material. The New Mexico Health Enhancement and Marathon Clinics Research Foundation (NMHEMC, Research Foundation) in Albuquerque NM, USA, carried out the analyses. The institutional review board of the NMHEMC Research Foundation approved the study. All necessary permits were obtained for the described study, which complied with all relevant regulations.

2.1. Scalp and Scalp Hair. A small piece $\sim 2 \times 5$ cm of brownish skin with reddish appearing hairs of varying length, in situ, was received for analysis. This was labeled "scalp skin of Zweeloo woman" without further description. Hair retrieved from bodies interred in bogs is usually, though not invariably, of a reddish discoloration because of the acidic environment of the bog.

2.2. Two-Photon and Confocal Laser Scanning Microscopy. We could not apply fluorescent stains to the tissue because of chemical changes in the skin-proteins (taphonomic changes) caused by the long immersion in the acidic bog.

Therefore, standard methods were used to visualize unstained images ($250 \mu\text{m}$ thick or single hairs) (Figures 1 and 4).

2.3. Scanning Electron Microscopy. The hair samples were coated with gold to provide better conductivity. A JEOL m 5800 electron microprobe (Figures 2 and 3) was used.

2.4. Biologic Rhythms. Our results were based on measuring the RI's of four hairs from controls yielding 212 data points and the RI's of six cropped hairs from Zweeloo woman's scalp yielding 504 data points.

The cropped hair remnants on the scalp skin were 10.4 mm, 9.1 mm, 11.4 mm, 12.2 mm, 17.9 mm, and 16.8 mm long.

2.5. Power Spectral Analysis of Repeat Intervals. We computed periodicities from the spectrum (periodogram) of a time series as a function of linear axis, such as, length along a strand of hair. We used growth rates in these measures to express frequency peaks in the spectrum as periodicities in units of days.

Determination of a high frequency peak is usually clear from the spectrum. However, determination of a low frequency peak can take several forms.

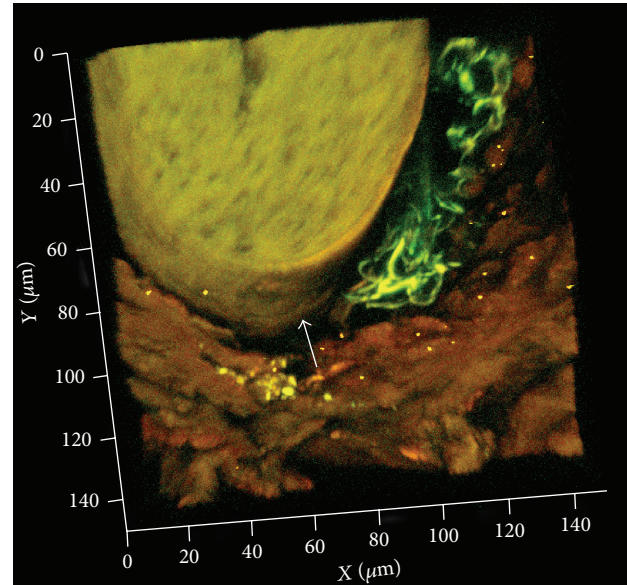


FIGURE 1: Three-dimensional image of the bog body's scalp skin by two-photon laser scanning microscopy. Unstained image ($250 \mu\text{m}$ thick) of an autofluorescent hair shaft with remnants of autofluorescent autonomic fibers in green adjacent to the hair root (arrow).

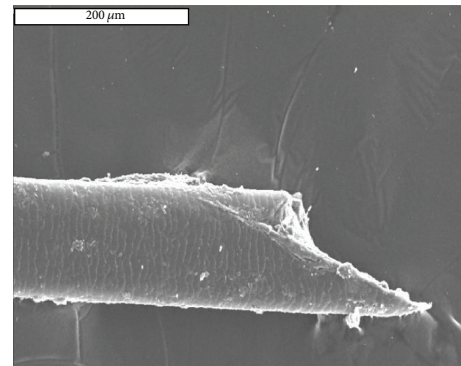


FIGURE 2: The end of a single scalp hair. Scissors would cut vertically across the hair; however, the shape of the cut suggests that this was made by a knife rather than scissors (scale bar in white above, $200 \mu\text{m}$).

In the time series of RI intervals (averaging 0.132 mm for short/medium hairs RI size = 0.214 mm for the longer hair remnants), there is a high frequency peak at 0.32 radians/RI in each series (see Figure 5(b)). The periodicity of this sinusoid cannot be 52 weeks, since the average long hair remnant length of 17.4 mm would represent 6.5 annual cycles with an improbable annual growth of only 3 mm per year (proof by contradiction).

The low frequency spectral peak for the Zweeloo long hair is at 0.045 radians/RI , which is a factor of 7 lower than the high frequency. Therefore, the high frequency represents a daily periodicity and the low frequency represents a weekly periodicity.

An identified spectral peak (i.e., a daily or annual cycle) can be used to compute hair growth rate; hence we then have

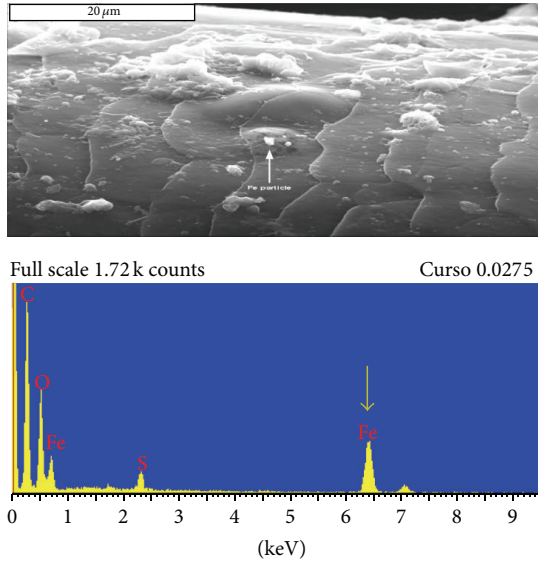


FIGURE 3: Particle (arrow) SEM image. This is the putative remnant of the hair cutting instrument, made of iron. Below, EDX of the particle showing the Fe peak of the spectrum (arrow).

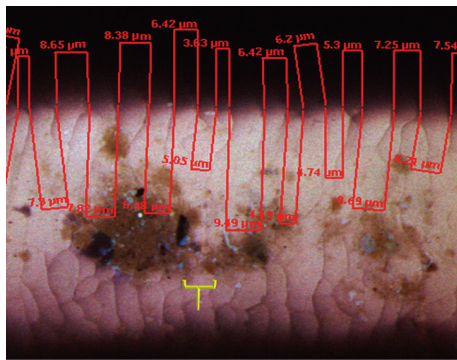


FIGURE 4: Confocal microscope image of single hair for measuring the repeat intervals (RI). The yellow bracket delineates the limits of one RI. Actual measures of some RI are shown in red. Brown patches are fungus growing on this hair.

an absolute time scale. The growth rate based on her longer hair remnant is estimated as (see formula below in legend to Figure 5) 153 cm/year ~10x the normal hair growth rate of 16 cm/year. Consider

$$\begin{aligned}
 &\text{Growth Rate} \\
 &= \frac{dt}{(\text{freq})(\text{Period})} \\
 &= \frac{0.214 \text{ mm/obs}}{(0.32 \text{ radians/obs})(1 \text{ day/cycle})} \frac{2\pi \text{ radians}}{\text{cycle}} \quad (1) \\
 &= 4.2 \text{ mm/day,}
 \end{aligned}$$

where each observation = a scale,
 which averaged = 0.214 mm/obs.

This formula is derived from [4]. The corresponding annual growth of 153 cm/year is ~10 times the average annual growth rate of 16 cm/year, consistent with hypertrichosis.

The spectra were computed using finite Fourier transform which decomposed time series into sums of sine and cosine waves of varying amplitudes and wave lengths. We used PROC SPECTRA from SAS version 9.3 for the statistical computations (Figures 6, 7, and 8).

The low frequency/high frequency (LFHF) ratios were significantly increased ($P < 0.02$) and the low frequency (LF) variance significantly decreased ($P = 0.02$) consistent with an increased sympathetic drive to metabolism and also increased heart rate and stress during life.

2.6. *Approximate Entropy (ApEn)*. To validate statistically our results we used approximate entropy (ApEn) [5]. This analysis can quantify the degree of regularity and unpredictability in the fluctuations of time series data such as those used in this study.

Here we used $m = 2$ and $m = 3$ windows. We found that values of 80% discriminated best for this analysis between controls and Zweeloo woman. The ApEn in Zweeloo woman was higher (Figure 8) thus her ANS was functioning well and reflected the robustness of her ANS function consistent also with sympathetic activation.

A typical case of hypertrichosis is illustrated in Figure 9. This shows why such excessive hair growth can be emotionally devastating leading to stress induced sympathetic activation and tachycardia as we surmise was present in Zweeloo woman before her death.

3. Results

Standard histological examination of the scalp was not possible due to protein degradation after 2000 years in a bog. However, using two-photon microscopy on 250 μm sections, we found preserved structures that appear to be hair and autonomic nerve fibers using the intrinsic fluorescence within the sample (Figure 1).

We then used the scanning electron microscope to visualize the end of her cut hair. This gave hints about the type of instrument used in her “hair cut” just before her death (Figure 2).

During the Roman period scissors and knives were made from either iron or copper [6]. We identify a particle on her hair by scanning electron microscopy, presumably, left from the “hair cut”; this was made of iron (Figure 3).

Energy-dispersive X-ray spectroscopy (EDX) is an accepted analytical tool used for elemental analysis applied here using the high-energy electron beam of the scanning electron microscope (SEM) used on the hair. We found iron particles on the surface of the hair (Figure 3), perhaps left by the cutting instrument. Additionally, this method of analysis revealed particles of the rare element, hafnium, which is, however, common in Dutch soil (not shown). Hafnium has also been found in hair and finger nail clipping of contemporaneous Scandinavian and Dutch people [7].

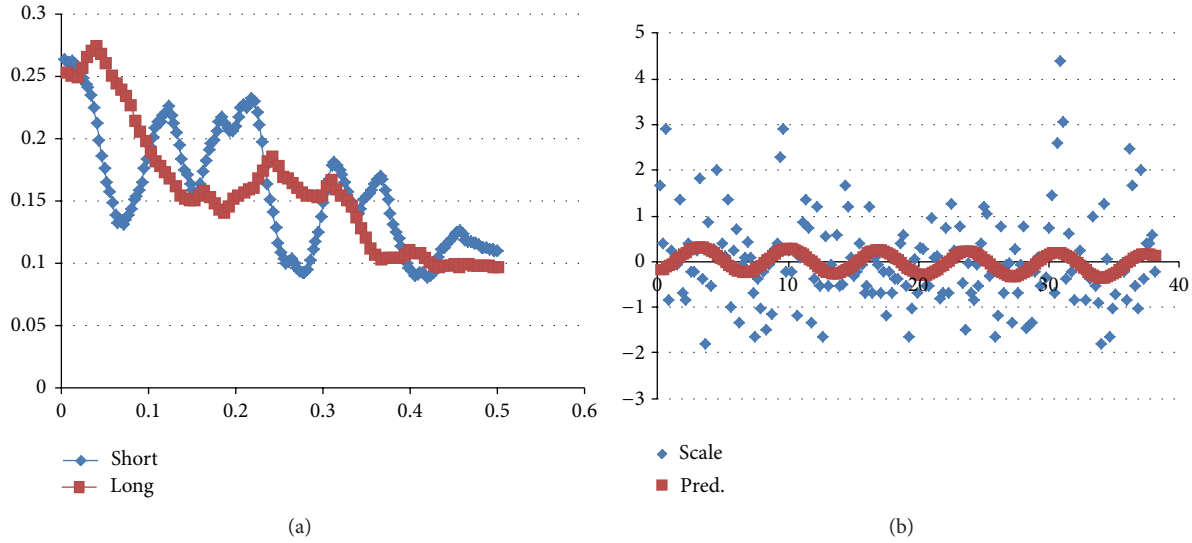


FIGURE 5: (a) Blue, control; red Zweeloo woman. Power spectra. (b) There is a high frequency peak at 0.32 radians/RI. The periodicity of this sinusoid cannot be 52 weeks, since the average long hair remnant length of 17.4 mm would represent 6.5 annual cycles with an improbable annual growth of only 3 mm per year (proof by contradiction).

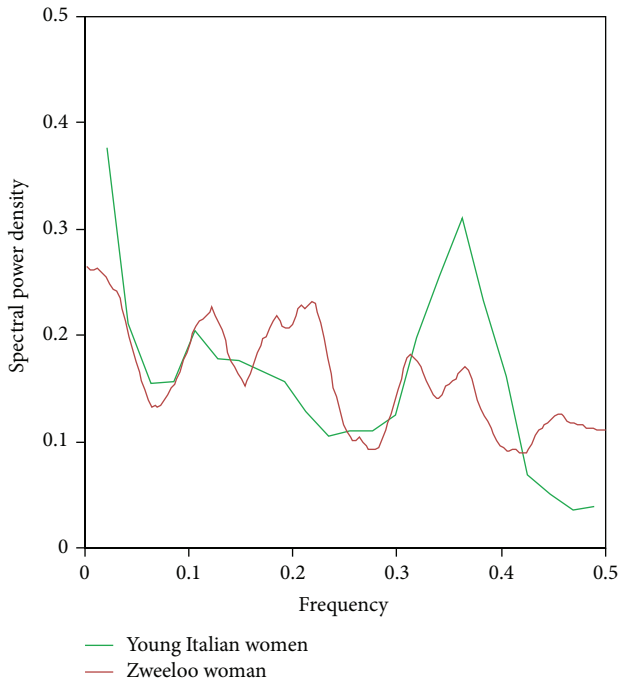


FIGURE 6: Comparative power spectra for a contemporary Italian woman's hair with normal growth rate of ~17 cm/year.

Using confocal microscopy images, we modeled the biologic rhythms by measuring the growth intervals, the widths of the repeat intervals (RI) on the hair (Figure 4) [8, 9].

Repeat intervals reflect hair growth; this in turn depends on metabolism which is affected by nutrition and environmental factors [8, 9]. Additionally, mental states in humans have overriding effects on the growth of the hair by affecting hormonal secretions and autonomic nervous system (ANS)

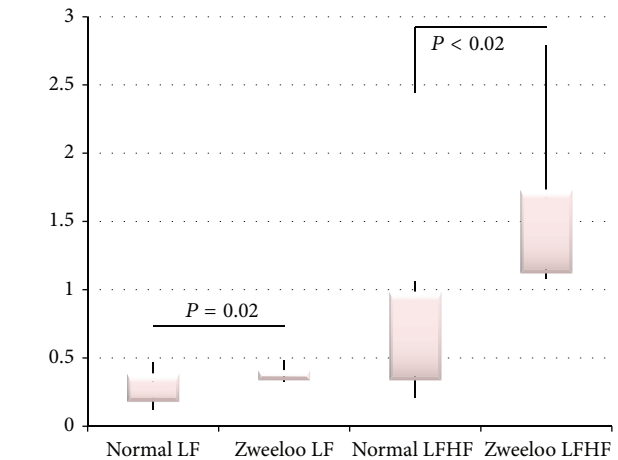


FIGURE 7: Modeled comparisons of Zweeloo woman's low frequency and LFHF ratios.

activity [10, 11]. Therefore, using modeling of the power spectra derived from the RIs inferences about the pathophysiology and mental state can be made [12].

The low frequency/high frequency (LFHF) ratios were significantly increased ($P < 0.02$) and the low frequency (LF) variance significantly decreased ($P = 0.02$) consistent with an increased ANS sympathetic drive (part of the ANS) to metabolism and also increased heart rate and stress during life.

To validate our model of metabolism we used approximate entropy (ApEn). This technique is used in the analysis of repetitive medical data such as heart rate variability [5, 13].

Approximate Entropy (ApEn). We used ApEn to measure the logarithmic likelihood that patterns of data length (m) that

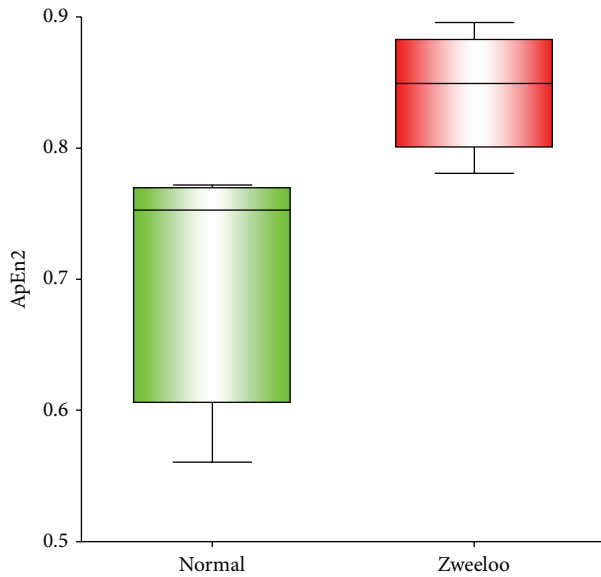


FIGURE 8: Approximate entropy (ApEn). The Low frequency/high frequency (LF/HF) ratios of the recurrent growth intervals (RI's) of normal (green) and Zweeloo woman's (red) time series.



FIGURE 9: Young girl with hypertrichosis (left) and similar aged control (right). Note exuberant hair on face and both forearms (arrows) (available at <http://www.mariasharapova.com/forum/>).

are similar remain so within a tolerance (r) on the next incremental ($m + 1$) comparison. In this analysis smaller values of ApEn indicate greater regularity in the data. Larger values are indicative of greater irregularities, more chaotic and more robust, systems (Figure 9).

4. Discussion

Bioarcheology is best described as the study of human remains from archeological excavations. This scientific endeavor deals with the examination of long dead tissues, mostly bone and hair. Therefore, life's activities such as metabolism, mood, and appearance cannot, usually, be determined from bioarcheological records. To do this suitable proxies are required using multiple methods to constrain inevitable uncertainties. Our study is based on a single specimen. Nevertheless, the multiple analytical methods and

proxies used allowed us to derive sufficient data to confirm our initial hypothesis.

Here we show that the archived records of hair growth in ancient specimens provide an opportunity to model metabolism, growth, physical appearance, and behavior of individuals who lived millennia ago.

We first confirmed from witness accounts of the exhumation in 1951 that the tissues were buried in a Dutch bog. This was also supported by typical deficiencies in histological staining of the tissues caused by long immersion in the acidic bog.

4.1. Skin and Hair. We could not assess the preservation of the skin by ordinary histological methods because of the degradation of proteins in the specimen caused by the acidic environment of the bog. However, thick sections revealed the structure of the hairs and remnants of autonomic nerve fibers surrounding the hair bulb by their retained autofluorescence (Figure 1).

Hair styling instruments such as knives and scissors during Roman times were made of either iron or copper [6]. The shape of the terminal end of the hair is consistent with a knife-cut rather than scissors because of its tapered appearance (Figure 2). Particles on the surface of the hair suggested that the knife may have been made of iron (Figure 3) rather than copper. Although other interpretations are also possible, notably, contamination from exhumation-instruments, these we consider unlikely in the context of this exhumation.

Using energy-dispersive X-ray spectroscopy (EDX) we also found remnants of bog-soil containing hafnium, on the surface of the hair. This rare element is commonly found in Netherland soil (P. van Gaans, personal communication).

4.2. Biologic Rhythms. Hair is a continuously growing tissue [11]. Like all growing tissues hair is subject to its own biologic time. The scale-like structures visible on the hair surface (Figure 4) reflect the rhythmic oscillations of growth and quiescence, the repeat intervals (RI) [9], paced by the hypothalamus, the "head ganglion" of the ANS, and master time-keeper of oscillating changes in gene expressions throughout all tissues [8, 10]. These signals, in turn, drive networks of intracellular proteins which affect the cycles of growth of the hair and other functions controlled by the ANS such as thermoregulation and especially metabolism [10]. Morphologically, the ANS signals can be identified; they correspond to the RI's of varying widths seen on microscopy of hairs (Figure 4) [8, 9].

Repetitive pattern in time series fluctuations, such as heart rate or metabolism, renders them more predictable whereas small numbers of repetitions in patterns make time series less predictable [5]. Time series with more repetitions have a small ApEn; those with fewer repetitions, therefore more chaotic patterns, have higher ApEn. We found that the ApEn of the low frequency/high frequency ratios in RI's were significantly larger in Zweeloo woman than in controls ($P = 0.01$) consistent with an enhanced sympathetic drive to metabolism (Figure 8).

The RI allowed us to determine the rate of annual hair growth [4], which for normal scalp hair is ~ 16 cm/year

[11]. We found a surprising 153 cm/year consistent with hypertrichosis, a condition characterized by an excessive hair growth [2]. Using the lengths of her cropped hair remnants we determined that she survived for ~3–5 days after the hair cut based on her excessive hair growth rate (~153 cm/year).

Biologic rhythms in living humans are often gleaned from heart rate variability which can be analyzed statistically by spectral methods [10, 14]. Such analyses give insights into health and disease of the subjects [10, 14].

We applied the same spectral methods to the analysis of the widths of the RI's in one of the best archived materials from archeological specimens, hair. Such analyses can also yield annual cycles of growth of the hair [4].

4.3. Cantú Syndrome. Previous studies based on her skeletal remains established that she suffered from Léri-Weill dyschondrosteosis which consists of bony abnormalities and clinically short stature [1]. This condition in combination with hypertrichosis and cardiomegaly constitutes a recently described syndrome designated Cantú syndrome [3].

Thus using archived material together with computational modeling we deduced her unusual physical appearance due to excessive hair growth and short stature and accelerated metabolic state including mental arousal. She survived for 3–5 days after the hair cut, as determined statistically 2000 years after death and burial in a Dutch bog.

Our results confirm that a record of metabolism and behavior is archived in the spectral power of the RI's of the hair which, in turn, gives insight into life as it was millennia ago and into other aspects of Zweeloo woman's last days before her burial in a Dutch bog.

Heart rate variability in health sciences has been extensively used as indicator of impending failure of metabolism (death) and for predicting progression of disease [10, 15]. Psychosocial investigations also use heart rate as a measure of emotions and arousal states of normal subjects [15]. We used the same computational methods applied to the RI of archived hair and were able to infer her unusual appearance during life and her emotional arousal for a few days before she died 2000 years ago.

4.4. Hirsutism. Idiopathic hirsutism is an inherited disorder associated with unusual physical features caused by excessive hair growth [16]. In the recent past, those afflicted with this disorder may have made their living by appearing in “freak-shows” such as Julia Pastrana born in 1834 in Mexico. She was sold to a freak show manager who exhibited human oddities throughout the United States and Canada. She suffered from hypertrichosis and gingival hyperplasia giving her an ape-like appearance. Darwin mentioned her in his book *The Variation of Animal and Plants under Domestication*. Because of her unusual appearance she was also considered the “missing link” between humans and apes. In modern times, this condition is usually associated with unexplained hairiness which affects 10% of otherwise normal women in the United States; the disorder implies abnormalities in androgen actions. Though hirsutism is not lethal, in severe cases, it causes significant mental trauma and anguish [16]. Zweeloo woman's hair grew at ~10 times the normal rate of

scalp hair [11] and she had excessive hair growing over her extremities (data not shown) which would have contributed to her unusual appearance.

Previous studies on Zweeloo woman [1] indicated short stature, otherwise normal health for that time in history, but failed to provide a definite clue for the reason of her unusual burial. We surmise that because of her marked hirsutism, short stature, and peculiar appearance that these physical features may have been decisive in leading to her burial in a bog.

4.5. Modeling. Advances in science can be made using computational modeling and validating the models with additional data. In bioarcheology and evolutionary genomics computational modeling has also recently been used [17, 18].

Here we use archived hair from the Roman period. We have validated our results in living people [12, 19] and in a variety of animals such as mammoths [20]. We also used RI's from different tissues such as teeth from humans and hominines [12] and confirmed our statistical methods in these additional growing materials.

The adoption of mathematical models successfully used in the analysis of repetitive physiological events such as power spectral analysis of heart rate variability [19] and in other repetitive physiological events, for example, growth and quiescence of growth, has numerous precedents [14]. In biology modeling has been applied to the analysis of tree ring repeat intervals and in ptilochronology [21], the biology of bird metabolism, deduced from repeat intervals found on bird feathers. In the analysis of ecological competition modeling using similar techniques is used to predict the abundance of bird species competing for food [22]. This method has also been applied to predict the size of industrial efforts necessary in producing materials such as concrete [14, 22].

Thus, power spectral analysis used in heart rate variability which yields insights into clinical states and emotional arousal of living people [15, 19] can be applied to the variation in the width of repeat intervals of growth and quiescence as evidenced in growth lines on ancient human hair. This application of a well established method promises to also broaden the scope of archeological and forensic investigations.

5. Conclusions

We show that valid deductions about metabolism, physical and mental states of long dead individuals can be made from archived hair by appropriate modeling.

Thus, we could derive metabolic data and evidence for emotional states of individuals who died millennia ago.

Our model could help in analyzing hair remnants in archeological remains and in forensic investigations.

Conflict of Interests

The authors declare that there is no conflict of interests regarding the publication of this paper.

References

- [1] R. Bianucci, D. Brothwell, W. van der Sanden et al., "A possible case of dyschondrosteosis in a bog body from the Netherlands," *Journal of Archaeology in the Low Countries*, vol. 4, pp. 37–64, 2012.
- [2] M. Palmetun Ekbäck, M. Lindberg, E. Benzein, and K. Arestedt, "Health-related quality of life, depression and anxiety correlate with the degree of hirsutism," *Dermatology*, vol. 227, no. 3, pp. 278–284, 2013.
- [3] B. Lazalde, R. Sánchez-Urbina, I. Nuño-Arana, W. E. Bitar, and M. de Lourdes Ramírez-Dueñas, "Autosomal dominant inheritance in Cantú syndrome (congenital hypertrichosis, osteochondrodysplasia and cardiomegaly)," *The American Journal of Medical Genetics*, vol. 94, no. 5, pp. 421–427, 2000.
- [4] Z. D. Sharp, V. Atudorei, H. O. Panarello, J. Fernández, and C. Douthitt, "Hydrogen isotope systematics of hair: archeological and forensic applications," *Journal of Archaeological Science*, vol. 30, no. 12, pp. 1709–1716, 2003.
- [5] S. M. Pincus and A. L. Goldberger, "Physiological time-series analysis: what does regularity quantify?" *The American Journal of Physiology—Heart and Circulatory Physiology*, vol. 266, no. 4, part 2, pp. H1643–H1656, 1994.
- [6] H. Eckardt and N. Crummy, *Styling the Body in Late Iron Age Roman Britain: A Contextual Approach to Toilet Instruments*, Éditions Monique Mergoïl Montagna, 2008.
- [7] J. S. Richman and J. R. Moorman, "Physiological time-series analysis using approximate and sample entropy," *The American Journal of Physiology—Heart and Circulatory Physiology*, vol. 278, no. 6, pp. H2039–H2049, 2000.
- [8] R. Paus and G. Cotsarelis, "The biology of hair follicles," *The New England Journal of Medicine*, vol. 341, no. 7, pp. 491–497, 1999.
- [9] T. G. Bromage, R. T. Hogg, R. S. Lacruz, and C. Hou, "Primate enamel evinces long period biological timing and regulation of life history," *Journal of Theoretical Biology*, vol. 305, pp. 131–144, 2012.
- [10] I. Cygankiewicz and W. Zareba, "Heart rate variability," *Handbook of Clinical Neurology*, vol. 117, pp. 379–393, 2013.
- [11] I. Rodushkin and M. D. Axelsson, "Application of double focusing sector field ICP-MS for multielemental characterization of human hair and nails. Part II. A study of the inhabitants of northern Sweden," *Science of the Total Environment*, vol. 262, no. 1-2, pp. 21–36, 2000.
- [12] O. Appenzeller, C. Qualls, F. Barbic, R. Furlan, and A. Porta, "Stable isotope ratios in hair and teeth reflect biologic rhythms," *PLoS ONE*, vol. 2, no. 7, article e636, 2007.
- [13] J. S. Richman and J. R. Moorman, "Physiological time-series analysis using Approximate entropy and sample entropy," *The American Journal of Physiology—Heart and Circulatory Physiology*, vol. 278, no. 6, pp. H2039–H2049, 2000.
- [14] T. Duque, M. A. Hassan Samee, M. Kazemian, H. N. Pham, M. H. Brodsky, and S. Sinha, "Simulations of enhancer evolution provide mechanistic insights into gene regulation," *Molecular Biology and Evolution*, 2013.
- [15] S. Wallot, R. Fusaroli, K. Tylén, and E.-M. Jegindø, "Using complexity metrics with R-R intervals and BPM heart rate measures," *Frontiers in Physiology*, vol. 4, article 211, 2013.
- [16] M. Ekbäck, K. Wijma, and E. Benzein, "It is always on my mind': women's experiences of their bodies when living with hirsutism," *Health Care for Women International*, vol. 30, no. 5, pp. 358–372, 2009.
- [17] L. J. Reitsema, "Beyond diet reconstruction: stable isotope applications to human physiology, health, and nutrition," *American Journal of Human Biology*, vol. 25, no. 4, pp. 445–456, 2013.
- [18] M. Roksandic and S. D. Armstrong, "Using the life history model to set the stage(s) of growth and senescence in bioarchaeology and paleodemography," *The American Journal of Physical Anthropology*, vol. 145, no. 3, pp. 337–347, 2011.
- [19] A. Malliani, M. Pagani, F. Lombardi, and S. Cerutti, "Cardiovascular neural regulation explored in the frequency domain," *Circulation*, vol. 84, no. 2, pp. 482–492, 1991.
- [20] M. Spilde, A. Lanzirotti, C. Qualls et al., "Biologic rhythms derived from Siberian Mammoths' Hairs," *PLoS ONE*, vol. 6, no. 6, Article ID e21705, 2011.
- [21] T. C. Grubb Jr., *Ptilochronology. Feather Time and the Biology of Birds*, Oxford University Press, 2006.
- [22] M. Scudellari, "Biology's coefficient," *The Scientist*, vol. 27, pp. 54–56, 2013.

Review Article

Frozen Mummies from Andean Mountaintop Shrines: Bioarchaeology and Ethnohistory of Inca Human Sacrifice

Maria Constanza Ceruti

Instituto de Investigaciones de Alta Montaña, Universidad Católica de Salta, Campus Castañares, 4400 Salta, Argentina

Correspondence should be addressed to Maria Constanza Ceruti; constanzaceruti@hotmail.com

Received 22 December 2014; Accepted 5 April 2015

Academic Editor: Andreas G. Nerlich

Copyright © 2015 Maria Constanza Ceruti. This is an open access article distributed under the Creative Commons Attribution License, which permits unrestricted use, distribution, and reproduction in any medium, provided the original work is properly cited.

This study will focus on frozen mummies of sacrificial victims from mounts Llullaillaco (6739 m), Quehuar (6130 m), El Toro (6160 m), and the Aconcagua massif. These finds provide bioarchaeological data from mountaintop sites that has been recovered in scientifically controlled excavations in the northwest of Argentina, which was once part of the southern province of the Inca Empire. Numerous interdisciplinary studies have been conducted on the Llullaillaco mummies, including radiological evaluations by conventional X-rays and CT scans, which provided information about condition and pathology of the bones and internal organ, as well as dental studies oriented to the estimation of the ages of the three children at the time of death. Ancient DNA studies and hair analysis were also performed in cooperation with the George Mason University, the University of Bradford, and the Laboratory of Biological Anthropology at the University of Copenhagen. Ethnohistorical sources reveal interesting aspects related to the commemorative, expiatory, propitiatory, and dedicatory aspects of human sacrifice performed under Inca rule. The selection of the victims along with the procedures followed during the performance of the *capacocha* ceremony will be discussed, based on the bioarchaeological evidences from frozen mummies and the accounts recorded by the Spanish chroniclers.

1. Introduction

The practice of human sacrifice has been known to occur cross-culturally throughout history. Humans have been sacrificed in order to celebrate special events, to mark royal funerals, in response to natural disasters, to atone for sins committed, to consecrate a special construction project or location, and to ensure fertility and health ([1]: 290; [2]). Sacrificial victims have also been executed in order to serve as retainers to high-ranking individuals in the afterlife. Inca human offerings should therefore be considered as being commemorative, expiatory, propitiatory, and or dedicatory sacrifices.

During the Late Post Classic Period in ancient Mesoamerica, the Aztecs embarked upon the practice of ritual of human sacrifice involving the removal of hearts in epic proportions (rooted in the Maya-Toltec tradition) based on their belief that human blood needed to be continuously offered to the Sun deity lest the god grow weak and not be able to continue his journey through the sky each day. Sacrifices celebrating

the completion of special constructions were conducted for such projects such as the dedication of the twin temples of Tlaloc and Huitzilopochtli in Mexico-Tenochtitlan. The Maya-Toltec sacrificial rites were not limited to the removal of the heart; they also included the flaying of the victim as well as the eating of his flesh ([3]: 51). The cruelty of these very public sacrificial events presumably served to reinforce the power of the Aztecs in the minds of allies as well as potential rivals.

In the ancient South American Andes, evidence of human sacrificial practices has been found depicted on Moche pottery (100 to 700 AD). The iconography of human sacrifice taking place on mountains seems to have been related to agricultural fertility rites and to the management of water resources ([4]: 35-36). But it was almost eight centuries later, under the rule of the Inca civilization, that the practice of human sacrifice on mountaintop shrines reached its highest level of cultural elaboration and expression.

The Inca Empire spread from its capital at Cuzco (located heartland in the Peruvian highlands) northwards to southern Colombia and as far south as central Chile. Since its

beginning in 1438 A.D. until the Spanish conquest in 1532 A.D. (a span of less than one hundred years), the *Tawantinsuyu* achieved the highest level of sociopolitical organization in the history of Andean civilization. During this period, the Incas constructed shrines on the summits of snow-capped peaks (over 5,000 m in elevation). These remote locations became the settings for the ritual performance of human sacrifice. The extraordinary preservation of the victims' bodies as well as of many of the grave goods recovered in the extremely cold and dry high elevation Andean environment provides exceptional bioanthropological evidence (both osteological as well as soft tissue) for the study of human sacrifice among the Incas.

The frozen bodies of three Inca children were discovered by Johan Reinhard and the author of this paper on the summit of mount Llullaillaco, at an elevation of 6715 m, at the world's highest archaeological site. They are considered to be among the best preserved Precolumbian mummies known to date. They have been previously analyzed in the context of the diversity of mummies worldwide [5]; as objects of dedication [6], in connection to the religious role of children in the Andes [7], as actors in the ceremonies of *capacocha* [8, 9], and as objects of paleopathological and medical research [10].

Numerous interdisciplinary studies were conducted on the frozen mummies from mount Llullaillaco during the years in which they were preserved at the Catholic University of Salta (see Figures 14 and 15). These studies included radiological evaluations by conventional X-rays and CT scans, which provided information about condition and pathology of the bones and internal organs; as well as dental studies oriented to the estimation of the ages of the three children at the time of death [11–13]. Ancient DNA studies and hair analysis were also performed in cooperation with academic institutions including the George Mason University, the University of Bradford and the Laboratory of Biological Anthropology at the University of Copenhagen [14–16].

The archaeology of mount Llullaillaco, including its architectural and landscape features, has been studied and published in the context of Inca religion and sacred landscape in the Andes [17–19]. The material offerings associated to the Llullaillaco mountaintop burials have been described and studied in terms of their social use and symbolic meaning [17]. Expert work has been undertaken on the technological analysis of the textile objects; and pottery items have been subjected to neutron activation analysis to help identify their geographical origin. The results of pottery analysis have demonstrated that the ceremonial items buried together with the Llullaillaco mummies had been manufactured in Cusco and around Lake Titicaca, while some of the pottery found at the foot of the volcano came from northern Chile [20]. This is in with what would be expected in the context of a state sponsored pilgrimage of *capacocha*, in which ceramic offerings carried to the summit of a mountain were customarily brought from Cusco or the Bolivian highlands, while utilitarian pottery used at base-camp could be of local origin.

This study will focus on the frozen mummies of sacrificial victims from mount Llullaillaco (6739 m), volcano Quehuar (6130 m), mount El Toro (6160 m), and the Pyramid of the

Aconcagua massif. These finds provide a robust and valuable amount of bioarchaeological data from Inca mountaintop shrines that has been recovered in scientifically controlled excavations in the northern and western regions of Argentina. Reference will also be made to mummies excavated under nonscientifically controlled digs from Mt. Chañi and Mt. Chuscha in Argentina, and from Mt. El Plomo and Cerro Esmeralda in Chile. These peaks are mainly located in areas of modern day northwestern Argentina, as well as north and central Chile, and were once part of the southern province of the Inca Empire, known as *Collasuyu*.

Ethnohistorical sources reveal interesting aspects related to the commemorative, expiatory, propitiatory, and/or dedicatory aspects of human sacrifice performed under Inca rule. The selection of the human victims along with a description of the procedures followed during the performance of the sacred *capacocha* ceremony will also be discussed, based on the bioarchaeological evidences from frozen mummies and the accounts recorded by the Spanish chroniclers.

2. Inca Human Sacrifice in the Historical Sources

An Inca *capacocha* ceremony involved the movement of sacrificial victims (along with various ceremonial goods) from the peripheral communities of the conquered provinces towards the centrally located capital city of Cuzco. After being ritually transformed into Inca-style offerings in the capital city, the sons and daughters of local chiefs, as well as the chosen Virgins of the Sun god, were then made to travel in ritual procession, to various sacred places located throughout the empire. They eventually would be sacrificed and buried at designated locations as vivid representations of the state cult to the sun god Inti, as well as an imperial homage to the local sacred sites, known as *huacas*.

The term *capacocha* consists of two Quechua words: “*capac*” meaning “royal” and “*cocha*” the word for “lake” or “body of water” ([21]: 134, 559). According to Reinhard [22], the *capacocha* would serve as a powerful public manifestation of the Inca's power to organize such propitiatory rituals. Based on the fact that the Quechua word *hucha* can signify “sin,” interpreted “*capac-hucha*” as the ritual procedure designed to atone for transgressions committed and to prevent misfortune that could affect the Inca ruler and his empire.

Human sacrifice being strictly under the control of the Inca State, ethnohistorical sources specify that the ritual killing of native Andean people could only occur with the explicit approval of the emperor:

...*Cuando el dicho Inca quería hacer algún sacrificio y aplacar alguna guaca [...] entonces por su orden mataban algunos indios y los sacrificaban a los cerros y guacas que enviaba a mandar el dicho Inca, y que sin su orden no podían sacrificar indios* ([23]: 330).

2.1. Celebratory Sacrifices. Certain events of the life of the emperor were celebrated by means of human sacrifices. The chroniclers report that sacrifices took place upon the coronation of a new Inca ruler ([24]: 92; [25]: 26). Reportedly,

two hundred children were sacrificed when a new ruler assumed the throne ([26]: 87) and even the birth of the son of the emperor was celebrated with sacrifices ([27]: 93). Other important events, such as the victorious return of the Inca from battle, called for the sacrifice of war prisoners in thanksgiving to the Sun God Inti for a successful military campaign ([28]: 143).

2.2. Funerary Sacrifices. Under the Inca rule, ritual killing of wives and servants was performed as *necropompa*, in order to provide a deceased emperor with a fitting cadre of servants in the afterlife. Chroniclers report that 1,000 persons were sacrificed upon the death of Inca Emperor Huayna Cápac ([29]: 118), although other sources mention that the number of victims was over 4,000 ([30]: 80). According to chronicler Bernabe Cobo, many victims would voluntarily offer to be sacrificed so that they could join those servants who had already been killed in order to serve the deceased ruler in the hereafter ([28]: 161). Chronicler Santa Cruz Pachacuti refers to the ritual homicide of wives and servants as an example of commemorative sacrifices undertaken by the Inca State after the death of an emperor:

Se entierra a muchos yanás, mujeres y criados amados del dicho Inca; todos estos eran escogidos, entendiendo que el Inca había de ser servido en la otra vida ([31]: 306).

2.3. Sacrifices of Atonement in Response to Natural Disasters. Sacrifices were often conducted in response to natural calamities, such as droughts, epidemics, earthquakes, and volcanic eruptions ([32]: 112; [33]: 155; [34]: 48). According to a Spanish chronicler:

...el sacrificar niños u hombres era para cosa de gran importancia, como pestilencia grande o mortandad... ([29]: 193).

These acts of atonement involving human sacrifice were based on their belief that illness and natural disasters were forms of supernatural punishment for sins committed or for the improper performance of various sacred rituals. Only a major offering such as a human life could serve to reestablish the spiritual equilibrium with the cosmos ([35, 36]: 426-427):

Tenían por opinión que todas las enfermedades venían por pecados que se hubiesen hecho. Y para el remedio usaban de sacrificios ([29]: 12).

Chronicler Martín de Murúa ([34]: 48) reports that during the devastating eruption of the Misti Volcano in 1440, Mama Ana Huarque Coya, queen and wife of Emperor Pachacutec Inca Yupanqui, ordered many sacrifices to be performed in various temples throughout Cuzco in the hopes that this would assuage the supernatural lord's (*apu*) anger. The volcanic activity ceased only after Pachacutec himself traveled with several priests and shamans to the massif (located near Arequipa, Peru) to personally make sacrificial offerings designed to calm the divine fury of the mountain:

Así mostró su incomparable ánimo y ser en un terrible terremoto que hubo en su tiempo en la ciudad de Arequipa, resultado de un volcán temeroso que está a tres leguas de la dicha ciudad. El cual cuentan los indios que lanzó de sí tanto fuego y con tan espantosas llamaradas, que en muchas

leguas quedaron los indios atónitos y absortos. Fue cierto haber revocado y salido del volcán tanta ceniza que llovió en todo el reyno, con universal admiración y miedo. Si no fuera por el ánimo de esta Coya Mama Ana Huarque se hubiera asolado la mayor parte de la gente de todas las provincias cercanas a Arequipa. La cual mando lo primero hacer grandísimos sacrificios a sus ídolos en el templo que ellos llaman Tipci Huaci, que quiere decir casa del universo, y en otros muchos que había en el Cuzco, hasta que sabido por el Inga Yupanqui, su marido, vino con suma prisa dentro de pocos días y se partió a Arequipa con muchos pontífices, adivinos y hechiceros, y llegado cerca, hizo diversos sacrificios... ([34]: 48).

2.4. Sacrifices to Consecrate a Special Construction Project or Location. Chronicler Betanzos reports that the construction of the Temple of the Sun in Cuzco was preceded by *capacocha* ceremonies in which several children sent by the local rulers were buried alive in the sanctuary as a way to consecrate the "sacred space" of the place of worship ([27]: 46). According to the chronicler Rodrigo Hernández Príncipe [37], the sacrifice and burial of a ten-year-old girl on a summit near her natal village was performed to assure successful completion of a new irrigation canal. Some human sacrifices may also have served as a means of establishing boundaries along the periphery of the ever expanding Inca Empire ([38]: 551; [39]: 371; [40]: 18).

2.5. Fertility and Health Sacrifices. The Incas dedicated human offerings to the Sun god Inti, to the Weather (Thunder) deity Illapa, and to the Creator god Viracocha, as well as to local deities (*huacas*) in order to ensure the fertility of the crops and to plead for favorable weather as well as to petition for the good health of the emperor. In the words of Cobo:

They made sacrifices to the Sun so that he would make the plants grow, to the Thunder, so that he would make it rain and not hail or freeze, and to the rest of the special gods and second causes. First they would speak with Viracocha and afterwards they would speak with the special gods. And in their sacrifices to all the universal huacas they would plead for the health of the Inca ([32]: 111).

In 1571, a group of Inca men informed the Spaniards that the *capacocha* offerings were made in order to ensure favorable weather for crops ([33]: 155). Reinhard and the author have extensively analyzed the symbolic link between the worship of sacred mountains, by means of offerings and sacrifices, and the propitiation of fertility in ancient and modern times in the Andes [19, 41].

3. Bioarchaeological Evidence of Inca Human Sacrifice on High Andean Mountains

The climax of the Inca *capacocha* ceremony involved the sacrifice of children and their burial with lavish grave goods, such as *cumbi* textiles, fine pottery, and figurines made of gold, silver and *Spondylus* shell. After the long processions to the sacred summits, these children would be sacrificed and thus be sent on a supernatural pilgrimage in the hereafter



FIGURE 1: Mount Chañi in northern Argentina (© Constanza Ceruti).

where they served as messengers to the world of the ancestors and deities.

Archeologically, the sacrifices performed in the context of an Inca *capacocha* can be identified by (a) the location of the burial site (often on mountaintops), (b) the age and sex of the victims, usually boys and girls under the age of ten, and/or (c) teenage women who were part of the so called “*acllas*” or “chosen ones.” Inca offerings for *capacocha* ceremonies include pottery of imperial style, textiles, and miniature figurines made of metal and shell, representing individuals of the same sex as the victim sacrificed (Figure 16). Alternatively, other kind of human sacrifices, such as those performed during the *necropompa* of a dead emperor, might include victims of older ages, selected among the spouses, concubines, and servants of the Inca.

One of the earliest sources of evidence for Inca human sacrifice on mountaintop shrines came from a case of looting that occurred in 1905, when the naturally mummified body of a child was extracted from the summit of Mt. Chañi, a 5896 m peak located in northern Argentina (Figure 1). Items included with the mummy were tunics, two belts, one comb, one bag covered in feathers and a pair of sandals [42, 43]. Various archaeological surveys were conducted by the author on the Chañi massif during 1996 and 1997 [44], and three years later, research at this same site was directed by Johan Reinhard and the author. This investigation resulted in the discovery of the burial place of the Chañi infant [45].

In 1922, looters removed the body of a young female mummy that was buried with associated offerings including a *cumbi* tunic, a textile bag, one belt, three combs, and a feather adornment made from tropical birds on her head [46]. Interdisciplinary research on the Chuscha mummy (Figure 2) was later coordinated by Dr. Juan Schobinger, Emeritus Professor of Archaeology at the National University of Cuyo [47]. The mummy had been extracted from one of the summits of Mt. Chuscha (over 5300 m), in northwestern Argentina. The burial site was relocated during a high-altitude survey by the author in 1996 [48].

It was the discovery by treasure hunters in 1954 of the frozen body of an 8-year-old boy on Mt. El Plomo in central Chile that captured the attention of the archaeological community. Although the artifacts were not recovered in



FIGURE 2: Mummy from mount Chuscha (© Constanza Ceruti).

a scientifically controlled excavation, they did yield a substantial amount of valuable data [49]. The child seems to have died of exposure to the cold or may have even been buried alive [50].

In 1964, mountain climbers Antonio Beorchia Nigris and Erico Groch came across the frozen body of an adult male that was found inside a circular stone structure (located near an Inca ceremonial rectangular structure) at over 6000 m in elevation on Mt. El Toro (Figure 4) in western Argentina. Archeologist Juan Schobinger recovered the mummy and conducted an investigation which revealed that the man had apparently been killed by strangulation. Wearing only a breechcloth, the victim had been buried with a set of objects including a mantle, two ordinary tunics, a woolen cap, two pair of sandals, a sling, and feathers [35]. A more recent survey of the southern slopes and summit of El Toro (Figure 3) did not reveal further traces of the prehispanic use of ritual space on the mountain [51].

In 1976, a road construction crew came across the burial of two females (1 child and 1 adult) near the summit of Mt. Esmeralda found along the north coast of Chile. Although this mountain is relatively low in elevation, it nevertheless still dominates the coast when viewed from the ocean. The human remains found at the site had been preserved by desiccation and many artifacts were found in association with the mummies, albeit not in a scientifically controlled excavation. Nonetheless, the items recovered, which included *cumbi* cloth, fine Inca pottery, and *Spondylus* shell, clearly indicated that this burial was a *capacocha* offering and furthermore, the victims seemed to have been killed by strangulation [52, 53].

In 1985, mountain climbers came across the frozen body of a seven-year-old boy who was found inside a semicircular stone structure (over 5300 m in elevation) on the slopes of Mt. Piramide located in the Aconcagua massif of western Argentina (Figure 5). The mummy and the offerings associated with it were recovered and studied by a team of scholars led by Juan Schobinger. The victim had been killed by a blow to the head, although he also had ribs broken by compression during the process of bundling the body. He was dressed in two tunics, wearing sandals and a necklace of stones. The bundle contained several textile mantles (one was covered in feathers of highland birds) and a feathered

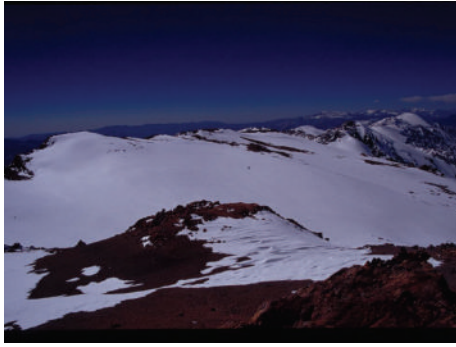


FIGURE 3: Summit of mount El Toro (© Constanza Ceruti).



FIGURE 4: Mummy from mount El Toro (© Constanza Ceruti).

headdress, woven belts, and five tunics, some of them woven in *cumbi*, three breechcloths, a pair of sandals, and two bags. Inside the tomb were found three male figurines made of gold, silver, and *Spondylus* shell, which were adorned with feathers of rainforest birds. In addition to these items, two llama figurines made of *Spondylus* shell and a silver figurine representing a camelid were found [54]. Red pigment was identified on the boy's skin, and on his tunic, traces of which were found in the victim's vomit and feces [55].

Mt. Misti is a steep sided, cone shaped volcano (5,822 m in elevation) found near the city of Arequipa in southern Peru (Figure 6). It is located in what once was the western Inca province of *Cuntisuyu*, (the Ampato and Sara Sara Volcanoes are also found in this region). Misti is one of the few active volcanoes that erupted during the historic Inca period, and various chroniclers (mentioned above) report that both ritual offerings and sacrifices were conducted at this site in response to this activity. In 1998, Johan Reinhard, José Chavez, Constanza Ceruti and a team of collaborators, excavated the Inca ceremonial site located inside the volcano's crater, which is marked by unimpressive rectangular and circular alignments of stones. The recovery of the bodies of six human sacrificial victims and more than forty statuettes (one of the largest *capacocho* assemblages ever found) demonstrated the importance of this site to the Incas [19]. Unfortunately, the preservation of the bodies and textile offerings on Misti was very poor, due to the high concentration of sulfur in the soil and the high temperatures within the crater.



FIGURE 5: Mummy from mount Aconcagua (© Constanza Ceruti).



FIGURE 6: Volcano Misti in Arequipa (© Constanza Ceruti).

Mt. Quehuar, a 6130 m extinct volcano in the highlands of northwestern Argentina, holds one of the most impressive Inca mountaintop shrines in the Andes (Figure 7). The summit's architectural complex included an artificial raised platform (*ushnu*) measuring over 6 m long and 1.7 m high, with a frontal ramp, as well as a circular stone structure with walls more than 2.2 m high and 1.2 m thick [19]. In 1999, Johan Reinhard, José Antonio Chávez and the author directed a National Geographic Society sponsored excavation of this particular Inca shrine. A human sacrificial victim had been originally buried inside the circular structure, but looters had employed dynamite to gain access to the tomb. The blast left scattered pieces of the offerings including textiles, fragmented pottery, corn seeds, meat, and bones from a sacrificed camelid strewn about the site. A typical Inca style female figurine made of *Spondylus* shell and dressed in miniatures of *cumbi* clothes was recovered from the *ushnu* platform [56]. Apparently, a small damaged tunic had also been found at the same structure in 1974 ([57]: 188–200). Subsequent DNA analysis conducted on the individual buried on the summit of Mt. Quehuar revealed that it was female [58] but given the poor preservation of the remains (stemming from the use of explosives in the recovery of the body), it was



FIGURE 7: Inca platform on the summit of mount Quehwar (© Constanza Ceruti).



FIGURE 9: The author climbs to the top of volcano Llullaillaco (© Constanza Ceruti).

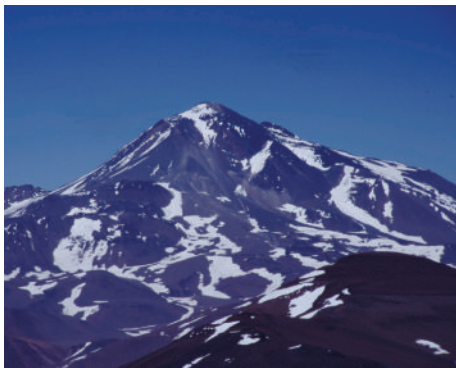


FIGURE 8: Volcano Llullaillaco in northern Argentina (© Constanza Ceruti).



FIGURE 10: Inca shrine on the summit of mount Llullaillaco, the highest ceremonial site in the world (© Constanza Ceruti).

impossible to establish the cause of death. However, due to the types of artifacts recovered in association with the body, it is parsimonious to conclude that this was a *capacocho* sacrifice. The victim was about twelve years old at the time of her sacrifice, according to estimations based on the length of her long bones, as they appeared in the X-rays.

On the summit of Mt. Llullaillaco (6739 m), in north-western Argentina (Figure 8), Johan Reinhard and the author of this paper directed an archaeological expedition funded by the National Geographic Society, which took place in March 1999 (Figure 9). At an elevation of 6.715 m, the summit shrine of Llullaillaco is the world's highest archaeological site (Figure 10). Excavations at the main ceremonial structure (a rectangular stone platform) revealed three separate burials and several offering assemblages. One young woman, one girl, and one boy were found together with more than one hundred offerings comprising metal figurines, *Spondylus* shell, fine imperial pottery, *cumbi* textiles, and feathered adornments of tropical birds, all in an excellent state of preservation (cf. [19, 59]).

The Llullaillaco boy, who was 7 years old, was wearing a red tunic, leather moccasins, fur anklets, a silver bracelet, and a sling wrapped around his head, with his forehead adorned with white feathers (Figure 13). Two figurines were found, one representing a man and the other a llama, which had been placed on the ground, close to the body. An aryballo (an Inca ceramic vessel) that had contained *chicha* (an Andean corn

beverage) was recovered in the fill of the tomb, as well as a *Spondylus* seashell [19]. The body of a six-year-old female had apparently been hit by lightning after she had been buried in the tomb. She was wearing a sleeveless dress and a shawl, both kept in place with metal pins, moccasins on her feet and a metal plaque on her forehead. Textile and ceramic items, as well as metal figurines, were placed around her body on the bottom of the tomb ([59]: 60-61).

The Llullaillaco maiden (Figure 12) was about 15 years old at the time of her sacrifice ([60]: 7). Her body was placed in the tomb facing northeast and was covered with two brown outer mantles. A feathered headdress was placed on her head and an exquisite *cumbi* tunic on her shoulder outside of the funerary bundle. Her hair was combed in numerous intricately woven braids. Her offering assemblage also included textile bags and belts, gold and silver figurines, and various ceramic items ([59]: 59-60). Excavations also brought to light several additional sets of offerings containing metal and *Spondylus* shell statuettes, some of which included two male figurines at the head of a row of metal and seashell figurines representing llamas.

4. Discussion

Bioarchaeological findings of frozen mummies on the summits of high altitude Andean peaks indicate a high degree of

correspondence with the ethnohistorical descriptions written by various chroniclers on the Inca ceremonies of human sacrifice with regards to the profile of the victims chosen and the sacrificial techniques involved. Ideological motifs that were invoked to legitimize the need for a *capacocha* ceremony would have contributed to the acceptance of the ritual violence exerted by the Inca Empire during its territorial expansion.

The chroniclers report that children were selected to serve as messengers to the gods because their “purity” made them the most fitting mediators between humans and deities ([61]: 233; [37]). The parents of sacrificial victims were expected to surrender their children willingly and were encouraged by the Inca to consider the selection of their offspring for *capacocha* as a great social honor as well as being an act of pious devotion ([32]: 112; [37]; [25]: 81).

Ethnohistorical sources state that the boys chosen for sacrifice during *capacocha* ceremonies were expected to be between four and ten years old ([62]: 342; [29]: 37; [28]: 235). Bioarchaeological findings are consistent with these reports as it has been determined that the Aconcagua and Lulllaillaco boys were approximately seven years old at the time of their deaths.

The Inca Empire institutionalized a system of selection, seclusion, and redistribution of “chosen women” or *acllas*, who were taken from their homes prior to the onset of puberty and kept in special houses or *acllahuasi*. Here they were kept under the close surveillance of consecrated women known as *mamacona* who would teach the young girls to weave and to prepare chicha ([62]: 333). At the age of 14, the young women were taken out of the *acllahuasi* and some would be selected to be given as secondary wives to nobles while others would be consecrated to serve as priestesses or Wives of the Sun. However, some of the girls were chosen for the *capacocha* ([63]: 241). The young female from Mt. Lulllaillaco (Figure 11), the famous “Ice Maiden” found on Mt. Ampato in Peru [64, 65] and the girl from the summit of Peru’s Mt Sara Sara [66] appear to have been *capacocha* sacrificial victims because they all were all females of approximately 14 to 15 years of age and they were found with various ceremonial goods that are the same items that ethnohistorical sources report as being *capacocha* ritual offerings ([27]: 77; [37]: 473; [62]: 319; [24]: 96). Reinhard has noted that girls found on mountaintop burials tend to be older than boys because they would have been kept as virgins until being sacrificed ([32]: 112), whereas there was no institution equivalent to the *acllahuasi* to ensure a virginal condition on the boys.

All different types of Inca human sacrifices described in the historical sources, including *capacocha* and necropompa, have been identified archaeologically in diverse funerary contexts excavated in the Andes of Peru, Chile, and Argentina. The bioarchaeological evidences discussed in this paper can all be interpreted as the outcome of Inca ceremonies of *capacocha*. The only exception could be the mummy found on Mt. El Toro, since an adult male cannot easily be considered a classic *capacocha* offering. This would also account for absence of statues or other sumptuous offerings in his burial.



FIGURE 11: Constanza Ceruti discovering an Inca female mummy on the summit of Lulllaillaco (© Constanza Ceruti).



FIGURE 12: The Lulllaillaco Ice Maiden (© Constanza Ceruti).

With regards to their social ranking, the chroniclers state that the children chosen for sacrifice were expected to be sons and daughters of nobles and local rulers ([27]: 78). Some of the victims were intentionally sent by their high status parents, in order to reinforce their political ties to the emperor and to be reaffirmed in their privileged positions of power ([37]: 472). From the bioanthropological perspective, the relatively good state of nutrition that the Lulllaillaco children seemed to have enjoyed in life, as reflected in the thick layer of fatty tissue appearing in CT-scans as well as the absence of Harris lines in the X-rays, [12, 13], serve as indicators of the high social rank of these victims. From an archaeological perspective, the fact that the bodies were recovered in association with sumptuous items such as *cumbi* tunics that served specific diplomatic functions (i.e., only the emperor could give such a gift to a local ruler as a token of his good will) indicate the high social status of these sacrificial victims [19].

4.1. Sacrificial Procedures. During *capacocha* ceremonies, children could alternatively be sacrificed by strangulation ([67]: 150), by a blow to the head ([28]: 235; [61]: 233; [25]: 25), by suffocation ([62]: 263; [25]: 26), or by being buried alive ([27]: 46; [28]: 235).

Strangulation seems to have brought about the death of the two female mummies on Cerro Esmeralda [52], as well as for the man from Mt. El Toro [35]. Radiological studies have



FIGURE 13: Inca mummy of the Llullaillaco boy (© Constanza Ceruti).



FIGURE 14: Interdisciplinary studies on the Llullaillaco maiden at the Catholic University of Salta (© Constanza Ceruti).

indicated that cranial trauma was the cause of death in the case of the Mt. Ampato maiden [65] as well as in the case of the female mummy found on Mt. Sara Sara [66]. This may also have been the sacrificial technique used to kill the boy on Mt. Aconcagua ([40]: 8). However, CT-scans and X-rays taken of the skulls of the three individuals from Llullaillaco indicated no evidence of trauma to the head [12, 13].

The practice of burying children alive or of suffocating them prior to burial is both compatible with the physical evidence of the Llullaillaco children [12] and the El Plomo boy [50]. Apparently, the reason for selecting this particular sacrificial procedure was rooted in the belief that only “complete” offerings were acceptable to a major deity. A victim who had shed blood would have been considered to be an “incomplete” offering in the eyes of the Incas ([62]: 263-264).

The case of the Llullaillaco boy suggests that death came to him as the result of exhaustion or high altitude sickness (or a combination of both), before he actually reached the summit. The relaxed position of his arms differs from the usual that mountain top sacrificial victims typically show (with their arms flexed over the body like in perimortem attempt to preserve body heat). The fetal position of the body and the tight wrapping of cords around his legs could also have been induced to facilitate the transportation of the corpse to the summit [17]. Additionally, the swap analysis of the lips of the boy has demonstrated the presence of blood in



FIGURE 15: Interdisciplinary studies on Llullaillaco mummies (© Constanza Ceruti).



FIGURE 16: Inca offerings from mount Llullaillaco (© Constanza Ceruti).

the saliva, which can be interpreted as a sign of pulmonary edema [10].

The sacrifice of children by means of burying them alive was still in use during the first decades of the Hispanic invasion. Chronicler Ramos Gavilan reports that in 1598, a ten-year-old Andean girl was found by a European miner still alive three days after she had been ritually walled inside a funerary tower (*chullpa*) by the local chiefs of the village of Sicasica, near Caracollo, in the Bolivian highlands ([25]: 66). Antonio de Herrera Tordesillas’s account tells of a young Andean boy who sought refuge among the Spaniards in the Xauxa Valley (in the Peruvian Sierra), after he narrowly escaped from being ritually buried alive in occasion of the death of a local chief ([30]: 67).

4.2. Mountaintop Capacochas as Commemorative, Expiatory, Propitiatory, and Dedicatory Inca Sacrifices. *Capacocha* ceremonies that took place on volcanoes located in remotely located areas of the empire, such as the arid Atacama highlands in the case of Llullaillaco, were most likely related to the commemoration of events in the life of an Inca emperor, rather than motivated by the need to ritually respond to locally occurring natural disasters. However, expiatory or propitiatory rituals conducted with the goal of affecting local conditions could have played a part in the sacrifices performed on mountains near well populated areas, such as in the case of Mt. Chañi (near Quebrada de Humahuaca)

or on Mt. Chuscha (near the Calchaquí Valley, in northern Argentina).

It is clear that both the archaeological and historical evidence support the hypothesis that human sacrifices seeking atonement were conducted on sacred summits in response to natural calamities (such as volcanic eruptions) in the hopes that such actions would put an end to the particular phenomena that was causing strife. This seems to have been the case with the offerings and human sacrifices performed inside the crater of the active Misti Volcano [19, 68].

The propitiation of fertility is suggested by the presence of *Spondylus* shell in the offerings recovered in the burials of the sacrificial victims on mounts Lullaillaco, Quehwar, Esmeralda, Chuscha, and Aconcagua. From pre-Inca times to this very day, *Spondylus* has been a ritual material of high symbolic importance in the Andes since it is believed to be related to both seawater and rain [22, 41]. Concerns about the fertility of camelids appear to be physically expressed in the assemblages of figurines on Lullaillaco and Misti, which seem to represent a caravan of llamas [17, 19].

Dedicatory rituals involving human sacrifice appear to have been performed by the Inca on mountaintop shrines because the burial of victims at these locations would have consecrated the summit ([37]: 473) and such actions would place the massifs' "natural sacredness" under the domain of the imperial cult [17]. Human sacrifices on mountains conducted at the southern border of the Inca territory (like at Aconcagua and at El Plomo) could also have been related to the consecration of boundaries during the expansion of the empire [40, 69].

4.3. Ideological Manipulation and Political Implications of Human Sacrifice on Mountains. Sacrificial techniques employed in Inca *capacocha* ceremonies seem to have been selected in order to avoid an overt display of cruelty. This was very different from Mesoamerican heart excision and the flaying, for these extremely bloody rituals were conducted in front of a large and presumably terrified audience. Contrastingly, Inca sacrificial victims were transported to largely uninhabited and inaccessible localities and were dispatched with a minimum amount of suffering (with the spilling of blood being avoided).

We can even infer that active sacrificial procedures (such as a blow to the head or strangulation) would only have been used by the priests as a last resort, as when death caused by exposure to the cold took too long to occur or if resistance was offered by the children. The sacrificial role of the priests was apparently reduced to a minimum, making the high altitude mountain environment (with its low temperatures and extreme atmospheric conditions) a key participant in the process of bringing about the deaths of the victims. In other words, the ritual was designed to allow the mountain deity to actually take the life of the victim with the Inca religious attendants serving as subordinate facilitators in the sacrificial ritual.

As stated above, the justification for local children to be offered on mountaintop shrines during Inca *capacocha* ceremonies would have been provided by commemorative,

propitiatory, or expiatory circumstances such as important events in the life of the Inca emperor, the universal Andean concern to appease the mountain deities who controlled both weather and fertility, or the need to stop locally occurring natural disasters.

The Inca sacrifice of Andean children would have been ideologically presented as having an important "mission" in which these "chosen ones" would continue living among the celestial and mountain deities as intercessors on behalf of the Inca emperor and for their own people. Their parents, their kinsmen, and local communities would have been encouraged by the Inca to believe that the payment of this type of "tribute" (consisting of their own children) was not only a religious obligation but more importantly, it was a great social "honor" as well [17].

The political implications of sacrificial ceremonies would have been utilized by local chiefs as mechanisms for creating and maintaining alliances with imperial Cuzco. Chronicler Hernandez Príncipe specifically mentions that a local leader from the Peruvian sierra (seeking to increase his political standing), volunteered his ten year old daughter for the state sponsored ritual of *capacocha* and was granted special privileges by a grateful Inca emperor as a result of his "generosity" [37].

The spectacle of these very public processions comprised of sacrificial victims (traveling with prestigious ceremonial items) radiating out from Cuzco towards the provinces would have contributed to the integration of the Inca territory by means of an intensification of the economic, political, and religious links between the center and the periphery of the empire [70–72].

5. Conclusions

In this presentation, we have focused on the frozen bodies from Inca high altitude shrines as objects for bioarchaeological and ethnohistorical research, providing an overview on the procedures and justifications of human sacrifice among the Incas. According to the historical sources written during the Hispanic conquest, the Inca human sacrifices were performed in response to natural catastrophes, the death of the Inca emperor, or to propitiate the mountain spirits that grant fertility. The selected children and the young *acllas* or "chosen women" were taken in processions to the highest summits of the Andes to be sacrificed. They were believed to become messengers into the world of the mountain deities and the spirits of the ancestors.

The sacrifice of young individuals on Andean mountaintop shrines at Lullaillaco, Quehwar, Aconcagua, Ampato, El Plomo, Chañi, Misti, and Chuscha was designed to celebrate special events, to ensure the well-being of the emperor, to mark a ruler's passing into the afterlife, to promote agricultural prosperity, to consecrate a specific construction project or location, to appease the deities, or to atone for sins. The Inca attributed commemorative, expiatory, propitiatory and or dedicatory motives to these sacrifices and this made the acceptance of the *capacocha* ritual by local Andean communities more feasible.

The ritual violence (inherent to Inca human sacrifice) was cloaked in a bloodless ritual conducted on remote mountaintops and was based on belief in the efficacy of sacrificed children as supernatural mediators to the mountain deities. Additionally, the “propaganda” value of convincing local elites that it was indeed an “honor” to have one’s offspring sacrificed in the *capacocha* ceremony would have constituted a very efficient ideological foundation for ensuring cooperation from local rulers during the phases of expansion and consolidation of the Inca Empire.

Conflict of Interests

The author declares that there is no conflict of interests regarding the publication of this paper.

Acknowledgments

The author would like to thank the institutional support of the National Council of Scientific Research in Argentina (CONICET), the Catholic University of Salta, and the National Geographic Society. She would like to express her gratitude towards Johan Reinhard, Carlos Previgliano, Facundo Arias Araoz, Josefina González Díez, Andrew Wilson, Timothy Taylor, Chiara Villa, Emma Brown, Tom Gilbert, Larry Cartmell, Keith Mc Kenney, Arnaldo Arroyo, Gerardo Vides Almonacid, Bob Brier, Arthur Aufderheide, Rubén Gurevech, Niels Lynnerup, Keith McKenney, Gael Lonergan, Angélique Corthals, Andrew Merriwether, Ian Farrington, Clara Abal, Vuka Roussakis, Craig Morris, Juan Schobinger, Thomas Besom, and Tamara Bray.

References

- [1] C. Mims, *When We Die. The Science, Culture, and Rituals of Death*, St. Martin’s Press, New York, NY, USA, 1999.
- [2] P. Tierney, *The Highest Altar*, Penguin Books, New York, NY, USA, 1989.
- [3] F. Robicsek and D. M. Hales, “Maya heart sacrifice: cultural perspective and surgical technique,” in *Ritual Human Sacrifice in Mesoamerica*, E. H. Boone, Ed., Dumbarton Oaks, Washington, DC, USA, 1984.
- [4] A. Zighelboim, “Escenas de Sacrificio en Montañas en la Iconografía Moche,” *Boletín del Museo Chileno de Arte Precolombino*, no. 6, pp. 35–70, 1995, Santiago.
- [5] M. Constanza Ceruti, *Embajadores del Pasado: los niños del Llullaillaco y otras momias del mundo*, Editorial de la Universidad Católica de Salta (EUCASA), Salta, Argentina, 2011.
- [6] C. Ceruti, “Human bodies as objects of dedication at Inca mountain shrines (north-western Argentina),” *World Archaeology*, vol. 36, no. 1, pp. 103–122, 2004.
- [7] M. C. Ceruti, “The religious role of children in the andes, past and present,” *AmS Skrifler*, vol. 23, pp. 125–133, 2010.
- [8] M. C. Ceruti, “Elegidos de los Dioses: Identidad y Status en las víctimas sacrificiales del volcán Llullaillaco y de otros santuarios de altura Inca,” *Boletín de Arqueología*, vol. 7, pp. 263–275, 2003, Pontificia Universidad Católica del Perú, Lima, Peru, 2005.
- [9] M. C. Ceruti, “Actores, ritos y destinatarios de las ceremonias incaicas de capacocha: una visión desde la arqueología y la etnohistoria,” *Xama*, vol. 15–18, pp. 287–299, 2002–2005.
- [10] C. Ceruti, “An overview of the frozen Inca mummies from Mount Llullaillaco,” *Journal of Glacial Archaeology*, vol. 1, no. 1, 2014.
- [11] M. C. Ceruti, C. Previgliano, J. G. Díez, F. Arias Aráoz, and J. Reinhard, “Síntesis de Estudios Interdisciplinarios en las Momias Congeladas del Volcán Llullaillaco,” in *Problemáticas de la Arqueología Contemporánea. Actas del XV Congreso Nacional de Arqueología Argentina*, vol. 2, pp. 639–645, Universidad Nacional de Río Cuarto, 2008.
- [12] C. H. Previgliano, C. Ceruti, J. Reinhard, F. A. Araoz, and J. G. Díez, “Radiologic evaluation of the llullaillaco mummies,” *American Journal of Roentgenology*, vol. 181, no. 6, pp. 1473–1479, 2003.
- [13] C. Previgliano, C. Ceruti, F. Arias Aráoz, J. González Díez, and J. Reinhard, “Radiología en estudios arqueológicos de momias incas,” *Revista Argentina de Radiología*, vol. 69, no. 3, pp. 199–210, 2005.
- [14] E. Brown, T. Taylor, M. Constanza Ceruti et al., “Evidence for coca and alcohol ingestion in the final months of the Llullaillaco Maiden’s life,” in *Proceedings of the Bioarchaeology Symposium*, Oxford, UK, 2008.
- [15] C. Villa, C. Previgliano, C. Ceruti, F. Arias Araoz, J. González Díez, and N. Lynnerup, “Anthropological and paleopathological analysis of the three Llullaillaco child mummies using 3D visualizations from CT-scans,” in *Proceedings of the 2nd Bolzano Mummy Congress*, Tyrol Museum of Archaeology, Bolzano, Italy, 2011.
- [16] A. S. Wilson, E. L. Brown, C. Villa et al., “Archaeological, radiological, and biological evidence offer insight into Inca child sacrifice,” *Proceedings of the National Academy of Sciences of the United States of America*, vol. 110, no. 33, pp. 13322–13327, 2013.
- [17] M. C. Ceruti, *Llullaillaco: Sacrificios y Ofrendas en un Santuario Inca de Alta Montaña*, Ediciones Universidad Católica de Salta (EUCASA), Salta, Argentina, 2003.
- [18] M. C. Ceruti, “Panorama de los santuarios Inca de alta montaña en Argentina,” *Revista Arqueología y Sociedad*, vol. 18, pp. 211–228, 2008.
- [19] J. Reinhard and C. Ceruti, *Inca Rituals and Sacred Mountains: A Study of the World’s Highest Archaeological Sites*, Cotsen Institute of Archaeology, UCLA, 2010.
- [20] T. Bray, L. Minc, M. C. Ceruti, J. A. Chávez, R. Perea, and J. Reinhard, “A compositional analysis of pottery vessels associated with the Inca ritual of *capacocha*,” *Journal of Anthropological Archaeology*, vol. 24, no. 1, pp. 82–100, 2005.
- [21] D. G. Holguín, [1608] *Vocabulario de la Lengua General de todo el Peru llamada Lengua Quichua del Inca*, Universidad Nacional de San Marcos, Lima, Peru, 1952.
- [22] J. Reinhard, “Las Montañas Sagradas: Un Estudio Etnoarqueológico de Ruinas en las Altas Cumbres Andinas,” *Cuadernos de Historia*, vol. 3, pp. 27–62, 1983.
- [23] J. de Ulloa Mogollón, “[1586] Relación de la provincia de los Collaguas,” in *Relaciones Geográficas de IndiasPerú*, M. J. de la Espada, Ed., vol. 1, pp. 326–333, Ediciones Atlas, Madrid, Spain, 1965.
- [24] C. de Molina, [1575] *Ritos y Fábulas de los Incas*, Editorial Futuro, Buenos Aires, Argentina, 1959.
- [25] G. A. Ramos, [1621] *Historia de Nuestra Señora de Copacabana*, Empresa Editorial Universo, La Paz, Bolivia, 1976.
- [26] F. Montesinos, [1570–1572] *Memorias Antiguas, Historiales y Políticas del Perú*, Imprenta de Miguel Ginesta, Madrid, Spain, 1882.

- [27] J. de Betanzos, [1551–1557] *Narratives of the Incas*, University of Texas Press, Austin, Tex, USA, 1996.
- [28] B. Cobo, [1652] *History of the Inca Empire*, edited by: R. Hamilton, University of Texas Press, Austin, Tex, USA, 1996.
- [29] J. P. de Ondegardo, [1571] *Informaciones Acerca de la Religión y Gobierno de los Incas*, Sanmarti y Ca, Lima, Peru, 1916.
- [30] A. de Herrera Tordesillas, [ca.1615] *Historia General de los Hechos de los Castellanos en las Isla, y Tierra Firme de el Mar Oceano*, Francisco Martínez Abad, Madrid, Spain, 1728.
- [31] J. D. Santa Cruz Pachacuti, [1571] *Relación de Antigüedades deste reyno del Perú*, Biblioteca de Autores Españoles, Madrid, Spain, 1968.
- [32] B. Cobo, [1653] *Inca Religion and Customs*, edited by R. Hamilton, University of Texas Press, Austin, Tex, USA, 1990.
- [33] R. Levillier, *Don Francisco de Toledo, supremo organizador del Perú. Su vida, su obra (1515–1582). Tomo II, Libro I: Sus informaciones sobre los Incas (1570–1572)*, Espasa Calpe, Buenos Aires, Argentina, 1940.
- [34] M. de Murúa, [1590] *Historia General del Perú*, Ediciones Historia 16, Madrid, Spain, 1992.
- [35] J. Schobinger, Ed., *La "momia" del Cerro El Toro: Investigaciones arqueológicas en la Cordillera de la Provincia de San Juan*, Universidad Nacional de Cuyo, Mendoza, Argentina, 1966.
- [36] "Bureaucracy and systematic knowledge in Andean civilization," in *The Inca and Aztec States, 1400–1800. Anthropology and History*, G. Collier, R. Rosaldo, and J. D. Wirth, Eds., pp. 419–458, Academic Press, New York, NY, USA, 1982.
- [37] R. Hernandez Príncipe, "[1621] Idolatría del Pueblo de Ocos, cabeza desta comunidad," in *Cultura Andina y Represión*, P. Duviols, Ed., pp. 442–448, Centro de Estudios Rurales Andinos Bartolomé de las Casas, Cuzco, Peru, 1986.
- [38] I. Farrington, "The concept of Cuzco," *Tawantinsuyu*, vol. 5, pp. 53–59, 1998.
- [39] C. McEwan and M. Van de Guchte, "Ancestral time and sacred space in Inca state ritual," in *The Ancient Americas. Art from Sacred Landscapes*, R. Townsend, Ed., pp. 359–371, The Art Institute of Chicago, Chicago, Ill, USA, 1992.
- [40] "Los santuarios de altura incaicos y el Aconcagua: Aspectos Generales e Interpretativos," *Relaciones de la Sociedad Argentina de Antropología*, vol. 24, pp. 7–27, 1999.
- [41] J. Reinhard, "Sacred Mountains: an ethno-archaeological study of high andean ruins," *Mountain Research and Development*, vol. 5, no. 4, pp. 299–317, 1985.
- [42] M. D. Millán de Palavecino, "Descripción de material arqueológico proveniente de yacimientos de Alta Montaña en el área de la Puna," *Anales de Arqueología y Etnología*, vol. 21, pp. 81–99, 1966.
- [43] M. C. Ceruti, "La Capacocha del Nevado de Chañi: Una Aproximación Preliminar desde la Arqueología," *Chungara*, vol. 33, no. 2, pp. 279–282, 2001.
- [44] M. C. Ceruti, "Sitios Rituales de Altura y Estrategias Sociales de Dominación: caso de estudio en el Nevado de Chañi (5.896 m., límite provincial Jujuy-Salta, Argentina)," *Revista Estudios Sociales del NOA*, vol. 1, pp. 127–154, 1997.
- [45] M. C. Ceruti, "Excavaciones arqueológicas de alta montaña en el Nevado de Chañi (5.896 m.) y el Nevado de Acay (5.716 m.) Provincia de Salta. Arqueología argentina en los inicios de un nuevo siglo," in *14th Congreso Nacional de Arqueología Argentina*, vol. 1, Universidad Nacional de Rosario, 2007.
- [46] J. Schobinger, "Informe sobre la relocalización de un hallazgo de alta montaña del noroeste Argentino: la llamada momia de los Quilmes," *Comechingonia*, vol. 8, pp. 47–65, 1995.
- [47] J. Schobinger, *El santuario incaico del nevado de Chuscha*, Universidad Nacional de Cuyo, Mendoza, Argentina, 2004.
- [48] "Revisión de los resultados de las prospecciones arqueológicas de alta montaña en el cerro Pabellón, el Nevado de Chuscha y el cerro Bayo," *Anales de Arqueología y Etnología* 56/8, Facultad de Filosofía y Letras de la Universidad de Cuyo, Mendoza, Argentina, 2004.
- [49] G. Mostny, Ed., *La Momia del Cerro El Plomo*, vol. 27, Boletín del Museo Nacional de Historia Natural, Santiago, Chile, 1957.
- [50] S. Quevedo and E. Duran, "Ofrendas a los dioses en las montañas: santuarios de altura en la cultura Inka," *Boletín del Museo Nacional de Historia Natural de Chile*, vol. 43, pp. 193–206, 1992.
- [51] C. Ceruti, "El Toro, el Potro y el Baboso: reconocimiento arqueológico de montañas con glaciares de la cordillera de San Juan y La Rioja," in *Actas de las IV Jornadas Arqueológicas Cuyanas*, INCIHUSA, Mendoza, Argentina, 2009.
- [52] J. Checura, "Funebría incaica en el cerro Esmeralda (Iquique, I Region)," *Estudios Atacameños*, vol. 5, pp. 125–141, 1977.
- [53] T. Besom, *Inca Human Sacrifice and Mountain Worship: Strategies for Imperial Unification*, University of New Mexico Press, Albuquerque, NM, USA, 2013.
- [54] J. Schobinger, *El Santuario Incaico del Cerro Aconcagua*, Universidad Nacional de Cuyo, Mendoza, Argentina, 2001.
- [55] R. Bárcena, "Pigmentos en el Ritual Funerario de la Momia del Cerro Aconcagua," *Xama*, vol. 2, pp. 61–116, 1989.
- [56] M. C. Ceruti, "Rescue archaeology of the Inca mummy on Mount Quehwar, Argentina," *Journal of Biological Research*, vol. 80, no. 1, pp. 303–307, 2006.
- [57] A. Beorchia, *El Enigma de los Santuarios Indígenas de Alta Montaña*, vol. 5, Revista del Centro de Investigaciones Arqueológicas de Alta Montaña, San Juan, Puerto Rico, 1985.
- [58] J. M. Castañeda, *Molecular genetic analysis of ancient human remains [M.S. thesis]*, George Washington University, Washington, DC, USA, 2000.
- [59] J. Reinhard and C. Ceruti, *Investigaciones Arqueológicas en el Volcán Lullaillo*, Universidad Católica de Salta, Salta, Argentina, 2000.
- [60] F. Arias Araóz, J. González Diez, and C. Ceruti, "Estudios Odontológicos de las momias del Lullaillo," *Boletín de la Asociación Argentina de Odontología para Niños*, vol. 31, no. 2-3, pp. 3–10, 2002.
- [61] P. Gutierrez de Santa Clara, [ca. 1603] *Quinquenarios o Historia de las Guerras Civiles del Perú*, vol. 166, Biblioteca de Autores Españoles, Ediciones Atlas, Madrid, Spain, 1963.
- [62] M. D. Murúa, [1590] *Historia del Origen y Genealogía Real de los Reyes Incas del Perú*, vol. 2, Biblioteca Missionalia Hispanica, Madrid, Spain, 1946.
- [63] J. de Acosta, [1590] *Historia Natural y Moral de las Indias*, Fondo de Cultura Económica, Mexico City, Mexico, 2nd edition, 1962.
- [64] J. Reinhard, "Peru's Ice Maidens," *National Geographic Magazine*, vol. 189, no. 6, pp. 62–81, 1996.
- [65] J. Reinhard, "Sharp eyes of science probe the mummies of Peru," *National Geographic*, vol. 191, no. 1, pp. 36–43, 1997.
- [66] J. Reinhard, "New Inca mummies," *National Geographic Magazine*, vol. 194, no. 1, pp. 128–135, 1998.
- [67] P. Cieza de León, [1553] *The Incas of Pedro Cieza de León*, University of Oklahoma Press, Norman, Okla, USA, 1959.
- [68] M. Chachani, P. Picchu, and M. C. Ceruti, "Pasado y presente de los volcanes sagrados de Arequipa," *Anuario de Arqueología*, vol. 5, no. 1, pp. 359–372, 2013.

- [69] M. Gentile, "La dimensión sociopolítica y religiosa de la capacocha del cerro aconcagua," *Bulletin de l'Institut Français d'Études Andines*, vol. 25, no. 1, pp. 43–90, 1996.
- [70] P. Duviols, "La Capacocha. Mecanismo y función del sacrificio humano, su proyección geométrica, su papel en la política integracionista y en la economía redistributiva del Tawantisuyu," *Allpanchis*, vol. 9, pp. 11–57, 1976, Cuzco.
- [71] F. Salomon, "The beautiful grandparents': Andean Ancestor Shrines and mortuary ritual as seen through colonial records," in *Tombs for the Living: Andean Mortuary Practices*, T. Dillehay, Ed., pp. 315–353, Dumbarton Oaks, Washington, DC, USA, 1995.
- [72] S. MacCormack, "Processions for the Inca: Andean and Christian ideas of human sacrifice, communion and embodiment in early colonial Peru," *Archiv für Religionsgeschichte*, vol. 2, no. 1, pp. 110–140, 2000.

Research Article

Resilience at the Transition to Agriculture: The Long-Term Landscape and Resource Development at the Aceramic Neolithic Tell Site of Chogha Golan (Iran)

S. Riehl,^{1,2} E. Asouti,³ D. Karakaya,¹ B. M. Starkovich,^{1,2} M. Zeidi,^{2,4} and N. J. Conard^{2,4}

¹Institute for Archaeological Sciences, University of Tübingen, Rümelinstraße 23, 72070 Tübingen, Germany

²Tübingen Senckenberg Center for Human Evolution and Palaeoenvironment, Rümelinstraße 23, 72070 Tübingen, Germany

³Department of Archaeology, Classics and Egyptology, University of Liverpool, 12-14 Abercromby Square, Liverpool L69 7WZ, UK

⁴Abteilung für Ältere Urgeschichte und Quartärökologie, Institut für Ur- und Frühgeschichte und Archäologie des Mittelalters, Universität Tübingen, Schloss Hohentübingen, 72070 Tübingen, Germany

Correspondence should be addressed to S. Riehl; simone.riehl@uni-tuebingen.de

Received 23 January 2015; Accepted 24 May 2015

Academic Editor: Otto Appenzeller

Copyright © 2015 S. Riehl et al. This is an open access article distributed under the Creative Commons Attribution License, which permits unrestricted use, distribution, and reproduction in any medium, provided the original work is properly cited.

The evidence for the slow development from gathering and cultivation of wild species to the use of domesticates in the Near East, deriving from a number of Epipalaeolithic and aceramic Neolithic sites with short occupational stratigraphies, cannot explain the reasons for the protracted development of agriculture in the Fertile Crescent. The botanical and faunal remains from the long stratigraphic sequence of Chogha Golan, indicate local changes in environmental conditions and subsistence practices that characterize a site-specific pathway into emerging agriculture. Our multidisciplinary approach demonstrates a long-term subsistence strategy of several hundred years on wild cereals and pulses as well as on hunting a variety of faunal species that were based on relatively favorable and stable environmental conditions. Fluctuations in the availability of resources after around 10,200 cal BP may have been caused by small-scale climatic fluctuations. The temporary depletion of resources was managed through a shift to other species which required minor technological changes to make these resources accessible and by intensification of barley cultivation which approached its domestication. After roughly 200 years, emmer domestication is apparent, accompanied by higher contribution of cattle in the diet, suggesting long-term intensification of resource management.

1. Introduction

Explaining the Beginnings of Agriculture: An Accumulated Record. Since the first half of the 20th century the importance of agriculture in the history of humankind has been continuously emphasized along with a steady development of models on the natural conditions and cognitive circumstances under which the neolithization process took place.

From a bioarchaeological perspective many questions on the associated changes seem to be well understood. During the last decades identification criteria for distinguishing wild and domesticated plant species have improved (e.g. [1]). In some cases it is even possible to distinguish between gathered and cultivated wild assemblages through consideration of grain size and the presence of weed species [2–4]. Similar

methodological developments in the study of faunal remains enabled novel insights into the emergence of animal domestication (e.g. [5, 6]). Radiocarbon dating of morphologically domesticated species and DNA analyses of modern species allowed the localization and timing of the first domesticated plant and animal species [7–10]. Archaeobotanical research resulted in the abandonment of the hypothesis of a single core area for the origins of agriculture within the Fertile Crescent [11, 12]. The accumulated record of archaeobotanical assemblages with different proportions of wild and domesticated species supported the model of protracted domestication lasting up to 2000 years ([2, 11, 13, 14], but see also [15] for a different opinion). The term “protracted domestication” is often used with absolute chronological designations, for example, marking the time range between

large-scale systematic gathering of wild cereals at Ohalo II around 23,000 BP and the appearance of the first domesticated species during the PPNB [13], contrasted with possible “rapid domestication” resulting from the intentional selection of domesticated phenotypes which may take place within a few cereal generations [16]. We, however, consider the qualitative connotation of the term to be less arbitrary and use “protracted” as a relative term, indicating an evolutionary process with phases of stasis or even reversal. With such an understanding “protracted domestication” can occur equally within a process of 1,000 or 15,000 years.

Climatic fluctuations following the end of the last glacial maximum have been comprehensively investigated and favored by some to represent a key catalyst for the development of agriculture under a combined contribution of changes in resource availability and demographic pressures [17–22]. Others use global palaeoclimate records to argue for the mandatory beginnings of agriculture during the Holocene, by linking them to the rate of innovation of subsistence technology or subsistence-related social organization [23–25]. With some exceptions [26], such generalizations rarely incorporate the regional climatic diversity that is fundamental in considerations of agricultural development during later periods (e.g. [27]), and that is evidenced in the palaeoclimatic record (e.g. [28–30]). One obstacle for integrating local palaeoclimate proxies and the archaeological record is the considerable distance of some archaeological sites from the locations of major palaeoclimate archives. In the archaeological record climatic fluctuations are often difficult to pinpoint, as the nature of the palaeoenvironmental evidence is superimposed by human activity. In addition, climate-relevant parameters in palaeoclimatic archives often show the character of creeping normalcy, thus would not necessarily have been recognized by ancient people, or may have allowed for adaptive measures provoking further environmental change through anthropogenic impacts [31].

Alongside the unknown mode of ancient people’s perceptions that shaped their individual interactions with the environment goes the socio-natural development of the human species itself that has been less frequently included into neolithization models. What has earlier been considered as the coevolution of domesticates and human subsistence strategies [32], has been further developed by integrating insights from cognitive science [33]. In focusing on the biological aspects of *Homo sapiens* evolution, the form and functionality of the human brain have often been considered to have changed little, although the cognitive and cultural faculties as tangible through the archaeological record have changed considerably over time (see also [34]).

This paper focuses specifically on two aspects of the archaeological record that are particularly relevant to the investigation of agricultural origins: archaeobotanical and zooarchaeological assemblages. Our goal is to address the major epistemological issue of building broad-scale, cross-regional generalizations on the basis of a fragmentary record.

An impediment to the investigation of the local, long-term transitional developments from cultivating wild and later domesticated species, is the generally short-term occupation at aceramic Neolithic sites, in most cases spanning

less than 2,000 years. The nature of the evidence on the beginnings of agriculture is therefore accumulated from disparate locations across the Fertile Crescent. Emerging problems from adding up snapshots from sites at different geographic locations with the goal of reconstructing a developmental sequence relate to the above described differences in local climatic and environmental conditions, as well as in socio-cultural identities, landscape perceptions and associated strategies of the prehistoric populations (see discussion in [35, 36]). The shorter the archaeological sequence at a particular site, the greater likelihood that our generalizations on evolutionary and developmental processes capture only a limited picture.

The long-term archaeobiological record from the aceramic Neolithic site of Chogha Golan, representing more than 2,000 years, allows the investigation of a multifactorial interplay of humans with their environment, including adaptive cycles at the transition to agriculture.

Chogha Golan and Its Significance for Understanding the Neolithization Process. The aceramic tell site of Chogha Golan is situated at the lower ranges of the Central Zagros Mountains, about 30 km north of Mehran (Amirabad plain/Illam Province/Iran) (Figure 1). Starting in 2009 the site was excavated by the Tübingen-Iranian Stone Age Research Project (TISARP) and the Iranian Center for Archaeological Research [37, 38].

Aceramic sites in western Iran have been poorly documented so far, and our knowledge of prehistoric populations in this area derives mainly from surveys and excavations undertaken in the 1950s and 1960s [39–41]. Therefore little is known about the archaeobotany and early human subsistence strategies in the region, including the emergence of plant cultivation and agriculture [4, 42–44]. Animal domestication is more well-studied in the region (e.g., [5, 6, 45–53]), though more work remains to be done.

Excavations at Chogha Golan revealed 8 m of deposits consisting of 11 archaeological layers (AH XI–I) and one geological horizon at the lowest level of the stratigraphic sequence spanning in all more than 2,000 years. The profile of the deep sounding has been consistently dated, with 17 AMS dates ranging from roughly 11,800 BP (geological horizon) to ca. 9,600 BP (AH I) (Table 1, Figure 2). With the earliest date at the end of the Younger Dryas, Chogha Golan represents one of the oldest aceramic Neolithic sites in Iran, together with Sheikh-e Abad [54]. Most of the archaeological sediments derive from a deep sounding measuring between five and one square meter into a depth of 8 meters. The different archaeological horizons contain ochre-painted plaster floors and mud brick walls interspersed with midden deposits that have been interpreted as the contemporary architecture and associated occupation debris of the site’s inhabitants.

The extraordinary richness of the archaeological sediments in artefacts and bioarchaeological remains at Chogha Golan permits a high-resolution investigation of the development of the cultural sequence, subsistence behaviors and the local environment. Large quantities of lithic debitage demonstrate the intensive nature of the activities of the prehistoric community.

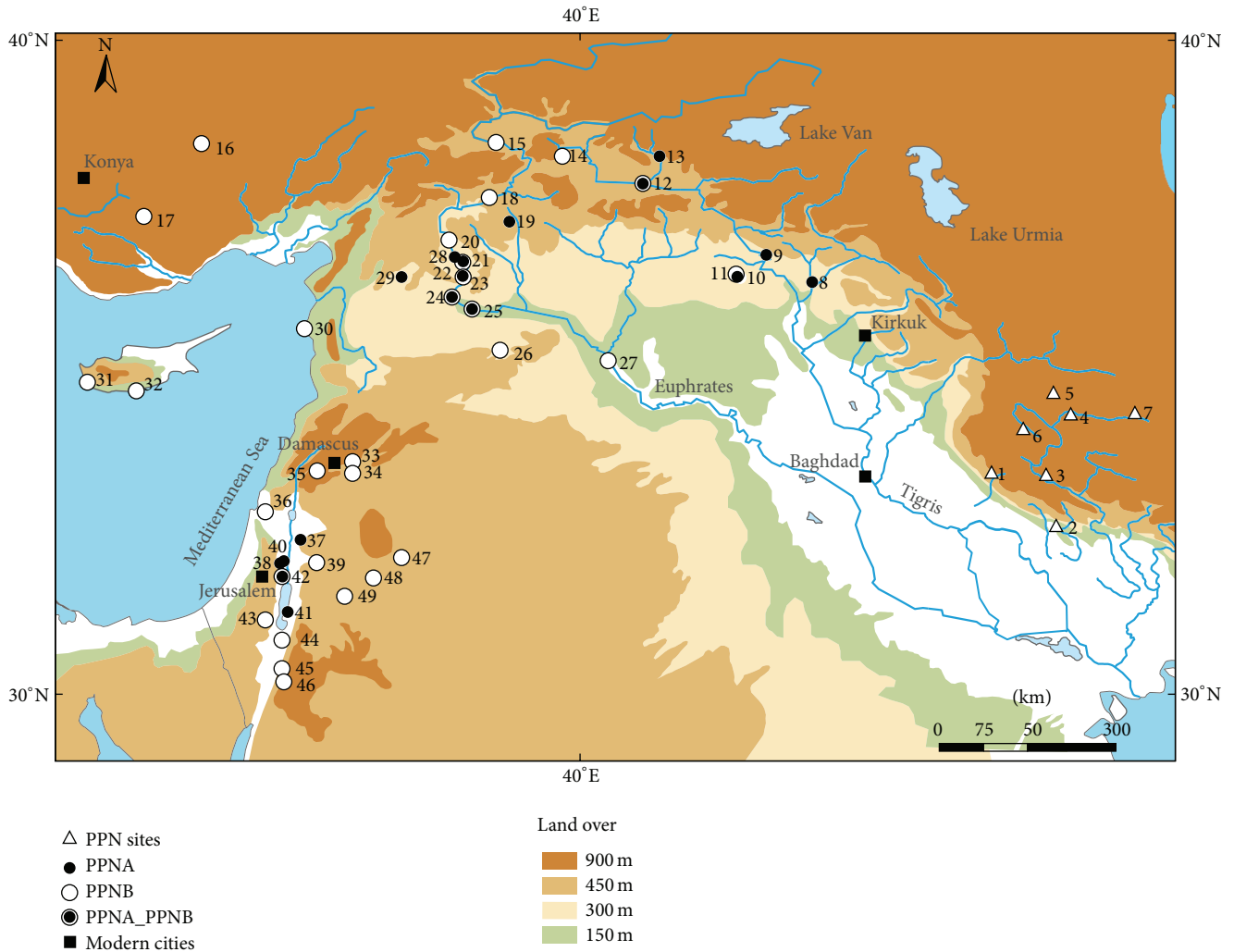


FIGURE 1: Chogha Golan (1) and its geographic position within the Fertile Crescent; (2) Ali Kosh, (3) Chia Sabz, (4) Ganj Dareh Tepe, (5) Sheikh-e Abad, (6) Jani, (7) Tepe Abdul Hosein, (8) M’lefaat, (9) Nemrik, (10) Qermez Dere, (11) Magzalia, (12) Körtik Tepe, (13) Hallan Cemi, (14) Cayonu, (15) Cafer Hoyuk, (16) Asikli Hoyuk, (17) Can Hasan III, (18) Nevali Cori, (19) Göbekli Tepe, (20) Akarcay Tepe, (21) Djade, (22) Halula, (23) Jerf al Ahmar, (24) Mureybet, (25) Abu Hureyra, (26) El Kowm I & II, (27) Bouqras, (28) Abr, (29) Qaramel, (30) Tell Ras Shamra, (31) Kissonerga, (32) Parekklisha-Shillourokambos, (33) Tell Ghoraifé, (34) Tell Aswad, (35) Tell Ramad, (36) Yiftahel, (37) Tell Ras Dubb, (38) Gilgal, (39) ‘Ain Ghazal, (40) Netiv Hagdud, (41) Dhra, (42) Jericho, (43) Nahal Hemar, (44) Wadi Fidan, (45) Beidha, (46) Basta, (47) Dhuweila, (48) Azraq 31, (49) Wadi Jilat 7; PPN is applied to Iranian sites, because PPNA and PPNB have additional cultural connotations that do only apply to sites in the western and northern part of the FC.

The development of the lithic industry over the sequence of 11 archaeological layers is relatively indistinct and may indicate relative stability in tool usage. All layers can be characterized by the systematic production of large numbers of bladelets and tools made on bladelets [38, 56]. The assemblage contains a large component of non-retouched bladelets. The tool diversity from Chogha Golan is relatively low, and most tools appear to have been used for cutting or perforating, with limited indications of scraping and harvesting. The amount of sickle blades with evidence of use wear is also consistently low throughout the archaeological horizons [56]. The comparison of the lithic assemblages at Chogha Golan with other early

Neolithic sites in the Zagros highlands and lowlands reveals similarities which place these sites within a cultural and behavioral group associated with the Mlefaatian industry which persisted for almost 2000 years (cf. [57, 58]).

The site’s inhabitants routinely exploited locally available raw materials as well as a very low percentage of imported obsidian. In archaeological horizon II and subsequently AH I obsidian occurs for the first time and comprises approximately 0.5% of the lithic material [56]. The presence of obsidian in the upper layers of Chogha Golan fits the diachronic trend of the region of increased obsidian finds around 9600–9500 cal BP [58]. At other sites in the region

TABLE 1: Radiocarbon AMS data from Chogha Golan. Dating has been conducted at the AMS laboratory of the Universities of Erlangen, Uppsala, and Kiel. Calibration BP with *calPal-online.de*, BC 2σ after Reimer et al. [64].

Species/archaeological horizon	Lab code	BP	Cal BP	Cal BC (2σ)
<i>Hordeum spontaneum</i> , geological horizon	KIA45647	9330 \pm 35 (base residue) 10125 \pm 45 BP (humic acid)	10549 \pm 37 (b.r.) 11740 \pm 187 (h.a.)	8658–8529 (b.r.) 10042–9651 (h.a.)
<i>Hordeum spontaneum</i> , AH XI	KIA44943	9790 + 120/–110	11162 \pm 220	9556–8812
<i>Hordeum spontaneum</i> , AH XIa	KIA45648	9320 \pm 120 BP (base residue) 10230 \pm 45 BP (humic acid)	10527 \pm 166 (b.r.) 11952 \pm 137 (h.a.)	8847–8283 (b.r.) 10155–9817 (h.a.)
<i>Hordeum spontaneum</i> , AH XI	KIA44944	9690 \pm 45	11054 \pm 129	9274–9119
<i>Hordeum spontaneum</i> , AH XI	KIA44942	9385 \pm 37 (base residue) 9590 \pm 40 (humic acid)	10622 \pm 45 (b.r.) 10945 \pm 123 (h.a.)	8754–8565 (b.r.) 9118–8872 (h.a.)
<i>Hordeum spontaneum</i> , AH VIII	KIA43836	9425 \pm 45	10656 \pm 53	8814–8602
<i>Hordeum spontaneum</i> , AH VI	Ua-44324	8812 \pm 53	9910 \pm 157	8117–7803
<i>Aegilops</i> sp., AH V	Ua-44323	8845 \pm 54	9954 \pm 148	8152–7856
<i>Hordeum spontaneum</i> , AH IV	Erl-14839	8887 \pm 37	10037 \pm 94	8234–7938
Poaceae, AH III	Erl-14840	8805 \pm 38	9839 \pm 81	8181–7731
<i>Hordeum spontaneum</i> , AH III	Erl-14838	8770 \pm 40	9788 \pm 84	7967–7648
<i>Aegilops</i> glume bases, AH II	KIA45649	8965 \pm 35	10091 \pm 107	8286–8181
Cerealia, AH II	KIA44941	9518 \pm 44	10887 \pm 147	8934–8713
<i>Hordeum spontaneum</i> , AH II	Beta336511	9110 \pm 40	10319 \pm 59	8460–8280
<i>Triticum</i> type species, AH II	Beta336510	8800 \pm 40	9831 \pm 82	8020–7750
Charcoal, AH I	Beta336509	8900 \pm 40	10045 \pm 95	8240–7950
Charcoal, AH I	Beta336508	8690 \pm 40	9637 \pm 54	7790–7600

obsidian has been found to originate from eastern Anatolia [59, 60] suggesting prehistoric mobility patterns dating from as early as the Palaeolithic (cf. [61]).

The first appearance of mudbrick walls, plaster floors and associated ground stone implements such as mortars, pestles and grinding slabs is recorded for AH X. Mortars and grinding slabs were at times found embedded in structure floors showing that they were permanent fixtures in the architecture of the site, while other mortars and grinding slabs were mobile [38, 62]. Although the first appearance of inhabited mudbrick structures with *in situ* preserved ground stone implements are from AH X, most of the mortars, grinding slabs and pestles were recovered from AH III onwards, and were likely used for processing foods. The available data, however, show an emphasis on pounding and little emphasis on grinding. This tendency could be related to the low volume of sediments excavated thus far, rather than an emphasis on pounding activities during the upper occupation. The presence of asphalt and pigments on ground stone tools also demonstrate that they were not exclusively used for food-processing activities. In fact, the available

records fit the observation that ground stone tools were often multifunctional devices during the aceramic Neolithic.

A total of 62 clay small objects from stratified deposits were recovered during the course of the 2009 and 2010 field seasons at Chogha Golan. Most clay objects are from ash and midden deposits. They are found with debris from daily activities and are not limited to obvious ritual contexts. Chogha Golan has provided evidence for the use of clay from the 10th millennium cal. BC onward. The clay usage in Chogha Golan is first evidenced by small and simply formed objects. The usage of clay increases through the sequence, probably reflecting social, economic and cultural development. Excavators recovered 10 clay animal figurines. While an unknown animal head and a goat horn were found from AH VI and III respectively, most of the animal figurines representing sheep/goat, cattle and pig were recovered from AH II and I.

Preliminary results of the ongoing archaeobotanical analyses suggest that cultivation of wild plants in the Zagros started equally early as at other places in the Fertile Crescent [4, 63], but here we provide a more detailed picture of the

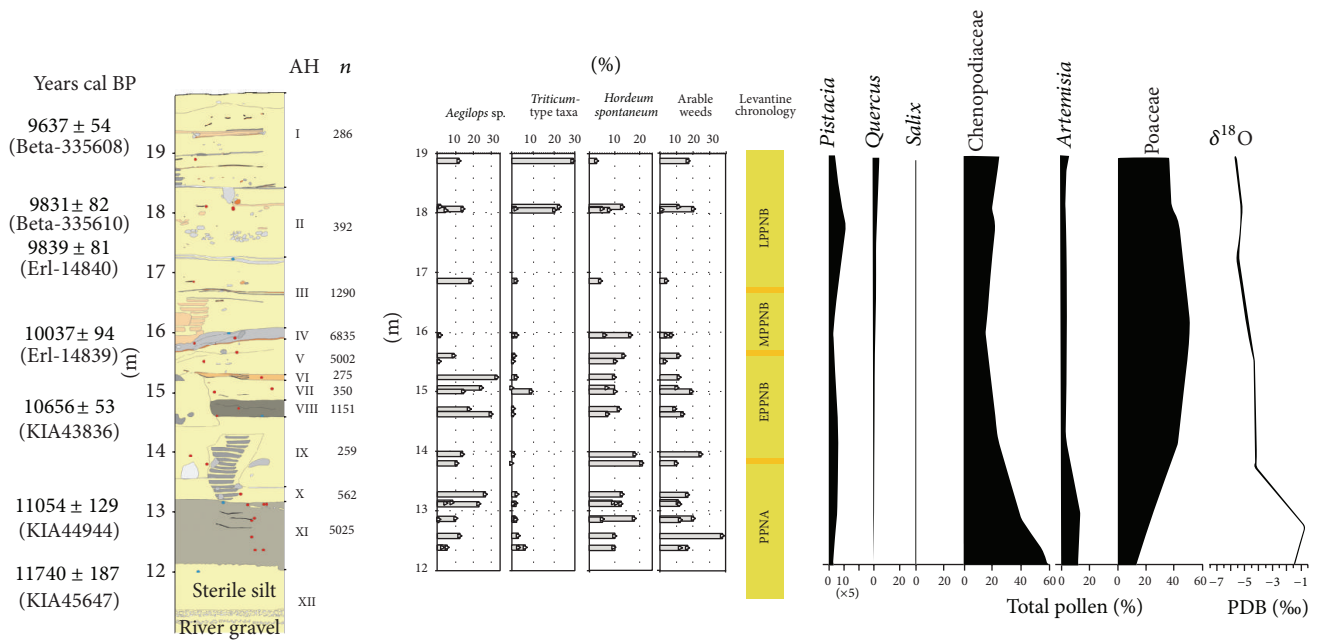


FIGURE 2: Stratigraphic profile from Chogha Golan with AMS dates in years cal BP (locations of dated samples indicated with blue dots in the profile) and archaeological horizons (AH) in Roman numbers. Percentages of taxa and groups of taxa relevant for the development of cultivation and domestication in each sample based on the total of all identifications from each AH (location of samples are indicated with red dots in the profile): *Aegilops* sp. (goat-grass), *Triticum*-type taxa: agglomeration of different *Triticum* taxa (including *Triticum boeoticum/dicoccoides* grains and glume bases, free-threshing wheat type rachis internodes and unidentified *Triticum* taxa), *Hordeum spontaneum* (wild barley), probable arable weeds acc. to Willcox [3] including *Trigonella* sp., *Silene* sp., *Reseda luteola*, *Ornithogalum/Muscari*, *Medicago radiata*, *Malva* sp., *Lithospermum* sp., *Heliotropium* sp., *Gypsophila* sp., *Galium* sp., *Fumaria* sp., *Erodium* sp., *Coronilla* sp., *Centaurea* sp. and *Adonis* sp.; (*n*) number of seed and chaff records identified in each horizon. The yellow bar indicates the equivalent Levantine cultural chronology. The palynological and stable oxygen isotope data (right) represent the relevant sequences of Lake Zeribar record extracted from [55].

changing economic and landscape practices of the Neolithic inhabitants of Chogha Golan, and their interplay with environmental and cultural shifts. Our aim is to contribute to the ongoing scientific debate concerning the socio-cultural, economic and environmental conditions that enabled the slow pace of the development of cultivation and herding practices and the transition to agriculture.

The Modern and Early Holocene Environment of the Region. The present-day climate of Iran is marked by extreme continental conditions (i.e., cold winters and hot, dry summers); the observed mesoclimatic heterogeneity is attributed to the region's complex topography. The strong north-south contrast in atmospheric pressure is due to Iran's position between summer dominating north-east trade winds and the winter dominating westerlies [65]. Chogha Golan is located in a region receiving today between 100–200 mm of mean annual precipitation, while mean annual temperatures range between 20–25°C. More important for considerations of past environmental conditions, however, is that calculated surplus and deficits of precipitation vary considerably over relatively short distances, particularly near the Elburz and Zagros ranges. According to the mapping of surplus and deficits of precipitation, Chogha Golan is situated in an area with more than 800 mm annual deficit in rainfall, but in less than 25 km distance from this region surpluses of 100–400 mm

annual precipitation have been calculated (see [65, p. 76]). Considering that isohyets may have shifted with past climatic fluctuations, environmental conditions at Chogha Golan may equally have been very variable throughout time.

The modern ecotope around Chogha Golan can be characterized as a desert type vegetation zone or Mesopotamian steppe bordering the *Acacietea* classes of the Sudanian flora as defined by Zohary (Figure 3; [66]). The region is, however, highly diversified hosting geobotanical units ranging from steppe-forests to desert vegetation, comprising elements of the Sudanian and sub-Sudanian flora as well as of the Saharo-Arabian desert vegetation, Irano-Turanian steppe, and Kurdo-Zagrosian steppe-forest sensu Zohary [66]. Characteristic plant associations include the *Acacietea flavae iranica*, *Anabasetea articulatae*, *Artemisietea herbae-albae mesopotamica*, *Pistacia-Amygdalus* steppe forest and *Quercetea brantii* xerophilous deciduous steppe-forest.

Another important landscape unit that is closely associated with Chogha Golan is the Konjan Cham River which is located 200 m from the site, and which would have provided suitable conditions for the growth of vegetation requiring alluvial wetland habitats.

Considering pollen diagrams in more detail to inform about late Quaternary vegetation, extant Lake Mirabad (800 m asl, [67]) is, the closest palaeovegetation proxy archive to Chogha Golan, at only 140 km away. Unfortunately the

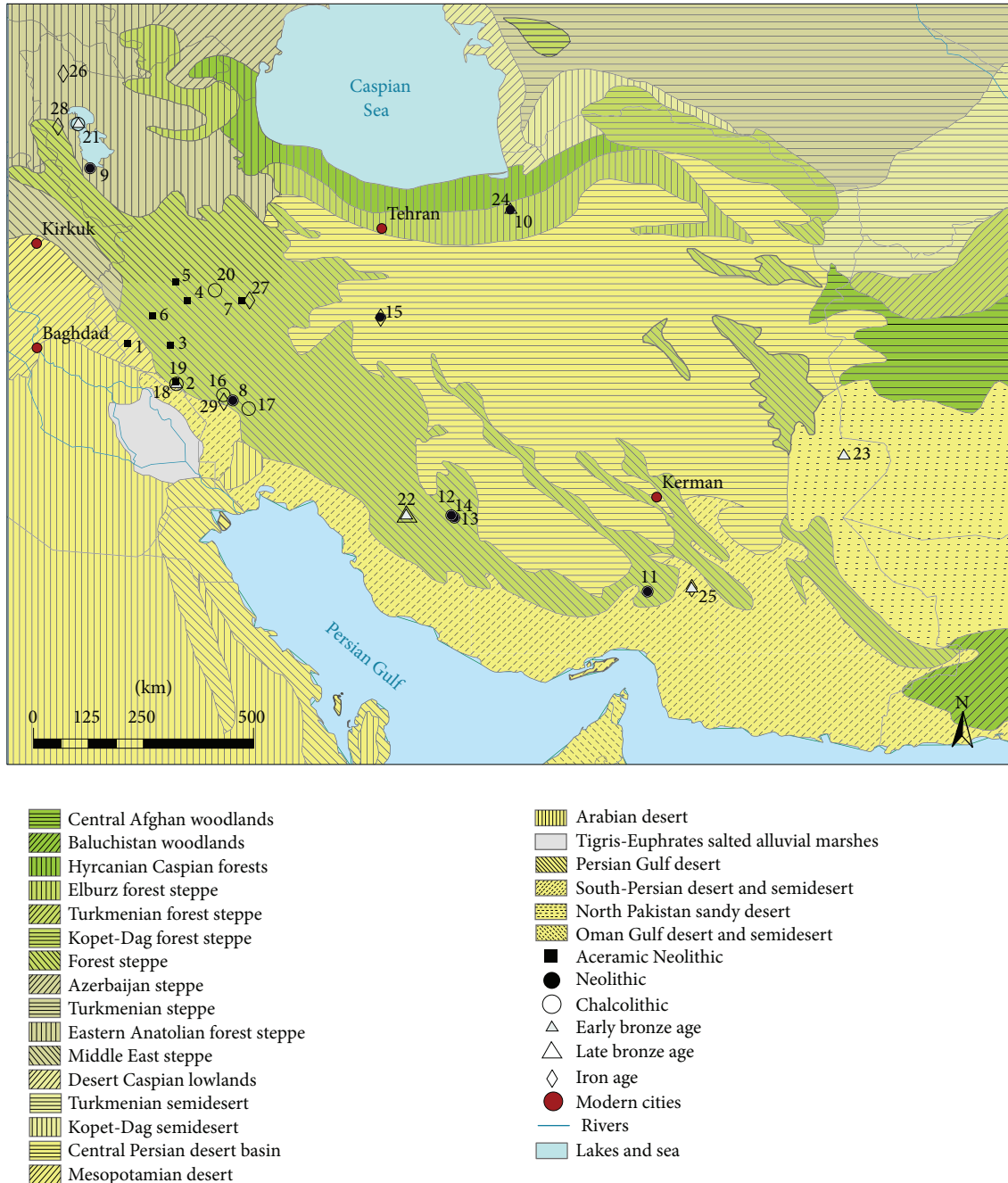


FIGURE 3: Ecotopes in Iran with archaeobotanically investigated sites: (1) Chogha Golan, (2) Ali Kosh, (3) Chia Sabz, (4) Ganj Dareh Tepe, (5) Sheikh-e Abad, (6) Jani, (7) Tepe Abdul Hosein, (8) Jaffarabad, (9) Tepe Hasanlu, (10) Tepe Musiyan, (11) Tepe Yahya, (12) Tall-e Mushki, (13) Tall-e Jari, (14) Tall-e Bakun, (15) Tepe Sialk, (16) Bendebal, (17) Sharafabad, (18) Tepe Farukhabad, (19) Tepe Sabz, (20) Godin Tepe, (21) Tappeh Gijlar, (22) Malyan, (23) Shahr-i Sokhta, (24) Tepe Hissar, (25) Konar Sandal, (26) Bastam, (27) Nush-i Jan, (28) Qal'eh Ismail Aqa, (29) Susa-Ville Royale.

only palynological analysis available from this location was conducted several decades ago, and is thus lacking a highly resolved chronology [68]. There is however one radiocarbon date (10.370 ± 120 BP) from the lowest core level placing the sequence into the Holocene. According to the authors, the vegetation development reflected in the diagram is very similar to that of the better investigated and dated core from

Lake Zeribar (1.285 m asl, 240 km north of Chogha Golan, [55, 69]; see also Figure 2). Palaeoclimate proxy archives are also available from Lake Urmia (1.270 m asl, [70, 71]) 500 km to the north of Chogha Golan (490 m asl).

For the Late Glacial/Early Holocene transition most researchers propose that temperatures were high, therefore so were evaporation rates. These factors, combined with low

precipitation led to low lake levels, water salinization and scattered occurrences of a very thin arboreal cover [55, 72]. El-Moslimany has suggested that the high percentages of Chenopodiaceae and *Artemisia* pollen, generally interpreted as indicators of dry steppe habitats and a cold-arid climate, do not necessarily indicate low annual precipitation, but instead a highly seasonal climate with cold winters and hot, dry summers [69].

At the onset of the early Holocene a rise in temperatures and a change to freshwater lake conditions as recorded in the shift in *Najas* species is indicated at Lake Urmia. Unstable and variable water levels are superimposed on generally low lake levels as indicated by the botanical macrofossils [72]. Some researchers have deduced changes in patterns of seasonality. According to Stevens et al. [55], summer rainfall or at least reduced summer drought occurred, while El-Moslimany [69] suggests that changes in seasonality resulted in the dominance of Poaceae pollen and the initial increase in arboreal pollen. Most grasses thrive in environments characterized by summer rainfall, while low pollen production is apparently due to reproductive strategies related to the summer-dry climate [69]. Upland vegetation shifted to a *Pistacia*-deciduous oak semi-arid grassland as low temperatures and aridity ameliorated [55], while winter-dominated precipitation after 10,000 BP is also suggested by low $\delta^{18}\text{O}$ values observed at Lake Mirabad [73].

Differences in the pace of Holocene expansion of oak within the Fertile Crescent from its refugia during the Late Glacial Maximum have been already outlined by Bottema and van Zeist [68, 74–77]. While oak in the Levant is represented with more than 20% in the pollen diagrams during the Younger Dryas and immediately increases with the beginning of the Holocene, it increases only some thousand years later at Lake Van and Lake Zeribar [78]. There is, however, a strong increase in Poaceae, concurrently with the decrease of *Artemisia* and Chenopodiaceae values at the end of the Younger Dryas event, supported by the $\delta^{18}\text{O}$ record of Lake Zeribar. However, precipitation levels are interpreted to have been low by comparison to the Mediterranean Levant.

Roberts has suggested that human activities such as vegetation burning and woodcutting might have played a role in the early Holocene delay of woodland expansion in the Zagros region [79]. The discovery of charred plant remains in Lake Zeribar sediments brings a new argument to this discussion. Charred particles of herbaceous plants in all sediment cores dating from the Pleniglacial to the present indicate that occasional fires occurred in the wider region, whether these were natural and/or anthropogenic is a matter of debate. Wasylikowa has interpreted the increased frequency of *Plantago lanceolata*-type pollen from about 10,000 cal yr BP as an indicator of the spread of this species in steppe plant communities due to vegetation disturbance by hunters and/or herders [30]. Asouti and Kabukcu [80] have proposed that early Holocene vegetation across the hilly flanks of the Irano-Anatolian region of Southwest Asia was dominated by semi-arid grasslands. The sparse arboreal vegetation was dominated by insect-pollinated Rosaceae associated with erratic pollen producers, such as *Pistacia* and deciduous oak shrubs. The delayed establishment of

deciduous woodlands was due to the very rapid response of grasses to the abrupt increase in precipitation values, which provided them with the competitive advantage over trees in seedling establishment. Contrasting with the Levantine littoral, the establishment of woodland vegetation on the mid to low elevation slopes and the plateaus of the Irano-Anatolian region became possible only with the widespread adoption of woodland management strategies and caprine herding. Such practices controlled the growth of grasslands thus enabling intensively managed woodland species such as *Pistacia* and deciduous *Quercus* to form widespread mature woodland pastures [80].

2. Materials and Methods

2.1. Seed and Chaff Remains. During the excavations in 2009 and 2010 more than 700 sediment samples were recovered and manually floated using 200 μm sieves, of which 45 archaeobotanical samples containing almost 32,000 carbonized seed and chaff remains have been analyzed to date. The mean volume of the sediment samples was 10 liters and find densities of seed and chaff remains in the different archaeological horizons were highly variable, ranging from very low find densities of 10–20 items per liter sediment in the two uppermost layers AH I and AH II to extremely high find densities of 296 items per liter sediment in AH IV (see also Figure 11). The mean find density of all 11 archaeological horizons was 65 seed and chaff remains per liter sediment which is high compared to contemporaneous sites in the Fertile Crescent, such as Tell 'Abr or Jerf el Ahmar (3 items/liter), Dja'de (5 items/liter) and Tell Qaramel (7 items/liter) [81, 82]. Even in comparison with later periods when settlements are based on fully established agriculture, such as the Bronze Age settlements in Syria [83] the find densities for seeds and chaff remains at Chogha Golan appear to be extremely high. This can be explained by several factors, including a general good preservation for this type of plant remains and the specific contextual situation, that is, their preservation mostly in midden (refuse) contexts, but is also related to the fine stratigraphic excavation of the layers and subsequent careful hand flotation.

All the samples derive from the deep sounding and do not allow a detailed consideration of context. However, an advantage is the long-term sequence of well-dated deposits and the direct comparability of the bioarchaeological remains obtained from the same samples.

Analysis of the seeds was conducted using a Leica GZ6 binocular microscope at the archaeobotanical laboratory of the Institute of Archaeological Science, Tübingen University, based on morphological criteria and the use of the botanical reference collection. In total, 110 botanical taxa were identified (Table 2). Basic numeric methods, such as percentage proportions of taxa and taxa groups and the ubiquity analysis were applied to compare the assemblages of the different archaeological horizons.

2.2. Wood Charcoal. Anthracological analyses are ongoing at the Archaeobotany Laboratory of the Department of

TABLE 2: Archaeobotanical taxa (seeds or fruits unless otherwise stated) and their overall find number, proportions, and frequencies in the deep sounding; · <0,01%, • <0,1%, and # <1%.

Family	Taxa	Σ	Proportion in %	Frequency in %
Amaranthaceae	<i>Amaranthus</i> sp.	2	•	18
Amaranthaceae	<i>Atriplex</i> cf. <i>prostrata</i> (fruit and perianth)	23	#	55
Amaranthaceae	<i>Suaeda</i> sp.	61	#	45
Anacardiaceae	<i>Pistacia</i> sp.	518	2	100
Anacardiaceae	<i>Pistacia terebinthus</i>	2	•	9
Apiaceae	Apiaceae indet.	1	·	9
Asteraceae	<i>Anthemis cotula</i>	1	·	9
Asteraceae	Asteraceae indet.	1	·	9
Asteraceae	<i>Centaurea</i> sp.	79	#	91
Asteraceae	cf. <i>Carthamus</i> sp.	1	·	9
Boraginaceae	<i>Arnebia</i> sp.	6	•	27
Boraginaceae	Boraginaceae indet.	4	•	27
Boraginaceae	<i>Heliotropium</i> sp.	94	#	100
Boraginaceae	<i>Lithospermum arvense</i> , uncarbonized	16	#	73
Boraginaceae	<i>Lithospermum tenuiflorum</i> , uncarbonized	2	•	9
Brassicaceae	<i>Alyssum</i> sp.	2	•	18
Brassicaceae	Brassicaceae indet.	275	1	100
Brassicaceae	<i>Lepidium/Sisymbrium</i>	2	•	18
Capparidaceae	<i>Capparis</i> sp.	1	·	9
Caryophyllaceae	<i>Arenaria</i> sp.	1	·	9
Caryophyllaceae	Caryophyllaceae indet.	114	#	91
Caryophyllaceae	<i>Gypsophila elegans</i> type	1	·	9
Caryophyllaceae	<i>Gypsophila</i> sp.	39	#	55
Caryophyllaceae	<i>Silene</i> sp.	118	#	91
Caryophyllaceae	<i>Silene/Arenaria</i>	3	•	9
Chenopodiaceae	<i>Beta vulgaris</i>	1	·	9
Chenopodiaceae	Chenopodiaceae/Amaranthaceae	52	#	36
Chenopodiaceae	<i>Chenopodium</i> sp.	18	#	64
Chenopodiaceae	<i>Salsola kali</i>	28	#	73
Convolvulaceae	<i>Convolvulus</i> type	2	•	18
Cyperaceae	<i>Carex</i> sp.	1	·	9
Cyperaceae	Cyperaceae indet.	5	•	9
Cyperaceae	<i>Scirpus</i> cf. <i>maritimus</i>	77	#	91
Cyperaceae	<i>Scirpus</i> sp.	74	#	91
Fabaceae	<i>Astragalus</i> sp.	1764	6	100
Fabaceae	cf. <i>Lathyrus</i> sp. (cylindric)	12	•	18
Fabaceae	cf. <i>Trigonella</i> sp.	17	#	9
Fabaceae	<i>Coronilla</i> sp.	50	#	55
Fabaceae	<i>Coronilla/Trigonella</i>	13	•	9
Fabaceae	Fabaceae indet., large	1	·	9
Fabaceae	Fabaceae indet., medium	55	#	64
Fabaceae	Fabaceae indet., small	1396	4	100
Fabaceae	<i>Galega/Ornithopus</i> type	4	•	9
Fabaceae	<i>Lathyrus/Pisum/Vicia</i>	317	1	100
Fabaceae	<i>Lathyrus/Vicia</i>	124	#	55
Fabaceae	<i>Lens</i> sp.	455	1	100
Fabaceae	<i>Medicago radiata</i>	103	#	91
Fabaceae	<i>Medicago</i> sp.	72	#	27
Fabaceae	<i>Pisum</i> sp.	2	•	9

TABLE 2: Continued.

Family	Taxa	Σ	Proportion in %	Frequency in %
Fabaceae	<i>Trifolium</i> type	1	.	9
Fabaceae	<i>Trigonella</i> sp.	2222	7	100
Fabaceae	<i>Trigonella/Astragalus</i>	37	#	9
Fabaceae	<i>Vicia</i> type	3	•	18
Geraniaceae	<i>Erodium</i> sp.	19	#	9
Lamiaceae	Lamiaceae indet.	1	.	9
Lamiaceae	<i>Ocimum/Salvia</i>	1	.	9
Liliaceae	<i>Ornithogalum/Muscari</i>	100	#	91
Malvaceae	cf. <i>Malva</i> sp.	258	1	100
Papaveraceae	<i>Fumaria</i> sp.	3	•	9
Papaveraceae	<i>Papaver</i> sp.	28	#	9
Plantaginaceae	<i>Veronica opaca</i> type	1	.	9
Poaceae	<i>Aegilops</i> sp.	139	#	91
Poaceae	<i>Aegilops</i> sp., glume base	4698	15	100
Poaceae	<i>Aegilops/Hordeum</i>	19	#	55
Poaceae	<i>Aegilops/Triticum</i> , glume base	18	#	18
Poaceae	<i>Agrostis</i> sp.	4	•	9
Poaceae	<i>Avena fatua</i> type	56	#	18
Poaceae	<i>Bromus</i> type	87	#	82
Poaceae	<i>Bromus/Brachypodium</i>	46	#	36
Poaceae	Cerealia	3	•	9
Poaceae	<i>Dasyphyrum</i> -type	18	#	9
Poaceae	<i>Echinaria capitata</i>	1	.	9
Poaceae	<i>Eragrostis</i> sp.	201	1	55
Poaceae	<i>Eremopyrum</i> sp.	1	.	9
Poaceae	<i>Hordeum</i> cf. <i>Spontaneum</i>	444	1	91
Poaceae	<i>Hordeum distichum</i> , rachis	25	#	45
Poaceae	<i>Hordeum distichum</i> type	17	#	64
Poaceae	<i>Hordeum</i> sp.	227	1	100
Poaceae	<i>Hordeum</i> sp., rachis	479	2	100
Poaceae	<i>Hordeum spontaneum</i> , rachis	1698	5	91
Poaceae	<i>Hordeum/Taeniatherum</i>	34	#	18
Poaceae	<i>Phalaris</i> sp.	1278	4	100
Poaceae	<i>Phleum</i> type	51	#	36
Poaceae	Poaceae indet., awn fragments	47	#	9
Poaceae	Poaceae indet., large	606	2	100
Poaceae	Poaceae indet., large, glume base fragments	997	3	100
Poaceae	Poaceae indet., medium	670	2	73
Poaceae	Poaceae indet., small	10372	33	100
Poaceae	<i>Secale</i> type	13	•	9
Poaceae	<i>Stipa</i> type	45	#	18
Poaceae	<i>Taeniatherum caput-medusae/crininum</i>	67	#	73
Poaceae	<i>Taeniatherum caput-medusae/crininum</i> , rachis	110	#	64
Poaceae	<i>Triticum boeoticum/dicoccoides</i> , glume base	28	#	64
Poaceae	<i>Triticum boeoticum/dicoccoides</i>	49	#	73
Poaceae	<i>Triticum</i> cf. <i>boeoticum</i>	27	#	9
Poaceae	<i>Triticum</i> cf. <i>boeoticum</i> (<i>thaouidar</i> , 2-grained)	10	•	9
Poaceae	<i>Triticum</i> cf. <i>dicoccum</i> , glume base	25	#	18
Poaceae	<i>Triticum</i> cf. <i>monococcum</i> , 1-grained	26	#	9
Poaceae	<i>Triticum</i> sp. glume base	205	1	82

TABLE 2: Continued.

Family	Taxa	Σ	Proportion in %	Frequency in %
Poaceae	<i>Triticum</i> sp.	10	•	36
Poaceae	<i>Triticum</i> , free-threshing type rachis	3	•	18
Poaceae	Triticoid type (acc. Van Zeist)	169	1	91
Polygonaceae	<i>Rumex/Polygonum</i>	4	•	9
Ranunculaceae	<i>Adonis</i> sp.	11	•	45
Resedaceae	<i>Reseda luteola</i>	8	•	9
Rosaceae	<i>Prunus</i> sp., fragment	1	•	9
Rubiaceae	<i>Galium</i> sp.	36	#	73
Solanaceae	<i>Solanum</i> sp.	1	•	9
	cf. <i>Vitis</i> sp.	1	•	9
Vitaceae	Indet.	53	#	45
	Ostracoda cf. <i>Candona</i> sp.	14	•	45

Archaeology, Classics and Egyptology, University of Liverpool. To date 45 anthracological samples have been analyzed from horizons AH XI and AH IX-I amounting to 1209 wood charcoal particles >2 mm. Judging from the small size of the retrieved charcoal particles (fragments >4 mm were only very occasionally present in the samples) the absence of fresh edges and the relatively low charcoal densities recovered from each archaeological horizon (Figure 11), it can be assumed that, on the whole, the anthracological assemblage had been subjected to a relatively high degree of post-depositional fragmentation prior to field sampling. This appears to be the case with the charcoal macro-remains retrieved from horizon AH VII, and especially from the latest sampled horizon AH I, both of which contained floors and other intensively maintained architectural features. It should also be noted that overall charcoal particles are very well preserved as indicated by the low number of unidentifiable fragments (ranging between 0–7 fragments per sample).

Depending on their size and shape individual charcoal fragments were fractured by hand or with a single edge razor blade across the transverse plane. Where applicable and necessary (also considering the small size of the examined fragments), the tangential and radial longitudinal planes were also obtained. Fresh charcoal surfaces were suspended in a sand bath and examined using high-power, epi-illuminating, dark-field microscopy (magnifications $\times 40$, $\times 50$, $\times 100$, $\times 200$, $\times 500$). Comparative reference materials consulted for wood charcoal identification include a modern charcoal reference collection from Southwest Asia, alongside published wood anatomical descriptions [84–87]. In total, 14 charcoal taxa have been identified. Preliminary results (raw/percentage fragment counts and sample presence) from the samples and size fractions already analyzed are presented in Table 3, tabulated by archaeological horizon.

2.3. Faunal Remains. While the archaeobotanical remains studied so far comprise only approximately 6% of the entire assemblage, about one fourth of the faunal remains from the deep sounding sequence have been analyzed, excluding microfaunal remains. We recorded over 5.800 specimens, 1.620 of which were identifiable to species or body class

and element. Unidentifiable fragments are recorded in order to document taphonomic processes on the materials. In relation to the archaeobotanical remains, the faunal remains are under-represented. This might be due to bone loss from taphonomic factors, or site use activities that concentrated faunal remains in parts of the tell that are unexcavated.

Faunal specimens were identified using the comparative collection in the Institute for Archaeological Sciences at the University of Tübingen. Documentation of the faunas follows standard zooarchaeological methods and counting units (e.g., [88–92]). All specimens were counted, weighed, and identified to species or body class, element, and portion of element. We recorded human and non-human taphonomic damage when available, as well as information to determine age. Typically, number of identified specimens (NISP) is the preferred counting unit for faunal assemblages [88, 93, 94]. However, during excavation, some horizons were fully (IV, V, VIII, X, XI) or partially (II, III, VI, VII, IX) wet screened, while others were not (I). Because of this, and the potential for NISP to underestimate small taxa in layers that were not wet screened, an alternative method based on weight is used to quantify the remains. Many authors have argued that bone weight represents a more accurate measure of meat mass because it corrects for differences in animal body size, and is less affected by fragmentation [88, 93, 94]. This is particularly true if bones are not mineralized and do not have surface concretions, and if the taphonomic conditions are similar throughout the sequence, which is the case at Chogha Golan.

For the data analysis we categorize individual taxa into groups based on body size and predator evasion tactics (following [95]), because the assemblage considered here is comparatively small. The groups include four sizes of ungulates, small carnivores, small fast, and small-slow moving animals (Table 4). This allows for less diagnostic remains (e.g., medium ungulates) to be included in the analysis.

2.4. Stable Carbon Isotope Data. Stable carbon isotope ratios were measured on 159 wild-type barley grains from the site. Measuring stable carbon isotopes in archaeobotanical remains is an established method for identifying past environmental conditions for plant growth in arid and semi-arid

TABLE 3: Quantified anthracological data from Chogha Golan (deep soundings; horizons AH XI, IX-IV, and III-I) tabulated by absolute fragment counts (C), percentage fragment counts (%), and sample presence (U).

	XI		IX		VIII		VII		VI		V		IV		III		II		I														
	C	%	U	C	%	U	C	%	U	C	%	U	C	%	U	C	%	U	C	%	U												
<i>Pistacia</i>	32	35.56	4	72	40.45	4	13	32.50	2	17	18.48	4	9	6.38	4	39	21.67	4	45	37.50	2	28	21.88	4	114	76.00	7	81	90.00	8			
<i>Amygdalus</i>	5	5.56	2	11	6.18	3	3	7.50	2	1	1.09	1	1	0.71	1	3	1.67	2	2	1.67	1	6	4.69	3	7	4.67	4	1	1.11	1			
<i>Prunus</i>																																	
cf. <i>Malvoideae</i>																																	
<i>Acer</i>				1	0.56	1										1	0.56	1															
<i>Salicaceae</i>	25	27.78	4	53	29.78	4	6	15.00	2	47	51.09	4	55	39.01	4	76	42.22	4	51	42.50	2	59	46.09	4	23	15.33	4	5	5.56	3			
<i>Tamarix</i>	23	25.56	4	31	17.42	4	17	42.50	2	21	22.83	4	70	49.65	4	51	28.33	4	11	9.17	2	31	24.22	4	4	2.67	4	1	1.11	1			
<i>Hippophae</i>	3	3.33	2	2	1.12	2	0																										
<i>Chenopodiaceae</i>	2	2.22	2	4	2.25	1	1	2.50	1	1	1.09	1	4	2.84	3	2	1.11	2	2	1.67	1	1	0.78	1	1	0.67	1	2	2.22	1			
<i>Palurus/Ziziphus</i>				1	0.56	1							2	1.42	2	1	0.56	1	2	1.67	2	1	0.78	1									
<i>Vitex</i>				1	0.56	1																											
<i>Leguminosae</i>				1	0.56	1				5	5.43	2				6	3.33	3	7	5.83	2	2	1.56	2	1	0.67	1						
cf. <i>Ephedra</i>																1	0.56	1															
cf. <i>Labiatae</i>				1	0.56	1																											
Total	90	100	(n = 4)	178	100	(n = 4)	40	100	(n = 2)	92	100	(n = 4)	141	100	(n = 4)	180	100	(n = 4)	120	100	(n = 2)	128	100	(n = 4)	150	100	(n = 7)	90	100	(n = 8)			

TABLE 4: Taxa categories based on body size and predator evasion tactics. Weight ranges from Nowack [96] and Silva and Downing [97].

	Weight range (kg)
Very large ungulate	
Aurochs (<i>Bos primigenius</i>)	500–1000
Large ungulate	
Red deer (<i>Cervus elaphus</i>)	75–340
Wild pig (<i>Sus scrofa</i>)	50–350
Medium ungulate	
Persian fallow deer (<i>Dama mesopotamica</i>)	50–120
Wild goat (<i>Capra aegagrus</i>)	40–90
Wild sheep (<i>Ovis sp.</i>)	40–90
Small ungulate	
Gazelle (<i>Gazella gazella</i>)	17–23
Small carnivore	
Eurasian lynx (<i>Lynx lynx</i>)	8–38
Red fox (<i>Vulpes vulpes</i>)	8–10
Wild cat (<i>Felis silvestris</i>)	3–8
Small fast-moving	
Cape hare (<i>Lepus capensis</i>)	1.3–7.0
Rock partridge (<i>Alectoris graeca</i>)	0.51–0.68
Fish (<i>Pices</i>)	
Small slow-moving	
Tortoise (<i>Testudo sp.</i>)	1–2+

environments, as $\delta^{13}\text{C}$ values in cereals provide a drought stress signal when the amount of water received during the grain-filling period is low [98–100]. Taking knowledge of intra-sample variability of $\delta^{13}\text{C}$ into account, a target of minimum measurements of six individual grains per archaeobotanical sample was taken. Well-developed grains were chosen to guarantee the exclusion of $\delta^{13}\text{C}$ values that would not reflect the average growing conditions, such as values obtained from immature grains. To eliminate inputs from sedimentary carbonate, the barley grains were reacted with 0.5 M HCl before measurement. The measurements were carried out at the Institute of Geosciences of the University of Tübingen, Germany on a FinniganMAT252 gas source mass spectrometer with a ThermoFinnigan GasBench II/CTC Combi-Pal autosampler.

The common standard of $\delta^{13}\text{C}$ VPDB (Vienna Peedee belemnite ‰) was applied to the measurements of $^{13}\text{C}/^{12}\text{C}$ ratios to calculate $\delta^{13}\text{C}$ in the barley grains. Changes in atmospheric CO_2 concentration ($\delta^{13}\text{C}$ air) over time were considered by calibrating the $\delta^{13}\text{C}$ from ancient barley into $\Delta^{13}\text{C}$ values using the approximation AIRCO2_LOESS [101].

3. Results

3.1. Long-Term Subsistence Development

3.1.1. *The Carpological Remains.* While 110 seed taxa are recorded for the entire assemblage, only up to 38% of these occur simultaneously in one of the archaeological horizons.

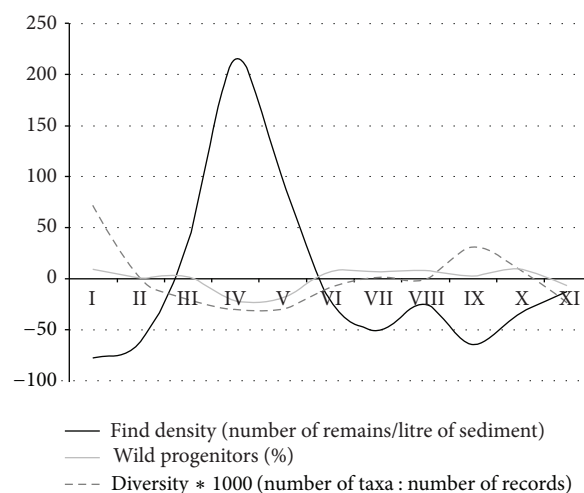


FIGURE 4: Find density, diversity and percentage of wild progenitor species of crops (all large-seeded grasses and pulses that were domesticated in the Neolithic period, i.e., mainly taxa of *Triticum*, *Hordeum*, and *Lens*) shown in their deviation from the mean represented by the x-axis.

Some of the taxa are represented in high numbers, such as the small-seeded Poaceae and Fabaceae, goatgrass and barley and thus characterize the different archaeological layers. Only 16 taxa occur throughout all the 11 archaeological layers, almost exclusively consisting of grasses and pulses (compare frequencies in Table 2).

The overall diversity, calculated as a ratio of the number of taxa and the number of records, was highest in layer I and IX which may indicate a bias, because these two layers were the poorest as concerns record numbers. The find density, that is, the number of records per liter of sediment, was highest in AH IV and V which is mostly due to a large number of small-seeded grasses in these two layers and correlates with low percentages of wild progenitor species of modern crops (Figure 4).

The main taxa groups show distinct developments over the stratigraphic sequence (Figure 5). Large-seeded grasses such as goatgrass (*Aegilops sp.*), the genome donor to free-threshing wheat species, and wild barley (*Hordeum spontaneum*) are very numerous from the beginning of the occupation. While wild barley decreases in relative proportions throughout the entire sequence, goatgrass appears abruptly reduced in layers V and IV. These trends are partially reflected in the potential arable weed species. These however increase from layer III onwards together with the wheat species (*Triticum spp.*). Large-seeded pulses, such as lentil (*Lens sp.*) and vetch (*Vicia sp.*) occur in lower proportions with a peak in layer VII and then continuously decrease until layer II. Small-seeded grasses strongly increase in layers V and IV and out-number all other taxa.

When the dominant small-seeded grass taxa are excluded from the assemblage, the proportion patterns change (Figure 6). The most conspicuous pattern becomes visible for wild barley, which is now comparatively higher

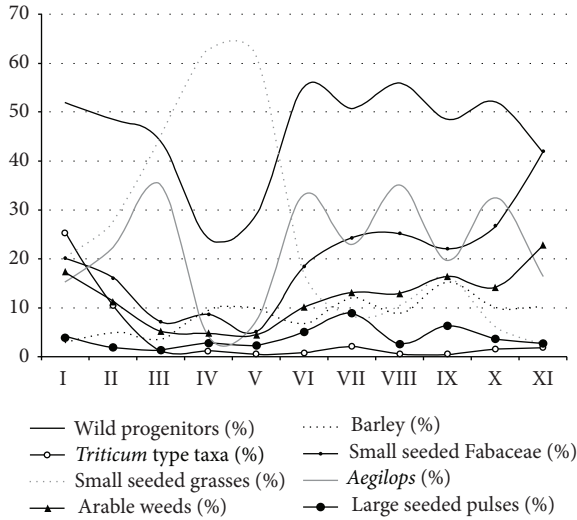


FIGURE 5: Proportions of the main taxa groups throughout the stratigraphic sequence; *Triticum* type taxa and barley include wild and domesticated taxa; total number of records on which percentage proportions are based for each archaeological horizon: I: 327, II: 1022, III: 2309, IV: 8875, V: 6584, VI: 1628, VII: 1298, VIII: 1550, IX: 614, X: 942, XI: 6621.

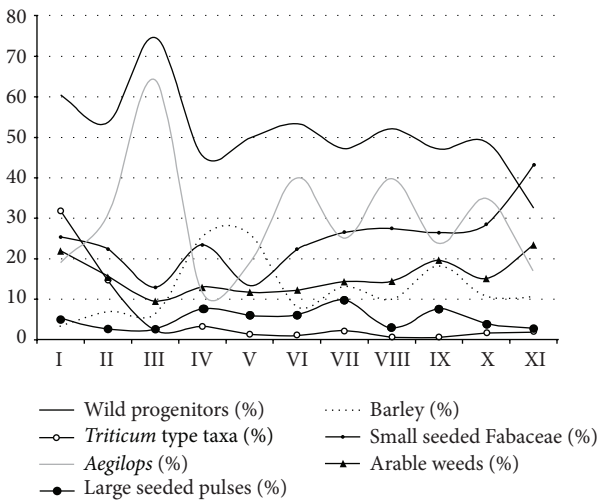


FIGURE 6: Development of the proportions of taxa groups without the small-seeded grasses.

in horizons V and IV, while other large-seeded grasses, goatgrass in particular, decrease.

Presuming that the percentages of taxa groups in the different layers are representative for the subsistence development of the entire site, shifts in plant use may be evident. Notable changes are visible in layers V and IV with decreasing proportions of large-seeded grasses, mostly represented by goatgrass, and an increase in proportions of barley and small-seeded grasses.

Size development of barley grains has been documented throughout the archaeological horizons (Figure 7). Seed size increase in wild cereal species has been linked to increased

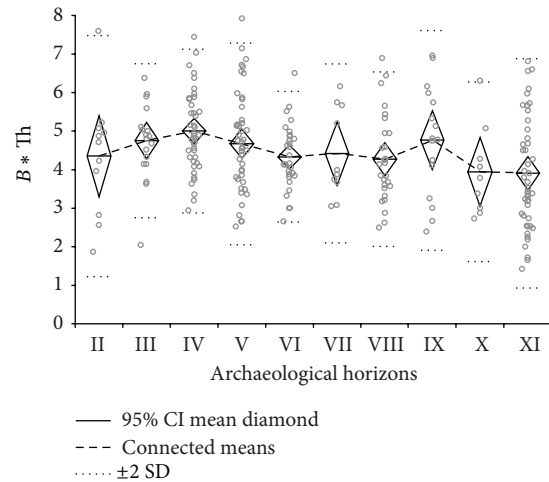


FIGURE 7: Development of barley grain sizes ($B * Th$: breadth multiplied by thickness) throughout the stratigraphic sequence.

plant management and cultivation [2]. An interesting observation is the correlation of the grain size development with the percentages of barley after exclusion of the small-seeded grasses from the assemblage. Both grain size mean values and proportion percentages of wild barley increase from layer XI to IX, then decrease and increase again in layers V and IV followed by a decrease from layer III onwards. In layer IV the first domesticated-type rachis segments of barley appear, indicating the emergence of potentially genetically changed barley cultivars by roughly 10.000 cal BP. This correlates with the increased proportions of wild barley in layers V to IV. However, the rachis internodes occur in very low proportions, consistent with the non-brittle lower rachis segments occurring in wild populations of barley as reported by Kislev [102]. Domesticated-type barley does not occur in the following layers III-I.

At the current stage of the analysis the earliest presence of unequivocally domesticated-type taxa occurs from layer II onwards with the presence of phenotypically domesticated emmer wheat chaff (*Triticum dicoccum*), corresponding with an increase of potential arable weed taxa and a decrease in goatgrass.

3.1.2. The Faunal Remains. Ungulates are the most commonly identified group, followed by fish (Figure 8), which are mostly represented by small vertebrae. Among the ungulates, sheep/goat (*Ovis* or *Capra* sp.), gazelle (*Gazella gazella*), pig (*Sus scrofa*), red deer (*Cervus elaphus*), and cattle (*Bos* sp.) are most common. Other taxa include tortoise (*Testudo* sp.), hedgehog (*Erinaceus europaeus*), red fox (*Vulpes vulpes*), Eurasian lynx (*Lynx lynx*), and unidentified medium-sized birds.

Large game, in particular medium ungulates such as sheep and goat, dominate the assemblage by mass throughout the sequence. There is a spike in small ungulates (i.e., gazelles) in horizons V and IV, which correlates to the changes of the

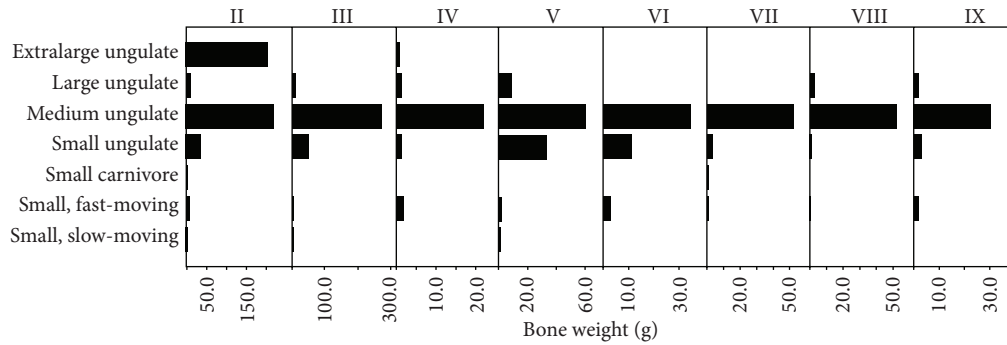


FIGURE 8: Taxa groups by bone weight for horizons with large samples (NISP > 50).

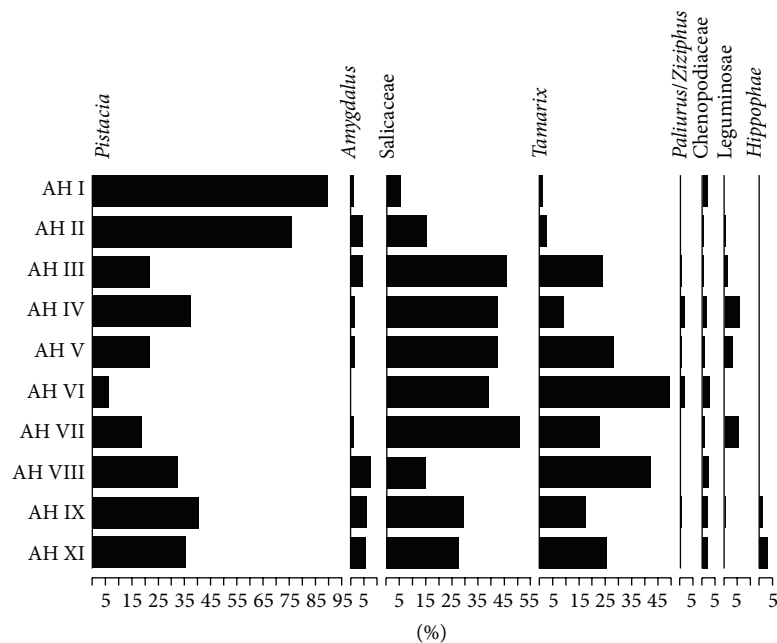


FIGURE 9: Anthracological diagram showing percentage fragment counts of the main taxa represented in the Chogha Golan deep sounding sequence (see also Table 3).

archaeobotanical assemblage. Bone weight values of extralarge ungulates (i.e., cattle) increase in horizon II, corresponding with the appearance of domesticated-type emmer chaff.

There are no temporal trends in the proportion of small to large game by mass through the sequence, nor are there changes in the small game component itself. There is, however, a statistically significant trend in the increase of cattle in later phases of the sequence (for detailed statistical results see [103]).

3.2. Environmental Dynamics

3.2.1. Wood Charcoal. The analysis of the anthracological remains points to the existence of two major arboreal vegetation catchments in the vicinity of Chogha Golan: the semi-arid *Pistacia*-*Amygdalus* woodland and riparian vegetation habitats dominated by *Salicaceae* and *Tamarix* (Table 3, Figure 9). *Chenopodiaceae* shrubs (likely present in both

zones) form a minor component of charcoal sample composition, although they are ubiquitous across the sampled sequence. Other less frequent taxa include *Paliurus/Ziziphus* and *Leguminosae* (subf. *Papilionoideae*), both of which might have been associated with riparian woodland habitats. The presence of *Hippophaë* is limited in the earliest sampled horizons (AH XI, AH IX). This taxon is considered by Zohary as tolerant of arid and cold conditions and its presence might represent a residual element from vegetation communities that were locally widespread during the Younger Dryas [66]. Other very rare taxa include *Vitex* (a riparian shrub), *Prunus* (diffuse porous; likely to represent some variety of wild cherry), *Maloideae* (subfamily of the *Rosaceae* including wild apples, pears and hawthorn), *Acer* (maple) and various shrubs (cf. *Ephedra*, cf. *Labiatae*). Fragments of grass stems (including charcoal particles identified as *Phragmites*) were also very occasionally present in the examined samples (not included in the wood charcoal counts). With the exception of *Vitex*, *Ephedra* and *Lamiaceae* the remaining wood charcoal

taxa are likely to have derived from vegetation catchments located at some distance from the site. In any case, their rarity suggests that they were not routinely and/or intensively collected as fuel wood.

The variations observed in the ubiquity (sample presence) and frequencies (percentage fragment counts; see also Table 3, Figure 9) of individual taxa provide some useful insights in the temporal fluctuations of the intensity of use and the availability of arboreal vegetation habitats near the site. An important first observation is that *Pistacia-Amygdalus* woodland was present and routinely used as a source of wood at Chogha Golan throughout the roughly 2000 years long habitation of the site, from its earliest sampled levels dated to the last phases of the Younger Dryas to the 10th millennium cal BP. *Pistacia* and *Amygdalus* charcoals account for >35% of charcoal sample composition in AH XI, AH IX-VIII (c. 11,740–10,650 cal BP). A decrease in both taxa is observed from AH VII and is more pronounced in AH VI. *Pistacia* values pick up very quickly in AH V (rising from 6.8% in AH VI to 21.67% in AH V) and continue to increase through the remainder of the sampled sequence, reaching 90% by AH I (currently dated to c. 9,640 cal BP). Overall, the wood charcoal samples corresponding to the much shorter time period represented by AH VII–IV (10650–10040 cal BP) are dominated by riparian taxa (particularly Salicaceae; the ubiquity of Papilionoideae charcoals is also noteworthy, representing in all cases young twig fragments). The wood charcoal samples derived from the chronologically latest part of the sequence (AH III–I; c. 10040–9640 cal BP) indicate yet another shift in sample composition from AH III, still dominated by Salicaceae, to AH II–I that are overwhelmingly dominated by *Pistacia*.

3.2.2. Stable Carbon Isotopes in Barley Grain. Most of the 159 measurements are available from archaeological layer XI (Figure 10). For horizons IX and VII only four measurements each could be obtained so far, while the remaining data distributes relatively equally on the other horizons. Despite the minimum target of six measurements per sample to cover the full range of variability in one sample [100], layers IX and VII show a sufficiently large range of values.

The range between 17‰ and 16‰ has elsewhere been defined to represent a transitional area between well-watered conditions for cereal growth (above 17‰) and drought stress (below 16‰) [99]. The measurements for each archaeological horizon demonstrate wide ranges, as is generally the case with increasing numbers of measurements. Most important are the mean and minimum values which represent the generalized signal (mean value) on one hand and the highest measured stress (minimum value) on the other. At Chogha Golan, there are no mean values below 16‰, indicating that drought stress was generally not a major impediment for plant growth. In some layers mean values were above 17‰, suggesting that the growing conditions for wild barley represented in layers VIII, VII, V and IV were generally under sufficient moisture availability. Archaeological layers XI, VI and III with mean values below 17‰ and minima values below 16‰ can be interpreted to show moderate drought stress signals in the plants.

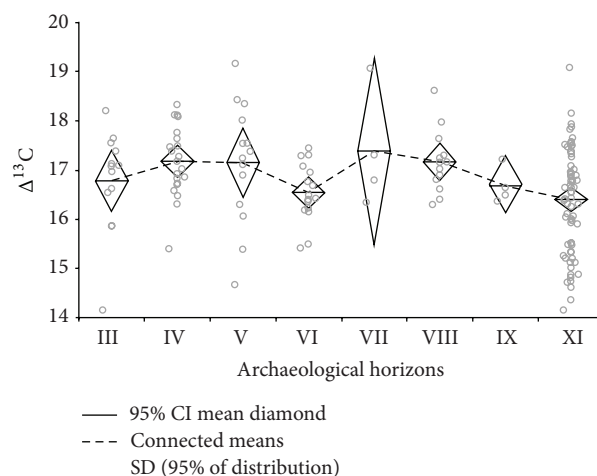


FIGURE 10: $\Delta^{13}\text{C}$ measurements of wild barley grains throughout the stratigraphic sequence of Chogha Golan. Each circle represents a measurement for a single grain.

Although the $\Delta^{13}\text{C}$ data do not indicate extreme drought stress signals in any of the sampled horizons, they suggest fluctuations of the moisture availability with reduced moisture levels available for plant growth particularly in horizon VI, which may have resulted in the reduction of or regional shifts in some plant populations.

4. Discussion

4.1. Environmental Fluctuations and Their Possible Impact on the Living Conditions at Chogha Golan. Various reasons have been discussed as influential factors on the development of domesticated species, attributing more influence to either humans in relation to their degree of consciousness and socio-cultural needs or to fluctuating natural conditions, such as moisture and temperature increase after the Younger Dryas or increasing atmospheric CO_2 concentration.

A major argument against multiple centers of origin of domesticated species and for the origins of domesticated plants in the Levant was formerly based on differences in vegetation development in the various geographic regions of the Fertile Crescent, in particular the later expansion of oak in the Zagros region compared to the Levant [68, 77]. Despite limited soil moisture availability in the eastern part of the Fertile Crescent, grasses expanded at the end of the Younger Dryas, suggesting that the principal resource situation as concerns the availability of grain food was relatively similar in the entire Fertile Crescent. Decreasing oxygen isotope values alongside declining Chenopodiaceae and *Artemisia* pollen as reflected in the Zeribar records that are synchronous with AH XI throughout AH IX at Chogha Golan, suggest increases in moisture. This is in agreement with the size development of barley grains and the $\delta^{13}\text{C}$ record from barley (Figures 7 and 10).

However, the position of Chogha Golan in a diversified region in terms of deficits or surpluses of rainfall suggests a

potential for considerable environmental fluctuations in relation to inter-annual weather variability and climate change.

As C3 plants are particularly sensitive to changes in atmospheric CO₂, the relatively low CO₂ concentrations during the Pleistocene have been used as an explanation for why agriculture only started in the Holocene and not earlier (e.g., [23, 24, 104]). Atmospheric CO₂ concentration during the critical sequence from large-scale gathering of wild cereals at Ohalo II around 23,000 BP increased from roughly 200 μmol mol⁻¹ to 270 μmol mol⁻¹ [105] until the end of the Younger Dryas when evidence of cultivating wild cereals started to become more frequent and remained relatively stable until approximately 1800 AD. Lower CO₂ concentrations are associated with reduced rates of photosynthesis which often results in the decreased production of storage carbohydrates and lowered plant productivity [104]. An increase from 200 to 270 μmol mol⁻¹ stimulates photosynthesis and biomass productivity of C3 plants by 25–50% which served as the main argument to explain the worldwide beginnings of agriculture only in the Holocene [23]. If we assume that this model is possible, we may further ask whether fluctuations in atmospheric CO₂ in the early Holocene may have resulted in extended phases of lower biomass productivity thus protracting the evolution of domesticated species.

The atmospheric concentration of CO₂ effects the water balance of C3 plants, because increased CO₂ reduces the stomatal aperture, thus lowering transpiration. This means that increasing CO₂ towards the end of the Pleistocene could have led to reductions in water consumption, reducing the intensity of drought stress experienced by the plants [23]. This has a theoretical impact on our interpretation of the Δ¹³C values in barley from Chogha Golan, as fluctuations toward decreased CO₂ could produce relative stress signals in the Δ¹³C record that are indicative of the short-term lowering of CO₂ concentration rather than for a reduction in water availability, as has been interpreted for the Δ¹³C values in barley from AH VI. However, this assumption is hypothetical as research on low CO₂ concentrations and vegetation responses are still very limited.

The Chogha Golan sequence falls into the early Holocene with CO₂ concentrations around 270 μmol mol⁻¹ and fluctuations in CO₂—for example, indicated in reconstructions of carbon-cycle dynamics based on trapped CO₂ at Taylor Dome [106]—may have influenced the productivity of the vegetation on a local and regional scale. In particular the data from the Byrd Station ice core indicate relatively low CO₂ concentrations around 10,000 BP which may be related to the low Δ¹³C values in AH VI. However, using raw data available from the World Data Center for Paleoclimatology, Boulder [107], lower CO₂ values occur towards the end of the occupation period at Chogha Golan, but are not chronologically related to AH VI. Given the relatively stable development of CO₂ concentrations between 11,800 and 10,000 BP, the lowered Δ¹³C values from Chogha Golan in horizon VI seem to support a moderate drought stress signal.

A peak in salt-tolerant *Tamarix* charcoal and the pronounced decrease of *Pistacia* and *Amygdalus* that may have

formed open woodland communities as observed in AH VI are consistent with the interpretation of slight drought stress, but could alternatively indicate a reduction in biomass productivity in relation to lower CO₂ concentrations.

Integrating the Lake Zeribar palaeoenvironmental record into our data sets we may delineate the following environment-subsistence-coupled developments.

Before the earliest occupation of the site, temperatures increased with the end of the Younger Dryas. High evaporation and low precipitation led to low lake levels, water salinization and scattered occurrence of a very thin arboreal cover, dominated by Chenopodiaceae. During the time of the first settlement horizon (AH XI), conditions were still relatively cold and dry, as indicated by the occurrence of *Hippophaë* charcoal, a moderate drought stress for wild barley at Chogha Golan, and high Chenopodiaceae and *Artemisia* pollen values at Lake Zeribar. At the same time *Pistacia* charcoal as well as grains of barley and goatgrass are already present in relatively high proportions and grain size mean values of barley increase, indicating intensive plant management. Environmental conditions changed until AH VIII when decreased Chenopodiaceae and *Artemisia*, and increased Poaceae pollen are indicated at Lake Zeribar which have been interpreted as reduced summer drought. Changes in seasonality resulted in the dominance of Poaceae pollen and an initial increase in arboreal pollen, represented by a *Pistacia*-deciduous oak semi-arid grassland. These shifts are reflected in abundant *Pistacia* charcoal at Chogha Golan and sufficient moisture availability for wild barley. However, grain size mean values and proportional percentages of wild barley decrease in AH VIII, suggesting some limitations in the use of barley which may have been compensated by goatgrass. In AH VII a few dung fragments and coprophilous fungi have been observed, while for the following sequence (AH VI) vegetation disturbance by hunters and/or herders has been suggested for the Lake Zeribar region. For this horizon the lowest *Pistacia* charcoal proportions have been documented, while Salicaceae and *Tamarix* percentages are increased. Drought and/or lowered biomass productivity may have limited the efficiency of plant management, which might also have resulted in a temporary change in animal prey availability. The latter becomes apparent in AH V with increased bone weight for gazelle. This is accompanied by large numbers of small-seeded grasses, a strong reduction in goatgrass and a relative peak in wild barley that may have been intensively cultivated under sufficient moisture availability in relation to the previous shortcomings in AH VI. Evidence for the intensified cultivation of wild barley is supported by increased grain size mean values. The conditions are unchanged in AH IV when first domesticated-type rachis segments of barley appear alongside a possible clay animal head.

In AH III the first evidence for the use of dung fuel is represented in the remains of a floor and suggests the intentional collection of dung for burning or construction, or increased access to dung from keeping certain species at the site. In this layer, grain size mean values and proportional percentages of wild barley decrease, whereas in the following layer AH II an increase of arable weed taxa and wheat species

is apparent. *Pistacia* pollen increases in a relative sense and oak pollen is also present at Lake Zeribar. This correlates with wood charcoal finds from Chogha Golan which show a steep increase in *Pistacia* percentages. In this horizon the first domesticated-type emmer chaff and an increase in cattle bone is documented. The first animal figurines representing cattle also occur in this horizon, as well as obsidian that comprises 0.5% of the lithic material. In AH I *Pistacia* charcoal increases further, and mortars, pestles and grinding slabs are frequent. Overall, the environment-subsistence-coupled developments suggest that despite the moderate fluctuations in biomass productivity for various reasons, the inhabitants of Chogha Golan created resilient living conditions through an increase in the use of large-bodied ungulates and cereal cultivation.

4.2. Changes in Resource Availability or Limitations to the Recognition of Spatial Patterns? Although the main seed and faunal taxa groups from Chogha Golan are relatively stable in composition throughout the archaeological layers, changing proportions of taxa in the middle (AH V and IV) and the late (AH II) parts of the sequence are considerable. While most of the archaeological horizons are dominated by large-seeded grasses, that is, goatgrass and barley, layers V and IV contain large amounts of small-seeded grasses and show signs of intensification of barley cultivation (Figure 6). The first domesticated-type rachis segments of barley and a relative seed size increase appear in layer IV. Resource stress, following on somewhat drier conditions for plant growth at the time of the formation of horizon VI, might have been present, which is corroborated by an increase in gazelle bones. The general lack of diachronic changes in the ratio of proportions of easy to procure small, slow-moving animals and more difficult to catch small, fast-moving game might be interpreted as an absence of resource stress [91, 95, 108, 109] (see [103] for an in-depth discussion of small game at Chogha Golan), though this might also reflect the small sample size of the current assemblage. There is also no significant change in the charcoal assemblages that are dominated by Salicaceae in AH V and IV. In general, AH VII–III are dominated by riparian taxa, while *Pistacia* (and to a lesser degree *Amygdalus*) register high values (percentage frequencies and ubiquity) in AH I–II. *Pistacia* and *Amygdalus* also have high values in the earlier part of the sampled sequence (AH XI–VIII). It is therefore possible that a different spatial pattern of fuel use and deposition of fuel debris is reflected in charcoal sample composition from AH VII–III (e.g., opportunistic clearance and use of riparian vegetation by mobile herders/hunters).

Preliminary micromorphological analyses have indicated that middens, as revealed throughout AH VII–III were likely accumulated inside abandoned structures [110]. Although there is no evidence to suggest that any of the sampled levels in the deep sounding could have been used as an animal penning area, very few dung fragments and coprophilous fungi were observed in AH VII [110, p. 129]. Small-seeded grasses and pulses are often interpreted as potential forage for herbivore species grazing in late summer. While the small-seeded grasses have very high frequencies in AH V and IV, small-seeded pulses are decreased by comparison

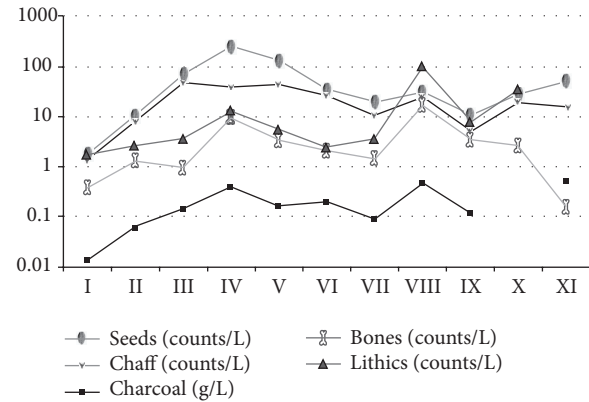


FIGURE 11: Find densities of the different find groups over the stratigraphic sequence.

in AH V, but increase in AH IV. It is possible that these levels represent a spatial pattern in the use of plant-derived resources compared to areas that are more likely to contain the debris of domestic wood fuel. Although dung spherulites were occasionally observed throughout the studied sequence, the first definitive evidence for the use of dung fuel derives from the remains of a floor preserved in AH III [110]. It is therefore possible that dung was used, alongside wood, as a complementary source of fuel or for the production of construction materials. However, the available evidence (including anthracological, seed botanical, micromorphological and stratigraphic data) does not support increasing use of dung fuel through time as a substitute for depleted woodland sources, but rather points to the resilient nature of the local landscape and its resources.

A major concern in interpreting our data is the question of the representativeness of a 1m² excavation area, and whether the fluctuations described above, particularly in AH V and IV, indeed indicate a shift in resource use or subsistence, or if the patterns only reflect the limitations of the excavation. Synchronous shifts in the proportions of some important plant and animal taxa, the correlation of barley proportions with grain size development, as well as the appearance of domesticated-type barley rachis internodes in AH IV and domesticated-type emmer chaff in AH II support the patterns as representative. The wood charcoal data, however, do not correlate with the changes in the seed and faunal assemblages. Instead they are in relatively good agreement with the $\Delta^{13}\text{C}$ values in barley.

Find densities of the different find groups may partially clarify the complex relationship of taphonomy and contextual differences in the different materials recovered from the deep sounding (Figure 11).

The general trend of the find densities is very similar in all of the groups and may indicate underlying contextual aspects of the deposits. Except for animal bones, find densities of the other categories are high in AH XI and decrease until AH IX, though densities of faunal remains must be examined with caution due to the differential wet screening methods mentioned above. Charcoal, animal bones and lithic artefacts

show their peak in find density in AH VIII. The densities of all find categories decrease after AH VIII, stagnate or slightly increase in AH VI and V, and again peak in finds in AH IV. After AH IV there is a continuous decrease in find densities in all categories, except for chaff remains, indicating their intense production in the settlement. In AH I the find densities are particularly low as a result of taphonomic processes in close proximity to the soil surface.

As concerns the specific question of AH V and IV reflecting some kind of bottleneck in subsistence, the high find densities in all categories suggest that a bias through selective preservation of the more fragile organic remains can be excluded (i.e. the reduced presence of large-seeded grasses and increased weights of gazelle bones very likely reflect the contextual characteristics of these layers).

5. Conclusions

The long-term subsistence reliance on cultivated wild plant species and wild game, with the first perpetual domesticated-type emmer appearing after almost 2,000 years of occupation suggests, despite a short-term depression in horizons V and IV, a generally proliferous environment, rich in resources at Chogha Golan.

The development of barley through time supports the model of protracted domestication. Both proportions and grain sizes of wild barley increase from AH XI to IX and correlate with $\Delta^{13}\text{C}$ signals of increasing moisture availability. The slight drought stress signal in AH VI, which can be easily understood as a plausible effect of inter-annual variation of precipitation, is followed by changes in the plant and faunal assemblages in layers V and IV. These layers show increased proportions of small-seeded grasses and gazelle bone, and a relative increase of wild barley proportions and its grain size. In AH IV, roughly around 10,200 cal BP barley rachis internodes also show domesticated-type features that disappear again in the following horizons. The short-term appearance of domesticated-type characteristics in barley suggest that the inhabitants at Chogha Golan were about to domesticate barley around 10,200 cal BP, but continued with the earlier practice of plant use (i.e. probably introducing again more wild types). Grain size and $\Delta^{13}\text{C}$ signals decrease again in AH III. With the transition to AH II further changes become apparent that include an increase in *Triticum* species, including phenotypically domesticated emmer wheat chaff (*Triticum dicoccum*), increasing percentages of potential arable weeds and increasing numbers of cattle bones.

In our previous work about Chogha Golan we argued that domestication of emmer may have evolved on-site [4], supported by the long tradition in cultivating a broad range of wild progenitor species of modern crops at the site, including the occurrence of domesticated-type barley rachis internodes non-recurring in layer IV, and biomolecular evidence of a separate gene pool in this area [111, 112]. There are, however, models suggesting the dispersal of wild and/or domesticated emmer from elsewhere [113] that are included in earlier archaeological hypotheses on transport of cereal grain into regions outside their original area of cultivation [114] and

supported by obsidian trade from southern Anatolia into our study region [60].

Hypotheses concerning the transport of grain from elsewhere, such as the western Fertile Crescent, can indeed be used to explain a protracted development of domesticated species. However, this argument is less convincing in a proliferous environment offering sufficient resources, and thus enabling a resilient way of living. Given the fact that there is evidence for the extensive use of plants, we may question whether the development of agriculture really required significant changes in human subsistence behavior or whether these changes were gradual and appear to be substantial only from our modern perspective.

Overall, the entire stratigraphic sequence at Chogha Golan can be seen as a continuously increasing intensification in the use of grasses, even in layers V and IV. However, a bottleneck in the availability of large-seeded grasses might have occurred during the formation of these two strata, which was attenuated by the increased gathering of small-seeded grasses, shift to small-bodied ungulates and intensified cultivation of barley, followed by emmer cultivation in the subsequent phases.

Conflict of Interests

The authors declare that there is no conflict of interests regarding the publication of this paper.

Acknowledgments

We thank the TISARP team and the Iranian colleagues, for their support during fieldwork and the directors of the Research Center of the ICHHTO and the Iranian Center for Archaeological Research for granting our permits. Funding of this research was provided by the Tübingen Senckenberg Center for Human Evolution and Palaeoecology (HEP) and the German Research Foundation (DFG).

References

- [1] K.-I. Tanno and G. Willcox, "Distinguishing wild and domestic wheat and barley spikelets from early Holocene sites in the Near East," *Vegetation History and Archaeobotany*, vol. 21, no. 2, pp. 107–115, 2012.
- [2] D. Q. Fuller, "Contrasting patterns in crop domestication and domestication rates: recent archaeobotanical insights from the old world," *Annals of Botany*, vol. 100, no. 5, pp. 903–924, 2007.
- [3] G. Willcox, "Searching for the origins of arable weeds in the Near East," *Vegetation History & Archaeobotany*, vol. 21, no. 2, pp. 163–167, 2012.
- [4] S. Riehl, M. Zeidi, and N. J. Conard, "Emergence of agriculture in the foothills of the Zagros mountains of Iran," *Science*, vol. 341, no. 6141, pp. 65–67, 2013.
- [5] M. A. Zeder and B. Hesse, "The initial domestication of goats (*Capra hircus*) in the Zagros mountains 10,000 years ago," *Science*, vol. 287, no. 5461, pp. 2254–2257, 2000.
- [6] M. A. Zeder, "Animal domestication in the Zagros: an update and directions for future research," in *Archaeozoology of the*

- Near East VIII: Proceedings of the Eighth International Symposium on the Archaeozoology of Southwestern Asia and Adjacent Areas*, L. G. E. Vila, A. Choyke, and H. Buitenhuis, Eds., pp. 243–277, Travaux de la Maison de l'Orient et de la Méditerranée (TMO), Lyon, France, 2008.
- [7] M. Heun, S. Haldorsen, and K. Vollan, "Reassessing domestication events in the Near East: einkorn and *Triticum urartu*," *Genome*, vol. 51, no. 6, pp. 444–451, 2008.
- [8] H. Ozkan, A. Brandolini, C. Pozzi, S. Effgen, J. Wunder, and F. Salamini, "A reconsideration of the domestication geography of tetraploid wheats," *Theoretical and Applied Genetics*, vol. 110, no. 6, pp. 1052–1060, 2005.
- [9] F. Salamini, H. Özkan, A. Brandolini, R. Schäfer-Pregl, and W. Martin, "Genetics and geography of wild cereal domestication in the Near East," *Nature Reviews Genetics*, vol. 3, no. 6, pp. 429–441, 2002.
- [10] S. Naderi, H.-R. Rezaei, F. Pompanon et al., "The goat domestication process inferred from large-scale mitochondrial DNA analysis of wild and domestic individuals," *Proceedings of the National Academy of Sciences of the United States of America*, vol. 105, no. 46, pp. 17659–17664, 2008.
- [11] D. Q. Fuller, G. Willcox, and R. G. Allaby, "Cultivation and domestication had multiple origins: arguments against the core area hypothesis for the origins of agriculture in the Near East," *World Archaeology*, vol. 43, no. 4, pp. 628–652, 2011.
- [12] G. Larson, K. Dobney, U. Albarella et al., "Worldwide phylogeography of wild boar reveals multiple centers of pig domestication," *Science*, vol. 307, no. 5715, pp. 1618–1621, 2005.
- [13] R. G. Allaby, D. Q. Fuller, and T. A. Brown, "The genetic expectations of a protracted model for the origins of domesticated crops," *Proceedings of the National Academy of Sciences of the United States of America*, vol. 105, no. 37, pp. 13982–13986, 2008.
- [14] K.-I. Tanno and G. Willcox, "How fast was wild wheat domesticated?" *Science*, vol. 311, no. 5769, p. 1886, 2006.
- [15] M. Heun, S. Abbo, S. Lev-Yadun, and A. Gopher, "A critical review of the protracted domestication model for Near-Eastern founder crops: linear regression, long-distance gene flow, archaeological, and archaeobotanical evidence," *Journal of Experimental Botany*, vol. 63, no. 12, pp. 4333–4341, 2012.
- [16] G. C. Hillman and M. S. Davies, "Domestication rates in wild-type wheats and barley under primitive cultivation," *Biological Journal of the Linnean Society*, vol. 39, no. 1, pp. 39–78, 1990.
- [17] L. R. Binford, "Post-Pleistocene adaptations," in *New perspectives in archaeology*, S. R. Binford and L. R. Binford, Eds., pp. 313–342, Aldine Publishing, Chicago, Ill, USA, 1968.
- [18] M. N. Cohen, *Food Crisis in Prehistory: Overpopulation and the Origins of Agriculture*, Yale University Press, New Haven, Conn, USA, 1977.
- [19] B. Byrne, "Climatic change and the origins of agriculture," in *Studies in the Neolithic and urban revolutions: The V. Gordon Childe Colloquium, Mexico*, L. Manzanilla, Ed., pp. 21–34, 1987.
- [20] D. O. Henry, *From Foraging to Agriculture: The Levant at the End of the Ice Age*, University of Pennsylvania Press, Philadelphia, Pa, USA, 1989.
- [21] H. E. Wright Jr., "Environmental determinism in Near Eastern prehistory," *Current Anthropology*, vol. 34, no. 4, pp. 458–469, 1993.
- [22] O. Bar-Yosef, "Climatic fluctuations and early farming in West and East Asia," *Current Anthropology*, vol. 52, supplement 4, pp. S175–S193, 2011.
- [23] R. F. Sage, "Was low atmospheric CO₂ during the Pleistocene a limiting factor for the origin of agriculture?" *Global Change Biology*, vol. 1, no. 2, pp. 93–106, 1995.
- [24] P. J. Richerson, R. Boyd, and R. L. Bettinger, "Was agriculture impossible during the Pleistocene but mandatory during the Holocene? A climate change hypothesis," *The American Antiquity*, vol. 66, no. 3, pp. 387–411, 2001.
- [25] O. Bar-Yosef, "Social changes triggered by the Younger Dryas and the early Holocene climatic fluctuations in the Near East," in *The Archaeology of Environmental Change: Socionatural Legacies of Degradation and Resilience*, C. T. Fisher, J. B. Hill and, and G. M. Feinman, Eds., pp. 192–208, The University of Arizona Press, Tucson, Ariz, USA, 2009.
- [26] K. V. Flannery, "The ecology of early food production in Mesopotamia: prehistoric farmers and herders exploited a series of adjacent but contrasting climatic zones," *Science*, vol. 147, no. 3663, pp. 1247–1256, 1965.
- [27] S. Riehl, "Variability in ancient Near Eastern environmental and agricultural development," *Journal of Arid Environments*, vol. 86, pp. 113–121, 2012.
- [28] I. J. Orland, M. Bar-Matthews, A. Ayalon et al., "Seasonal resolution of Eastern Mediterranean climate change since 34ka from a Soreq Cave speleothem," *Geochimica et Cosmochimica Acta*, vol. 89, pp. 240–255, 2012.
- [29] T. Litt, S. Krastel, M. Sturm et al., "PALEOVAN, International Continental Scientific Drilling Program (ICDP): site survey results and perspectives," *Quaternary Science Reviews*, vol. 28, no. 15-16, pp. 1555–1567, 2009.
- [30] K. Wasylkova, A. Witkowski, A. Walanus, A. Hutorowicz, S. W. Alexandrowicz, and J. J. Langer, "Palaeolimnology of Lake Zeribar, Iran, and its climatic implications," *Quaternary Research*, vol. 66, no. 3, pp. 477–493, 2006.
- [31] S. Riehl, "A cross-disciplinary investigation of cause-and-effect for the dependence of agro-production on climate change in the ancient Near East," in *Knochen pflastern ihren Weg. Festschrift for Hans-Peter and Margarete Uerpman*, S. Münzel, R. de Beauchair, and H. Napierala, Eds., pp. 217–226, Marie Leidorf, Rahden, Germany, 2009.
- [32] D. Rindos, *The Origins of Agriculture. An Evolutionary Perspective*, Academic Press, London, UK, 1984.
- [33] T. Watkins, "Neolithisation needs evolution, as evolution needs neolithisation," *Neolithics*, vol. 2, pp. 5–10, 2013.
- [34] J. Diamond, *The World Until Yesterday: What Can We Learn from Traditional Societies?* Viking Adult, 2012.
- [35] E. Asouti and D. Q. Fuller, "From foraging to farming in the Southern Levant: the development of epipalaeolithic and pre-pottery neolithic plant management strategies," *Vegetation History and Archaeobotany*, vol. 21, no. 2, pp. 149–162, 2012.
- [36] E. Asouti and D. Q. Fuller, "A contextual approach to the emergence of agriculture in southwest Asia: reconstructing early neolithic plant-food production," *Current Anthropology*, vol. 54, no. 3, pp. 299–345, 2013.
- [37] M. Zeidi and N. J. Conard, "Preliminary report on the chipped lithic assemblage from Chogha Golan, a PPN site in the foothills of the Zagros mountains, Ilam Province, Iran," *Ex Oriente*. In press.
- [38] M. Zeidi, S. Riehl, H. Napierala, and N. Conard, "Chogha Golan: a PPN site in the foothills of the Zagros Mountains, Ilam Province, Iran (report on the first season of excavation in 2009)," in *Proceedings of the 7th International Congress on the Archaeology of the Ancient Near East*, R. Matthews and J. Curtis, Eds., pp. 259–275, Harrassowitz, Wiesbaden, Germany, 2012.

- [39] R. Braidwood, "The earliest village communities of southwestern Asia," *Journal of World History*, vol. 1, pp. 278–310, 1953.
- [40] R. J. Braidwood and B. Howe, *Prehistoric Investigations in Iraqi Kurdistan*, University of Chicago Press, Chicago, Ill, USA, 1960.
- [41] F. Hole, *The Archaeology of Western Iran: Settlement and Society from Prehistory to the Islamic Conquest*, Smithsonian Institution Press, 1987.
- [42] H. Helbaek, "Plant collecting, dry-farming, and irrigation agriculture in prehistoric Deh Luran," in *Prehistory and Human Ecology of the Deh Luran Plain. An Early Village Sequence from Khuzistan, Iran*, F. Hole, K. V. Flannery, and J. A. Neely, Eds., pp. 383–426, University of Michigan, Ann Arbor, Mich, USA, 1969.
- [43] L. Costantini, "Seeds," in *Archaeological Discoveries and Methodological Problems in the Excavations of Shahr-i Sokhta*, R. Biscione, G. M. Bulgarelli, L. Costantini, M. Pierno, and M. Tosi, Eds., plates 33–36, pp. 48–50, E.J. Brill, Leiden, The Netherlands, 1974.
- [44] N. Miller, "Archaeobotany in Iran, past and future," in *Yeki Bud, Yeki Nabud: Essays on the Archaeology of Iran in Honor of William M. Sumner*, N. Miller and K. Abdi, Eds., pp. 9–15, The Cotsen Institute of Archaeology, University of California, Los Angeles, Calif, USA, 2003.
- [45] F. Hole, K. V. Flannery, and J. A. Neely, *Prehistory and Human Ecology of the Deh Luran Plain*, Memoirs of the Museum of Anthropology, University of Michigan Press, Ann Arbor, Mich, USA, 1969.
- [46] S. Bökönyi, *Animal Remains from Four Sites in the Kermanshah Valley, Iran*, BAR Supplementary Series, British Archaeological Reports, Oxford, UK, 1977.
- [47] H.-P. Uerpmann, "Metrical analysis of faunal remains from the Middle East," in *Approaches to Faunal Analysis in the Middle East*, R. H. Meadow and M. A. Zeder, Eds., pp. 41–45, Peabody Museum, Cambridge, Mass, USA, 1978.
- [48] H.-P. Uerpmann, *Probleme der Neolithisierung des Mittelmeerraums*, Reichert, Wiesbaden, Germany, 1979.
- [49] B. Hesse, *Evidence for Husbandry from the Early Neolithic Site of Ganj Dareh in Western Iran*, Columbia University, 1978.
- [50] B. Hesse, "Slaughter patterns and domestication: the beginnings of pastoralism in western Iran," *Man*, vol. 17, no. 3, pp. 403–417, 1982.
- [51] B. Hesse, "These are our goats, the origins of herding in West Central Iran," in *Animals and Archaeology: 3. Early Herders and Their Flocks*, J. Clutton-Brock and C. Grigson, Eds., BAR International Series, pp. 243–264, BAR International, Oxford, UK, 1984.
- [52] M. A. Zeder, "A View from the Zagros: new perspectives on livestock domestication in the fertile crescent," in *The First Steps of Animal Domestication: New Archaeozoological Approaches*, J.-D. Vigne, J. Peters, and D. Helmer, Eds., pp. 125–146, Oxbow Books, Oxford, UK, 2005.
- [53] M. A. Zeder, "Domestication and early agriculture in the Mediterranean Basin: origins, diffusion, and impact," *Proceedings of the National Academy of Sciences of the United States of America*, vol. 105, no. 33, pp. 11597–11604, 2008.
- [54] R. Matthews, W. Matthews, and Y. Mohammadifar, *The Earliest Neolithic of Iran: 2008 Excavations at Sheikh-E Abad and Jani. Central Zagros Archaeological Project*, vol. 1, Oxbow Books, Oxford, UK, 2013.
- [55] L. R. Stevens, H. E. Wright, and E. Ito, "Proposed changes in seasonality of climate during the Lateglacial and Holocene at Lake Zeribar, Iran," *Holocene*, vol. 11, no. 6, pp. 747–755, 2001.
- [56] M. Zeidi and N. J. Conard, "Chipped stone artifacts from the aceramic Neolithic site of Chogha Golan, Ilam Province, western Iran," in *Stone Tools in Transition: From Hunter-Gatherers to Farming Societies in the Near East*, F. Borrell, J. J. Ibanez, and M. Molist, Eds., pp. 313–326, Universitat Autònoma de Barcelona Press, Barcelona, Spain, 2013.
- [57] S. K. Kozłowski, "From Zawi Chemi to M'lefaat," in *Neolithic Chipped Stone Industries of the Fertile Crescent, and Their Contemporaries in Adjacent Regions*, S. K. Kozłowski and H. G. K. Gebel, Eds., pp. 161–170, Ex oriente, Berlin, Germany, 1996.
- [58] S. K. Kozłowski, *The Eastern Wing of the Fertile Crescent*, BAR International Series, BAR International, Oxford, UK, 1999.
- [59] K. Abdi, "Obsidian in Iran from the Epipalaeolithic period to the Bronze Age," in *Persiens antike Pracht*, T. Stöllner, R. Slotta, and A. Vatandoust, Eds., pp. 148–153, Bochum Museum, Bochum, Germany, 2004.
- [60] H. Darabi and M. D. Glascock, "The source of obsidian artefacts found at East Chia Sabz, Western Iran," *Journal of Archaeological Science*, vol. 40, no. 10, pp. 3804–3809, 2013.
- [61] T. Watkins, "Supra-regional networks in the Neolithic of Southwest Asia," *Journal of World Prehistory*, vol. 21, no. 2, pp. 139–171, 2008.
- [62] N. J. Conard and M. Zeidi, "The ground stone tools from the aceramic neolithic site of Chogha Golan, Ilam Province, western Iran," in *Stone Tools in Transition: From Hunter-Gatherers to Farming Societies in the Near East*, F. Borrell, J. J. Ibanez, and M. Molist, Eds., pp. 365–375, Universitat Autònoma de Barcelona Press, Barcelona, Spain, 2013.
- [63] S. Riehl, M. Benz, N. J. Conard et al., "Plant use in three Pre-Pottery Neolithic sites of the northern and eastern Fertile Crescent: a preliminary report," *Vegetation History & Archaeobotany*, vol. 21, no. 2, pp. 95–106, 2012.
- [64] P. J. Reimer, M. G. L. Baillie, E. Bard et al., "Intcal09 Terrestrial radiocarbon age calibration 0–26 cal kyr BP," *Radiocarbon*, vol. 46, no. 3, pp. 1029–1058, 2004.
- [65] E. Ehlers, *Iran. Grundzüge einer Geographischen Landeskunde*, Wissenschaftliche Buchgesellschaft, Darmstadt, Germany, 1980.
- [66] M. Zohary, *Geobotanical Foundations of the Middle East*, Swets & Zeitlinger Publishers, Stuttgart, Germany, 1973.
- [67] H. I. Griffiths, A. Schwalb, and L. R. Stevens, "Environmental change in southwestern Iran: the Holocene ostracod fauna of Lake Mirabad," *The Holocene*, vol. 11, no. 6, pp. 757–764, 2001.
- [68] W. van Zeist and S. Bottema, *Late Quaternary Vegetation of the Near East*, Dr. Ludwig Reichert, Wiesbaden, Germany, 1991.
- [69] A. P. El-Moslimany, "The late Pleistocene climates of the Lake Zeribar region (Kurdistan, western Iran) deduced from the ecology and pollen production of non-arboreal vegetation," *Vegetatio*, vol. 72, no. 3, pp. 131–139, 1987.
- [70] S. Bottema, "A late quaternary pollen diagram from Lake Urmia (Northwestern Iran)," *Review of Palaeobotany and Palynology*, vol. 47, no. 3–4, pp. 241–261, 1986.
- [71] M. Djamali, J.-L. de Beaulieu, M. Shah-hosseini et al., "A late Pleistocene long pollen record from Lake Urmia, NW Iran," *Quaternary Research*, vol. 69, no. 3, pp. 413–420, 2008.
- [72] K. Wasylkowa, "Palaeoecology of Lake Zeribar, Iran, in the Pleniglacial, Lateglacial and Holocene, reconstructed from plant macrofossils," *The Holocene*, vol. 15, no. 5, pp. 720–735, 2005.
- [73] L. R. Stevens, E. Ito, A. Schwalb, and H. E. Wright Jr., "Timing of atmospheric precipitation in the Zagros Mountains inferred from a multi-proxy record from Lake Mirabad, Iran," *Quaternary Research*, vol. 66, no. 3, pp. 494–500, 2006.

- [74] S. Bottema and W. van Zeist, "Palynological evidence for the climatic history of the Near East 50000–6000 BP," in *Colloques Internationaux du C.N.R.S.*, vol. 598, pp. 111–132, Paris, France, 1981.
- [75] W. van Zeist and S. Bottema, "Palynological investigations in western Iran," *Palaeohistoria*, vol. 19, pp. 19–85, 1977.
- [76] W. van Zeist and S. Bottema, "Vegetational history of the eastern Mediterranean and the Near East during the last 20000 years," in *Palaeoclimates, Palaeoenvironments and Human Communities in the Eastern Mediterranean Region in Later Prehistory*, J. L. Bintliff and W. van Zeist, Eds., pp. 277–319, British Archaeological Reports, Oxford, UK, 1982.
- [77] S. Bottema, "The younger dryas in the eastern mediterranean," *Quaternary Science Reviews*, vol. 14, no. 9, pp. 883–891, 1995.
- [78] H. E. Wright and J. L. Thorpe, "Climatic change and the origin of agriculture in the Near East," in *Global Change in the Holocene*, A. Mackay, R. Battarbee, J. Birks, and F. Oldfield, Eds., pp. 49–62, Arnold, London, UK, 2003.
- [79] N. Roberts, "Did prehistoric landscape management retard the post-glacial spread of woodland in Southwest Asia?" *Antiquity*, vol. 76, no. 294, pp. 1002–1010, 2002.
- [80] E. Asouti and C. Kabukcu, "Holocene semi-arid oak woodlands in the Irano-Anatolian region of Southwest Asia: natural or anthropogenic?" *Quaternary Science Reviews*, vol. 90, pp. 158–182, 2014.
- [81] G. C. Hillman, "Cereal remains from Tell Ilbol and Tell Qaramel," in *The River Qoueiq, Northern Syria, and Its Catchment: Studies Arising from the Tell Rifaat Survey 1977–79*, J. Matthers, Ed., pp. 503–507, British Archaeological Reports, Oxford, UK, 1981.
- [82] G. Willcox, "Charred plant remains from a 10th millennium B.P. kitchen at Jerf el Ahmar (Syria)," *Vegetation History & Archaeobotany*, vol. 11, no. 1–2, pp. 55–60, 2002.
- [83] S. Riehl, "Plant production in a changing environment—the archaeobotanical remains from Tell Mozan," in *Ausgrabungen 1998–2001 in der Zentralen Oberstadt von Tall Mozan/Urkeš: The Development of the Environment, Subsistence and Settlement of the City of Urkeš and Its Region*, K. Deckers, M. Doll, P. Pfälzner, and S. Riehl, Eds., pp. 13–158, 2010.
- [84] P. Greguss, *Holz-anatomie der europäischen Laubhölzer und Sträucher*, Akademiai Kiado, Budapest, Hungary, 1959.
- [85] A. Fahn, E. Werker, and P. Baas, *Wood Anatomy and Identification of Trees and Shrubs from Israel and Adjacent Regions*, The Israel Academy of Sciences and Humanities, Jerusalem, Israel, 1986.
- [86] F. H. Schweingruber, *Anatomie europäischer Hölzer. Ein Atlas zur Bestimmung europäischer Baum-, Strauch- und Zwergstrauchhölzer*, Paul Haupt, Stuttgart, Germany, 1990.
- [87] A. Crivellaro and F. H. Schweingruber, *Atlas of Wood, Bark and Pith Anatomy of Eastern Mediterranean Trees and Shrubs*, Springer, Dordrecht, The Netherlands, 2013.
- [88] H.-P. Uerpman, "Animal bone finds and economic archaeology: a critical study of 'osteological' method," *World Archaeology*, vol. 4, no. 3, pp. 307–322, 1973.
- [89] D. K. Grayson, *Quantitative Zooarchaeology*, Academic Press, Orlando, Fla, USA, 1984.
- [90] R. L. Lyman, *Vertebrate Taphonomy*, Cambridge University Press, Cambridge, UK, 1994.
- [91] M. C. Stiner, *The Faunas of Hayonim Cave, Israel: a 200,000-Year Record of Paleolithic Diet, Demography and Society*, Peabody Museum of Archaeology and Ethnology, Harvard University, Cambridge, Mass, USA, 2005.
- [92] E. J. Reitz and E. S. Wing, *Zooarchaeology*, Cambridge University Press, Cambridge, UK, 2nd edition, 2008.
- [93] E. J. Reitz and D. Cordier, "Use of allometry in zooarchaeological analysis," in *Animals and Archaeology 2. Shell Middens, Fishes and Birds*, C. Grigson and J. Clutton-Brock, Eds., pp. 237–252, British Archaeological Reports, Oxford, UK, 1983.
- [94] E. J. Reitz, I. R. Quitmyer, H. S. Hale, S. J. Scudder, and E. S. Wing, "Application of allometry to zooarchaeology," *American Antiquity*, vol. 52, no. 2, pp. 304–317, 1987.
- [95] M. C. Stiner, N. D. Munro, and T. A. Surovell, "The tortoise and the hare: small-game use, the broad-spectrum revolution, and paleolithic demography," *Current Anthropology*, vol. 41, no. 1, pp. 39–73, 2000.
- [96] R. M. Nowack, *Walker's Mammals of the World*, The Johns Hopkins University Press, Baltimore, Md, USA, 6th edition, 1999.
- [97] M. Silva and J. A. Downing, *Handbook of Mammalian Body Masses*, CRC Press, Boca Raton, Fla, USA, 1995.
- [98] J. L. Araus, J. P. Ferrio, J. Voltas, M. Aguilera, and R. Buxó, "Agronomic conditions and crop evolution in ancient Near East agriculture," *Nature Communications*, vol. 5, article 3953, 2014.
- [99] S. Riehl, K. E. Pustovoytov, H. Weippert, S. Klett, and F. Hole, "Drought stress variability in ancient Near Eastern agricultural systems evidenced by $\delta^{13}\text{C}$ in barley grain," *Proceedings of the National Academy of Sciences*, vol. 111, no. 34, pp. 12348–12353, 2014.
- [100] G. Fiorentino, J. P. Ferrio, A. Bogaard, J. L. Araus, and S. Riehl, "Stable isotopes in archaeobotanical research," *Vegetation History and Archaeobotany*, vol. 24, no. 1, pp. 215–227, 2015.
- [101] J. P. Ferrio, J. Voltas, and J. L. Araus, *A Smoothed Curve of $\delta^{13}\text{C}$ of Atmospheric CO_2 from 16.100 BCE to 2.010 CE*, edited by AIRCO2-LOESS, University of Lleida, 2012.
- [102] M. E. Kislev, "Early agriculture and paleoecology of Netiv Hagdud," in *An Early Neolithic Village in the Jordan Valley: Part 1. The Archaeology of Netiv Hagdud*, O. Bar-Yosef and A. Gopher, Eds., chapter 8, pp. 209–236, Peabody Museum of Archaeology and Ethnology, Harvard University, Cambridge, Mass, USA, 1997.
- [103] B. M. Starkovich, S. Riehl, M. Zeidi, and N. J. Conard, "Subsistence strategies in the aceramic Neolithic at Chogha Golan, Iran," in *Bones and Identity: Zooarchaeological Approaches to Reconstructing Social and Cultural Landscapes in Southwest Asia*, N. Marom, R. Yeshurun, L. Weissbrod, and G. Bar-Oz, Eds., Oxbow Books, Oxford, UK.
- [104] S. A. Cowling and M. T. Sykes, "Physiological significance of low atmospheric CO_2 for plant-climate interactions," *Quaternary Research*, vol. 52, no. 2, pp. 237–242, 1999.
- [105] J. D. Shakun, P. U. Clark, F. He et al., "Global warming preceded by increasing carbon dioxide concentrations during the last deglaciation," *Nature*, vol. 484, no. 7392, pp. 49–54, 2012.
- [106] A. Indermühle, T. F. Stocker, F. Joos et al., "Holocene carbon-cycle dynamics based on CO_2 trapped in ice at Taylor Dome, Antarctica," *Nature*, vol. 398, no. 6723, pp. 121–126, 1999.
- [107] J. B. Pedro, S. O. Rasmussen, and T. D. van Ommen, "Tightened constraints on the time-lag between Antarctic temperature and CO_2 during the last deglaciation," *Climate of the Past*, vol. 8, no. 4, pp. 1213–1221, 2012.
- [108] M. C. Stiner, "Thirty years on the 'Broad Spectrum Revolution' and paleolithic demography," *Proceedings of the National Academy of Sciences of the United States of America*, vol. 98, no. 13, pp. 6993–6996, 2001.

- [109] N. D. Munro, "Zooarchaeological measures of hunting pressure and occupation intensity in the Natufian: implications for agricultural origins," *Current Anthropology*, vol. 45, no. 4, pp. S5–S33, 2004.
- [110] A. Zaroni, *Using Micromorphology and Microfacies Analysis to Understand the Settlement History of the Aceramic Tell of Chogha Golan, Ilam Province, Iran*, edited by Institut für Naturwissenschaftliche Archäologie, Mathematisch-Naturwissenschaftliche Fakultät, Eberhard-Karls-Universität Tübingen, 2014.
- [111] P. L. Morrell and M. T. Clegg, "Genetic evidence for a second domestication of barley (*Hordeum vulgare*) east of the Fertile Crescent," *Proceedings of the National Academy of Sciences of the United States of America*, vol. 104, no. 9, pp. 3289–3294, 2007.
- [112] P. L. Morrell and M. T. Clegg, "Hordeum," in *Wild Crop Relatives: Genomic and Breeding Resources—Cereals*, C. Kole, Ed., pp. 309–319, Springer, Berlin, Germany, 2011.
- [113] P. Civián, Z. Ivaničová, and T. A. Brown, "Reticulated origin of domesticated emmer wheat supports a dynamic model for the emergence of agriculture in the fertile crescent," *PLoS ONE*, vol. 8, no. 11, Article ID e81955, 2013.
- [114] G. Willcox, S. Fornite, and L. Herveux, "Early Holocene cultivation before domestication in northern Syria," *Vegetation History and Archaeobotany*, vol. 17, no. 3, pp. 313–325, 2008.

Research Article

The Use and Effectiveness of Triple Multiplex System for Coding Region Single Nucleotide Polymorphism in Mitochondrial DNA Typing of Archaeologically Obtained Human Skeletons from Premodern Joseon Tombs of Korea

Chang Seok Oh,^{1,2} Soong Deok Lee,^{1,3} Yi-Suk Kim,⁴ and Dong Hoon Shin^{1,2}

¹Bioanthropology and Paleopathology Lab, Institute of Forensic Science, Seoul National University College of Medicine, 28 Yongon-dong, Chongno-Gu, Seoul 110-799, Republic of Korea

²Department of Anatomy, Seoul National University College of Medicine, 28 Yongon-dong, Chongno-Gu, Seoul 110-799, Republic of Korea

³Department of Forensic Medicine, Seoul National University College of Medicine, 28 Yongon-dong, Chongno-Gu, Seoul 110-799, Republic of Korea

⁴Department of Anatomy, Ewha Womans University School of Medicine, 911-1 Mok-6-dong, Yangcheon-Gu, Seoul 158-710, Republic of Korea

Correspondence should be addressed to Dong Hoon Shin; cuteminjae@gmail.com

Received 19 December 2014; Accepted 16 March 2015

Academic Editor: Otto Appenzeller

Copyright © 2015 Chang Seok Oh et al. This is an open access article distributed under the Creative Commons Attribution License, which permits unrestricted use, distribution, and reproduction in any medium, provided the original work is properly cited.

Previous study showed that East Asian mtDNA haplogroups, especially those of Koreans, could be successfully assigned by the coupled use of analyses on coding region SNP markers and control region mutation motifs. In this study, we tried to see if the same triple multiplex analysis for coding regions SNPs could be also applicable to ancient samples from East Asia as the complementation for sequence analysis of mtDNA control region. By the study on Joseon skeleton samples, we know that mtDNA haplogroup determined by coding region SNP markers successfully falls within the same haplogroup that sequence analysis on control region can assign. Considering that ancient samples in previous studies make no small number of errors in control region mtDNA sequencing, coding region SNP analysis can be used as good complimentary to the conventional haplogroup determination, especially of archaeological human bone samples buried underground over long periods.

1. Introduction

Ancient DNA (aDNA) analysis is very important for understanding the origin and evolution of mankind in history. Of various aDNA studies, analysis on mitochondrial DNA (mtDNA) is one of the best methods to know the phylogeny of archaeologically obtained human samples. mtDNA shows maternal haplotype lineage that is passed down throughout each generation without changing and reshuffling of DNA. In fact, it could be analyzed successfully even in case where nuclear DNA (nDNA) is degraded seriously [1].

Recently, about the determination of East Asian mtDNA haplogroups, Lee et al. [2] showed that Korean mtDNA could be allocated into 15 haplogroups by two different multiplex systems for 21 coding region SNP markers and one deletion motif. As Koreans do have many D4 subhaplogroups, the third set of PCR multiplex systems was also used for defining them in much detail. Authors showed that East Asian mtDNA haplogroups, especially those of Koreans, could be successfully assigned by the multiplex analysis system they developed [2]. As many previously published works exhibited that some of mtDNA data from degraded samples

were not sufficiently authentic, the establishment of more tools for detecting possible sequence errors looks valuable to concerned researchers.

The multiplex system was originally designed for mtDNA analysis of the degraded samples frequently met in the field of forensic science [2]. However, the technique looks very suggestive to the anthropologists in East Asia as well. Like forensic scientists, the biological anthropologists always tried to analyze the aDNA that is seriously degraded, remaining in archaeological human samples by small amounts. Therefore, sequencing errors in aDNA analysis have always been the researchers' concern. Since archaeological and forensic DNA typing share common subjects to be considered for making their studies on the degraded samples more successful and authentic, many experimental methods developed for forensic science have been also applied to aDNA researches.

In this respect, we wonder if the mtDNA typing by use of coding region SNP analysis could be also applicable to ancient samples from archaeological sites in East Asia. As the technique was proven to be time-, cost-, and target DNA-saving [2], it can be used as a good complimentary to conventional aDNA sequencing if both methods could show well-matching results from archaeologically obtained samples. However, regretfully enough, there were not any previous researches on how perfectly this multiplex system can be applied to archaeologically obtained human samples buried underground for several hundred to thousand years.

For the past several years, we tried to build a skeletal series consisting of human bones collected from 16th to 18th century Joseon tombs in South Korea. Our previous reports on the collection have revealed information concerning the health and disease status of premodern Korean people [3–9]. Using the same human skeleton collection, we undertook the experiments to compare haplogroup-directed data made by two different methods: conventional control region sequencing and analysis of coding region SNP markers. It determines whether the analysis of the triple multiplex system for coding region SNP analysis, like the forensic cases, could be also useful for the mtDNA analysis of hundred-year-old human bones from archaeological sites.

2. Materials and Methods

Human skeletons ($n = 11$) collected from 16th to 18th century Korean tombs (Joseon Dynasty) were used in this study. Sex determination was made on the basis of morphological differences manifest in the pelvic bone, by the examination of greater sciatic notch, preauricular sulcus, ischiopubic ramus, subpubic angle, subpubic concavity, and ventral arc [10, 11]. Considered ancillary indicators for sex determination were skull structures, specifically the nuchal crest, the mastoid process, the supraorbital margin, the glabella, and the mental eminence [12, 13]. Age was also estimated by auricular-surface degeneration of the hipbone, based on the degree of transverse organization, granularity, apical activity, retroauricular area degeneration, and auricular-surface porosity [14].

The age was accordingly categorized into eight phases: 1-2, young adult (20–35 years old); 3–6, middle-aged (36–50 years old); and 7-8, old adult (over 50 years old).

The femur fragments from the skeletal remains were used for aDNA analysis in this study. The surfaces of the bones were removed using a sterilized knife, after which they were exposed to UV irradiation for 20 min and subsequently immersed in 5.4% (w/v) sodium hypochlorite. After the samples were washed with distilled water and absolute ethanol, they were air-dried and pulverized to a fine powder using a SPEX 6750 Freezer/Mill (SPEX SamplePrep, Metuchen, NJ) [15, 16]. Bone powder (0.5 g) was incubated in 1 mL of lysis buffer (EDTA 50 mM, pH 8.0; 1 mg/mL of proteinase K; SDS 1%; 0.1 M DTT) at 56°C for 24 h. Total DNA was extracted with an equal volume of phenol/chloroform/isoamyl alcohol (25:24:1) and then was treated with chloroform/isoamyl alcohol (24:1). DNA isolation and purification were performed using a QIAmp PCR purification kit (Qiagen, Hilden, Germany). The purified DNA was eluted in 50 μ L of EB buffer (Qiagen) [17–20].

During sampling or lab work, we always wore protection gloves, masks, gowns, and head caps. Our aDNA lab facilities were set up in accordance with the protocol of Hofreiter et al. [21]. The rooms for aDNA extraction or PCR preparation were physically separated from our main PCR lab. The DNA extraction/PCR preparation rooms were equipped with night UV irradiation, isolated ventilation, and a laminated flow hood. The other procedures for authentic aDNA analysis, suggested by Hofreiter et al. [21], were also followed by us.

Three multiplex PCR systems used in this study were originally designed to detect 21 SNPs and a 9-bp deletion motif [2], and the sizes of each PCR amplicon were originally designed below 200 bp, for increasing success yields during DNA typing with degraded samples. By multiplex PCR reactions I and II, major 15 haplogroups could be detected from East Asian samples. Briefly, multiplex I reaction consisted of primers for eight different SNP loci (s4491, s5417, s7642, s8793, s8794, s10397, s10400, and s14668), typing the haplogroups M9, N9, M11, M10, A, D5, M, and D4, respectively. Multiplex II reaction also tested seven SNP loci (s3970, s4833, s4883, s7196, s8281-8289d, s9824, and s12705) for decision of the haplogroups R9, G, D, M8, B, M7, and R, respectively. Haplogroup D4, one of the most frequent haplogroups in East Asian population, was further subdivided into D4, D4a, D4b, D4e, D4g, D4h, and D4j by seven SNP loci (s3010, s14979, s8020, s11215, s8701, s5048, and s11696) of multiplex III reaction [2, 22–25].

Multiplex PCR amplification was done in a 20 μ L reaction volume, containing 40 ng of template DNA, AmpliTaq Gold 360 Master Mix (Life Technologies, USA), and appropriate concentrations of each primer. Thermal cycling was conducted on a PTC-200 DNA engine (MJ Research): 95°C for 10 min; 45 cycles of 95°C for 20 s, 58°C for 20 s, and 72°C for 30 s; and a final extension at 72°C for 10 min. To purify PCR products, 5 μ L of the PCR products was treated with 1 μ L of ExoSAP-IT (catalogue number 78201; USB, Cleveland,

OH, USA) at 37°C for 45 min. After that, the enzyme was inactivated by incubation at 80°C for 15 min.

We used twenty-two single base extension (SBE) primers recommended by Lee et al. [2]. SBE reactions were carried out using a SNaPshot Kit (Applied Biosystems, USA) according to the manufacturer's instructions. Thermal cycling conditions for SBE were as follows: denaturation at 96°C for 10 sec; annealing at 50°C for 5 sec; extension at 60°C for 30 sec. SBE was performed using a PTC-200 DNA Engine (Bio-Rad Laboratories, Hercules, CA). For postextension treatment, reaction mixtures were mixed with 1.0 unit of shrimp alkaline phosphatase (SAP), incubated at 37°C for 45 min, and followed by heat inactivation at 80°C for 15 min. The reactants were analyzed by an ABI PRISM 3100 Genetic Analyzer (Applied Biosystems, USA), using GeneMapper ID software, v3.2.1 (Applied Biosystems, USA). SNP scoring at each locus was confirmed by sequencing two samples for each of the observed alleles.

We also did direct sequencing of mtDNA control region of the samples. By sequencing of hypervariable regions I, II, and III, we could get haplotype of the bones and further determined haplogroups of them. The results could be compared with haplogroup determination by coding region SNP analysis on the same samples. Briefly, after quantification was done by NanoDrop ND-1000 Spectrophotometer (Thermo Fisher Scientific, MA, USA), 40 ng of aDNA was mixed with premix containing 1X *AmpliTaq* Gold 360 Master Mix (Life Technologies, USA) and 10 pmol of each primer (Integrated DNA Technology, USA). PCR conditions used in this study were as follows: predenaturation at 94°C for 10 min; 45 cycles of denaturation at 94°C for 30 sec; annealing at 50°C for 30 sec; extension at 72°C for 30 sec; final extension at 72°C for 10 min. PCR amplification was performed using a PTC-200 DNA Engine (Bio-Rad Laboratories, Hercules, CA). Primer sets used for this study were as follows: for 267-bp HV1A, F15971 (5'-TTA ACT CCA CCA TTA GCA CC-3') and R16237 (5'-TGT GTG ATA GTT GAG GGT TG-3'); for 267-bp HV1B, F16144 (5'-TGA CCA CCT GTA CAT AA-3') and R16410 (5'-GAG GAT GGT GGT CAA GGG AC-3'); for 226-bp HV2A, F015 (5'-CAC CCT ATT AAC CAC TCA CG-3') and R240 (5'-TAT TAT TAT GTC CTA CAA GCA-3'); for 235-bp HV2B, F155 (5'-CTA TTA TTT ATC GCA CCT-3') and R389 (5'-CTG GTT AGG CTG GTG TTA GG-3'); for 167-bp HV3, F403 (5'-TCT TTT GGC GGT ATG CAC TTT-3') and R569 (5'-GGT GTA TTT GGG GTT TGG TTG-3') [26].

The PCR products were separated on 2.5% agarose gel, stained with ethidium bromide, and then isolated using a Qiagen gel extraction kit (Qiagen, Germany). The sequencing of each amplicon was performed by ABI Prism 3100 Genetic Analyzer (Applied Biosystems, USA), using ABI Prism BigDye Terminator Cycle Sequencing Ready Reaction Kit (Applied Biosystems, USA). The obtained DNA sequences were compared with the revised Cambridge Reference Sequence (rCRS; accession number: NC_012920), to identify the sequence differences between them. The resultant control region mutation motifs were imported into program mtDNAmanager (<http://mtmanager.yonsei.ac.kr/>), with which

most Korean mtDNA haplotypes can be automatically classified into East Asian mtDNA haplogroups and their subhaplogroups [27], or another web-based program for mtDNA haplogroup analysis (<http://dna.jameslick.com/mthap/>) [28, 29].

In order to guard against any modern DNA contamination of ancient samples, the mtDNA profiles of all of the researchers involved in this study were determined (with the permission of the Institutional Review Board of Seoul National University, H-0909-049-295). They were then compared with the mtDNA profiles from the Joseon skeletons to rule out the possibility of modern DNA contamination.

3. Results

The sex and age of the samples determined in this study are summarized in Table 1. By direct sequencing of mtDNA control region, every Joseon skeleton could be assigned to relevant existing haplo- or subhaplogroups of mtDNA. In multiplex PCR analyses to detect 21 SNP markers in mtDNA coding region, eight (multiplex I) and seven (multiplexes II and III) primer extension peaks for different haplogroups could be observed. Most samples exhibited no missing or extra assignment peaks in the results (Figures 1 and 2).

When the coding region SNP typing data were further compared with control region direct sequencing results, well-matching patterns can be observed between the outcomes of two methods. The mtDNA haplogroup expected by coding region SNP could fall successfully within the same haplogroup that control region sequencing could make (Table 1, Figure 1). However, as far as haplogroup subclades are concerned, the results of direct sequencing on control region mutation motif were far better than SNP marker analysis on coding region. The haplogroup subclades of the cases numbers 024, 034, 036, 038, 040, 045, 100, and 238 were much successfully determined in direct sequencing of control region than in coding region SNP analysis (Table 1, Figure 2).

The absence of modern DNA contamination could be confirmed by the comparison of mtDNA haplotypes obtained from the current Joseon skeleton and participating researchers' samples. As we did not see any identical sequence between them (Table 1), mtDNA obtained from Joseon samples should have been the endogenous DNA of the ancient people but not the outcome of modern DNA contamination from researchers.

4. Discussion

Coding region SNP analysis attracts forensic scientists' interest because it is a time-, cost-, and target DNA-saving method for mtDNA analysis of degraded samples [2, 30–35]. Multiplex PCR system for coding region SNP used in this study was originally designed for the detection of major haplogroups of forensic samples from East Asia. In the study, the triple multiplex system on coding region SNP markers was proven

TABLE I: Sequencing analysis result of mtDNA coding and control region.

Subject	Sex	Age	Hypervariable region			Haplogroup (control region)	Haplogroup (coding region)
			HVI (15991–16390)	HVII (034–369)	HVIII (423–548)		
004	Male	Old	16223T, 16235G, 16290T	73G, 235G, 263G, 315.1C	rCRS	A	A
005	Female	Young	16171G, 16223T, 16248T, 16298C, 16327T, 16344T, 16357C	73G, 248d, 263G, 315.1C	489C	M8	M8
024	Male	Middle	16129A, 16223T, 16309G, 16362C	73G, 152C, 263G, 309.1C, 315.1C	489C, 533G	D4a1b1	D4a
034	Male	Old	16189C, 16232A, 16249C, 16304C, 16311C, 16344T	73G, 263G, 310C	489C	M1a3b1	M
036	Male	Old	16150T, 16183C, 16185T, 16189C	73G, 151T, 197G, 263G, 315.1C	546G	B4d3	B
038	Male	Old	16129A, 16223T, 16362C	73G, 194T, 263G, 315.1C	489C	D4b2b	D4b
040	Male	Middle	16188.1C, 16193.1C, 16223T, 16311C	73G, 263G, 309.1C, 315.1C	489C	M4''67	M
045	Male	Old	16223T, 16234T, 16311C, 16316G, 16362C	73G, 263G, 309.1C, 315.1C	489C	M9a1a1c1b1	M9
100	Male	Middle	16111T, 16229A, 16257A, 16261T, 16362C	73G, 150T, 263G, 309.2C, 315.1C	rCRS	N9a	N9
225	Male	Middle	16209C, 16223T, 16362C	73G, 195C, 234G, 263G, 315.1C	489C	D4	D4
238	Female	Old	16223T, 16295T, 16319A	73G, 146C, 263G, 309.1C, 315.1C	489C, 513d, 514d	M7cla3	M7
Researcher 1	—	—	16172C, 16174T, 16223T, 16362C	73G, 263G, 309.1C, 315.1C	—	D4g	—
Researcher 2	—	—	16183C, 16189C, 16220C, 16254G, 16298C, 16362C	73G, 248d, 263G, 310.1C	—	F3b	—
Researcher 3	—	—	16129A, 16182C, 16183C, 16189C, 16232A, 16249C, 16304C, 16311C, 16344T	73G, 152C, 248d, 263G, 310.1C	—	D6c	—

to be very useful for analysis on forensic materials [2]. Briefly, when they tried to do the coding region SNP-based mtDNA analysis on the long bone or molar samples from about 50-year-old skeletal remains of war victims in the Korean War (1950–1953), mtDNA haplogroup could be determined successfully, even with a limited volume of degraded DNA [2]. In fact, as the triple multiplex system makes very high success rate in haplogroup determination, the combined consideration of coding region SNP markers and control region polymorphism can become a very useful tool for the genetic analysis of degraded samples collected from East Asian populations.

This technique is also very suggestive for anthropologists who deal with several hundred- to thousand-year-old

samples from archaeological sites. Most of the archaeological human bones were maintained under the worst preservation conditions for a long while. To make matters worse, it is very hard for researchers to get authentic outcomes from the ancient samples because only the limited volume of the samples can be allowed for the analysis of archaeologically important cases. We therefore admit that mtDNA analyses with highly degraded ancient samples are sometimes too risky because sequencing errors commonly occurred during analysis, and they could not be corrected easily by a due course of repeated experiments with a sufficient amount of samples.

In this regard, if another time-, cost-, and sample-saving mtDNA analysis could be also established for the assignment

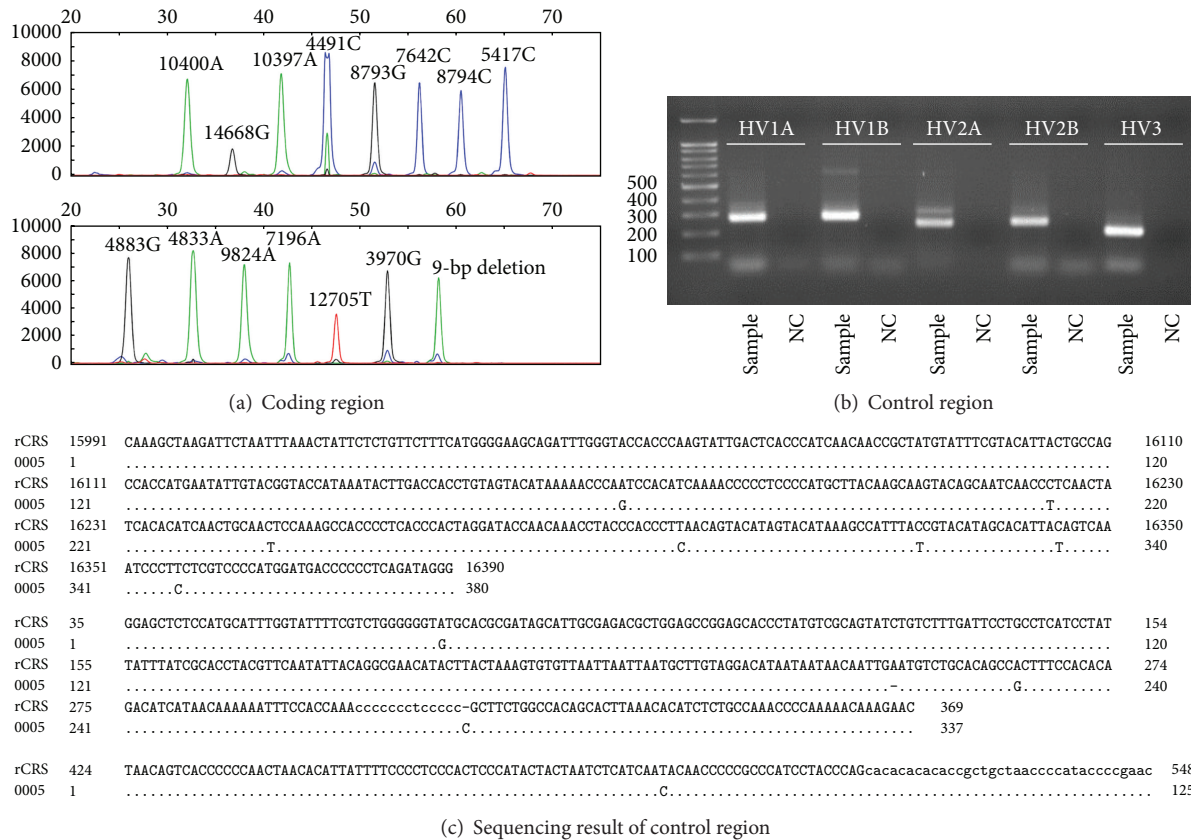


FIGURE 1: Analysis on sample number 005. (a) SNP analysis of mtDNA coding region by a SNaPshot Kit. ((b), (c)) Direct sequencing analysis on mtDNA control region. (b) Electrophoresis of PCR amplicons. (c) Direct sequencing result. rCRS, revised Cambridge Reference Sequence. Haplogroups (M8) determined by coding region SNP analysis (a) and control region direct sequencing ((b)/(c)) are the same for this case.

of ancient skeleton samples to relevant existing haplogroups, it will become a convenient method indeed for counterchecking the possible errors hidden in the conventional mtDNA sequencing. Our current results showed that most haplogroup results determined by coding region SNP analysis on Joseon archaeological samples can fall successfully within the same haplogroups that were decided by control region sequencing analysis. In fact, the results confirm coding region SNP analysis' error-screening role in the mtDNA haplogroup determination even for the ancient samples.

However, as for the current ancient samples, we must also admit some technical limits of haplogroup determination based on coding region SNP analysis. Briefly, a coding region SNP analysis on a few samples did not show the subhaplogroup results as completely as observed in the analysis of control region mutation motifs. This means that multiplex SNP analysis could not completely replace the conventional control region mtDNA sequencing, at least for the ancient cases from archaeological fields in South Korea. Even so, considering coding region SNP analysis' superb potential

for reconfirmation of haplogroups determined by mtDNA control region sequencing in time-, cost-, and target DNA-saving manner, the use of this method can be expedient for making mtDNA haplogroup determination of archaeological samples much authentic.

5. Conclusion

Obtaining authentic mtDNA outcomes from archaeological bone samples still remains a significant challenge to concerned researchers. The identification of possible errors in conventional sequencing as quickly as possible is thus significant for authentic mtDNA analysis of archaeologically obtained samples. In this study, we can show that mtDNA haplogroup determination can also be successfully carried out by coding region SNP analysis, in a time-, cost-, and target DNA-saving manner. Although the mtDNA subhaplogroups could not be determined by the coding region SNP analysis as completely seen in the control region sequencing, the former can be used as good supplementary to the latter, for making

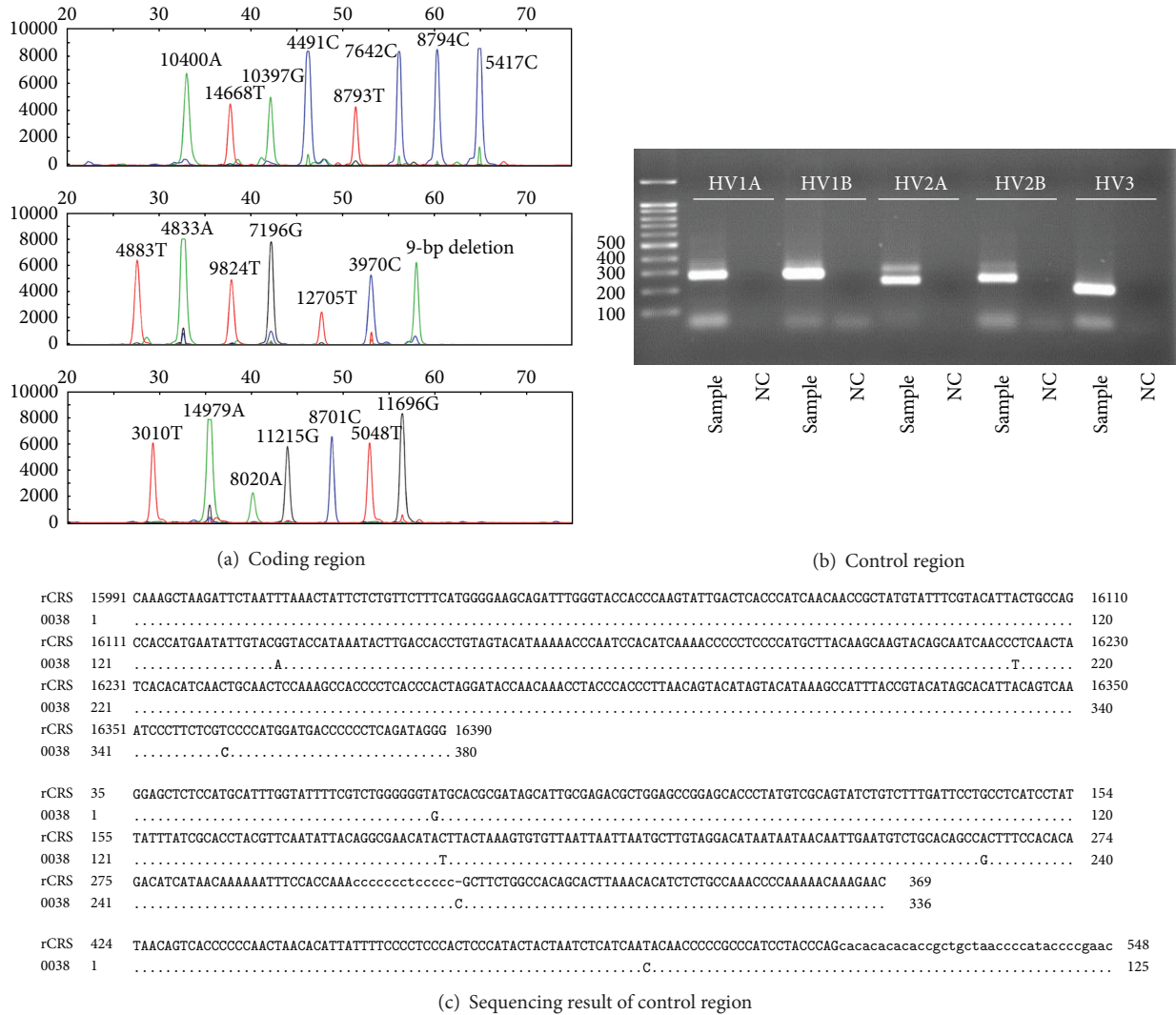


FIGURE 2: Analysis on sample number 038. (a) SNP analysis of mtDNA coding region by a SNaPshot Kit. ((b), (c)) Direct sequencing analysis on mtDNA control region. (b) Electrophoresis of PCR amplicons. (c) Direct sequencing result. rCRS, revised Cambridge Reference Sequence. Although mtDNA haplogroup expected by coding region SNP analysis could fall successfully within the same haplogroup that control region sequencing could make, haplogroup subclade made by SNP analysis (D4b) was not as successful as seen in control region sequencing (D4b2b).

the mtDNA typing of archaeological human bones much authentic.

Conflict of Interests

The authors declare that there is no conflict of interests regarding the publication of this paper.

Acknowledgments

This study was supported by the Seoul National University Hospital (SNUH) research fund (04-2011-0900; 2011-1350) and by the Basic Science Research Program through the National Research Foundation of Korea (NRF) funded by

the Ministry of Education, Science and Technology (2012-0002118).

References

- [1] J. M. Butler, *Forensic DNA Typing: Biology and Technology behind STR Markers*, Elsevier, Burlington, Mass, USA, 2nd edition, 2005.
- [2] H. Y. Lee, J.-E. Yoo, M. J. Park, U. Chung, C.-Y. Kim, and K.-J. Shin, "East Asian mtDNA haplogroup determination in Koreans: haplogroup-level coding region SNP analysis and subhaplogroup-level control region sequence analysis," *Electrophoresis*, vol. 27, no. 22, pp. 4408–4418, 2006.
- [3] M. J. Kim, C. S. Oh, I. S. Lee et al., "Human mummified brain from a medieval tomb with lime-soil mixture barrier of

- the Joseon Dynasty, Korea," *International Journal of Osteoarchaeology*, vol. 18, no. 6, pp. 614–623, 2008.
- [4] D. K. Kim, I. S. Lee, W.-L. Kim et al., "Possible rheumatoid arthritis found in the human skeleton collected from the tomb of Joseon Dynasty, Korea, dating back to the 1700s AD," *International Journal of Osteoarchaeology*, vol. 21, no. 2, pp. 136–149, 2011.
 - [5] Y. S. Kim, C. S. Oh, S. J. Lee, J. B. Park, M. J. Kim, and D. H. Shin, "Sex determination of Joseon people skeletons based on anatomical, cultural and molecular biological clues," *Annals of Anatomy*, vol. 193, no. 6, pp. 539–543, 2011.
 - [6] D. K. Kim, M. J. Kim, Y. Kim et al., "Long bone fractures identified in the Joseon Dynasty human skeletons of Korea," *Anatomy & Cell Biology*, vol. 46, no. 3, pp. 203–209, 2013.
 - [7] S. S. Han, K.-W. Baek, M. H. Shin et al., "Dental caries prevalence of medieval Korean people," *Archives of Oral Biology*, vol. 55, no. 7, pp. 535–540, 2010.
 - [8] D. H. Shin, C. S. Oh, Y.-S. Kim, and Y.-I. Hwang, "Ancient-to-modern secular changes in Korean stature," *American Journal of Physical Anthropology*, vol. 147, no. 3, pp. 433–442, 2012.
 - [9] J. Beom, E. J. Woo, I. S. Lee et al., "Harris lines observed in human skeletons of Joseon Dynasty, Korea," *Anatomy & Cell Biology*, vol. 47, no. 1, pp. 66–72, 2014.
 - [10] T. W. Phenice, "A newly developed visual method of sexing the os pubis," *American Journal of Physical Anthropology*, vol. 30, no. 2, pp. 297–301, 1969.
 - [11] W. M. Krogman and M. Y. Iscan, *The Human Skeleton in Forensic Medicine*, Charles C Thomas Publisher, Springfield, Ill, USA, 2nd edition, 1986.
 - [12] J. E. Buikstra and D. H. Ubelaker, *Standards for Data Collection from Human Skeletal Remains*, vol. 44 of *Arkansas Archaeological Survey Research Series*, Arkansas Archeological Survey, Fayetteville, Ark, USA, 1994.
 - [13] D. H. Ubelaker, *Human Skeletal Remains: Excavation, Analysis, Interpretation*, vol. 2 of *Manuals on Archeology*, Taraxacum, Washington, DC, USA, 3rd edition, 1999.
 - [14] C. O. Lovejoy, R. S. Meindl, T. R. Pryzbeck, and R. P. Mensforth, "Chronological metamorphosis of the auricular surface of the ilium: a new method for the determination of adult skeletal age at death," *American Journal of Physical Anthropology*, vol. 68, no. 1, pp. 15–28, 1985.
 - [15] D. H. O'Rourke, M. G. Hayes, and S. W. Carlyle, "Ancient DNA studies in physical anthropology," *Annual Review of Anthropology*, vol. 29, pp. 217–242, 2000.
 - [16] N. Rohland and M. Hofreiter, "Ancient DNA extraction from bones and teeth," *Nature Protocols*, vol. 2, no. 7, pp. 1756–1762, 2007.
 - [17] D. Y. Yang, B. Eng, J. S. Wayne, J. C. Dudar, and S. R. Saunders, "Improved DNA extraction from ancient bones using silica-based spin columns," *The American Journal of Physical Anthropology*, vol. 105, no. 4, pp. 539–543, 1998.
 - [18] M. J. Casas, E. Hagelberg, R. Fregel, J. M. Larruga, and A. M. González, "Human mitochondrial DNA diversity in an archaeological site in *al-Andalus*: genetic impact of migrations from North Africa in Medieval Spain," *American Journal of Physical Anthropology*, vol. 131, no. 4, pp. 539–551, 2006.
 - [19] M. J. Blow, T. Zhang, T. Woyke et al., "Identification of ancient remains through genomic sequencing," *Genome Research*, vol. 18, no. 8, pp. 1347–1353, 2008.
 - [20] S. Calvignac, S. Hughes, C. Tougaard et al., "Ancient DNA evidence for the loss of a highly divergent brown bear clade during historical times," *Molecular Ecology*, vol. 17, no. 8, pp. 1962–1970, 2008.
 - [21] M. Hofreiter, D. Serre, H. N. Poinar, M. Kuch, and S. Pääbo, "Ancient DNA," *Nature Reviews Genetics*, vol. 2, no. 5, pp. 353–359, 2001.
 - [22] T. Kivisild, H. V. Tolk, J. Parik et al., "The emerging limbs and twigs of the East Asian mtDNA tree," *Molecular Biology and Evolution*, vol. 19, no. 10, pp. 1737–1751, 2002.
 - [23] Q.-P. Kong, Y.-G. Yao, M. Liu et al., "Mitochondrial DNA sequence polymorphisms of five ethnic populations from northern China," *Human Genetics*, vol. 113, no. 5, pp. 391–405, 2003.
 - [24] Q.-P. Kong, H.-J. Bandelt, C. Sun et al., "Updating the East Asian mtDNA phylogeny: a prerequisite for the identification of pathogenic mutations," *Human Molecular Genetics*, vol. 15, no. 13, pp. 2076–2086, 2006.
 - [25] M. Tanaka, V. M. Cabrera, A. M. González et al., "Mitochondrial genome variation in Eastern Asia and the peopling of Japan," *Genome Research*, vol. 14, no. 10, pp. 1832–1850, 2004.
 - [26] M. M. Holland and E. F. Huffine, "Molecular analysis of the human mitochondrial DNA control region for forensic identity testing," in *Current Protocols in Human Genetics*, vol. 14.7, chapter 14, unit 14.7, 2001.
 - [27] H. Y. Lee, I. Song, E. Ha, S.-B. Cho, W. I. Yang, and K.-J. Shin, "mtDNAmanager: a Web-based tool for the management and quality analysis of mitochondrial DNA control-region sequences," *BMC bioinformatics*, vol. 9, no. 1, article 483, 2008.
 - [28] E. D. Aulicino, *Genetic Genealogy: The Basics and Beyond*, AuthorHouse, Bloomington, Ind, USA, 2013.
 - [29] D. Kennett, *DNA and Social Networking: A Guide to Genealogy in the Twenty-First Century*, The History Press, London, UK, 2012.
 - [30] H. J. Bandelt, P. Lahermo, M. Richards, and V. Macaulay, "Detecting errors in mtDNA data by phylogenetic analysis," *International Journal of Legal Medicine*, vol. 115, no. 2, pp. 64–69, 2001.
 - [31] H.-J. Bandelt, L. Quintana-Murci, A. Salas, and V. Macaulay, "The fingerprint of phantom mutations in mitochondrial DNA data," *The American Journal of Human Genetics*, vol. 71, no. 5, pp. 1150–1160, 2002.
 - [32] H. J. Bandelt, A. Salas, and S. Lutz-Bonengel, "Artificial recombination in forensic mtDNA population databases," *International Journal of Legal Medicine*, vol. 118, no. 5, pp. 267–273, 2004.
 - [33] P. Forster, "To err is human," *Annals of Human Genetics*, vol. 67, no. 1, pp. 2–4, 2003.
 - [34] Y. G. Yao, C. M. Bravi, and H. J. Bandelt, "A call for mtDNA data quality control in forensic science," *Forensic Science International*, vol. 141, no. 1, pp. 1–6, 2004.
 - [35] A. Salas, A. Carracedo, V. Macaulay, M. Richards, and H.-J. Bandelt, "A practical guide to mitochondrial DNA error prevention in clinical, forensic, and population genetics," *Biochemical and Biophysical Research Communications*, vol. 335, no. 3, pp. 891–899, 2005.

Research Article

Reconstructing Ancient Egyptian Diet through Bone Elemental Analysis Using LIBS (Qubbet el Hawa Cemetery)

Ghada Darwish Al-Khafif¹ and Rokia El-Banna²

¹*Anthropology and Mummy Conservation Laboratory, Conservation and Research Center, Ministry of Antiquities, 4 Nobar Street, Ismail Pasha Palace, Lazoghli, Cairo 11521, Egypt*

²*Biological Anthropology Department, National Research Center, El Buhouth Street, Dokki, Cairo 12311, Egypt*

Correspondence should be addressed to Ghada Darwish Al-Khafif; hatshepsout1980@hotmail.com

Received 18 December 2014; Revised 19 March 2015; Accepted 10 May 2015

Academic Editor: Otto Appenzeller

Copyright © 2015 G. D. Al-Khafif and R. El-Banna. This is an open access article distributed under the Creative Commons Attribution License, which permits unrestricted use, distribution, and reproduction in any medium, provided the original work is properly cited.

One of the most important advantages of LIBS that make it suitable for the analysis of archeological materials is that it is a quasi-nondestructive technique. Archeological mandibles excavated from Qubbet el Hawa Cemetery, Aswan, were subjected to elemental analysis in order to reconstruct the dietary patterns of the middle class of the Aswan population throughout three successive eras: the First Intermediate Period (FIP), the Middle Kingdom (MK), and the Second Intermediate Period (SIP). The bone Sr/Ca and Ba/Ca ratios were significantly correlated, so the Sr/Ca ratios are considered to represent the ante-mortem values. It was suggested that the significantly low FIP Sr/Ca compared to that of both the MK and the SIP was attributed to the consumption of unusual sorts of food and imported cereals during years of famine, while the MK Sr/Ca was considered to represent the amelioration of climatic, social, economic, and political conditions in this era of state socialism. The SIP Sr/Ca, which is nearly the same as that of the MK, was considered to be the reflection of the continuity of the individualism respect and state socialism and a reflection of agriculture conditions amelioration under the reign of the 17th Dynasty in Upper Egypt.

1. Introduction

Generally, social, economic, and belief system of a society can be reflected in food [1]. Information about the ancient Egyptians diet is mainly provided by artistic and textual sources [2]. But it is important to note that there many difficulties that interrupt the precise identification of food types consumed in ancient Egypt such as problems of translation [3]. However, as calcified tissues as bones and teeth can contain the indicators of diet and the environmental conditions, they are considered as the biological “archives” of the living organisms [4]. Thus, elemental analysis of archeological bones can be used as an important tool for paleodiet reconstruction.

From the Neolithic era and throughout the historic era, the base of masses daily diet was cereal foods. Beside bread and beer, the ancient Egyptian meals were mainly set from vegetables, fruit, milk, dairy products, and fish. Also, many species of fattened poultry or wild birds were eaten in ancient

Egypt. The regular consumption of beef is observed in the higher social class [5].

Dietary calcium ions may be accompanied by Sr and Ba ions that are removed through a food chain due to what is called “*biopurification*” which is defined by Burton [6] as “*the collection of processes that tend to preferentially remove these ions from calcium as it progress through the food chain from lower to higher consumers.*”

The intestinal absorption ratio for Ca, Sr, and Ba is 10 : 5 : 1, respectively [7]. Once strontium is absorbed, it will be distributed throughout the body but its deposition will be mostly in bone and teeth [8].

Many techniques of elemental analysis are used to evaluate the apatite elemental composition of archeological bone and teeth samples, for example, atomic absorption spectroscopy (AAS) [9–12], atomic emission spectroscopy (AES) [13–18], and neutron activation analysis (NAA) [19, 20].

Although Samek et al. [21] reported on the use of laser induced breakdown spectroscopy (LIBS) in the quantitative detection of trace elements in human teeth and bones by creation of calibration curves for aluminum, lead, and strontium, few studies applied LIBS technique in the elemental analysis of archeological skeletal remains, such as the studies of Alvira et al. [22, 23], El-Tayeb [24], Galiová et al. [25], and Kasem et al. [26]. While, as indicated by Giakoumaki et al. [27], one of the most important advantages of LIBS—that makes it suitable for archeological science applications is that it is nearly a non-invasive method of analysis as there is no sample preparation, in addition, destruction caused by the ablation of tens to hundred nanograms from the target surface is microscopic.

The aim of the current study is to reconstruct the paleodiet of the Elephantine nobles followers and descendants (the middle class of the archeological Aswan population) through three successive historical eras: the First Intermediate Period (FIP), the Middle Kingdom (MK), and the Second Intermediate Period (SIP) using LIBS technique for the elemental analysis of mandibular bones.

2. Materials and Methods

2.1. Materials. Qubbet el Hawa is the cemetery of nobles of “Abu” (Elephantine), the first Upper Egyptian Nome capital. The cemetery consists of a large number of graves cut into the sand stone of the eastern mountain slope of the Nile west bank of Aswan. The human remains content of the graves are not only that of noble families, but also that of followers. The social rank was estimated according to the position of the corpus within the grave: the nuclear noble family was buried in the central grave chambers, while in shaft fillings and in the grave chambers followers or later descendants (middle class) were buried [28, 29]. The excavated bones were stored in the magazine grave number 30 on the site [30].

69 mandibles of the archeological site Qubbet el Hawa consist of the sample of the current work. The mandibles under investigation, which are stored now in the Anthropology and Mummy Conservation Lab., Ministry of Antiquities, belong to the archeological period including the FIP (7th–11th early Dynasties), the MK (the second part of the 11th–12th Dynasties) and the SIP (13th–17th Dynasties) as indicated in Table 1.

Only mandibles of adult individuals of the middle class were used in the current study.

Two soil samples were extracted from inside the archeological bones: one for elemental analysis and the other for pH measurement.

2.2. Methods. Soft brushes were used for a dry mechanical cleaning; then ethanol was applied on cotton buds to ensure a complete removal of dust and soil particles as directed by Hillson [31].

The eruption of the third molar is considered as an indication of an age exceeding 18 years [32]. The soil sample pH was measured using a calibrated portable pH meter (METTLER TOLEDO, Seven Go™, pH meter SG2, Electrode: In Lab Surface).

TABLE 1: Number of mandibles for each epoch.

Grave number	Sample size	Era
26	17	FIP
89	19	MK
88	33	SIP

All elemental determinations were carried out in the Laser Atomic Spectroscopy Laboratory (I) of the Department of Laser Applications in Metrology, Photochemistry and Agriculture (LAMPA), The National Institute of Laser Enhanced Sciences (NILES), Cairo University.

Laser-induced plasma was obtained using Q-switched Nd:YAG laser (Brio, Quantel, France) operating at its fundamental wavelength ($\lambda = 1064$ nm). The laser pulse energy was 100 mJ with a pulse duration 5 ns. Laser light was focused onto the target surface using a lens of focal length 10 cm. The collected plasma emission was transmitted through the optical fiber to the echelle spectrometer coupled to the coupled to the ICCD camera. The gate and the delay time are controlled through a personal computer that is used also for displaying and storing the obtained spectra. The gate time and the delay time were adjusted at 1000 ns for each. All measurements were performed in air at atmospheric pressure. Two laser pulses were applied to the desired position for surface cleaning. Bone analysis was performed by irradiating each mandible at 2 different positions on the surface of the cortical bone of the mandibular body, each by 5 laser pulses. The 10 obtained spectra were averaged.

Prior to elemental analysis, soil sample was prepared to form a pellet. The soil was finely grounded; then it was pressed using a hydraulic piston without using any sort of fillers. The elemental analysis of the soil sample was carried out by shooting 4 different positions on the surface of the soil pellet, each by 5 laser pulses. The 20 obtained spectra were averaged.

Finally, the analysis of the emission spectra was performed using the LIPS++ software. To minimize the effect of experimental parameters fluctuations, emission line of carbon at 2478 Å was used for normalization of relative intensities of all spectral lines.

A data base of collected qualitative and quantitative data was created using Microsoft Office Excel 2007 (Microsoft).

Sr calibration curve created by Samek et al. [21] was used to obtain quantitative data. Samek et al. [21] used artificial reference samples of calcium CaCO_3 with known amount of SrCO_3 (10–10000 ppm relative to Ca content of the matrix). Relative intensities of strontium were obtained at 461 nm and that of calcium at 432 nm. The line equation and r^2 value is obtained after El-Tayeb [24].

Sr/Ca ratio and Ba/Ca ratios were transformed into the logarithmic form as Burton et al. [33] stated that “*The log-transform creates a more normal distribution than the strongly positively skewed ppm data and obviates some of the bias of anomalous outliers.*”

The statistical analysis was performed using the SPSS statistics software (version 17) (IBM).

TABLE 2: Comparison between soil and bone elemental relative intensities for the three epochs under investigation.

	Soil	Bone		Diff.	<i>t</i> -value	<i>P</i> value
		Mean	SD			
FIP						
Ca	3.31	10.108	4.241	6.798	6.61	<i>P</i> = <0.001*
Sr	0.44	0.830	0.406	0.3901	3.958	<i>P</i> = <0.001*
Ba	2.14	0.831	0.37	-1.309	-14.581	<i>P</i> = <0.001*
MK						
Ca	3.31	56.126	26.577	52.816	8.662	<i>P</i> = <0.001*
Sr	0.44	9.351	8.668	8.911	4.481	<i>P</i> = <0.001*
Ba	2.14	5.687	1.876	3.547	8.24	<i>P</i> = <0.001*
SIP						
Ca	3.31	17.551	23.244	14.241	3.52	<i>P</i> = <0.001*
Sr	0.44	2.641	4.578	2.201	2.762	<i>P</i> = 0.007*
Ba	2.14	1.676	2.163	-0.464	-1.231	<i>P</i> = 0.223

SD: standard deviation.

*Significant at *P* < 0.05; *P* > 0.05 (nonsignificant), *P* < 0.05 (significant), and *P* < 0.01 (highly significant).

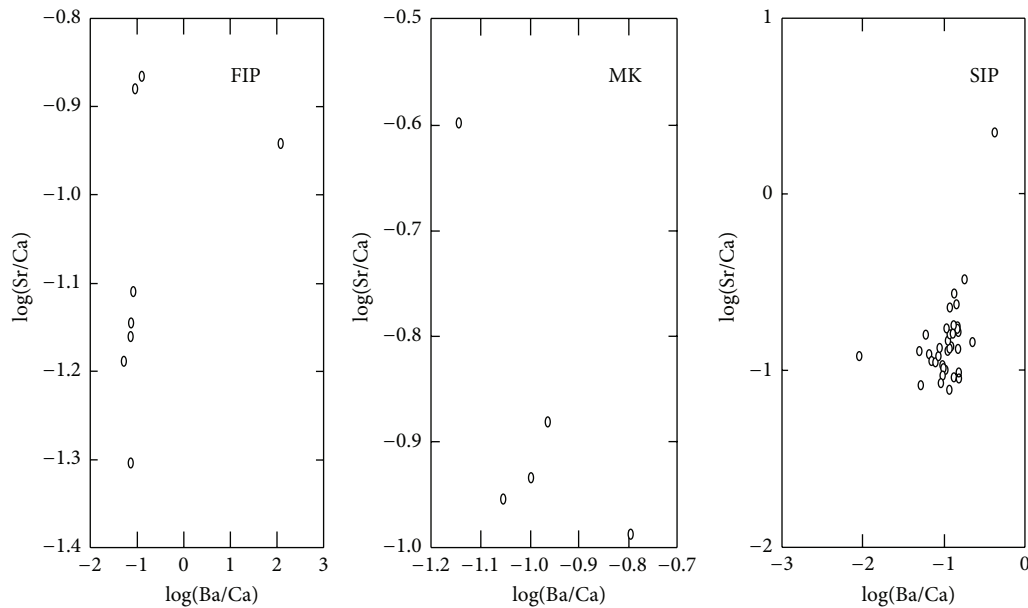


FIGURE 1: Bivariate plot of log(Ba/Ca) and log(Sr/Ca) for the three epochs.

3. Results

3.1. Comparison between Soil and Bone Elemental Relative Intensities. The soil pH measured for Qubbet el Hawa Cemetery was 6.6 (i.e., neutral). The elemental analysis of bone and soil samples using LIBS was performed: Ca was detected at 432 nm, Sr at 461 nm, and Ba at 455.5 nm. The emission line intensity (a.u.) of an element represents the relative concentration of this element in the sample. The mean and the standard deviation were calculated as shown in Table 2.

3.2. Correlation between Bone Ba/Ca and Sr/Ca. The correlation coefficients of log(Ba/Ca) and log(Sr/Ca) for the FIP, the MK, and the SIP were 0.403, 0.721, and 0.486 for

the three epochs, respectively; this positive significant correlation between Ba/Ca and Sr/Ca (Figure 1) indicates that they reflect intact biological values.

3.3. Determination of Strontium Concentrations in the Three Epochs. Using the strontium calibration curve created by Samek et al. [21] strontium concentration relative to calcium (Sr/Ca ratio) was obtained in ppm for the three historical epochs (FIP, MK, and SIP). Results of ANOVA test comparing the log(Sr/Ca) between the 3 historical eras revealed that there is a significant difference between the three epochs (*P* = 0.002). Post hoc comparisons LSD test indicated that the log(Sr/Ca) of the FIP was significantly lower than that of both the MK and the SIP as shown in Table 3 and Figure 2.

TABLE 3: Strontium concentration and $\log(\text{Sr}/\text{Ca})$ in mandibular bodies belonging to the three epochs.

Era	Sr (ppm)	$\log(\text{Sr}/\text{Ca})$
FIP	71.4 ^a	1.85 ^a
MK	187.5 ^b	2.272 ^b
SIP	156.7 ^b	2.1948 ^b

Different small letters indicate significant difference between different age groups according to Tukey LSD pairwise comparison.

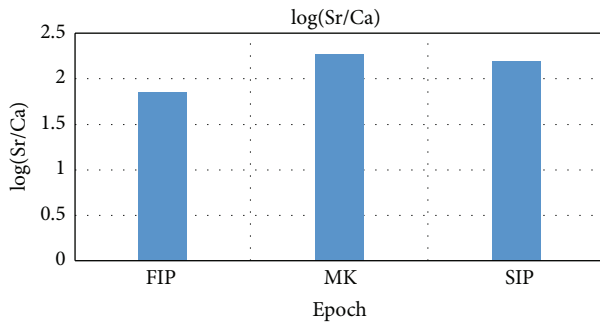


FIGURE 2: Comparison of $\log(\text{Sr}/\text{Ca})$ for the three epochs under investigation.

4. Discussion

4.1. Discussion of Methodology. The studies concerning elemental analysis of ancient Egyptians archeological bones are very rare. This may be attributed to the higher anthropologists' interest in more classic studies such as anthropometrical and pathological researches. The published anthropological studies concerning the skeletal collection of the Aswan population had covered many domains except diet reconstruction through elemental analysis of bones; that is why it was recommended by Rösing [34] to conduct researches concerning this item.

Benefiting from LIBS technique as a quasiondestructive technique the multielemental analysis of archeological mandibles belonging to Aswan population and dated to FIP, MK, and SIP was performed without the destruction of the mandibles that are considered as "precious" bones as the mandible represents a part of the skull.

The analysis of mandibles was restricted to the mandibular body which is considered as one of the sites containing the highest mineralized regions in the mandible [35]. It was chosen to use the cortical bone of mandibles because the high mineralization of the cortical bone and its small surface area in comparison to spongy bone render it more resistant to the diagenetic processes [36] and also because the skull cortical bone remodeling rate is slower than that in spongy bones [37]. During remodeling trace elements can be removed or deposited from bone apatite [38].

The cortical bone elemental analysis provides data concerning the last 6–10 years of the individual life [39], as the cortical bone is characterized by a lower biological activity than trabecular bone and it can be represented as the site of

elemental storage, while the spongy bone is characterized by a greater biological activity and greater turnover rate because it is closest to bone marrow and blood plasma and hence a more rapid metabolism is available [38].

In the current study only mandibles were analyzed, as it is recommended according to Grupe [36], to use compact bone from corresponding anatomical site in the studies of paleodiet reconstruction. That is because the rate of turnover of compact bone may differ in the same individual according to the anatomical location [40].

Only adult individuals were included in this work as the bones of immature individuals are more susceptible to diagenetic changes as they are characterized by their thinner compact bone and lower level of mineralization in comparison to the bones of adult individuals [41].

4.2. Diagenesis Evaluation. Diagenetic alterations can change the elemental content of archeological bones both by physical contamination and by chemical reaction [6].

In order to evaluate the extent of diagenesis the measurement of soil pH was conducted. The soil in Qubbet el Hawa is nearly neutral. The neutrality of the soil may be considered as an indicator of the good preservation state of bones [42]. Thanks to the ancient Egyptians burial customs the stability of the burial conditions over years is enhanced by the dryness of tomb environment as generally ancient Egyptians buried their dead in arid areas.

But, according to Nicholson [43], "*The pH alone is insufficient as a predictor of skeletal preservation,*" so the elemental content of soil was determined and compared to that of bones.

The significant higher levels of Sr and Ca in bones in comparison to that in soil was considered as an indication that Sr and Ca levels represent the biological levels, but the main argument against diagenesis was the results showed by the significant correlation between the Sr/Ca ratio and the Ba/Ca ratio that indicate that these ratios reflect the biological values. This test was used not only for its effectiveness over classic tests [33] but also because the target of analysis was the mandible which represents a "precious" bone because it is a part of the skull, so the use of any destructive method for assessing the extent of diagenesis was avoided.

4.3. Diet Reconstruction. Many studies used the Sr/Ca ratio as a quantitative indication of the plant to meat ratio basing on the biopurification of strontium through the food chain, for example, that of Schoeninger and Peebles [20], El-Tayeb [24]; however, this way of interpretation had been criticized because the relationship between bone Sr/Ca and the plant/meat ratio is not linear, also, as bone Sr/Ca ratio is negatively affected by calcium-rich food consumption, the low bone Sr/Ca ratio is not necessarily the result of reliance on meat [44].

It is important to note that ethanol consumption causes a decrease in bone strontium and barium, while a low-protein diet accompanied by ethanol consumption increases the bone strontium and decreases that of barium [45]. Also, ways of cooking may affect Sr content of food [46]. In addition, it is indicated by Katzenberg [47] that the concentration of

strontium in plant tissues depends on many factors such as the soil type.

Before discussing the results it is important to note that differences in the Sr/Ca ratio between the three groups could not be attributed to alcoholism, as, in contrast to beer, wine was available mainly for the higher social class [48]. In addition, prohibition of some sorts of food is not expected as taboos concerning eating some sorts of food in the ancient Egyptian culture were very few [49]. Also, as little is known about ancient Egypt methods of cooking [50], it is impossible to conclude to what extent ancient Egyptian processing could affect strontium levels in foods.

That $\log(\text{Sr}/\text{Ca})$ ratio in case of the FIP is significantly lower than that of MK and SIP. The FIP was a period accompanied by the rise of nomarchs authority and the dissolution of the central government: it was the period of feudalism [51]. According to Welc and Marks [52], at the end of the Old Kingdom, failure of the rains over the Ethiopian Highlands led into the failure of Nile floods. According to Bell [53], this situation that extended for decades during the FIP was the “*crisis that shattered a weakened central government utterly unable to cope with the problem, and decimated the Egyptian people.*” As explained by Erman [54], there is an indication in the text named “*Admonitions of an Egyptian Sage*” that famine pushed the people to eat which they used to feed to the domesticated birds and mammals. Then, the introduction of “unusual” sorts of foods or plants in the diet of Elephantine nobles followers and descendants during years of famine is suggested by this study. The high calcium or very low strontium contents of these newly and “exceptionally” introduced food types may be the cause of low Sr/Ca ratio relative to that in following eras, the MK and the SIP.

In addition, as indicated by Vandier [55] one of the adopted strategies against famine in ancient Egypt was the loans of cereals between nomes, for example, Ankhtifi, the nomarch of “Edfu” and “Hierakonpolis” during the early FIP supported the neighboring cities, including Elephantine, during years of famine, as he described in his tomb. Thus, it is expected that the consumption of cereals-staple food-exported from other nomes, that is, from regions with different chemical soil composition, caused this low level of Sr/Ca during years of famine where Aswan population cannot be considered as self-sufficient.

During the MK, the whole situation had been changed: Egypt was reunified and feudalism disappeared [51]. The social revolution during the FIP led to radical changes in moral values that led in turn to equal opportunities availability. Thus, the rise of a new class of officials that were proud to be self-made was allowed [56], and the flourishing of the ancient Egyptian middle class [51] that was “safeguarded from famine” [57] took place. The current study suggested that considering the amelioration of conditions, especially for the middle class to which the population under investigation is belonging, it is expected that dietary habits of Elephantine nobles followers and descendants had been differed from that of the FIP. The typical Dynastic diet consumption was adopted with no need for the consumption of “exceptional” sorts of food nor cereals import.

The Sr/Ca ratio of the group of the SIP is nearly equal to that of the MK. According to Ryholt [58] famines struck Egypt during the reign of the two competing Dynasties, the 13th and the 14th ones, as well as during the reign of the 16th Dynasty that governed the south of Upper Egypt. Although the anarchy swept all over the country during the SIP, the dissolution of the central government did not appear as the feudalism disappeared [51]. According to Abu-Taleb [59], by the disappearance of feudalism during the MK and the SIP, the individualism associated with state socialism flourished. That means that although the SIP was a period of weakness, general conditions were different from that of the FIP which is reflected in a Sr/Ca ratio that is nearly similar to that of the MK: despite the anarchy and famines, the calcium sources of the population under investigation remained the same during the MK and the SIP which may reflect an indication that food intake during the SIP in Elephantine was not hardly affected to the same extent of the FIP, taking in mind that as indicated by Vandier [55] few texts concerning famine during the SIP are available. One of these texts reflects the amelioration of political and economical conditions at the end of the SIP during the reign of the 17th Dynasty in Upper Egypt to the extent that the legitimate authority in the South was ready to struggle the Asiatics that ruled Lower Egypt (The Hyksos). In Carnarvon Tablet, the pharaoh Kamose recorded his discussion with the counselors about the situation in Egypt where they said “*We are tranquil in our part of Egypt. Elephantine is strong, and the middle part (of the land) is with us as far as Cusae. Men till for us the finest of their lands. Our cattle pasture in the Papyrus marshes. Corn is sent for our swine. Our cattle are not taken away. . . He holds the land of the Asiatics; we hold Egypt*” (quotation from Gardiner [60]).

It is recommended to conduct isotopic studies on the Aswan population to achieve more detailed interpretations about food customs of this area during ancient epochs. This will be completed with detailed paleoclimatological, zooarcheological, archeobotanical, and land use studies.

Conflict of Interests

The authors declare that there is no conflict of interests regarding the publication of this paper.

Acknowledgments

Sincere acknowledgments are expressed to Professor Dr. Friedrich Rösing, Faculty of Medicine, Ulm University, Germany, for his valuable help and advice specially during the early stages of work. Deep thanks are offered to Dr. Tamer Mahmoud Ahmed, Lecturer of Physical Anthropology, Institute of African Research and Studies, Cairo University, for his great help during the performance of statistical analysis. Profound gratitude is offered to researchers in the Research and Conservation of Antiquities Center, Ministry of Antiquities, specially the staff of the Anthropology and Mummy Conservation Lab., for great assistance.

References

- [1] D. W. Samuel, "Cereal foods and nutrition in ancient Egypt," *Nutrition*, vol. 13, no. 6, pp. 579–580, 1997.
- [2] M. R. Buzon and A. Bombak, "Dental disease in the Nile Valley during the New Kingdom," *International Journal of Osteoarchaeology*, vol. 20, no. 4, pp. 371–387, 2010.
- [3] A. Touzeau, R. Amiot, J. Blichert-Toft et al., "Diet of ancient Egyptians inferred from stable isotope systematics," *Journal of Archaeological Science*, vol. 46, no. 1, pp. 114–124, 2014.
- [4] Z. A. Abdel-Salam, A. H. Galmed, E. Tognoni, and M. A. Harith, "Estimation of calcified tissues hardness via calcium and magnesium ionic to atomic line intensity ratio in laser induced breakdown spectra," *Spectrochimica Acta—Part B, Atomic Spectroscopy*, vol. 62, no. 12, pp. 1343–1347, 2007.
- [5] E. Strouhal, *Life of the Ancient Egyptians*, The American University in Cairo Press, Cairo, Egypt, 1992.
- [6] J. Burton, "Bone chemistry and trace element analysis," in *Biological Anthropology of the Human Skeleton*, M. A. Katzenberg and S. R. Saunders, Eds., Wiley-Liss, Hoboken, NJ, USA, 2008.
- [7] C. Gilbert, J. Sealy, and A. Sillen, "An investigation of barium, calcium and strontium as palaeodietary indicators in the southwestern Cape, South Africa," *Journal of Archaeological Science*, vol. 21, no. 2, pp. 173–184, 1994.
- [8] A. R. Johnson, W. D. Armstrong, and L. Singer, "The incorporation and removal of large amounts of strontium by physiologic mechanisms in mineralized tissues of the rat," *Calcified Tissue Research*, vol. 2, no. 1, pp. 242–252, 1968.
- [9] M. Arnay-de-la-Rosa, E. González-Reimers, A. Gámez-Mendoza, and L. Galindo-Martín, "The Ba/Sr ratio, carious lesions, and dental calculus among the population buried in the church La Concepción (Tenerife, Canary Islands)," *Journal of Archaeological Science*, vol. 36, no. 2, pp. 351–358, 2009.
- [10] M. Arnay-de-la-Rosa, A. Gámez-Mendoza, J. F. Navarro-Mederos et al., "Dietary patterns during the early prehispanic settlement in La Gomera (Canary Islands)," *Journal of Archaeological Science*, vol. 36, no. 9, pp. 1972–1981, 2009.
- [11] M. J. Martínez-García, J. M. Moreno, J. Moreno-Clavel et al., "Heavy metals in human bones in different historical epochs," *Science of the Total Environment*, vol. 348, no. 1–3, pp. 51–72, 2005.
- [12] V. Scattarella, S. S. Saponetti, L. Laraspata, F. Bartoli, and F. Bertoldi, "The individual of the early Neolithic of Balsignano (Bari, Italy): a study of some skeletal indicators of stress and palaeonutritional analysis," *Human Evolution*, vol. 17, no. 3–4, pp. 143–155, 2002.
- [13] J. H. Burton and T. Douglas Price, "Evaluation of bone strontium as a measure of seafood consumption," *International Journal of Osteoarchaeology*, vol. 9, no. 4, pp. 233–236, 1999.
- [14] J. H. Burton, T. D. Price, L. Cahue, and L. E. Wright, "The use of barium and strontium abundances in human skeletal tissues to determine their geographic origins," *International Journal of Osteoarchaeology*, vol. 13, no. 1–2, pp. 88–95, 2003.
- [15] A.-F. Maurer, M. Gerard, A. Person et al., "Intra-skeletal variability in trace elemental content of Precolumbian Chupicuaro human bones: the record of *post-mortem* alteration and a tool for palaeodietary reconstruction," *Journal of Archaeological Science*, vol. 38, no. 8, pp. 1784–1797, 2011.
- [16] C. Stadlbauer, C. Reiter, B. Patzak, G. Stingeder, and T. Prohaska, "History of individuals of the 18th/19th centuries stored in bones, teeth, and hair analyzed by LA-ICP-MS: a step in attempts to confirm the authenticity of Mozart's skull," *Analytical and Bioanalytical Chemistry*, vol. 388, pp. 593–602, 2007.
- [17] K. Özdemir, Y. S. Erdal, and Ş. Demirci, "Arsenic accumulation on the bones in the Early bronze Age İkiztepe Population, Turkey," *Journal of Archaeological Science*, vol. 37, no. 5, pp. 1033–1041, 2010.
- [18] J. Zapata, C. Pérez-Sirvent, M. J. Martínez-Sánchez, and P. Tovar, "Diagenesis, not biogenesis: two late Roman skeletal examples," *Science of the Total Environment*, vol. 369, no. 1–3, pp. 357–368, 2006.
- [19] M. Busetto, L. Giordani, A. Brandone, C. Cattaneo, and A. Mazzucchi, "Dietary investigation by trace element content in bones of ancient inhabitants of Northern Italy," *Journal of Radioanalytical and Nuclear Chemistry*, vol. 275, no. 2, pp. 355–363, 2008.
- [20] M. J. Schoeninger and C. S. Peebles, "Effect of mollusc eating on human bone strontium levels," *Journal of Archaeological Science*, vol. 8, no. 4, pp. 391–397, 1981.
- [21] O. Samek, D. C. S. Beddows, H. H. Telle et al., "Quantitative laser-induced breakdown spectroscopy analysis of calcified tissue samples," *Spectrochimica Acta Part B: Atomic Spectroscopy*, vol. 56, no. 6, pp. 865–875, 2001.
- [22] F. C. Alvira, F. R. Rozzi, and G. M. Bilmes, "Laser-induced breakdown spectroscopy microanalysis of trace elements in homo sapiens teeth," *Applied Spectroscopy*, vol. 64, no. 3, pp. 313–319, 2010.
- [23] F. C. Alvira, F. V. Ramirez Rozzi, G. A. Torchia, L. Roso, and G. M. Bilmes, "A new method for relative Sr determination in human teeth enamel," *Journal of Anthropological Sciences*, vol. 89, pp. 153–160, 2011.
- [24] E. A. El-Tayeb, *Laser elemental analysis of ancient Egyptians teeth [M.S. thesis]*, National Institute of Laser Enhanced Science, Cairo University, Giza, Egypt, 2006.
- [25] M. Galiová, J. Kaiser, F. J. Fortes et al., "Multielemental analysis of prehistoric animal teeth by laser-induced breakdown spectroscopy and laser ablation inductively coupled plasma mass spectrometry," *Applied Optics*, vol. 49, no. 13, pp. C191–C199, 2010.
- [26] M. A. Kasem, R. E. Russo, and M. A. Harith, "Influence of biological degradation and environmental effects on the interpretation of archeological bone samples with laser-induced breakdown spectroscopy," *Journal of Analytical Atomic Spectrometry*, vol. 26, no. 9, pp. 1733–1739, 2011.
- [27] A. Giakoumaki, K. Melessanaki, and D. Anglos, "Laser-induced breakdown spectroscopy (LIBS) in archaeological science-applications and prospects," *Analytical and Bioanalytical Chemistry*, vol. 387, no. 3, pp. 749–760, 2007.
- [28] F. W. Rösing, "Discreta des menschlichen skeletts—ein kritischer überblick," *HOMO*, vol. 33, pp. 100–125, 1982.
- [29] F. W. Rösing, "Kith or kin? On the feasibility of kinship reconstruction inskeletons," in *Science in Egyptology*, A. R. David, Ed., Manchester University Press, Manchester, UK, 1986.
- [30] F. W. Rösing, "Sexing immature human skeletons," *Journal of Human Evolution*, vol. 12, no. 2, pp. 149–155, 1983.
- [31] S. Hillson, *Dental Anthropology*, Cambridge University Press, Cambridge, UK, 1996.
- [32] W. M. Bass, *Human Osteology: A Laboratory Field Manual*, Missouri Archeological Society, Columbia, SC, USA, 1987.

- [33] J. H. Burton, T. D. Price, and W. D. Middleton, "Correlation of bone Ba/Ca and Sr/Ca due to biological purification of calcium," *Journal of Archaeological Science*, vol. 26, no. 6, pp. 609–616, 1999.
- [34] F. W. Rösing, *Qubbet el Hawa und Elephantine: Zur Bevölkerungsgeschichte von Ägypten*, G. Fischer, Stuttgart, Germany, 1990.
- [35] K. Maki, A. J. Miller, T. Okano et al., "Cortical bone mineral density in asymmetrical mandibles: a three-dimensional quantitative computed tomography study," *European Journal of Orthodontics*, vol. 23, no. 3, pp. 217–232, 2001.
- [36] G. Grupe, "Impact of the choice of bone samples on trace element data in excavated human skeletons," *Journal of Archaeological Science*, vol. 15, no. 2, pp. 123–129, 1988.
- [37] A. Sillen and M. Kavanagh, "Strontium and paleodietary research: a review," *The American Journal of Physical Anthropology*, vol. 59, no. 3, pp. 67–90, 1982.
- [38] J. J. Prutsman-Pfeiffer, *Lead in the human femoral head: relationships of pathology, environmental exposure, micro-architecture, and biocultural contributions to bone quality [Ph.D. thesis]*, Faculty of Graduate School, University of New York, New York, NY, USA, 2008.
- [39] B. L. Beard and C. M. Johnson, "Strontium isotope composition of skeletal material can determine the birth place and geographic mobility of humans and animals," *Journal of Forensic Sciences*, vol. 45, no. 5, pp. 1049–1061, 2000.
- [40] J. Calcagno, *The seasonal and anatomical variation in compact bone remodeling in adult sheep [Ph.D. thesis]*, Faculty of California Polytechnic State University, San Luis Obispo, Calif, USA, 2011.
- [41] J. B. Edward and R. A. Benfer, "The effects of diagenesis on the Paloma skeletal material," in *Investigations of Ancient Human Tissue: Chemical Analyses in Anthropology*, M. K. Sandford, Ed., Gordon and Breach Science Publishers, Amsterdam, The Netherlands, 1993.
- [42] A. M. Child, "Microbial taphonomy of archeological bone," *Studies in Conservation*, vol. 40, pp. 19–30, 1995.
- [43] R. A. Nicholson, "Bone degradation, burial medium and species representation: debunking the myths, an experiment-based approach," *Journal of Archaeological Science*, vol. 23, no. 4, pp. 513–533, 1996.
- [44] J. H. Burton and L. E. Wright, "Nonlinearity in the relationship between bone Sr/Ca and diet: paleodietary implications," *American Journal of Physical Anthropology*, vol. 96, no. 3, pp. 273–282, 1995.
- [45] E. Gonzalez-Reimers, F. Rodriguez-Moreno, A. Martinez-Riera et al., "Relative and combined effects of ethanol and protein deficiency on strontium and barium bone content and fecal and urinary excretion," *Biological Trace Element Research*, vol. 68, no. 1, pp. 41–49, 1999.
- [46] M. A. Katzenberg, S. R. Saunders, and S. Abonyi, "Bone chemistry, food and history: a case study from 19th century Upper Canada," in *Biogeochemical Approaches to Paleodietary Analysis*, S. H. Ambrose and M. A. Katzenberg, Eds., Kluwer Academic/Plenum Publishers, New York, NY, USA, 2000.
- [47] M. A. Katzenberg, *Chemical Analysis of Prehistoric Human Bone from Five Temporally Distinct Populations in Southern Ontario*, National Museums of Canada, Ottawa, Canada, 1984.
- [48] W. J. Darby, P. Ghalioungui, and L. Grivetti, *Food: The Gift of Osiris*, vol. 2, Academic Press, London, UK, 1976.
- [49] W. J. Darby, P. Ghalioungui, and I. Grivetti, *Food: The Gift of Osiris*, vol. 1, Academic Press, London, UK, 1977.
- [50] E. Bresciani, *Food and Drink: Life Resources in Ancient Egypt*, Maria Pacini Fazzi Editore, Lucca, Italy, 1997.
- [51] T. G. H. James, *A Short History of Ancient Egypt: From Predynastic to Roman Egypt*, Librairie du Liban, Beirut, Lebanon, 1995.
- [52] F. Welc and L. Marks, "Climate change at the end of the Old Kingdom in Egypt around 4200 BP: new geoarchaeological evidence," *Quaternary International*, vol. 324, pp. 124–133, 2014.
- [53] B. Bell, "The dark ages in ancient history. I. The First Dark Age in Egypt," *The American Journal of Archaeology*, vol. 75, no. 1, pp. 1–26, 1971.
- [54] A. Erman, *The Ancient Egyptians: A Source Book for Their Writings*, Harber Torchbooks and The Academy Library, New York, NY, USA, 1966.
- [55] J. Vandier, *La Famine Dans L'Égypte Ancienne*, L'Imprimerie de L'Institut Français d'Archéologie Orientale, Cairo, Egypt, 1936.
- [56] M. B. Mahran, *The First Social Revolution in Egypt of The Pharaohs*, Dar El-Maarefa El-Gameiyia, Cairo, Egypt, 1999, (Arabic).
- [57] S. H. Aufrère, "The middle kingdom," in *The Pharaohs*, C. Ziegler, Ed., Bompiani Art, Milan, Italy, 2002.
- [58] K. S. B. Ryholt, *The Political Situation in Egypt During the Second Intermediate Period*, University of Copenhagen and Museum Tusulanum Press, Copenhagen, Denmark, 1997.
- [59] S. H. Abu-Taleb, *Legal History Principles*, Dar Al-Nahda Al-Arabia, Cairo, Egypt, 1965, (Arabic).
- [60] A. H. Gardiner, *Egypt of the Pharaohs*, Oxford University Press, New York, NY, USA, 1961.

Review Article

Invasive versus Non Invasive Methods Applied to Mummy Research: Will This Controversy Ever Be Solved?

Despina Moissidou,¹ Jasmine Day,² Dong Hoon Shin,³ and Raffaella Bianucci^{4,5,6}

¹Department of Histology and Embryology, Medical School, National Kapodistrian University of Athens, 75 M. Asias Street, 11527 Athens, Greece

²The Ancient Egypt Society of Western Australia Inc., P.O. Box 103, Ballajura, WA 6066, Australia

³Division of Paleopathology, Institute of Forensic Science, Seoul National University College of Medicine, Seoul 110-799, Republic of Korea

⁴Department of Public Health and Paediatric Sciences, Legal Medicine Section, University of Turin, Corso Galileo Galilei 22, 10126 Turin, Italy

⁵Center for Ecological and Evolutionary Synthesis (CEES), Department of Biosciences, University of Oslo, P.O. Box 1066, Blindern, 0316 Oslo, Norway

⁶Anthropologie Bioculturelle, Droit, Ethique et Santé, Faculté de Médecine-Nord, Aix-Marseille Université, 15 boulevard Pierre Dramard, 13344 Marseille Cedex 15, France

Correspondence should be addressed to Dong Hoon Shin; cuteminjae@gmail.com and Raffaella Bianucci; raffaella.bianucci@unito.it

Received 18 December 2014; Accepted 21 April 2015

Academic Editor: Timothy G. Bromage

Copyright © 2015 Despina Moissidou et al. This is an open access article distributed under the Creative Commons Attribution License, which permits unrestricted use, distribution, and reproduction in any medium, provided the original work is properly cited.

Advances in the application of non invasive techniques to mummified remains have shed new light on past diseases. The virtual inspection of a corpse, which has almost completely replaced classical autopsy, has proven to be important especially when dealing with valuable museum specimens. In spite of some very rewarding results, there are still many open questions. Non invasive techniques provide information on hard and soft tissue pathologies and allow information to be gleaned concerning mummification practices (e.g., ancient Egyptian artificial mummification). Nevertheless, there are other fields of mummy studies in which the results provided by non invasive techniques are not always self-explanatory. Reliance exclusively upon virtual diagnoses can sometimes lead to inconclusive and misleading interpretations. On the other hand, several types of investigation (e.g., histology, paleomicrobiology, and biochemistry), although minimally invasive, require direct contact with the bodies and, for this reason, are often avoided, particularly by museum curators. Here we present an overview of the non invasive and invasive techniques currently used in mummy studies and propose an approach that might solve these conflicts.

1. Introduction

Mummies represent a unique source of information about past diseases and their evolution. The question as to how to best maintain the integrity of archaeological and anthropological specimens in the course of examining this evidence has been a major cause for dispute among scholars.

The advent of non invasive techniques (e.g., X-ray, CAT scanning, and MRI) for examining mummified remains

has been a breakthrough in paleopathology as retrospective diagnoses can now be achieved without dissection.

However, mainly because of the structural differences between modern and ancient soft tissues, the efficiency of non invasive techniques has been questioned repeatedly. Many scholars insist that an accurate diagnosis can be correctly made only through direct examination of the corpse (i.e., autopsy, endoscopy). However, this approach creates concern among curators and archaeologists.

Here we address the debate from a broader perspective considering the advantages and disadvantages of both invasive and non invasive methods and propose the creation of an examination protocol for the analysis of ancient mummified remains based upon strict scientific and ethical criteria.

2. The Use of Non Invasive Techniques in Paleopathology

A new era in mummy studies began when the first group of Egyptian mummies was subjected to computed tomography (CT) in 1979 [1]. Scientists were given the opportunity to inspect the ancient Egyptians' bodies without resorting to the use of invasive methods [2, 3]. Both hard and soft tissues could be differentiated from multiple textile layers and artifacts (amulets, death masks, or portraits) and their pathologies diagnosed.

Although diagenetic alterations of ancient tissues often generate interpretative biases, CT scans have allowed differentiation between tissue structures and embalming materials. Similarly, antemortem traumas could be distinguished from postmortem manipulations associated with the embalming process [4], generating greater knowledge about the ways in which ancient populations treated and preserved their dead.

Artificial mummification is the deliberate act of preservation of a body after death [5]. This practice is aimed at slowing and/or halting soft tissues' degradation [6]. Different types of treatments (e.g., evisceration, use of natron, and coating with complex mixtures with antibacterial and antiputrefactive properties) allowed long-term preservation of the Egyptian mummies [7, 8].

Apart from exceptional cases, in which some steps of the mummification procedure were documented (i.e., the coffin of Djedbastiuefankh, Pelizaeus Museum, Hildesheim, Late Period; the Rhind Magical Papyrus, ca. 200 BC; three papyri in Cairo, Durham Oriental and Louvre Museums, around 1st century AD), the Egyptians did not leave written or illustrated records of their mummification methods [5].

Gaps in direct evidence have, therefore, been filled with information derived from numerous written sources. Herodotus (5th century AD) provided the earliest written accounts of mummification (Book II of *The Histories*). This is coupled with the records of Diodorus Siculus (1st century BC) and further augmented by the writings of Porphyry (3rd century AD). These principal sources have long provided the basis of modern knowledge about Egyptian mummification techniques [9]. CT scans have thus helped scientists and Egyptologists to increase their knowledge, which had hitherto been biased by the cultural stereotyping of Egypt in classical sources. New and more detailed knowledge about the evolution of artificial mummification has emerged [10, 11].

Over the last decade, a new generation of CAT scanners with increased power of resolution has been released and virtual autopsy has become one of the basic steps in any scientific investigation of mummified remains [12]. Visualization technology is an efficient tool in hard and soft tissue paleopathology [13]. Dental diseases (e.g., severe teeth abrasion, carious lesions, cists/abscesses, inflammation, and tooth loss) [14] and many degenerative disorders (e.g., rheumatoid

arthritis of the Iceman [15], anthro-paleopathological in Egyptian mummies [16], bone and soft tissue malignant tumours and/or soft tissue adenomas [17], or atherosclerosis [18, 19]) can now be diagnosed.

The latest developments in CT resolution (MicroCT) have even enabled the observation of architectural structures of bones [20].

Variations in wavelength radiation or use of Terahertz imaging have also been applied to mummified remains. Depending on the degree of hydration of a mummified corpse, this technique enables scientists to distinguish between features of soft tissues or bone and various artifacts, identifying objects [21] wrapped within textiles.

MRI (magnetic resonance imaging) has been similarly advantageous, especially in the study of hydrated mummies (i.e., bog bodies, South Korean mummies) [22]. MRI application on a 17th century Korean body showed unique clear organ structures, which could not be visualized by CT [23]. Less satisfactory results were obtained from MRI applied to dehydrated and embalmed bodies (i.e., Egyptian mummies) [24–26].

Despite the increased use of non invasive techniques, scholars still debate whether virtual inspection should be regarded as the “gold standard” in mummy studies or not.

In general, the CT methodological reference standards applied to the study of ancient remains are those determined from living patients [27]. Any kind of modification to CT scanning methodology (e.g., slice thickness or the introduction of other non invasive methods such as ionizing radiation on mummified cells) is still on an experimental level and is applied mainly in pilot studies of uncertain potential [28].

As a result of the differences between modern and ancient tissues and the absence of well-established methodological standards in mummy studies, misdiagnosis can occur. Gravitational force modifies both the morphology and location of the organs that elapses between burial and exhumation. Organs are displaced to the dorsal portion and their contraction is severe. While the difference in radiodensity is very important at a diagnostic level for living patients, radiodensity does not differ from organ to organ in mummies. Diagenetic processes can be misidentified as pathological conditions and vice versa [20]. To avoid misinterpretations, the complementary use of invasive methods (i.e., endoscopy, histology) is of utmost importance, either to support or to reject an initial diagnosis.

Another problem associated with the exclusive use of non invasive techniques is the lack of multidisciplinary teams involved in the interpretations of the data. Valid scientific research should include trained radiologists, whose experience lies mostly in diagnosing living patients, physical anthropologists or paleopathologists, and archaeologists who provide background information [4, 19, 22, 29].

To some extent concerning the scope of non invasive techniques applied to the study of ancient mummies generates confusion; therefore, the scientific purpose of non invasive methods often loses its meaning.

Museum curators and conservation experts usually prefer to resort to CT scanning in order to avoid specimen sampling

and usually disregard the need for an overall anthropopa-leopathological investigation. As a result, the broader use of non invasive techniques has become a fad, a spectacle misused by some scientists and curators for “infotainment” or advertising purposes. In many cases, the motivation for the employment of visual imaging is to take a curious glimpse inside a mummy [12] and perform animated 3D rendering for public display in exhibits rather than acquire sound scientific data.

3. The Role of Invasive Methods in Mummy Studies

Prior to recent advances in paleoradiology, invasive methods were the only available means of examining anthropological materials scientifically. Precious information about ancient lifestyles and diseases was acquired over decades, allowing scholars to gain a more profound historical and biological knowledge about populations of the past. The first invasive examination of ancient mummies began during the early 19th century, albeit as a form of public entertainment [2]. Many mummy unwrappings were carried out on the basis of mere curiosity and limited scientific knowledge. Therefore, many specimens were partially or completely destroyed.

Gradually, mummy autopsy became a more meticulous postmortem and provided scientists with information about both pathologies and possible causes of death [30].

Pioneering palaeopathologists adapted modern laboratory techniques to tiny mummified tissue biopsies in order to identify ancient tissue structures. They successfully diagnosed many diseases (e.g., tuberculosis, atherosclerosis, and parasitic diseases) [31–35].

Step by step, scientists have developed new methods to sample inner organ tissues, for example, endoscopy through natural orifices (i.e., mouth, nasal cavities, and use of forceps), and have progressively reduced the damage caused to mummies [36, 37].

Where endoscopes could not be introduced through natural or postmortem openings, a small perforation was made in the mummy’s back [38], so that tissue samples could be taken for histological studies.

As in forensic pathology [39], microscopic examination of small tissue biopsies (0.7×0.7 cm) is a requisite to complement non invasive methods because it allows an initial diagnosis to be precisely confirmed or infirmed [17, 35, 40, 41].

Similar developments in gas chromatography/mass spectrometry (GC/MS), isotopic analysis, and synchrotron analysis of minimal amounts of mummy hair have provided remarkable information about the daily lives of ancient populations within various social classes [42–44] and detected chronic or acute exposure to heavy metals [45–47].

Advances in paleoimmunology [48–50] and paleomicrobiology through soft/hard tissue analysis and secretion swabs led to the retrospective diagnosis of several pathogens (e.g., salmonellosis, tuberculosis, malaria, human leishmaniasis, and Chagas disease) in mummies [51–67] and revealed some of their evolutionary patterns [68]. However, not all scientists agree that it is possible to recover ancient endogenous human and pathogenic DNAs from Egyptian mummies [69–71].

Sampling of small skin tissue biopsies (0.7×0.7 cm) and textiles (1×1 cm) proved to be a reliable method for assessing potential biodeterioration of a mummified body or its external contamination. Microorganism identification through cultivation and molecular techniques is extremely useful for conservation purposes and to minimize the risk of potential hazards to the public, especially when mummies are on display [72].

Biochemical investigations (a combination of gas chromatography-mass spectrometry, GC-MS, and thermal desorption/pyrolysis, TD/Py-GC-MS) applied to skin and textiles and to dental calculus provide a plethora of information concerning the recipes used in embalming procedures [73–77] and the diets of ancient populations [78, 79].

Nowadays, the use of invasive methods for examining mummies is widely regarded with skepticism. While some researchers consider autopsies unavoidable, many consider them a destructive procedure [80].

Full autopsy has often been performed mainly to see inside a mummy and take samples for experimental research rather than obtain confirmation of a disease tentatively identified via a non invasive method.

The archaeological value of a human/animal specimen must always be a primary concern, especially when it is on display. When mummies are completely wrapped, fully dressed, and accompanied by funerary equipment, the prospect of a full autopsy threatens their integrity [20]. Whereas CT imaging requires only careful transportation of the mummy, invasive examination is more complex but can potentially be performed in a manner that respects the integrity of the corpse [29].

Equally significant is the ethical issue concerning lack of respect for a human body. A mummy is a deceased person, not an artifact, and burial customs should not be ignored [81]. If this assumption is followed, no sampling or limited sampling should be allowed in order to respect the deceased, and it is equally true that presenting 3D virtual renderings of undressed dead bodies to a lay public also raises ethical concerns.

Questions concerning the analyses of anthropological remains have been raised in many countries and these call for a specific set of bioethical guidelines [82].

The extent of invasive examination to which ancient mummies should be subjected is the cause of much debate. In the absence of specific laboratory guidelines and protocols, there is a lack of consistency; this has allowed people without sufficient if any scientific background to decide how valuable samples should be investigated. In most countries, decisions rely mostly upon the protocols established by individual institutes, museums, or team supervisors. Decisions based upon such independent judgments may therefore vary from full autopsy permission to total prohibition of the use of any invasive technique.

4. Discussion and Conclusion

4.1. Is the Examination Method the Real Issue? The controversy over the necessity of invasive versus non invasive

techniques calls for some appropriate and standardized protocols to be applied to mummy research. The issue is not the effectiveness of invasive or non invasive studies but their suitability for mummy research, which at present does not consistently achieve scientific standards.

Firstly, the purposes of many studies are inconsistent. A mummy must be investigated in order to provide scholars with answers related to specific biological or historical questions. An investigation performed simply to observe a mummy macroscopically or microscopically is not useful and is not ethical. Curiously, only a limited number of studies focusing upon specific diseases or historical developments in funerary artifact types found upon mummies have been performed to date.

Secondly, artificial mummification techniques vary considerably according to environmental conditions and cultural practices. Various factors, temperature, humidity, soil acidity, and time, cause various cell system modifications; these can be pinpointed both through invasive and non invasive techniques. The state of preservation, fully intact or partially preserved, is significant even for mummies of similar type, which means that every mummy is a unique case.

Despite the numerous studies performed upon mummies, methodological consistency and scientific comparison are lacking. Validity of results cannot be cross-checked for the lack of comparative studies and when scientists from various disciplines collaborate in multidisciplinary studies, conflict of interests is not uncommon.

4.2. Mummy Research Guidelines: The Need for an International Ethical and Scientific Committee. The aim of this review is to show that the current controversy is mainly caused by a lack of internationally established guidelines in mummy research. This, in turn, calls for an international mummy research protocol to be instituted. Composed of scholars of high repute, whose integrity is widely recognized, a committee should reestablish a series of priorities in the study of mummified bodies.

Firstly, ethical issues should be considered [83]. Scientists need to pay respect to the funerary beliefs of the deceased. With advice from cultural anthropologists, ethnologists, and bioethicists, a specific protocol to approach each type of cultural/religious context should be designed.

Secondly, mummy studies should be allowed for scientific and educational purposes but not for business (i.e., public entertainment or commercial movies). The purpose of a given study, either medical or archaeological, should be disclosed before any kind of investigation is performed, its value being widely recognized by the scientific community. Similarly, as many neophytes approach the field without proper training, strict selection criteria should be applied.

Obviously, it is impossible to apply a rigid and inflexible scientific protocol to all mummy cohorts. While some universal principles and rules will apply, technical protocols will necessarily need to be adjusted depending upon the type of mummy (i.e., dry or hydrated) and its state of preservation (i.e., fully wrapped, intact, partially destroyed, etc.). Nonetheless, all parameters used for mummy investigations should be clearly detailed and results fully published.

More transparency should be demanded when genetic studies are released. Entire datasets should be published rather than selected sequences. This would enable other researchers to provide the scientific community with their own interpretations and critical assessments of the data. The absence of transparency through selective data publication only gives rise to accusations of secrecy that taint the name of science and reputation of the data.

Along with an international protocol for mummy investigations, the creation of a worldwide network of tissue banks would be an optimal solution. Scientists could be provided with samples for laboratory research without frequent examination of the original remains [84] and their research would generate a comparative database with which to enable more targeted scientific applications.

Mummies represent the most precious anthropological material with which ancient cultures have provided us. Since mummified bodies attract scientists from different fields, an international protocol is now essential and required urgently. This protocol should clearly answer three main questions: “Are we showing adequate respect to the corpse we are analyzing?”, “Which scientific hypothesis necessitates our study of mummified remains?”, and “Do we propose to study mummies for scientific/cultural purposes or for business?”

With the aim of creating a scientific committee and, subsequently, of promoting the standardisation of a bioethical protocol on mummified remains, the authors plan to organise a dedicated symposium within the next World Congress on Mummy Studies (Lima, July 27–30, 2016).

Conflict of Interests

The authors declare that there is no conflict of interests.

Authors’ Contribution

Despina Moissidou, Jasmine Day, Dong Hoon Shin, and Raffaella Bianucci all contributed equally to this work.

References

- [1] D. C. F. Harwood-Nash, “Computed tomography of ancient Egyptian mummies,” *Journal of Computer Assisted Tomography*, vol. 3, no. 6, pp. 768–773, 1979.
- [2] A. R. David, *The Manchester Museum Mummy Project*, Manchester University Press, Manchester, UK, 1979.
- [3] D.-S. Lim, I. S. Lee, K.-J. Choi et al., “The potential for non-invasive study of mummies: validation of the use of computerized tomography by post factum dissection and histological examination of a 17th century female Korean mummy,” *Journal of Anatomy*, vol. 213, no. 4, pp. 482–495, 2008.
- [4] A. D. Wade and A. J. Nelson, “Radiological evaluation of the evisceration tradition in ancient Egyptian mummies,” *HOMO—Journal of Comparative Human Biology*, vol. 64, no. 1, pp. 1–28, 2013.
- [5] S. Ikram, *Death and Burial in Ancient Egypt*, Longman, Harlow, UK, 2003.

- [6] N. Shved, C. Haas, C. Papageorgopoulou et al., "Post mortem DNA degradation of human tissue experimentally mummified in salt," *PLoS ONE*, vol. 9, no. 10, Article ID e110753, 2014.
- [7] B. Brier and R. S. Wade, "The use of natron in human mummification: a modern experiment," *Zeitschrift für Ägyptische Sprache und Altertumskunde*, vol. 124, no. 2, pp. 89–100, 1997.
- [8] S. A. Buckley and R. P. Evershed, "Organic chemistry of embalming agents in Pharaonic and Graeco-Roman mummies," *Nature*, vol. 413, no. 6858, pp. 837–841, 2001.
- [9] S. Wisseman, "Preserved for the afterlife," *Nature*, vol. 413, no. 6858, pp. 783–784, 2001.
- [10] R. Gupta, Y. Markowitz, L. Berman, and P. Chapman, "High-resolution imaging of an ancient Egyptian mummified head: new insights into the mummification process," *American Journal of Neuroradiology*, vol. 29, no. 4, pp. 705–713, 2008.
- [11] A. D. Wade, G. J. Garvin, J. H. Hurnanen et al., "Scenes from the past: multidetector CT of Egyptian mummies of the Redpath Museum," *Radiographics*, vol. 32, no. 4, pp. 1235–1250, 2012.
- [12] J. J. O'Brien, J. J. Battista, C. Romagnoli, and R. K. Chhem, "CT imaging of human mummies: a critical review of the literature (1979–2005)," *International Journal of Osteoarchaeology*, vol. 19, no. 1, pp. 90–98, 2009.
- [13] A. S. Wilson, "Digitised diseases: preserving precious remains," *British Archaeology*, vol. 136, pp. 36–41, 2014.
- [14] L. Pacey, "Ancient mummies reveal impact of dental disease," *British Dental Journal*, vol. 216, no. 12, p. 663, 2014.
- [15] R. Ciranni, F. Garbini, E. Nerie, L. Melai, L. Giusti, and G. Fornaciari, "The 'Braids lady' of Arezzo: a case of rheumatoid arthritis in a 16th century mummy," *Clinical and Experimental Rheumatology*, vol. 20, no. 6, pp. 745–752, 2002.
- [16] W. K. Taconis and G. J. R. Maat, "Radiological findings in the human mummies and human heads," in *Egyptian Mummies: Radiological Atlas of the Collections in the National Museum of Antiquities at Leiden*, J. R. Maarten, W. K. Taconis, and G. J. R. Maat, Eds., Brepols, Turnhout, Belgium, 2005.
- [17] G. Fornaciari, M. Castagna, A. Naccarato, P. Collecchi, A. Tognetti, and G. Bevilacqua, "Adenocarcinoma in the mummy of Ferrante I of Aragon, King of Naples," *Paleopathology Newsletter*, vol. 82, pp. 7–11, 1993.
- [18] A. H. Allam, R. C. Thompson, L. S. Wann, M. I. Miyamoto, and G. S. Thomas, "Computed tomographic assessment of atherosclerosis in ancient Egyptian mummies," *Journal of the American Medical Association*, vol. 302, no. 19, pp. 2091–2094, 2009.
- [19] R. C. Thompson, A. H. Allam, G. P. Lombardi et al., "Atherosclerosis across 4000 years of human history: the Horus study of four ancient populations," *The Lancet*, vol. 381, no. 9873, pp. 1211–1222, 2013.
- [20] N. Lynnerup, "Mummies," *Yearbook of Physical Anthropology*, vol. 50, pp. 162–190, 2007.
- [21] L. Öhrström, A. Bitzer, M. Walther, and F. J. Rühli, "Technical note: terahertz imaging of ancient mummies and bone," *American Journal of Physical Anthropology*, vol. 142, no. 3, pp. 497–500, 2010.
- [22] C. Papageorgopoulou, K. Rentsch, M. Raghavan et al., "Preservation of cell structures in a medieval infant brain: a paleohistological, paleogenetic, radiological and physico-chemical study," *NeuroImage*, vol. 50, no. 3, pp. 893–901, 2010.
- [23] D. H. Shin, I. S. Lee, M. J. Kim et al., "Magnetic resonance imaging performed on a hydrated mummy of medieval Korea," *Journal of Anatomy*, vol. 216, no. 3, pp. 329–334, 2010.
- [24] H. Piepenbrink, J. Frahm, A. Haase, and D. Matthaei, "Nuclear magnetic resonance imaging of mummified corpses," *American Journal of Physical Anthropology*, vol. 70, no. 1, pp. 27–28, 1986.
- [25] F. J. Rühli, R. K. Chhem, and T. Böni, "Diagnostic paleoradiology of mummified tissue: interpretation and pitfalls," *Canadian Association of Radiologists Journal*, vol. 55, no. 4, pp. 218–227, 2004.
- [26] S. J. Karlik, R. Bartha, K. Kennedy, and R. Chhem, "MRI and multinuclear MR spectroscopy of 3,200-year-old Egyptian mummy brain," *American Journal of Roentgenology*, vol. 189, no. 2, pp. W105–W110, 2007.
- [27] L. Zweifel, T. Büni, and F. J. Rühli, "Evidence-based palaeopathology: meta-analysis of PubMed-listed scientific studies on ancient Egyptian mummies," *HOMO*, vol. 60, no. 5, pp. 405–427, 2009.
- [28] J. Wanek, R. Speller, and F. J. Rühli, "Direct action of radiation on mummified cells: modeling of computed tomography by Monte Carlo algorithms," *Radiation and Environmental Biophysics*, vol. 52, no. 3, pp. 397–410, 2013.
- [29] E.-J. Lee, C. S. Oh, S. G. Yim et al., "Collaboration of archaeologists, historians and bioarchaeologists during removal of clothing from Korean Mummy of Joseon Dynasty," *International Journal of Historical Archaeology*, vol. 17, no. 1, pp. 94–118, 2013.
- [30] M. R. Zimmerman and A. C. Aufderheide, "The frozen family of Utqiagvik: the autopsy findings," *Arctic Anthropology*, vol. 21, pp. 53–64, 1984.
- [31] M. A. Ruffer, "Pathological notes on the royal mummies of the Cairo Museum," in *Studies in the Paleopathology of Egypt*, R. L. Moodie, Ed., pp. 166–178, University of Chicago Press, Chicago, Ill, USA, 1921.
- [32] P. J. Turner and D. B. Holtom, "The use of a fabric softener in the reconstitution of mummified tissue prior to paraffin wax sectioning for light microscopical examination," *Stain Technology*, vol. 56, no. 1, pp. 35–38, 1981.
- [33] E. Fulcheri, E. Rabino Massa, and C. Fenoglio, "Improvement in the histological technique for mummified tissue," *Verhandlungen der Deutschen Gesellschaft für Pathologie*, vol. 69, p. 471, 1985.
- [34] A.-M. Mekota and M. Vermehren, "Determination of optimal rehydration, fixation and staining methods for histological and immunohistochemical analysis of mummified soft tissues," *Biotechnic & Histochemistry*, vol. 80, no. 1, pp. 7–13, 2005.
- [35] A. C. Aufderheide, "History of mummy studies," in *The Scientific Study of Mummies*, A. C. Aufderheide, Ed., pp. 1–17, Cambridge University Press, Cambridge, UK, 2003.
- [36] M. Manialawi, R. Meligy, and M. Bucaille, "Endoscopic examination of Egyptian mummies," *Endoscopy*, vol. 10, no. 3, pp. 191–194, 1978.
- [37] G. Castillo-Rojas, M. A. Cerbón, and Y. López-Vidal, "Presence of *Helicobacter pylori* in a Mexican pre-columbian mummy," *BMC Microbiology*, vol. 8, article 119, 2008.
- [38] E. Tapp, "Histology and histopathology of the Manchester mummies," in *Science in Egyptology*, A. R. David, Ed., pp. 347–350, Manchester University Press, Manchester, UK, 1986.
- [39] F. Collini, S. A. Andreola, G. Gentile, M. Marchesi, E. Muccino, and R. Zoja, "Preservation of histological structure of cells in human skin presenting mummification and corification processes by Sandison's rehydrating solution," *Forensic Science International*, vol. 244, pp. 207–212, 2014.
- [40] G. Grévin, R. Lagier, and C.-A. Baud, "Metastatic carcinoma of presumed prostatic origin in cremated bones from the first century A.D.," *Virchows Archiv*, vol. 431, no. 3, pp. 211–214, 1997.

- [41] G. Kahila Bar-Gal, M. J. Kim, A. Klein et al., "Tracing hepatitis B virus to the 16th century in a Korean mummy," *Hepatology*, vol. 56, no. 5, pp. 1671–1680, 2012.
- [42] F. Musshoff, C. Brockmann, B. Madea, W. Rosendahl, and D. Piombino-Mascalì, "Ethyl glucuronide findings in hair samples from the mummies of the Capuchin Catacombs of Palermo," *Forensic Science International*, vol. 232, no. 1–3, pp. 213–217, 2013.
- [43] A. H. Thompson, A. S. Wilson, and J. R. Ehleringer, "Hair as a geochemical recorder: ancient to modern," in *Treatise on Geochemistry (Volume 14): Archaeology & Anthropology*, T. E. Cerling, Ed., pp. 371–393, Elsevier, Cambridge, UK, 2nd edition, 2014.
- [44] A. S. Wilson, E. L. Brown, C. Villa et al., "Archaeological, radiological, and biological evidence offer insight into Inca child sacrifice," *Proceedings of the National Academy of Sciences of the United States of America*, vol. 110, no. 33, pp. 13322–13327, 2013.
- [45] R. Bianucci, M. Jeziorska, R. Lallo et al., "A pre-hispanic head," *PLoS ONE*, vol. 3, no. 4, Article ID e2053, 2008.
- [46] G. Lombardi, A. Lanzirotti, C. Qualls, F. Socola, A.-M. Ali, and O. Appenzeller, "Five hundred years of mercury exposure and adaptation," *Journal of Biomedicine and Biotechnology*, vol. 2012, Article ID 472858, 10 pages, 2012.
- [47] A. Lanzirotti, R. Bianucci, R. LeGeros et al., "Assessing heavy metal exposure in Renaissance Europe using synchrotron microbeam techniques," *Journal of Archaeological Science*, vol. 52, pp. 204–217, 2014.
- [48] V. A. Sawicki, M. J. Allison, H. P. Dalton, and A. Pezzia, "Presence of *Salmonella* antigens in feces from a Peruvian mummy," *Bulletin of the New York Academy of Medicine: Journal of Urban Health*, vol. 52, no. 7, pp. 805–813, 1976.
- [49] R. Bianucci, G. Mattutino, R. Lallo et al., "Immunological evidence of *Plasmodium falciparum* infection in an Egyptian child mummy from the early dynastic period," *Journal of Archaeological Science*, vol. 35, no. 7, pp. 1880–1885, 2008.
- [50] A. Corthals, A. Koller, D. W. Martin et al., "Detecting the immune system response of a 500 year-Old Inca Mummy," *PLoS ONE*, vol. 7, no. 7, Article ID e41244, 2012.
- [51] W. L. Salo, A. C. Aufderheide, J. Buikstra, and T. A. Holcomb, "Identification of *Mycobacterium tuberculosis* DNA in a pre-Columbian Peruvian mummy," *Proceedings of the National Academy of Sciences of the United States of America*, vol. 91, no. 6, pp. 2091–2094, 1994.
- [52] A. G. Nerlich, C. J. Haas, A. Zink, U. Szeimies, and H. G. Hagedorn, "Molecular evidence for tuberculosis in an ancient Egyptian mummy," *The Lancet*, vol. 350, no. 9088, p. 1404, 1997.
- [53] É. Crubézy, B. Ludes, J. D. Poveda, J. Clayton, B. Crouau-Roy, and D. Montagnon, "Identification of *Mycobacterium* DNA in an Egyptian Pott's disease of 5400 years old," *Comptes Rendus de Académie des Sciences—Serie III*, vol. 321, no. 11, pp. 941–951, 1998.
- [54] A. Zink, C. J. Haas, U. Reischl, U. Szeimies, and A. G. Nerlich, "Molecular analysis of skeletal tuberculosis in an ancient Egyptian population," *Journal of Medical Microbiology*, vol. 50, no. 4, pp. 355–366, 2001.
- [55] A. R. Zink, W. Grabner, U. Reischl, H. Wolf, and A. G. Nerlich, "Molecular study on human tuberculosis in three geographically distinct and time delineated populations from Ancient Egypt," *Epidemiology and Infection*, vol. 130, no. 2, pp. 239–249, 2003.
- [56] A. R. Zink, C. Sola, U. Reischl et al., "Characterization of *Mycobacterium tuberculosis* complex DNAs from Egyptian mummies by spoligotyping," *Journal of Clinical Microbiology*, vol. 41, no. 1, pp. 359–367, 2003.
- [57] A. R. Zink and A. G. Nerlich, "Molecular analyses of the 'Pharaohs': feasibility of molecular studies in ancient Egyptian material," *American Journal of Physical Anthropology*, vol. 121, no. 2, pp. 109–111, 2003.
- [58] A. R. Zink and A. G. Nerlich, "Long-term survival of ancient DNA in Egypt: reply to Gilbert et al," *American Journal of Physical Anthropology*, vol. 128, pp. 115–118, 2005.
- [59] A. R. Zink, M. Spigelman, B. Schraut, C. L. Greenblatt, A. G. Nerlich, and H. D. Donoghue, "Leishmaniasis in Ancient Egypt and Upper Nubia," *Emerging Infectious Diseases*, vol. 12, no. 10, pp. 1616–1617, 2006.
- [60] A. C. Aufderheide, W. Salo, M. Madden et al., "A 9,000-year record of Chagas' disease," *Proceedings of the National Academy of Sciences of the United States of America*, vol. 101, no. 7, pp. 2034–2039, 2004.
- [61] A. G. Nerlich, B. Schraut, S. Dittrich, T. Jelinek, and A. R. Zink, "*Plasmodium falciparum* in Ancient Egypt," *Emerging Infectious Diseases*, vol. 14, no. 8, pp. 1317–1319, 2008.
- [62] Z. Hawass, Y. Z. Gad, S. Ismail et al., "Ancestry and pathology in King Tutankhamun's family," *The Journal of the American Medical Association*, vol. 303, no. 7, pp. 638–647, 2010.
- [63] H. D. Donoghue, O. Y.-C. Lee, D. E. Minnikin, G. S. Besra, J. H. Taylor, and M. Spigelman, "Tuberculosis in Dr Granville's mummy: a molecular re-examination of the earliest known Egyptian mummy to be scientifically examined and given a medical diagnosis," *Proceedings of the Royal Society B: Biological Sciences*, vol. 277, no. 1678, pp. 51–56, 2010.
- [64] H. D. Donoghue, "Insights gained from palaeomicrobiology into ancient and modern tuberculosis," *Clinical Microbiology and Infection*, vol. 17, no. 6, pp. 821–829, 2011.
- [65] A. Lalremruata, M. Ball, R. Bianucci et al., "Molecular identification of *falciparum malaria* and human tuberculosis co-infections in mummies from the Fayum Depression (Lower Egypt)," *PLoS ONE*, vol. 8, no. 4, Article ID e60307, 2013.
- [66] J. Z.-M. Chan, M. J. Sergeant, O. Y.-C. Lee et al., "Metagenomic analysis of tuberculosis in a mummy," *The New England Journal of Medicine*, vol. 369, no. 3, pp. 289–290, 2013.
- [67] R. Khairat, M. Ball, C.-C. H. Chang et al., "First insights into the metagenome of Egyptian mummies using next-generation sequencing," *Journal of Applied Genetics*, vol. 54, no. 3, pp. 309–325, 2013.
- [68] E. Anastasiou and P. D. Mitchell, "Palaeopathology and genes: investigating the genetics of infectious diseases in excavated human skeletal remains and mummies from past populations," *Gene*, vol. 528, no. 1, pp. 33–40, 2013.
- [69] M. T. P. Gilbert, I. Barnes, M. J. Collins et al., "Long-term survival of ancient DNA in Egypt: response to Zink and Nerlich," *American Journal of Physical Anthropology*, vol. 128, no. 1, pp. 115–118, 2005.
- [70] E. D. Lorenzen and E. Willerslev, "King Tutankhamun's family and demise," *Journal of the American Medical Association*, vol. 303, no. 24, pp. 2471–2475, 2010.
- [71] J. Marchant, "Ancient DNA: curse of the Pharaoh's DNA," *Nature*, vol. 472, no. 7344, pp. 404–406, 2011.
- [72] G. Piñar, D. Piombino-Mascalì, F. Maixner, A. Zink, and K. Sterflinger, "Microbial survey of the mummies from the Capuchin Catacombs of Palermo, Italy: biodeterioration risk and contamination of the indoor air," *FEMS Microbiology Ecology*, vol. 86, no. 2, pp. 341–356, 2013.

- [73] J. Koller, U. Baumer, Y. Kaup, H. Etspuler, and U. Weser, "Embalming was used in Old Kingdom," *Nature*, vol. 391, no. 6665, pp. 343–344, 1998.
- [74] R. P. Evershed, K. I. Arnot, J. Collister, G. Eglinton, and S. Charters, "Application of isotope ratio monitoring gas chromatography–mass spectrometry to the analysis of organic residues of archaeological origin," *The Analyst*, vol. 119, no. 5, pp. 909–914, 1994.
- [75] S. A. Buckley, A. W. Stott, and R. P. Evershed, "Studies of organic residues from ancient Egyptian mummies using high temperature-gas chromatography-mass spectrometry and sequential thermal desorption-gas chromatography-mass spectrometry and pyrolysis-gas chromatography-mass spectrometry," *Analyst*, vol. 124, no. 4, pp. 443–452, 1999.
- [76] S. A. Buckley, K. A. Clark, and R. P. Evershed, "Complex organic chemical balms of Pharaonic animal mummies," *Nature*, vol. 431, no. 7006, pp. 294–299, 2004.
- [77] J. Jones, T. F. Higham, R. Oldfield, T. P. O'Connor, S. A. Buckley, and L. Bondioli, "Evidence for prehistoric origins of Egyptian mummification in late Neolithic burials," *PLoS ONE*, vol. 9, no. 8, Article ID e103608, 2014.
- [78] S. Buckley, D. Usai, T. Jakob, A. Radini, K. Hardy, and D. Guatelli-Steinberg, "Dental calculus reveals unique insights into food items, cooking and plant processing in prehistoric central Sudan," *PLoS ONE*, vol. 9, no. 7, Article ID e100808, 2014.
- [79] A. C. Aufderheide, L. R. Cartmell, M. Zlonis, and P. Horne, "Chemical dietary reconstruction of Greco-Roman mummies at Egypt's Dakhleh Oasis," *The Journal of the Society for the Study of Egyptian Antiquities*, vol. 30, pp. 1–10, 2003.
- [80] H. Pringle, *The Mummy Congress. Science, Obsession, and the Everlasting Dead*, Hyperion, New York, NY, USA, 2001.
- [81] S. Holm, "The privacy of Tutankhamen—utilising the genetic information in stored tissue samples," *Theoretical Medicine and Bioethics*, vol. 22, no. 5, pp. 437–449, 2001.
- [82] R. Downey, *Riddle of the Bones: Politics, Science, Race, and the Story of Kennewick Man*, Springer, Copernicus, New York, NY, USA, 2000.
- [83] I. M. Kaufmann and F. J. Rühli, "Without 'informed consent'? Ethics and ancient mummy research," *Journal of Medical Ethics*, vol. 36, no. 10, pp. 608–613, 2010.
- [84] P. Lambert-Zazulak, "The international ancient Egyptian mummy tissue bank at the Manchester Museum," *Antiquity*, vol. 74, no. 283, pp. 44–48, 2000.

Research Article

Modeling Metabolism and Disease in Bioarcheology

Clifford Qualls¹ and Otto Appenzeller²

¹Health Sciences Center, University of New Mexico, Albuquerque, NM 87131, USA

²New Mexico Health Enhancement and Marathon Clinics Research Foundation, Albuquerque, NM 87122, USA

Correspondence should be addressed to Clifford Qualls; clifford.qualls@gmail.com

Received 13 December 2014; Accepted 25 February 2015

Academic Editor: Carlo Baldari

Copyright © 2015 C. Qualls and O. Appenzeller. This is an open access article distributed under the Creative Commons Attribution License, which permits unrestricted use, distribution, and reproduction in any medium, provided the original work is properly cited.

We examine two important measures that can be made in bioarcheology on the remains of human and vertebrate animals. These remains consist of bone, teeth, or hair; each shows growth increments and each can be assayed for isotope ratios and other chemicals in equal intervals along the direction of growth. In each case, the central data is a time series of measurements. The first important measures are spectral estimates in spectral analyses and linear system analyses; we emphasize calculation of periodicities and growth rates as well as the comparison of power in bands. A low frequency band relates to the autonomic nervous system (ANS) control of metabolism and thus provides information about the life history of the individual of archeological interest. Turning to nonlinear system analysis, we discuss the calculation of SM Pinus' approximate entropy (ApEn) for short or moderate length time series. Like the concept that regular heart R-R interval data may indicate lack of health, low values of ApEn may indicate disrupted metabolism in individuals of archeological interest and even that a tipping point in deteriorating metabolism may have been reached just before death. This adds to the list of causes of death that can be determined from minimal data.

1. Introduction

Big data sets are revolutionizing science. They promote insights, facilitate comprehension, and order priorities for further studies using models and powerful computers. In the past decade important advances have been made using big data sets; they range from astronomy to climate change and from biology to geology. Bioarcheology, however, has not benefited from this trend, seemingly, because big data in bioarcheology are difficult to obtain.

Bioarcheology, as defined here, is cross-disciplinary research encompassing the study of human and animal remains. The best preserved tissues are bones, teeth, and occasionally hair.

Here we show that such archived materials provide sufficient data to model life's activities such as metabolism, growth, and biologic rhythms of individuals who have died decades or even millennia ago.

Many preserved tissues have growth marks left during life which reflect the rates of growth and by extension metabolism. For example, there are "scale like" markings on hair shafts which occur at more or less regular intervals which can be measured (Figure 1). Similarly on teeth surfaces or bone

sections growth lines can easily be discerned. For all of these we use the term repeat intervals (RIs) from Bromage et al. [1] to denote the histological evidence on archived remains that betray life's activities such as metabolism and growth.

We hypothesized that the growth lines (GL) in hair, measured by microscopy as a time series, provide direct measurements of hair growth rate, which in turn depends on metabolism and therefore is a proxy for that individual's metabolism during life [1, 2]. By analogy heart rate time series variability provides insight into autonomic nervous system (ANS) function and can hint at diseased states [3, 4].

In death, forensic time series have been linked to ANS function and may reflect on the individual's life history; these time series include the repeat intervals between growth lines (RIs) in scalp hair expressed as sizes of hair scales measured by microscopy. Also the repeat intervals between *Perikymata Grooves* (PG) or *Striae of Retzius* (SR) in the enamel in human teeth and growth lines in archosaur teeth provide other time series [1, 2, 5]. In addition, there are time series of osteocyte density in bone [6]. Oxygen, hydrogen, or carbon isotope ratios as well as other chemicals in hair measured along fixed intervals in the direction of growth provide time series. Here we use spectral analysis of such time series as proxies of

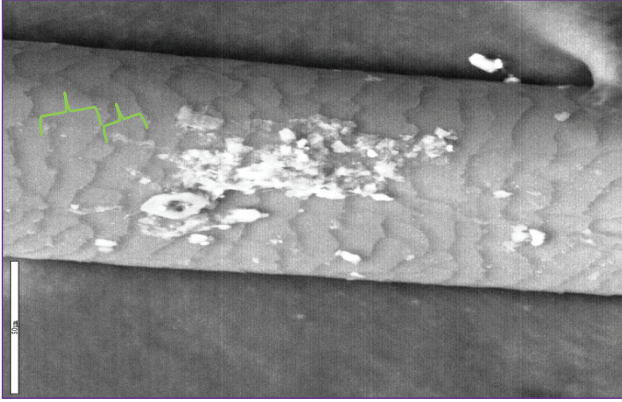


FIGURE 1: Human hair with repeat intervals (RIs) marked in green, 50 μm vertical bar in white.

metabolism, which provide insight into dynamic processes in operation in the individual's past life.

2. Materials and Methods

The annual growth rate can often be computed in the time domain.

2.1. Annual Growth Rate and Preprocessing Forensic Time Series. The forensic time series may be discrete time Y_i , $i = 1, \dots, N$, as in the growth lines in bone and teeth or for the scale sizes in hair, or a sample $Y_i = Y(t_i)$, $i = 1, \dots, N$, and $t_i = i\Delta t$ from a continuous time process such as chemicals measured in successive sections of bone of equal length Δt . For the discrete time process take $\Delta t = 1$, so that in both cases we have a discrete time series $\{Y_i\}$ of sample size (length) N . Usually this series will need to be preprocessed before it can be considered stationary Gaussian, the typical assumption for its spectral analysis.

Examining the plot Y versus time t , that is, Y_i versus i , it may show a nonzero mean, a trend over time, or an obvious annual cycle. We detrend the series if necessary by fitting a regression line $\hat{Y}_i = b + mt_i$ and replacing the series Y_i by its residuals $Y_i - \hat{Y}_i$ thereafter. The mean of the series is subtracted; the mean corresponds to the power at the zero frequency on the spectra, but our interest in spectral analysis sets aside consideration of the mean for separate analysis.

The next step in standardizing the time series $\{Y_i\}$ is to divide by its standard deviation. This preserves all the frequency content of the series and makes two different time series (perhaps even with different units of measurement) comparable. The situations where we would not standardize both series to variance = 1 is when our interest is the comparison of the variability (variances or the power in specified frequency bands) between the series.

If examination of the plot Y versus distance t along the hair shows an obvious annual cycle, then we can proceed directly to computing the annual growth rate of the hair.

Example 1 (mammoth). The hydrogen isotope ratio measurements (dD) at multiples of 0.3 cm are taken along a hair from a mammoth [7, 8]. There is a partial annual sinusoid evident, whose periodicity is 52 weeks.

Fitting the annual sinusoid as well as a trend yields the function of length along the hair in cm: Predicted $dD = -158 - 0.727 * \text{cm} + 8.69 * \sin(-0.196 * \text{cm} + 3.98)$ as reported in [7]. The frequency of the sinusoid is 0.196 radians/cm. Converting radians to cycles we have frequency = $(0.196 \text{ radians/cm}) / (2\pi \text{ radians/cycle}) = 0.0312 \text{ cycles/cm}$. This times the annual growth rate (cm/year) gives the number of cycles per year, which is equated to 1 cycle/year. Thus

$$\begin{aligned} \text{growth rate} &= \frac{1}{(\text{freq})(\text{period})} \\ &= \frac{1}{(0.0312 \text{ cycles/cm})(1 \text{ year/cycle})} \\ &= 32 \text{ cm/yr.} \end{aligned} \quad (1)$$

This is the growth rate reported in Sharp et al. [7].

2.2. Computing Periodicities by Spectral Analysis of Forensic Time Series. To identified periodicities that are more frequent than annual and less frequent than daily we compute the power spectrum of the discrete time standardized version of our annually adjusted time series using SAS PROC SPECTRA and the Fast Fourier Transform [9]. The mean is removed because it corresponds only to the power at frequency = 0, which is not our interest. Dividing each series by its own standard deviation (SD) removes the last difference in units between series, which is appropriate if we are not interested in comparing variances. In other settings the comparison of means or variance may be the goal, so this information is retained for such an analysis. Note that t -axis is no longer measured in cm but in the number of Δt , just as, in the mammoth Example 1 where $\Delta t = 0.3 \text{ cm}$. Now we give the spectral parameter definitions.

To be explicit, let the discrete time, stationary, Gaussian time series representing a series of measured intervals be $\{Y(t), \text{ for } t = 1, \dots, N\}$ with continuous spectral density $f(\lambda)$, where λ is the frequency on the x -axis. Then the periodogram $I(\lambda)$ is an estimate of $f(\lambda)$. One has

$$I(\lambda) = \frac{1}{2\pi N} \left| \sum_{t=1}^N Y(t)e^{-i\lambda t} \right|^2, \quad \text{for } -\pi < \lambda \leq \pi. \quad (2)$$

Note that each sinusoid $e^{i\lambda t}$ as a function of t has a frequency λ (radians per unit of t ; in this case, radians per observation) and a corresponding period $2\pi/\lambda$. Dividing λ by 2π radians per cycle gives a unit of cycle per observation as an alternative scale. For heartbeat, the frequency unit would be cycles per RR interval. For teeth, frequency units would be cycles per PG deposition (SR, Lines of Anderson (LA), or GL deposition). For the mammoth hair, the frequency units would be cycles per Δt increment. The units of the periodogram (and the spectral density) can be seen from the fact (proof not shown) that the sum of $I(\lambda_j)\Delta\lambda_j$ is the

variance of the $Y(t)$'s. The unit for power density on the y -axis is the measurement unit squared divided by the unit of the x -axis.

There is a well-known problem with the periodogram as an estimator of the spectral density; it is not consistent; it does not become better as the sample size N gets larger. Thus, the usual (and better) estimate of $f(\lambda)$ is the spectral density estimator $\hat{f}(\lambda)$, which is a smoothed and locally weighted average of the periodogram [10, 11]. One has

$$\hat{f}(\lambda_i) = \frac{2}{N} \sum_{j=1}^{\lfloor N/2 \rfloor} W(\lambda_i - \lambda_j) I(\lambda_j), \tag{3}$$

$$\text{for } \lambda_j = \frac{2\pi j}{N}, \quad j = 1, \dots, \left\lfloor \frac{N}{2} \right\rfloor.$$

The symbol $[x]$ represents the integer part of x . Spectral density $f(\lambda)$ is symmetric about $\lambda = 0$ by definition (definition not shown) and $I(\lambda)$ is symmetric. Since W , called the spectral window, is taken to be symmetric, the estimated spectral density is symmetric, which allows one to plot the spectral density only for the nonnegative frequencies $0 \leq \lambda_j \leq 2\pi$. Note that $4\pi/N = 2\Delta\lambda_j$, where the extra 2 represents the sum over the negative λ and the y -axis should also be scaled by dividing by 2π , and finally that $(4\pi/N) \div 2\pi = 2/N$ is the coefficient in (2).

Let us return to the mammoth example; the estimate of the spectral density of the standardized series in Figure 2(b) is Figure 2(c).

There are high frequency (0.42) and a low frequency (0.15) spectral peaks. Rearranging (1) above and including Δt provide the formula for computing periodicity. One has

$$\text{period} = \frac{\Delta t}{(\text{freq})(\text{growth rate})}. \tag{1'}$$

For the low frequency peak, we compute a periodicity of 3.25 weeks. Consider

$$\begin{aligned} \text{Period} &= \frac{\Delta t}{(\text{freq})(\text{growth})} \\ &= \frac{0.3 \text{ cm/obs}}{(0.15 \text{ cycles/obs})(32 \text{ cm/52 wk})} \\ &= 3.25 \text{ wk/ cycle}, \end{aligned} \tag{4}$$

where each observation represents one measurement interval with $\Delta t = 0.3 \text{ cm/obs}$.

Similarly, the periodicity of the high frequency peak is 1.2 weeks.

2.3. Nyquist Folding Frequency. There is a remaining issue; forensic time series are not measured continuously and the use of Δt affects the computed spectral density; one cannot hope to measure frequencies higher than a certain value taking place within an interval of length Δt . Furthermore, the spectral density is folded over at the Nyquist folding frequency ω_N with the high frequency content above ω_N

being added to the low frequency content below ω_N . For the Smithsonian mammoth hair,

Nyquist folding frequency

$$\omega_N = \frac{.5}{\Delta t} = \frac{.5 \text{ cycles/obs}}{0.3 \text{ cm/obs}} = 1.67 \text{ cycles/cm.} \tag{5}$$

This folding frequency times the growth rate gives a frequency of 1.03 cycles/week with a corresponding periodicity of 1/1.03 or approximately 1.0 week. Since we are not examining periodicities this low or lower, there may be no fold-back contamination in the above results. We have excluded the daily cycles from our interest; a much smaller Δt would have been necessary for this purpose. Though we are not examining the daily cycles directly, it could be folded back and contaminate our spectral density computation. The high frequency that folds back to a low frequency is called an alias. The aliasing problem sometimes requires a detailed discussion. The aliases of a given frequency λ are $\lambda + 2k\omega_N$, where $k = \pm 1, \pm 2, \pm 3, \dots$. The daily frequency is 7 cycles/week, and for $k = -3$, it is the alias of +0.82 cycles/week, but the observed peak is at $1/1.2 = 0.83$ cycles/week. Now we are uncertain whether the observed high frequency peak is real at a periodicity 1.2 weeks or it is a contamination from the daily cycle at 1/7 weeks. See discussion. It is clear that one should formally consider the effect of the Nyquist folding frequency.

2.4. Low Frequency-High Frequency Ratio. To compute the power in a given band of frequencies, the spectral density is integrated over the band; that is, the spectral density times $\Delta\lambda$ is summed over the frequencies λ_j in the band.

Thus, the total power or power in frequency bands is obtained as areas under the curve where the units of the x -axis cancel. While the computation of power as areas (AUCs) under the spectral density from (2) above is typical, we also wish to compute the asymptotic standard error of such estimates. The formulae for power in a frequency band are adapted from Priestley [12, page 427]. One has

$$\begin{aligned} \text{AUC} &= \sum_{\lambda_j \text{ in band}} 2\hat{f}(\lambda_j) \Delta\lambda_j, \\ \text{Variance} &= \sum_{\lambda_j \text{ in band}} 4\hat{f}^2(\lambda_j) \Delta\lambda_j^2, \quad \text{where } \Delta\lambda_j = \frac{2\pi}{N}, \\ \text{SE} &= \sqrt{\text{Variance}}. \end{aligned} \tag{6}$$

Again the factor of 2 represents the negative frequencies. When the time series is standardized, these formulae are dimensionless and can give a measure of the spectral shape. With these asymptotic means and SEs, one can compute a t -statistic and P value for the comparison of two AUCs. Note that these formulae in Priestley were developed for the periodogram $I(\lambda)$ instead of the locally smoothed periodogram, the estimated spectral density function $\hat{f}(\lambda_j)$. Both are approximately equal to the spectral density function $f(\lambda)$. Koopmans [13] uses the estimated spectral densities $\hat{f}(\lambda_j)$ for these formulae.

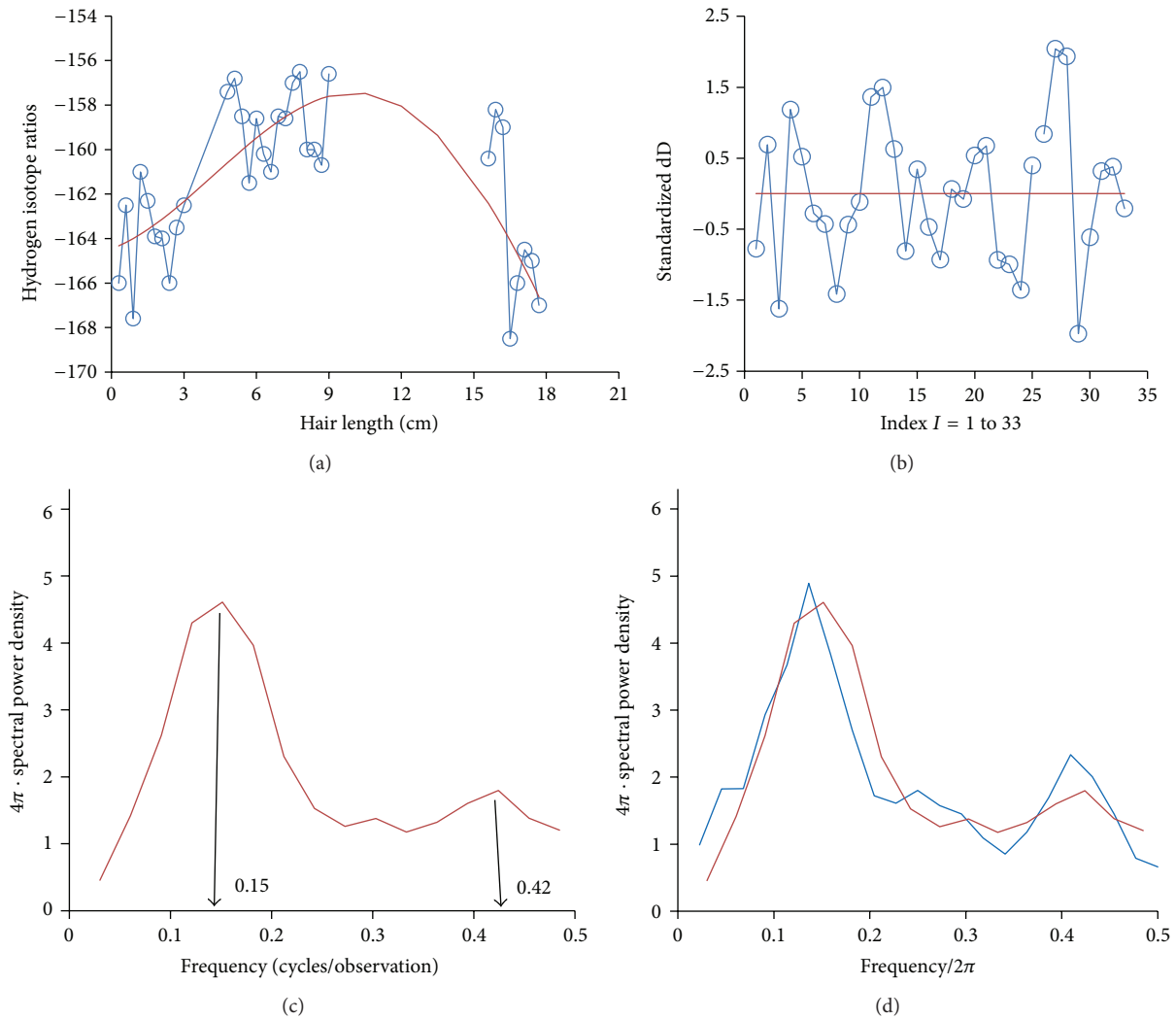


FIGURE 2: (a) Hydrogen isotope measured in 0.3 cm intervals of a hair of a Siberian mammoth loaned from the Smithsonian and published in [7]. (b) Standardized hydrogen isotope data in Figure 2(a) computed as the residuals of fitting the annual sinusoid, which have been standardized to mean = 0 and SD = 1. (c) Hydrogen isotope spectra of Smithsonian mammoth (red line) hair measured every 0.3 cm. Series standardized to mean = 0 and SD = 1. The low frequency peak marked at 0.15 and high frequency peak at 0.42 are marked. Frequency axis (radians/observation) is divided by 2π radians/cycle to obtain cycles/observation. (d) Hydrogen isotope spectra of Smithsonian mammoth (red line) and of Jarkov mammoth (blue line) hair measured every 0.3 cm. Series standardized to mean = 0 and SD = 1. Frequency axis is divided by 2π ; multiplying y-axis by 2π maintains AUCs; multiplying y-axis by 2 represents contribution from negative frequencies.

2.5. *Distribution of Estimates.* The distribution of the AUC estimator is based on the distribution of single estimated spectral densities $\hat{f}(\lambda_j)$, which in turn depends on the effective degrees of freedom (EDF) of spectral window $W(\lambda)$; see Koopmans [13, Table 8.1, page 279]. The standard result is $r(\hat{f}(\lambda)/f(\lambda)) \approx \chi_r^2$, where the random variable on the left hand side is chi-square-distributed with $r = \text{EDF}$. Now we write the random AUC $\approx \sum_{\lambda_j \text{ in band}} (2f(\lambda_j)\Delta\lambda_j/r)X_j$, where X_j are independent χ_r^2 , chi-square random variables. Since $EX_j = r$, the expected value of the random AUC is the targeted AUC. The variance of the random AUC is the targeted variance in (3). We now model the complicated

distribution of the random AUC, a weighted sum of chi-square random variables, as a single distribution $\approx c\chi_R^2$ by the standard method of equating moments. One has estimates

$$E(c\chi_R^2) = cR, \quad \text{Var}(c\chi_R^2) = 2c^2R. \quad (7)$$

In terms of the moments in (3) we have

$$r \frac{\hat{f}(\lambda)}{f(\lambda)} \text{ is approximately distributed as } a \chi_r^2,$$

chi-square random variable;

$$\text{AUC} \approx c\chi_R^2, \text{ where}$$

$$c = \frac{1}{2} \frac{\text{Var}(AUC)}{E(AUC)} \text{ and } R = 2 \frac{E^2(AUC)}{\text{Var}(AUC)} \text{ with}$$

$E(AUC), \text{Var}(AUC)$ computed as the

moments of AUC in (3).

(8)

Example 2. Let us compute the 95% confidence intervals for the low frequency power for the Smithsonian mammoth (red line, Figure 2(d)). First for the low frequency band, $0.07 \leq \lambda < 0.27$, we have $AUC_2 = 0.587, V_2 = 0.064$. Second, $c = .5 * .064 / .587 = 0.0545, R = .587 / .0545 = 10.8$. Third, the upper and lower critical values for the χ^2_R distribution are 3.7 and 21.6. Since $c * 21.6 > 1$, we compute the one-sided confidence interval with critical value 4.45. Finally, $P[c * 4.45 < AUC] = 0.95$ and $[0.24, 1.0]$ is the 95% one-sided confidence interval for the power in this low frequency band. The upper bound is 1.0 since the area under the whole curve is 1.0 for the standardized series.

Example 3. Now the ratio $(LF/HF) = AUC_2/AUC_3 = 0.587/0.322 = 1.82$. Is this different than 1.0? Here, the high frequency band is $0.27 < \lambda < 0.5$ with a width of 0.23, which introduces a bias relative to low frequency band width of 0.20. We could rerun our statistics for the comparable interval $0.30 < \lambda < 0.5$, but we modify our estimate of AUC_3 to be $(0.20/0.23) * 0.322 = 0.28$ and $LF/HF = 2.10$. So, we develop the following two-tailed F -test. In spectral theory, the two AUCs are based on disjoint frequencies and are nearly independent. They would be more independent if the spectral windows did not overlap. We have already computed $c = 0.0545$ and $R = 10.8$ for the statistic AUC_2 .

For the modified AUC_3 , we have $E(AUC_3) = 0.28$ and variance $V_3 = 0.0102$. Second, $c_3 = 0.5 * 0.0102 / 0.28 = 0.0182$ and $R_3 = 0.28 / 0.0182 = 15.4$. Third, the distribution of

$$\frac{AUC_2}{AUC_3} \approx \frac{c_2 \chi_{R_2}}{c_3 \chi_{R_3}} = \frac{c_2 R_2}{c_3 R_3} F_{R_2, R_3},$$

$$\frac{c_2 R_2}{c_3 R_3} = \frac{0.0545 * 10.8}{0.0182 * 15.4} = 2.10,$$

(9)

where $F = F_{R_2, R_3}$ is an F -statistic. Finally, $P[F > 2.1] = 0.09$ and the two-sided $P = 0.18$.

For an example of comparison between two spectra, we add the data for a hair sample from a Jarkov Siberian mammoth (Figure 2(d), in blue). For the frequency band $0.07 \leq \lambda < 0.27$, including the low frequency peaks, we have $AUC_2 = 0.587 \pm 0.253$ (SE) for Smith and $AUC_2 = 0.527 \pm 0.199$ (SE) for Jarkov.

A test of the difference shows no difference:

$$t = \frac{AUC_{\text{Smith}} - AUC_{\text{Jarkov}}}{\sqrt{SE_{\text{Smith}}^2 + SE_{\text{Jarkov}}^2}} = \frac{0.587 - 0.527}{\sqrt{.253^2 + .199^2}}$$

$$= \frac{0.06}{0.322} = 0.19, \quad P = 0.85.$$

(10)

Comment. For a spectral analysis, these sample sizes are small: $N = 33$ and $N = 44$. For chemical analyses these can be larger.

2.6. Tipping Points and Telogen Duration (Quiescence in Growth). Longer quiescence in hair growth (telogen [14]) indicates disrupted metabolism (longer intervals of oscillations of the system) and may be a marker of the tipping point in metabolism before complete cessations of rhythmic oscillations that are the hallmarks of biological systems. Here we compute the quiescent period in a basic model of reduced annual growth rate in hair. In normal human hair the telogen phase lasts approximately 3 months divided into approximately 4 periods. Hair grows for approximately 8 years and then, normally, falls out (metabolism ceases in this particular hair). Stress is known to lengthen the telogen; hormonal levels, age, and metabolism also affect the duration of the telogen. We cannot know at the time of modeling of the hair growth in what stage each hair is at the time of death. The basic model assumes (1) hair growth rate after the telogen continues independently of the telogen preceding it and independent of the telogen duration and (2) metabolism continues during the telogen phase as it was before and after, but since the hair is not growing, information about metabolism is missing in the hair record.

Let Q be the annual quiescence period measured in weeks and let G and G' be the reference and reduced annual growth rates of the hair, respectively. G' is reduced because of the augmented quiescence period AQ . The relationship is

$$G' = \frac{52 - AQ}{52 - Q} G, \text{ and conversely, } AQ = 52 - \frac{G'}{G} (52 - Q).$$

(11)

If $A = 1$ then $G' = G$ and G' is not reduced; if $A > 1$ then $G' < G$ and G' is reduced. For normal human hair growth, $Q = 13$ weeks. The augmented quiescence period AQ can only be computed by comparison of the reduced G' to a reference G unless direct observation can be made in life.

Example 4. For the 16th century Spanish royals at the end of life, King Ferrante had an annual hair growth rate of 12 cm/year and Queen Isabella had a growth rate of 2 cm/year. Thus assuming $G = 16$ cm/year, the augmented quiescence periods were $AQ = 52 - (12/16)(52 - 13) = 52 - 29.25 = 22.7$ weeks for Ferrante and $AQ = 52 - (2/16)(52 - 13) = 52 - 4.88 = 47.2$ weeks for Isabella. These are longer than the normal 13 weeks and Isabella's is extreme. The historical record may contain information about metabolism; for example, Isabella had marked hair loss before she died. However, since direct measurement of quiescence was unlikely to be recorded, computations based on comparison of growth rates give information on quiescence periods as illustrated above.

We now show graphically how the quiescence period AQ in our basic model affects the observed sinusoid representing the annual growth cycle. We will also check whether AQ affects the observed low frequency sinusoid representing autonomic neural system (ANS) control. Normal annual

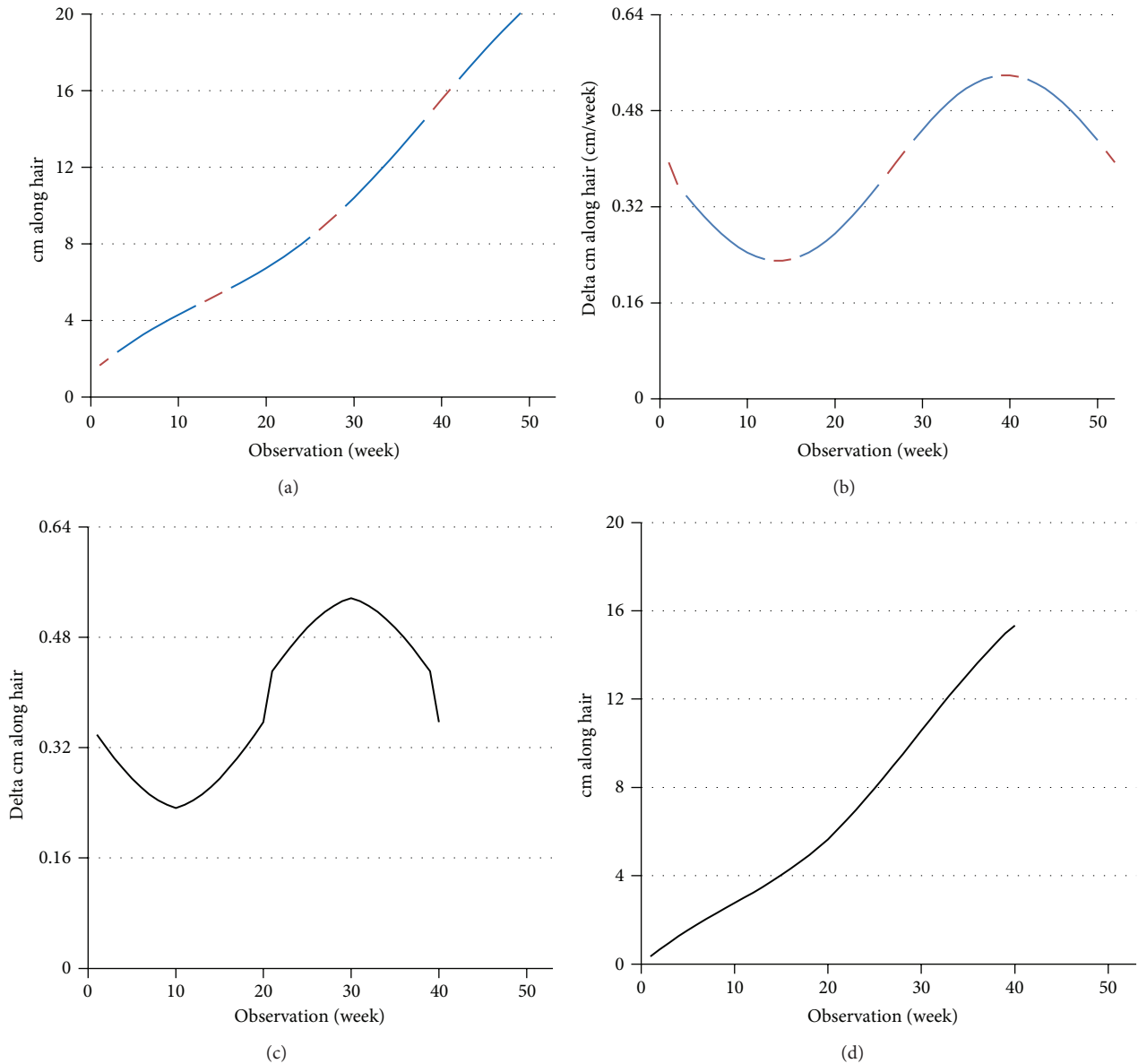


FIGURE 3: (a) Distance (cm) along a hypothetical hair (blue) that grows continuously for 52 weeks to a length of 20 cm as though there were no quiescence periods; now the quiescence periods are superimposed and marked (red). (b) Incremental weekly growth of the hypothetical hair (blue) with quiescence periods (red), mathematically obtained as the derivative of (a). (c) Observable incremental weekly growth for 39 weeks out of the year, periodic but not a sinusoid though a sinusoid of periodicity 39 weeks fits very well (not shown). (d) Distance (cm) along the observable hair for 39 weeks for an observed length of approximately 16 cm for the year, mathematically obtained as the integral of (c).

hair growth rate measured in hair growth is approximately 16 cm/year. Thus we begin with growth of 20 cm/year when there is no quiescence period ($Q = 0$ and $AQ = 0$) and weekly measurements that average 0.385 cm (see Figure 3(a)). The annual sinusoid as a function of weeks is followed by differentiation (see Figure 3(b)). Now three (3) months of quiescence are marked as missing (red) in Figures 3(a) and 3(b).

However the quiescence periods are not observed; thus the observable result is in Figures 3(c) and 3(d).

When the periodic function in Figure 3(c) is identified as an annual cycle, computations would consider the cycle as

though on a 52-week x -axis. Thus, the annual growth rate is computed as 16 cm/year. We have shown how a growth rate of 20 cm/year becomes 16 cm/year in our basic model with $Q = 3$ months out of the year.

2.7. Nonlinear Time Series Analysis. We have examined spectral analysis in the frequency domain, which can be considered as linear systems analysis. There are also methods for nonlinear time series analyses and their application to chaos in dynamical systems [15]. The name most associated with this field is Takens [16]. The field provides measure of chaos, which can arise from nonlinear dynamical equations. There

is also a more purely mathematical analysis [17]. We illustrate just one practical method from this large field.

2.7.1. Approximate Entropy Measure. Approximate entropy (ApEn) as described by Pincus et al. [18, 19] quantifies regularity in time series data. ApEn and other measures have been used extensively in the analysis of biological time series [20]. In heart rate variability the low frequency/high frequency ratios reflect the autonomic nervous system (ANS) control of the activity of the cardiac pacemaker; in our analysis these ratios reflect the ANS pacemaker of metabolism and thus the ANS control of metabolism. In heart rate variability, disease such as diabetes decreases the variability; the heart rate is fixed at a higher rate but the variability in heart rate is reduced, a sign of ANS failure due to the disease. Conversely, high variability in ApEn reflects the robustness of the system. Bone, teeth, and hair also reflect metabolism and as such reflect ANS control.

ApEn depends on three parameters: the length of the time series (N), the width of the window that defines the patterns (m), and the tolerance that defines the closeness of the patterns (r). ApEn measures how the pattern (m) repeats itself within tolerance (r) over the course of the time series. ApEn(m, r) is a statistic that estimates the logarithmic difference for m and $m + 1$ in the conditional probability that runs of patterns that are close for previous repetitions remain close. Consequently, a large ApEn corresponds to an irregular time series and a small ApEn corresponds to a regular time series. ApEn for lengths of $N > 50$ has been found to be reproducible, but the literature suggests it can also be used with $N \leq 50$. The pattern matching window can vary, but values between 1 and 3 are generally used. We used $m = 2$ and $m + 1 = 3$. A small tolerance value (r) corresponds to a fine pattern matching and a large r value corresponds to a coarser comparison. Our r was selected to be scale invariant as a percentage of the standard deviation of the time series being analyzed. We found values of r between 60% and 70% discriminated best for our analysis.

Thus, we use ApEn to measure the logarithmic likelihood that similar patterns of data length (m) that are similar remain so within a tolerance (r) on the next incremental ($m + 1$) comparison. In this analysis smaller values of ApEn indicate greater regularity in the data. Larger values are indicative of greater irregularities, more chaotic systems.

Example 5. The “Zwelloo woman” was exhumed from a bog in Netherlands in 1951.

We examined six scalp hairs, 2000 years after her death. The approximate entropy (ApEn) was computed for the repeat intervals (RIs) defined by the sizes of hair scales along the length of the hair and for each of her six hairs separately; with $N = 64$ –105 repeat intervals, pattern width $m = 2$ and tolerance $r = 80\%$ of the total standard deviation of the time series. The mean ApEn for Zwelloo’s hairs was 0.84 ± 0.05 (SD). Since tolerance (r) and, to a limited extent, pattern (m) are “free” parameters, these choices can be partially validated by comparison to a control group using the same parameters.

Here a control group of 4 individuals had a mean ApEn of 0.71 ± 0.10 .

3. Results and Discussion

For the methods outlined above, some operational aspects are now considered.

The Nyquist folding frequency probably is not a problem for measured RIs, since generally they are not sampling from a more continuous series. The RIs for hair are deposited in multiple of whole days with the multiple of days being related in an allometric fashion to the species’ body mass; the whole days for periodic deposits to tooth enamel were 1 day for smallest bodied primates to 11 days for largest bodied primates and 8 days for humans [1]. Thus the daily cycles are not explicitly present in the RI data. This is not so for the continuous chemical record. The usual engineering solution to the Nyquist folding frequency problem is to design so that there is no power for frequencies beyond ω_N . This is a consideration for the chemical time series, since the sampling rate Δt may be under the experimenter’s control. Even if this is not an option open to us, this spectral peak could still be real (uncontaminated), provided we knew the power of the daily cycle was low.

The data segments caused by missing values are pooled, laid end-to-end. The laying short time series end-to-end (concatenated) to form a longer series may cause difficulty. However, this difficulty is handled automatically in a similar situation for the spectral analysis of heart rate recordings where gaps occur due to technical problems or are introduced to eliminate periods of anomalous heartbeats for separate consideration. We follow this convention unless the difficulties become too large.

An important assumption for the distributions of spectral estimates in the section so named is that the choice of band width for the spectral window is wide enough for that the smoothed estimate of each spectral density function is consistent and narrow enough that estimates of adjacent spectral densities are approximately independent. The series length N must be large enough that the two conditions on the spectral window can be met.

Among several additional methods in use for nonlinear time series analysis, there are generalizations of the two basic methods (ApEn and FFT) used herein. First is the replacement of the deterministic rules used in approximate entropy (ApEn) with fuzzy logic rules yielding an improved algorithm (fApEn) that could help with the choice of the tolerance parameter (r) [21, 22]. Second is the Hilbert-Huang Transform (HHT) which is designed as a time-frequency analysis of nonlinear, nonstationary time series [23]. Compared to the spectral analysis using Fast Fourier Transform (FFT), which is designed as a frequency analysis of linear time series that are stationary in time, the HHT could help with periodicity estimation. The Hilbert-Huang Transform is implemented in a file exchange (hht) in MATLAB and in a package (hht) in the R language.

For our basic model of quiescence, we assume that the growth rate when the hair is growing is always constant

and normal. Then the length of the quiescence intervals is the major effect on the annual growth rate and the effect is algebraic. If the disruption in metabolism affects both Q and the growth rate when the hair is growing, then we would need a model that connects increased quiescence to change (lowering) in the (instantaneous) growth rate when growing.

Does quiescence affect the frequency (periodicity) of the low frequency peak, the peak most related to autonomic nervous system (ANS) control? No doubt it does in the same manner that quiescence affects the annual growth cycle. Nonetheless, the computation of the periodicity of the low frequency peak is from the same hair growth record where we compute the growth rate usually reported. As such, it is comparable and useable on its face.

Conflict of Interests

The authors declare that there is no conflict of interests regarding the publication of this paper.

References

- [1] T. G. Bromage, R. T. Hogg, R. S. Lacruz, and C. Hou, "Primate enamel evinces long period biological timing and regulation of life history," *Journal of Theoretical Biology*, vol. 305, pp. 131–144, 2012.
- [2] O. Appenzeller, C. Qualls, F. Barbic, R. Furlan, and A. Porta, "Stable isotope ratios in hair and teeth reflect biologic rhythms," *PLoS ONE*, vol. 2, no. 7, article e636, 2007.
- [3] A. Malliani, M. Pagani, F. Lombardi, and S. Cerutti, "Cardiovascular neural regulation explored in the frequency domain," *Circulation*, vol. 84, no. 2, pp. 482–492, 1991.
- [4] I. Cygankiewicz and W. Zareba, "Heart rate variability," *Handbook of Clinical Neurology*, vol. 117C, pp. 379–393, 2013.
- [5] O. Appenzeller, H.-C. Gunga, C. Qualls et al., "A hypothesis: autonomic rhythms are reflected in growth lines of teeth in humans and extinct archosaurs," *Autonomic Neuroscience: Basic and Clinical*, vol. 117, no. 2, pp. 115–119, 2005.
- [6] T. G. Bromage, R. S. Lacruz, R. Hogg et al., "Lamellar bone is an incremental tissue reconciling enamel rhythms, body size, and organismal life history," *Calcified Tissue International*, vol. 84, no. 5, pp. 388–404, 2009.
- [7] Z. D. Sharp, V. Atudorei, H. O. Panarello, J. Fernández, and C. Douthitt, "Hydrogen isotope systematics of hair: archeological and forensic applications," *Journal of Archaeological Science*, vol. 30, no. 12, pp. 1709–1716, 2003.
- [8] M. Spilde, A. Lanzirotti, C. Qualls et al., "Biologic rhythms derived from Siberian Mammoths' Hairs," *PLoS ONE*, vol. 6, no. 6, Article ID e21705, 2011.
- [9] J. W. Cooley and J. W. Tukey, "An algorithm for the machine calculation of complex Fourier series," *Mathematics of Computation*, vol. 19, pp. 297–301, 1965.
- [10] R. W. Hamming and J. W. Tukey, *Measuring Noise Color*, Bell Telephone Laboratories Memorandum, 1949.
- [11] R. B. Blackman and J. W. Tukey, *The Measurement of Power Spectra: From the Point of View of Communications Engineering*, Dover, New York, NY, USA, 1959.
- [12] M. B. Priestley, *Spectral Analysis and Time Serie*, vol. 1, Academic Press, London, UK, 1981.
- [13] L. H. Koopmans, *The Spectral Ananlysis of Times Series*, Academic Press, 1974.
- [14] M. Roksandic and S. D. Armstrong, "Using the life history model to set the stage(s) of growth and senescence in bioarchaeology and paleodemography," *American Journal of Physical Anthropology*, vol. 145, no. 3, pp. 337–347, 2011.
- [15] H. Tong, *Non-linear Time Series. A Dynamical System Approach*, Oxford University Press, 1990.
- [16] F. Takens, "Detecting strange attractors in turbulence," in *Dynamical Systems and Turbulence, Warwick 1980*, D. A. Rand and L.-S. Young, Eds., vol. 898 of *Lecture Notes in Mathematics*, pp. 366–381, Springer, Berlin, Germany, 1981.
- [17] W. A. Beyer, B. R. Ebanks, and C. R. Qualls, "Convergence rates and convergence-order profiles for sequences," *Acta Applicandae Mathematicae*, vol. 20, no. 3, pp. 267–284, 1990.
- [18] S. M. Pincus, I. M. Gladstone, and R. A. Ehrenkranz, "A regularity statistic for medical data analysis," *Journal of Clinical Monitoring*, vol. 7, no. 4, pp. 335–345, 1991.
- [19] S. M. Pincus and A. L. Goldberger, "Physiological time-series analysis—what does regularity quantify?" *The American Journal of Physiology—Heart and Circulatory Physiology*, vol. 266, no. 4, part 2, pp. H1643–H1656, 1994.
- [20] J. S. Richman and J. R. Moorman, "Physiological time-series analysis using approximate and sample entropy," *The American Journal of Physiology—Heart and Circulatory Physiology*, vol. 278, no. 6, pp. H2039–H2049, 2000.
- [21] W. Chen, J. Zhuang, W. Yu, and Z. Wang, "Measuring complexity using FuzzyEn, ApEn, and SampEn," *Medical Engineering and Physics*, vol. 31, no. 1, pp. 61–68, 2009.
- [22] H.-B. Xie, J.-Y. Guo, and Y.-P. Zheng, "Fuzzy approximate entropy analysis of chaotic and natural complex systems: detecting muscle fatigue using electromyography signals," *Annals of Biomedical Engineering*, vol. 38, no. 4, pp. 1483–1496, 2010.
- [23] N. E. Huang, Z. Shen, S. R. Long et al., "The empirical mode decomposition and the Hilbert spectrum for nonlinear and non-stationary time series analysis," *The Royal Society of London. Proceedings, Series A: Mathematical, Physical and Engineering Sciences*, vol. 454, no. 1971, pp. 903–995, 1998.